Università degli Studi di Ferrara

DOTTORATO DI RICERCA IN
"FARMACOLOGIA E ONCOLOGIA MOLECOLARE"

CICLO XXVIII

COORDINATORE Prof. Cuneo Antonio

Validation of the anti-chondrogenic properties of the microRNA-221 and Slug transcription factor by different *in vitro* and *in vivo* models: new perspectives for cartilage regeneration

Settore Scientifico Disciplinare BIO/10

Dottorando
Dott. Lolli Andrea

Tutore
Prof. Piva Roberta

Anni 2013/2015

Table of contents

Preface of the thesis

The research described in this thesis was mainly aimed at the design of novel strategies based on the use of human Mesenchymal Stromal Cells (hMSCs) for the repair of articular cartilage. Specifically, we focused on (i) the characterization of yet unidentified molecular mechanisms sustaining the processes of hMSCs chondrogenic commitment and differentiation, and (ii) the manipulation of hMSCs by gene silencing to enhance their chondrogenic and therapeutic potential, for possible applications in cartilage tissue engineering. The structure of the work is organized as follows.

Chapter 1 provides a general background and state-of-the-art in cartilage regeneration. Current therapies as well as issues and future trends in the application of cell-based approaches for cartilage reconstruction are taken into account.

Chapters 2-6 aim at the description of the experimental work, as outlined by the scheme in Fig. 1. In **Chapters 2 and 3** hMSCs and healthy/osteoarthritic chondrocytes 2D-monolayer cultures were respectively established. Molecular studies were performed with the aim of identifying critical regulators and mechanisms that could be targeted by gene silencing tools to optimize the cell chondrogenic potential. **Chapters 4, 5 and 6** are focused on the development of specific 3D-culture models that, being one step closer to the *in vivo* microenvironment, allowed us to broaden the validity of our data. In **Chapter 6**, we eventually assessed the ability of the newly developed hMSCs-based bioactive constructs to promote the repair of cartilage tissue defects *in vivo*.

Chapter 7 aims to place the findings reported in this thesis in a general context, and to address the translational significance and future development of the work.

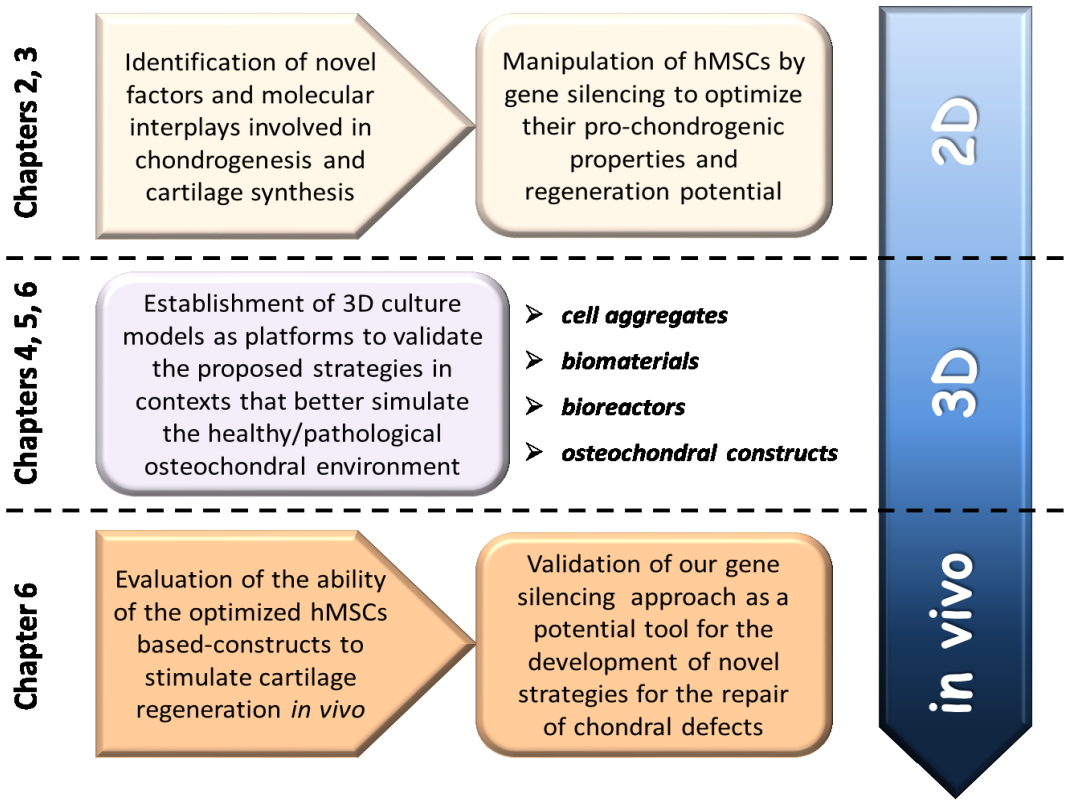

Figure 1. *Schematic diagram of the experimental work of the thesis.*

Chapter 1

Background

1. Overview

The rapid increase in the mean age of the population, and the even more striking increase in the portion of the population over age 60, is deeply changing the demands placed on our health care system. Data from the United Populations Fund (UNFPA) indicate that people aged 60 and older make up over 11% of the global population, and by 2050, that number is expected to rise to about 22% (*http://www.unfpa.org/ageing*). A wide variety of impairments and diseases have a close relationship to aging, and their prevalence and impact are increasing as the population ages. While dramatic progress has been made in defining age-related alterations in brain, bone and skeletal muscle, far less attention has been paid to the changes in articular cartilage. This is a serious concern as aging of articular cartilage involves a complex cascade of events resulting in a progressive loss of the tissue structure and function, with consequent pain, chronic inflammatory states and ultimately seriously impaired movement (*Baugé & Boumédiene, 2015*). As a matter of fact, no disease is more closely correlated with advancing age than osteoarthritis (OA), the most common complication associated with cartilage disfunctions, and no disease causes more impairment of mobility (*Martin & Buckwalter, 2001*).

Even if cartilage malformation and degeneration diseases affect the lifespan and quality of life of many humans from birth to senior age, most of them remain poorly treatable or incurable. Nowadays these clinical conditions represent a tremendous burden for the adult population: data from 2007 to 2009 showed that 1 in 5 (50 million) U.S. adults reported diagnosed arthritis in that period, while 1 in 9 (21 million) had arthritis-related activity limitations. In 2003 the costs attributable to arthritis and other rheumatic conditions were $128 billion, nearly 1% of that year's U.S. gross domestic product (*Murphy & Helmick, 2012*) . Most recent data showed that in 2013 half of the world's population aged 65 and older suffered from OA (*Li et al., 2013*). Moreover, cartilage degeneration is not exclusively related to aging or congenital diseases, but may also arise as a complication of many different events, such as infection, obesity, malnutrition, traumas and fractures.

For these reasons, regenerating articular cartilage is one of the most highly sought-after goals facing researchers in the orthopaedic field today. Attempts over the last two decades to regenerate functional hyaline cartilage using both cell-based and cell-free approaches have fallen short, and this was not due to lack of trying or investments. As a consequence, there is an urgent need for novel approaches and interventions that may specifically target the aberrant mechanisms in case of joint dysfunction, and restore the structure and function of the tissue. Remarkably, thanks to the most recent findings and discoveries in the fields of tissue engineering, cellular and molecular biology and biomaterials, it appears that progress in this field might have finally turned a corner and important results in basic and clinical research are being achieved towards the reparability of the articular tissue.

2. Cartilage damage

Cartilage is a flexible connective tissue found in many areas of the human body, including the joints, ribs, nose, ear, trachea and intervertebral discs, where not only it acts as a structural support, but also maintains shape and absorbs shocks during movement or physical exercise (*Oseni et al., 2011*). In particular, hyaline cartilage is the most abundant type of cartilage tissue, being present on the articular surfaces of joints (articular cartilage) and in the nasal septum. In the articular environment, cartilage permits congruency between the two opposing skeletal elements, facilitates the transfer of forces between them and their frictionless movement, and acts as an adsorber of weight during sustained static loading (*Hunziker et al., 2015*). Unlike most other connective tissues, cartilage is aneural, alymphatich and, most importantly, largely avascular, thus creating a hypoxic environment that greatly limits cell growth and consequently the regeneration potential of the tissue. The cartilage tissue itself actively resists vascularization by producing antiangiogenic components such as thrombospondin-1, chondromodulin-1, secreted protein acidic and rich in cysteine (SPARC), collagen type II derived N-terminal propeptide (PIIBNP), and the type XVIII derived endostatin. In addition, the calcified cartilage and the tidemark (the interface between calcified and non-calcified cartilage) are two anatomical barriers for the vascularization of articular cartilage (*Tiku & Sabaawy, 2015*). The only cells normally present in the cartilage tissue, the chondrocytes, are few and highly specialized, and exhibit an extremely low proliferation rate and a declining functionality with tissue aging. Chondrocytes themselves exist in an environment that does not support healing, as they are trapped in *lacunae* and cannot migrate to damaged areas to initiate repair processes.

All in all, cartilage tissue is virtually incapable of self-repair in the event of damage, with tissue injury being typically followed by necrosis as opposed to the process of inflammation and repair found in vascularized tissues. Accordingly, a cartilage injury does not involve fibrin clot formation, recruitment of inflammatory cells or angiogenesis (*Kessler & Grande, 2008*).

In 1743, William Hunter stated that "an ulcerated cartilage is a troublesome problem and, once destroyed, it never repairs". Surprisingly, and in spite of the great advances that have been made in the field of cartilage repair and tissue regeneration, this statement holds mostly true even three centuries later (*Bhosale & Richardson, 2008*). As mentioned previously, structural lesion of the articular cartilage layer can be induced either traumatically or during the course of a disease-based process, but once this alteration has begun, it cannot be arrested and progresses inexorably with time, the reason for which is not completely clear. Superficial injuries of the articular layer, i.e. defects that are confined to the cartilage layer itself and do not penetrate the subchondral-bone plate, do not heal spontaneously. With the lapse of time, these lesions would only broaden and lengthen, such that what is initially a discrete condition progresses insidiously towards a crippling disease (*Hunziker et al., 2015*), or even towards the onset of osteoarthritis. Unfortunately, once that the progressive lesioning process is initiated, no prophylactic or interventional measures are available to arrest it, and, likewise, there is a lack of biologically-based treatments that may induce an efficacious or complete healing of the structural defects.

2.1 Osteoarthritis (OA)

Osteoarthritis (OA) is the most common joint disorder, with well characterized clinical manifestations including progressive loss of articular cartilage, cartilage calcification, osteophyte formation, subchondral bone remodeling, and mild to moderate inflammation of the synovial lining. OA can occur in any joint but usually affects the joints of the hand, knee, and hip. It is described as a complex and progressive multifactorial disease which is impacted by aging, genetic predisposition, abnormal biomechanics, obesity, and trauma, and influenced by co-morbidities such as cardiovascular disease, metabolic syndrome, and diabetes (*Goldring & Berenbaum, 2015*). While OA was once viewed as a disease of purely mechanical cartilage degradation, it is now known to be a much more complex condition: the whole joint is affected, including the synovium, subchondral bone, capsule, ligaments, periarticular muscles and the sensory nerves whose termini lie within these tissues (*Baugé et al., 2014*).

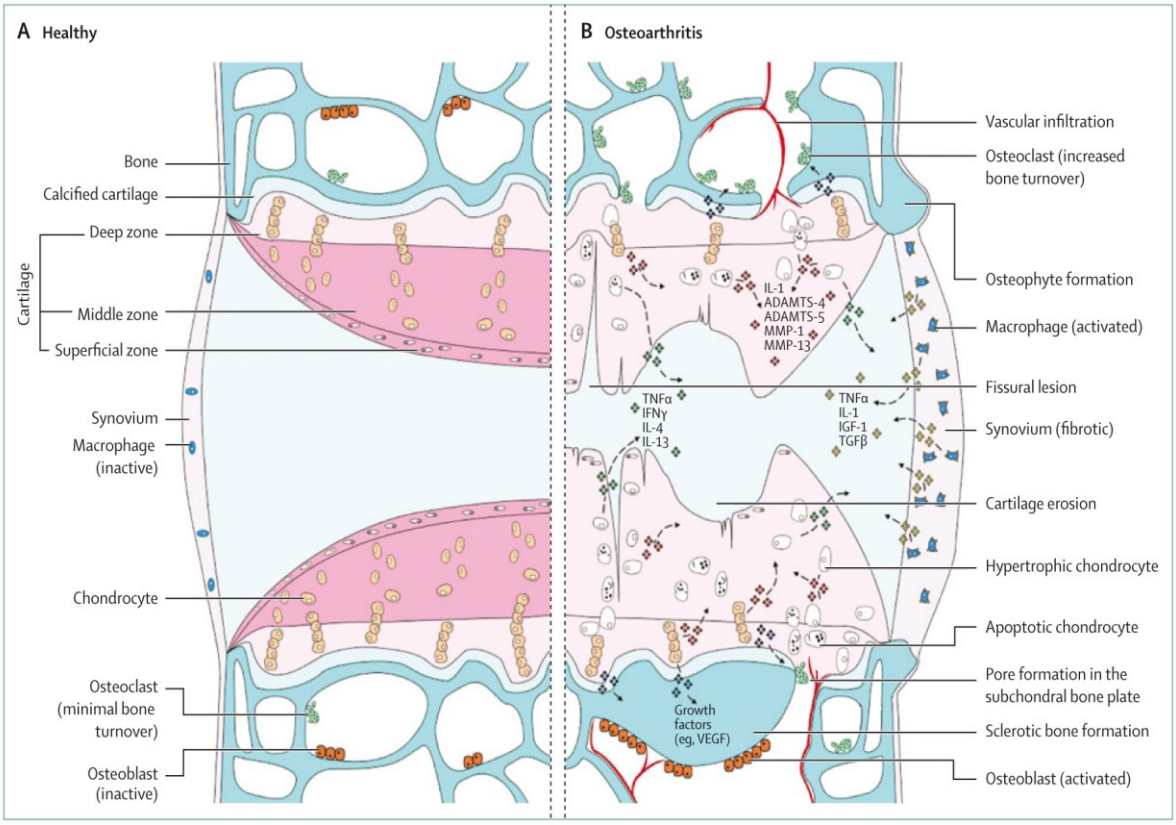

Figure 1. *Major signalling pathways and structural changes involved in the development of OA.* ADAMTS = A disintegrin and metalloproteinase with thrombospondin motifs, IL = interleukin, MMP = matrix metalloproteinase, TNF = tumour necrosis factor, IFN = interferon, IGF = insulin-like growth factor, TGF = transforming growth factor, VEGF = vascular endothelial growth factor (*Glyn-Jones et al., 2015*).

Accordingly, OA may also result from abnormalities in any of the above tissues. While the cartilage, subchondral bone and synovium are the main structures being destroyed during the progression of the disease, further research is revealing that OA is not simply a biomechanical process placing excess load on the affected joint, but contributions from catabolic cytokine cascades and production of inflammatory mediators also play a significant role and are potential targets for intervention (Fig. 1) (*Fibel et al., 2015*). In physiological conditions, signals generated by cytokines, growth factors, and cartilage matrix regulate chondrocyte metabolic activity. There is mounting evidence that in OA catabolic and pro-inflammatory mediators (cytokines, nitric oxide, prostaglandins and neuropeptides) are produced by the inflamed synovium, leading to enhanced production of the proteolytic enzymes responsible for cartilage breakdown, thereby disturbing the balance of cartilage matrix degradation and repair. In turn, these alterations induce further synovial inflammation, establishing a vicious cycle that causes progressing synovitis,

severe clinical symptoms and eventually further joint degradation (*Mobasheri et al., 2014*). To date, no efficacious structure-modifying agent has been approved by any regulatory agency and, as a consequence, conventional OA treatment consists of pain management with joint replacement for end-stage disease (*Glyn-Jones et al., 2015*). As available pain therapies are not only limited in efficacy but also related to severe side effects, there is an urgent need for novel approaches able to target the structural changes of the disease rather than the symptoms only.

3. Cartilage repair: cell-free approaches

Typically, cartilage injuries exhibit similar clinical sign and symptoms, with pain, swelling and impaired movement of the joint. The first line of treatments is represented by conservative medical options aimed at reducing pain and improving joint manipulation, such as non-steroidal anti-inflammatory drugs (NSAIDs), opiate pain killers and hyaluronic acid or corticosteroid injections (*Gardner et al., 2013*). When these interventions are not effective, a variety of conventional surgical options may be considered, depending on the patient factors and the nature, location and size of the lesions. Nevertheless, it is to be highlighted that thus far no surgical technique has ever been completely successful in stimulating the repair of articular cartilage.

- The earliest surgical procedures for cartilage healing were **debridement and lavage**. Loose cartilage bodies or fragments are arthroscopically removed from the joint capsule, while rough areas are smoothed. Debridement is simple to perform, relatively cheap and has low levels of post-operative morbidity, and is considered potentially useful to reduce pain and increase joint mobility, as well as to slow the progress of joint degeneration. However, in a controlled trial of arthroscopic surgery in the setting of OA, arthroscopic lavage or debridement had similar outcomes to placebo surgery. As a result, the therapeutic value of these techniques is limited (*Moseley et al., 2002*).
- **Bone marrow stimulation techniques**, such as Pridie drilling, abrasion arthroplasty and microfracture, are based on the principle that when full-thickness cartilage defects cross the subchondral bone, bleeding from the bone marrow leads to recruitment of marrow stromal cells containing progenitor cells, platelets and other factors that will aid the process of tissue repair. Microfracture is the most recent of these approaches and makes use of a surgical awl to create holes in the subchondral plate (approximately 3-4 mm apart), which allow blood to enter the defect from the bone marrow below.

The common problem of marrow stimulation approaches is that, although the clot fills the defect and produces repair tissue, this is mostly fibrocartilaginous and therefore less than optimal for long-term outcomes, being characterized by insufficient functionality in the context of the joint microenvironment (*Ye et al., 2014*).

- **Mosaicplasty** and **osteochondral transfer system (OATS)** are reconstructive bone grafting techniques that involve the harvesting of osteochondral plugs from low weight-bearing regions of the joint or from an allogeneic or cadaveric donor, and the transplantation into the cartilage defect. The transplantation of mature hyaline cartilage into the affected area is an advantage of the procedure. Indeed these techniques have proved useful to decrease pain and improve the mechanical function of the joint, but there is evidence of extensive cell death at the donor site in autologous donors, leading to tissue degeneration. Besides, allografts may lead to disease transmission and immunological response, while the long-term viability of transplanted grafts is a concern with any allografting procedure. Finally, poor cartilage integration is usually observed, with consequent degeneration of the implant site and therefore graft failure (*Badekas et al., 2013*).
- Other techniques used for the repair of damaged cartilage include **osteotomy**, which is useful to correct malalignment of joints hence preventing further degeneration due to abnormal loading, and **soft tissue grafts** of perichondrium or periosteum, that are thought to stimulate a repair response (*Gardner et al., 2013*).
- The final solution for severe damage is **total joint replacement or arthroplasty**, an invasive procedure aimed at replacing the damaged joint with a prosthesis. This approach has represented a striking advance in the treatment of painful and disabling joint pathologies and can be performed on any joints of the body, including the hip, knee, ankle, foot, shoulder, elbow, wrist, and fingers. Among these procedures, hip and knee total joint replacements are definitely the most common. Unfortunately, when joint replacement procedures are carried out in younger patients, revision surgery becomes necessary, and this is much more complex than the initial surgery, with a higher rate of complications (*Callaghan et al., 2015*).

Cell type	Advantages	Disadvantages
Autologous chondrocyte	Native phenotype Minimal risk of immunological problem	Small initial cell number De-differentiation on expansion
Allogeneic chondrocyte	Larger cell number Off-the-shelf solution	Limited donor availability Risk of disease transmission
Adult mesenchymal stem cells	Potential to produce large numbers Various harvest sites Additional paracrine signaling potential	Potential for hypertrophy Heterogeneous population of cells Stable and reproducible differentiation still problematic
Induced pluripotent stem cells (iPS)	Large source of patient specific cells Multiple cell types can be produced	Stable and reproducible differentiation still problematic Potential for teratoma
Embryonic stem cells	Off-the-shelf solution Multiple cell types can be produced	Stable and reproducible differentiation still problematic Potential for teratoma Ethical considerations

Table 1. *Cell sources for cartilage repair.* The main advantages and disadvantages of the cell sources currently under investigation for cartilage repair are reported (*Johnstone et al., 2013*).

4. Cartilage repair: cell-based approaches

In 1987 it was reported that chondrocytes could be cultured and implanted into chondral defects where the subchondral bone had remained intact (*Grande et al., 1987*). Few years later, Brittberg and Peterson reported a first case series where they used a new procedure with a considerable potential for cartilage regeneration named autologous cartilage transplantation, later referred to as autologous chondrocyte implantation (ACI) (*Brittberg et al., 1994*). Since then, ACI and cell-based tissue engineering techniques in general for cartilage or osteochondral repair have gained an increasing amount of interest (*Caldwell & Wang, 2015*). In the field of cell-based tissue engineering, selection of the source cells is a major critical point, as several criteria needs to be considered, including ease of access and availability, capacity for differentiation ("performance" of the cells), and lack of immunogenic or tumourigenic/teratogenic ability (*Seo & Na, 2011*). Specifically for cartilage repair, different cell sources have been proposed as good candidates, although each cell type has its limitations and advantages due to its intrinsic biological properties (Table 1). For the purposes of this work, the cell sources that will be further discussed are autologous chondrocytes and adult mesenchymal stem/stromal cells (hMSCs), as they represent the most promising alternatives thus far.

4.1 Chondrocytes: autologous chondrocyte implantation (ACI)

Nowadays, ACI is one of the most widely used cell-based strategies for the repair of articular cartilage (the technique is outlined in Fig. 2). The rationale in ACI is to fill up the cartilage defect with autologous chondrocytes, combining the surgical treatment with *in vitro* and cell culture techniques. In detail, a cartilage biopsy is surgically harvested from a non weight-bearing area and subsequently used as the source of autologous chondrocytes, after enzymatic treatment. Chondrocytes are then expanded *in vitro*, in order to obtain a sufficient cell number, and implanted into the affected joint during a second surgical procedure. Usually, a periosteal flap is further sewed over the defect, to confine the cells at the site of implantation and to prevent the mass from floating away (*Mobasheri et al., 2014*). ACI has been in clinical use since 1987 and has been performed on thousands of patients worldwide, showing encouraging clinical results. As a matter of fact, the technique has proved useful not only to reduce pain in patients, but also to produce cartilage-like tissue, with patients being overall satisfied.

Even though the ACI procedure has represented a considerable advance in the field of cartilage repair, the production of cartilage tissue exhibiting long-term stability and hyaline-like features is still an unfulfilled promise. Results after 3 to 9 years of follow-up are positive, but the repair of the defect is not uniform in all the areas of the joint. Published studies have compared ACI and microfracture, showing that both methods provided satisfactory results in 77% of the patients, but were not able to reveal a significant difference in the clinical and radiographic results between the two approaches (*Knutsen et al., 2007*). Taken as a whole, there are still considerable limitations to the use of ACI, and these are mainly due to 1. the complexity and cost of the two surgeries, 2. the biological response of the periosteal flap, and 3. the de-differentiation and consequent loss of chondrogenic potential associated with the *in vitro* expansion of isolated chondrocytes. While the second generation of ACI procedure (Fig. 2) has dramatically reduced the complications related to the periosteal flap and the adverse events, chondrocyte de-differentation still represents a major hurdle (*Kean & Dennis, 2015*). The intimate interaction between chondrocytes and the cartilage extracellular matrix (ECM) is an essential factor for the maintenance of the chondrogenic phenotype, function and biosynthetic program. As a consequence, damaged or absent ECM will inevitably lead to a significant change in chondrocyte gene expression.

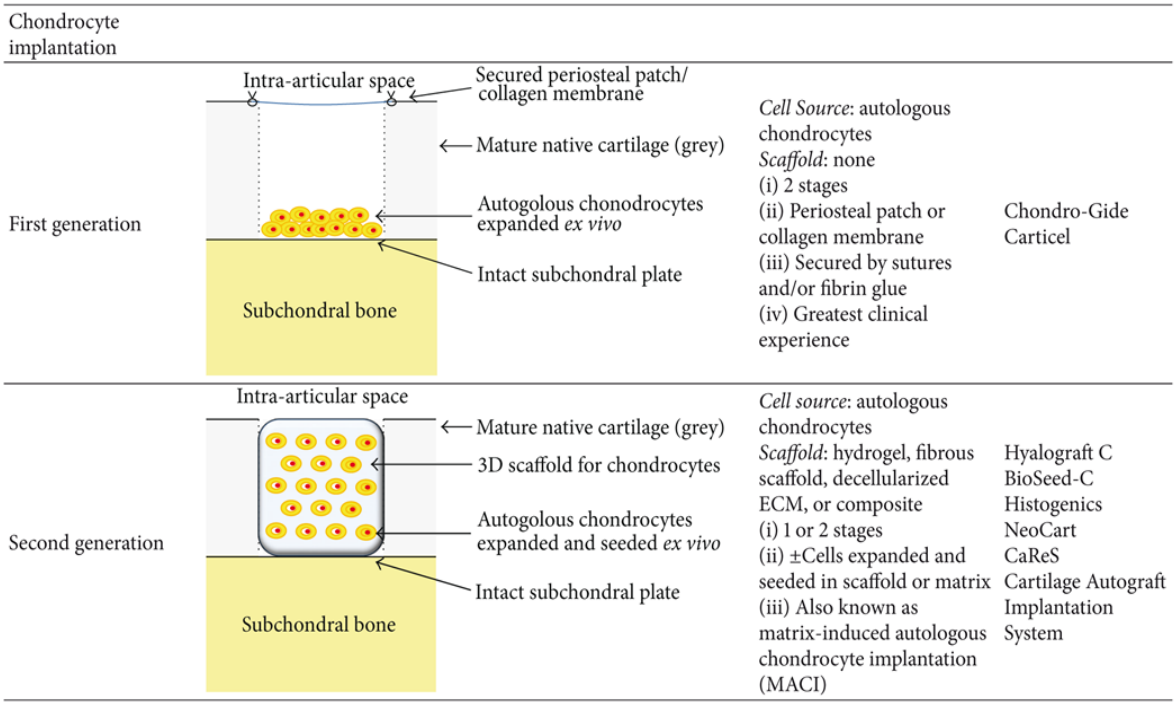

Figure 2. *Evolution of autologous chondrocyte implantation (ACI) approaches for cartilage repair.* The main features (components, scaffolds, commercial products) of the first and second generation of ACI techniques are reported. The second generation approaches are mainly characterized by the incorporation of a scaffold or substrate to promote chondrocyte expansion, and thereby are also known as matrix-induced autologous chondrocyte implantation (MACI) techniques *(Dewan et al., 2014)*.

Indeed, while mature chondrocytes produce cartilage-specific proteoglycans (PGs) and collagen type II, monolayered chondrocytes gradually switch to synthesizing non-specific PGs and collagen type I, and these matrix components are not suitable for sustaining the biomechanical stimuli and theresilience of articular cartilage. These deep changes in chondrocyte morphology, function and molecular signature are the reasons why fully de-differentiated chondrocytes are no longer capable of re-differentiation and synthesis of hyaline cartilage ECM when re-implanted in a defect. To avoid or at least slow down chondrocyte de-differentiation during *in vitro* expansion, different strategies have been explored, such as the use of chondrogenic growth factors, three-dimensional culture conditions and scaffolds or decellularized matrixes (*Chen et al., 2015b; Caron et al., 2012; Bittencourt et al., 2009; Pei et al., 2011; De Ceuninck et al., 2004*). However, the optimal *in vitro* culture conditions allowing the obtainment of a sufficient number of cells while preserving unaltered chondrocyte function and biosynthetic properties are yet to be found.

4.2 Mesenchymal Stem/Stromal Cells (hMSCs)

While chondrocytes are still of great interest as they represent the only cell source approved for clinical use, a great advance in the field has been made with the identification of multiple cell populations that can potentially provide a large number of undifferentiated chondroprogenitors (*Johnstone et al., 2013*). Specifically, hMSCs isolated from different sources have shown promising features for cartilage tissue engineering, such as hMSCs from bone marrow, fat, synovial fluid and umbilical cord blood or jelly tissue (Wharton's jelly). Indeed, among the different populations of multipotent adult stem cells, hMSCs are considered to be the cell type of choice, due to the ease of access and *in vitro* expansion, and their multi-lineage differentiation capacities. In addition, as well as maintaining their ability to produce cartilage-like repair tissue longer than chondrocytes in culture, hMSCs also have a higher rate of proliferation which, unlike chondrocytes, does not decrease when the cells are cultured in monolayer or when harvested from older donors (*Gardner et al., 2013*). Notably, hMSCs produces a variety of ECM macromolecules involved in cartilage function, such as collagens, fibronectin, glycosaminoglycans (GAGs) and proteoglycans (PGs), as well as a wide repertoire of growth factors, cytokines and immunomodulatory factors, that potentially mediate a variety of paracrine effects on the surrounding cells (*Mardones et al., 2015*).

Results of several pre-clinical and clinical studies utilizing hMSCs for cartilage repair have evidenced that the transplantation procedure is not substantially different from ACI, in terms of feasibility and safeness (Table 2). It is also very relevant that intra-articular injections of hMSCs proved to be effective in reducing pain, improving tissue function and generating hyaline-like cartilage. Nonetheless, there are still several challenges that must be overcome before hMSCs-based tissue engineering might become an effective regeneration therapy. Importantly, hMSCs, unlike chondrocytes, are prone to undergo hypertrophic differentiation following chondrogenic induction and the possibility to obtain stable and reproducible differentiation has proved difficult (*Chen et al., 2015b*). These issues (which are discussed in detail in par. 5.1.1) still represent a major hurdle, and in part explain why, despite the great advances concerning the use of hMSCs for cartilage repair, there are no published consensus statements relating to the optimal conditions needed to drive differentiation of hMSCs towards a stable chondrocyte phenotype. As a consequence, nowadays much effort is focused on the identification of the biomolecular and mechanical cues that might be exploited *in vitro*, prior to cell transplantation, to guide the cells towards the acquisition of the proper chondrogenic phenotype.

Cartilage lesion	Cell type	Number of patients	Most significant findings	Reference
Knee articular	ACI	431	Mild or no effects	*(a)*
Knee osteoarhritis	MSC	41	Significant improvement in knee evaluation tests and MRI scores	*(b)*
Knee articular	ACI or MSC	72	Both cell types produce no significant differences in knee evaluation tests (IKDC, Lysholm, Tegner). However, patients receiving MSC, but not ACI, improve evaluation tests and require less surgery	*(c)*
Knee osteoarthritis	MSC	18	No adverse events, improvement in knee evaluation tests, size of defect decreased, hyaline-like cartilage regeneration	*(d)*
Knee osteoarthritis	MSC	6	In 3/6 patients, cartilage thickness and knee evaluation tests improved (6 months); increase in extension of repair tissue; decrease in edematous subchondral patches	*(e)*

Table 2. *Use of hMSCs for cartilage repair.* Relevant clinical studies assessing the feasibility and safeness to repair cartilage defects by autologous chondrocyte (ACI) or hMSCs transplantation (MSC) (adapted from: *Mardones et al., 2015*). References: *(a) Vasiliadis et al., 2010, (b) Wakitani et al., 2011, (c) Nejadnik et al., 2010, (d) Jo et al., 2014, (e) Emadedin et al., 2012.*

This step normally requires the use of exogenous differentiating agents able to trigger the chondrogenic process and/or biocompatible scaffolds that may provide a 3D microenvironment, favourable and permissive to cell differentiation, while sustaining cell viability and metabolism (*Mazor et al., 2014*). These tools are widely used and considered extremely useful to stimulate and promote the differentiation process *in vitro*. Nonetheless, several aspects need to be taken into account in relation to the translational process, mostly concerning the long-term and side effects that exogenous agents introduced *in vitro* may produce on the articular microenviroment *in vivo*.

5. Chondrogenic differentiation of hMSCs

Most frequently, hMSCs needs to be chondrogenically differentiated *in vitro* prior to implantation in the cartilage defect, in order to induce the acquisition of a chondrocyte-like phenotype and the synthesis of cartilage ECM. In addition, the experimental models of chondrogenesis of hMSCs *in vitro* are valuable tools allowing a meticoulous characterization of the regulation of the differentation process, an aspect that has been elucidated only partially (*Kozhemyakina et al., 2015*). As it is generally accepted that natural tissue regeneration mimics developmental processes, hMSCs chondrogenesis *in vitro* strives to recapitulate, at least in part, the process of endochondral ossification.

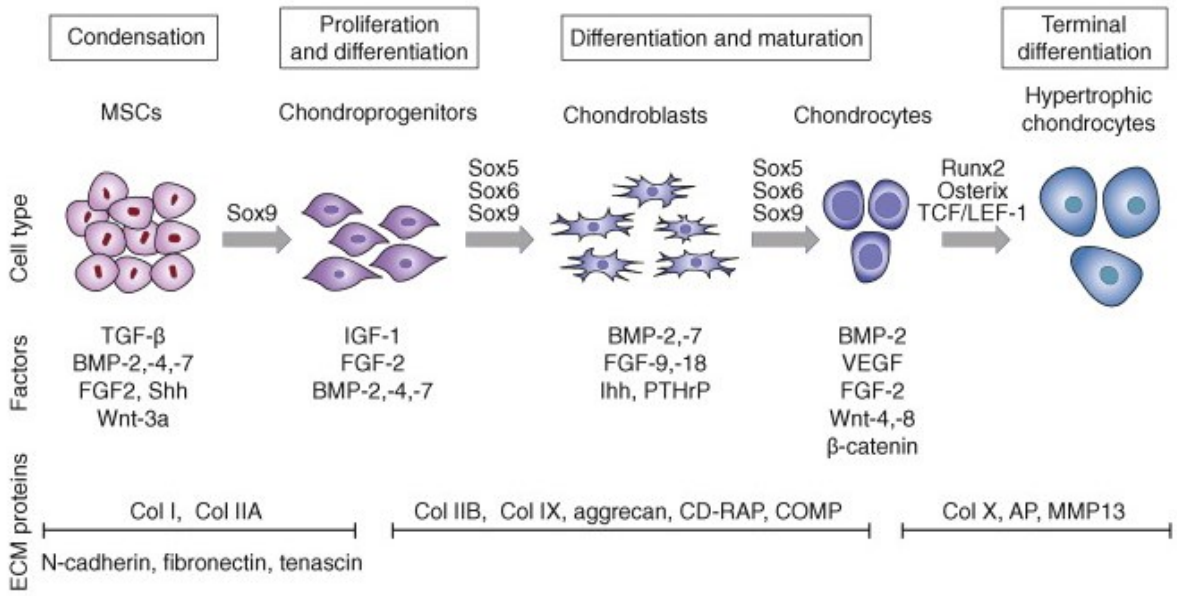

Figure 3. *Chondrogenic differentiation of hMSCs.* The different stages of chondrogenesis, the main transcription factors and growth factors involved in each stage, and the accompanying alterations in the ECM are outlined. The process requires a strict control of the expression of early to late chondrogenic regulators and markers *(Vinatier et al., 2009b)*.

This event that takes place at an embryonic stage, and involves the formation of a cartilage template that will eventually undergo ossification (*Oseni et al., 2011*). hMSCs chondrogenesis is a tightly regulated process that requires the expression of early to late chondrogenic markers and that may be subdivided into 5 stages (outlined in Fig. 3): hMSCs condensation, rise of chondroprogenitors, chondrogenesis and eventually terminal differentiation and ossification. It is believed that, in order to induce chondrogenesis of hMSCs, cells need to be in close contact, as well as being exposed to the correct bioactive agents, usually growth factors, and supported by proper scaffold matrixes.

5.1 Growth factors as chondrogenic inducers: the TGF-β family

Ideally, bioactive factors used for cartilage tissue engineering should promote proliferation, differentiation, and maturation of the cellular component of the construct. In addition, they should have chemotactic activity and maintain sufficient ECM production by the cells (*Ahmed & Hincke, 2014*). There are five most relevant families of growth factors involved in chondrogenic differentiation and thereby employed as pro-chondrogenic stimuli to

induce the differentiation of hMSCs: the transforming growth factor-β superfamily (TGF-β), the fibroblast growth factor family (FGF), the insulin-like growth factor family (IGF), the wingless family (Wnt) and the hedgehog family (HH) (*Vinatier et al., 2009b*). A considerable number of bioactive agents belonging to these families has been investigated for the development of tissue-engineered cartilage substitutes. However, the three TGF-β isoforms (TGF-β1, TGF-β2 and TGF-β3) are definitely the most widely applied pro-chondrogenic agents, alone or in combination with other growth factors, as they have been shown to strongly and efficiently promote chondrogenesis in a variety of experimental models, *in vitro* and *in vivo* (*Ahmed & Hincke, 2014*). While the effects of TGF-β2 appear rather controversial, the chondro-inductive effects of TGF-β1 and TGF-β3 on hMSCs are powerful and very similar (*Gardner et al., 2013*). These proteins are among the first factors to be expressed during the initial condensation of mesenchymal cells that precedes differentiation, and are also required for triggering chondrocyte maturation and synthesis of GAGs later in the process. As well as these direct chondrogenic effects on hMSCs and chondrocytes, there is also evidence for TGF-βs possessing chemotactic effects, as TGF-β3 was used *in vivo* to induce the migration of stromal cells found in tissues around the joint (*Mendelson et al., 2011*). This potential ability to recruit chondroprogenitors with regenerative potential from neighbouring tissues would provide an extra advantage to a cellular technique using TGF-β within a scaffold (*Khan et al., 2011*).

5.1.1 Potential effects of TGF-β in the joint: angel or devil?

In vivo, the TGF-β signalling is required for normal cartilage development and is crucial for differentiation of hMSCs into chondrocytes and maintenance of articular chondrocyte homeostasis in synovial joints. Accordingly, it has been shown that ablation of TGF-β signalling in cartilage causes imbalance in chondrocyte function and metabolism, ultimately resulting in cartilage degeneration. As a consequence, stimulation of the TGF-β pathway has been repeatedly proposed not only to induce differentiation of hMSCs-based constructs for cartilage tissue engineering, but also to restore or preserve the integrity of articular cartilage during OA or other cartilage-related diseases (*Bush & Beier, 2013*).

Despite the encouraging results and the considerable clinical potential related to the use of TGF-βs for cartilage repair, almost 30 years after its first description as a "cartilage-inducing factor" (*Seyedin et al., 1986*), an ideal protocol using TGF-β for hMSCs chondrogenesis has yet to be defined and the clinical translation is still worryingly limited.

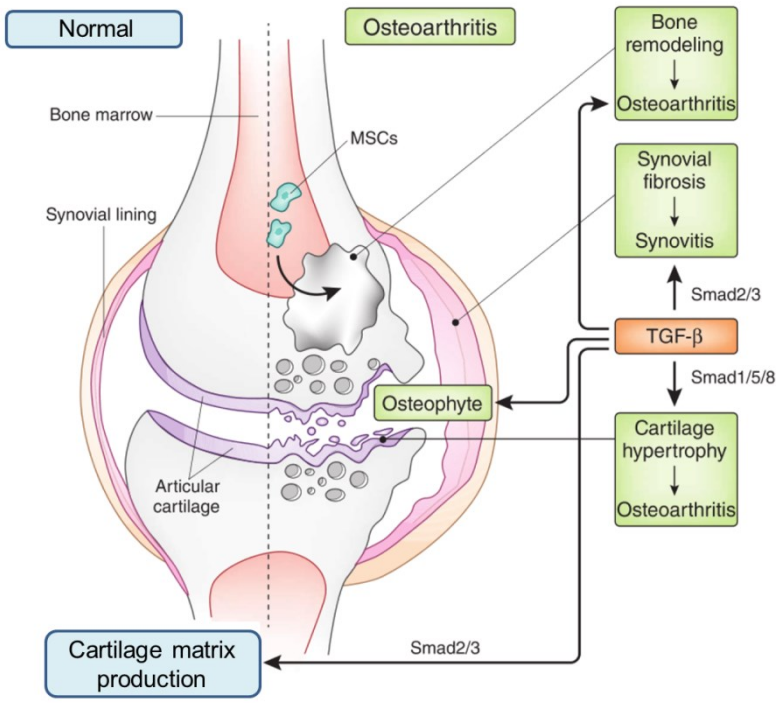

Figure 4. *Effects of TGF-β on the joint in vivo.* In the articular microenvironment, TGF-β promotes the anabolic activity of cartilage (blue squares), but it is also thought to be involved in the induction of other processes that are related to the pathogenesis of OA (green squares). Specifically, TGF-β stimulates the production of cartilage matrix through the classical Smad 2/3 pathway, while may also induce hypertrophy and the associated catabolic events via the Smad 1/5/8 pathway. TGF-β signalling also triggers synovial fibrosis and osteophyte formation, features of OA (*Bush & Beier, 2013*).

As a matter of fact, serious concerns have been raised in relation to a potential use of TGF-β in clinics, especially due to its involvement in the pathogenesis of OA and the dual effects on the expression of fibrotic and hypertrophic markers in chondrocytes and hMSCs. The precise role of TGF-β in OA is not understood (*Shen et al., 2014*). On the one hand, it exerts a protective effect against cartilage-degrading events, and its deficiency induces susceptibility to OA. On the other hand, a sustained and prolonged stimulation of TGF-β signalling in joints leads to OA-related changes, such as synovial fibrosis and osteophyte formation (Fig. 4). It is conceivable that this effects are due to an aberrant and undesired activation of TGF-β signalling in tissues that are in contact with articular cartilage, and in particular the subchondral bone, the synovium, the capsule and the ligaments. As a result, the use of TGF-β as a therapeutic agent should be carefully evaluated as side effects will likely occur if TGF-β exposure is not confined to articular cartilage, a goal that would be

extremely difficult to achieve. To clarify the role of TGF-β signalling in cartilage degeneration during OA progression, Zhen and co-workers used a mouse model of OA in which the anterior cruciate ligament was transected to destabilize knee joints leading to the development of OA, with increased thickening of the calcified cartilage, neo-vascularization and disruption of the articular cartilage (*Zhen et al., 2013*). The study showed that TGF-β is involved in aberrant bone remodeling and cartilage degeneration in OA and increased TGF-β activity in the subchondral bone may be a primary cause of OA and initiate pathology. In addition, it was shown that hMSCs are the target cells of aberrant TGF-β signalling during OA progression. These results does not only suggest that inhibition of TGF-β signalling might be beneficial in certain forms of OA, but also that the implantation of tissue engineered constructs supplemented with high doses of TGF-β in sites of cartilage injury may potentially induce or further worsen OA-related events.

As well as inducing chondrogenic factors, TGF-βs may also cause upregulation of typical markers of the last stage of chondrogenic differentiation (terminal or hypertrophic stage), that normally anticipates the mineralization phase, thereby preventing the cells from being therapeutically useful for the regeneration of cartilage (*Gardner et al., 2013*). At a molecular level, these conflicting actions depend on the alternative activation of different signalling pathways (*Mariani et al., 2014*). TGF-β signals via its type II receptor which then engages the type I receptors, normally represented by the activin-like-kinase (ALK) 1 or 5. The activation of the ALK receptors leads to the phosphorylation of downstream targets of the Sma and Mad Related Family (Smads), which exhibit both stimulatory and inhibitory effects on hypertrophic differentiation. ALK5 activates the Smad2/3 pathway directly leading to inhibition of hypertrophy and induction of chondrogenesis with stimulation of aggrecan and collagen type II production. This is due to the stabilization of the Sox9 transcription complex, while Runx2 becomes inhibited through epigenetic regulation. Conversely, the activation of the Smad1/5/8 pathway by ALK1 cooperates with Runx2 to stimulate hypertrophy, with consequent production of collagen type X, matrix metalloproteinase (MMP) 13, osteopontin, alkaline phosphatase, osteocalcin and vascular endothelial growth factor (VEGF). Accordingly, the addition of TGF-β to induction media during pellet culture of hMSCs is not sufficient to suppress the onset of hypertrophy and, remarkably, TGF-β1-supplemented expansion media has further shown to redirect chondrocytes towards hypertrophy (*Narcisi et al., 2012a*). A famous study by Pelttari and co-workers is particularly emblematic (*Pelttari et al., 2006*), as it was evaluated whether bone marrow-derived hMSCs adopted natural differentiation stages during TGF-β-induced chondrogenesis in pellet culture.

It was shown that the stimulation of chondrogenic factors was accompanied by the concomitant expression of typical fibrotic or hypertrophic markers, such as collagen type X, MMP13, osteopontin, osteonectin and alkaline phosphatase. Notably, these negative features influenced the fate of the hMSCs-derived cartilage-like tissue after transplantation *in vivo*, as it stained positive for GAGs and collagen type II, but also for collagen type I and X, and also displayed mineralization potential. The concomitant presence of hyaline, fibrous and hypertrofic/calcified cartilage features demonstrated that the natural differentiation process was not recapitulated by TGF-β-differentiated hMSCs.

The reported studies highlight how the impact of TGF-βs on the joint microenvironment is much more complex than initially hypothesized and explain why the clinical use of these molecules has encountered major hurdles. This emerging body of evidence is leading the researchers to pay special attention to feasible alternatives to the use of growth factors, that could allow to achieve sustained and stable chondrogenesis while better or fully exploiting the intrinsic chondrogenic potential of the cells.

5.2 Biomaterials: scaffold-based versus scaffold-free approaches

Traditional tissue engineering-based strategies for the repair of articular cartilage require a suitable biocompatible scaffold material in which the cells can propagate and differentiate with subsequent production of new tissue. The choice of the specific scaffold is not a secondary issue, as even a naked matrix (no cells or biomolecules) must be considered as an information-carrying device. Its 3D-structure and peculiar geometrical configuration will accordingly guide, or at least influence, the process of tissue growth, while the physicochemical properties of its surface will affect cell attachment and the binding of growth factors in the niche microenvironment (*Hunziker et al., 2015*). Ideally, scaffolds for articular cartilage tissue engineering should exert the following effects, in order to promote and/or sustain the process of tissue regeneration (*Ahmed & Hincke, 2014*):

- mimic the effect of native cartilage ECM on cell adhesion, proliferation, interaction and differentiation;
- be biodegradable but stable for an adequate length of time until being replaced gradually by the cartilage-like ECM produced by the cells (remodeling process);
- have suitable porosity and interconnectivity to allow cell migration and efficient exchange of nutrients and wastes;
- facilitate uniform cell distribution while retaining the cells at the lesion site and promoting integration with the surrounding native cartilage;

- have sufficient mechanical properties to withstand the *in vivo* forces and support tissue growth under native mechanical loads.

A plethora of scaffolding matrices has been evaluated for tissue engineering-mediated cartilage repair, either natural polymers extracted from living organisms or synthetic materials obtained from various chemical processes (*Zhang et al., 2009*). While some of them are already in clinical use, many others, and especially the synthetic ones, are still being tested in preclinical trials. The most extensively used scaffolds include protein-based (collagen, fibrin and gelatin), carbohydrate-based (agarose, alginate, chitosan and hyaluronan), and synthetic polymers such as polyglycolic acids (PGA), polylactic acid (PLA), copolymers of glycolic and lactic acids (PLGA), poly(ethylene glycol) (PEG), and poly(ε-caprolactone) (PCL).

In general, natural biomaterials are the scaffolds of choice for cartilage repair and regeneration due to their superior biocompatibility for cell attachment and differentiation. For instance, as a non-sulfated GAG derived from the ECMs of many tissues, hyaluronan has been used to support chondrocyte growth or stimulate chondrogenesis of hMSCs. A hyaluronan-based scaffold (Hyaff-11) seeded with autologous chondrocytes has proved to be effective in regenerating cartilage *in vivo* (*Grigolo et al., 2001*). Agarose and alginate are widely used as biocompatible 3D-scaffolds to encapsulate cells for cartilage tissue engineering, as both of them have exhibited excellent cytocompatibility for cell growth. Alginate forms biocompatible, biodegradable and shape-adaptable hydrogels which can be employed as cell carriers allowing bidirectional exchange of nutrient, oxygen and cell waste products, but protecting the delivered cells from the host immune system. However, the poor degradation properties and the difficulty to modify the stability of agarose and alginate-based scaffolds have partially hindered their clinical application for tissue regeneration. In this regards, we recently investigated the possibility to enhance the structural and biomimetic properties of alginate-based scaffolds for cartilage tissue engineering by producing alginate-gelatin and alginate-urinary bladder matrix (UBM) composite microfibers (*Angelozzi et al., submitted*). Collagens normally contribute to cell adhesion, proliferation and differentiation, and therefore are among the most common scaffold materials for cartilage tissue engineering as well. Many studies have shown that a combination of collagens (such as collagen type I and type II) with chondrocytes and hMSCs sustained cartilage tissue growth *in vitro* and *in vivo*. The second generation of ACI procedures, namely matrix-induced autologous chondrocyte implantation (MACI® implant, Genzyme), involves the expansion of chondrocytes in a collagen membrane prior to implantation of the constructs into the articular cartilage defect without suturing.

Furthermore, other natural scaffold materials like the biodegradable fibrin, chitosan or composites thereof are widely studied and have shown potential to enhance cartilage tissue regeneration. Among the great advances in this field, it should be mentioned that it has now become common to use biphasic scaffolds consisting of two different materials: an upper one that has pro-chondrogenic properties and thereby destined for the cartilaginous compartment of osteochondral defects, and a lower one of a ceramic-like substance, which can be fitted as a plug into the subchondral bone (*Da et al., 2013*).

Apart from the obvious issues that must be taken into account when testing a scaffold, such as biocompatibility, biodegradability, toxicity and immunological response (also related to the degradation byproducts), its integration with native cartilage is a serious concern, and one that has not yet been overcome (*Zhang et al., 2009*). In the effort to investigate alternative strategies, scaffold-free approaches have been developed as suitable modalities to engineer functional tissues ("scaffoldless" tissue engineering) (Fig. 5). Scaffold-free methods have been employed with success for musculoskeletal cartilages, such as articular cartilage, meniscus, temporomandibular joint disc and intervertebral disc, as they better mimic the condensation and differentiation stages that occur during the development of native cartilage (*DuRaine et al., 2014*). Within scaffold-free approaches, two distinct categories can be identified: self-organization methods, that include cell-sheet and aggregate engineering, and self-assembling methods (Fig. 5).

- **Cell sheet engineering** falls within the self-organization category of scaffold-free approaches as it requires external manipulation to form a desired structure. Cells are expanded to high confluence in order to form a cohesive layer (sheet), which is then lifted as a whole by temperature variations. The sheets are then further manipulated to stimulate ECM remodeling and tissue fusion, prior to transplantation in the organism. Regarding musculoskeletal cartilages, cell sheet engineering has been used to engineer neo-tissues with clinically relevant dimensions and properties. RevaFlex (ISTO Technologies) is a phase III clinical trial that involves the use of sheets of expanded juvenile allogeneic chondrocytes for the repair of articular cartilage (*McCormick et al., 2013*). Layered articular chondrocyte sheets have also been used to treat full-thickness cartilage defects in miniature pigs (*Sato et al., 2014*). Despite the encouraging results, cell-sheet engineering for cartilage repair has a number of limitations, such as chondrocytes de-differentation during monolayer expansion and technical hurdles encountered in maintaining a desired size and structure of the sheet or when producing thicker tissues of defined shapes. At the same time, the main advantage of this technique is the possibility to expand cells and form a cell sheet in a single step.

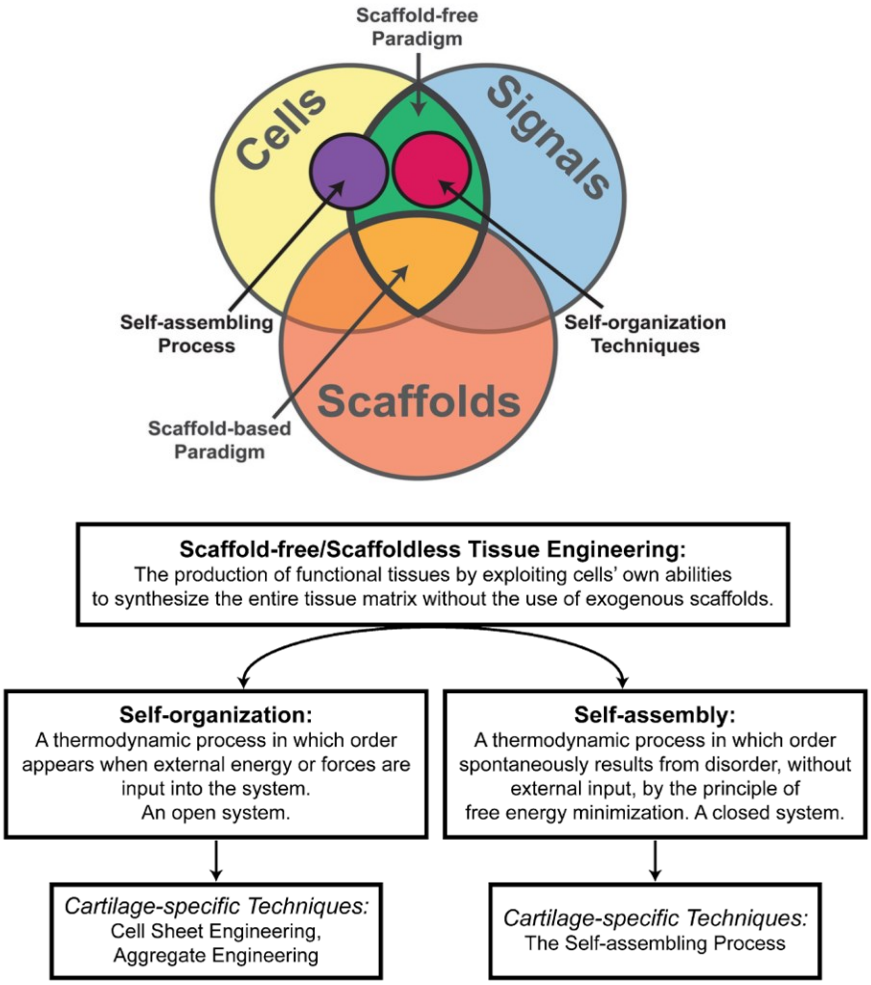

Figure 5. *Scaffoldless tissue engineering.* Traditionally, tissue engineering is based on an optimal combination of cells, scaffolds and signalling molecules. More recently, scaffold-free approaches based on the processes of self-organization or self-assembly have been proposed as well (*DuRaine et al., 2014*).

- **Cell aggregates** are commonly formed in culture by applying a rotational force to cells in a suspension or other non-adherent culture. Particularly relevant examples are rotational culture and pellet culture, where the rotational forces produced by the bioreactor or centrifuge, respectively, are directly responsible for the formation of cell aggregates. Rotational culture provides a better diffusion and nutrient/gas exchange compared to static cultures, making it an appealing tissue engineering strategy (*Furukawa et al., 2008*). Pellet culture is commonly used to chondrogenically (re-) differentiate chondrocytes and hMSCs, as this culture method is thought to mirror cell aggregation and matrix production that occur during the development of native cartilage (*Babur et al., 2013*). Commercial products based on aggregate tissue

engineering already exist, such as Chondrosphere® (co.don AG), which uses autologous cell aggregates/spheroids and is currently in phase III clinical trials in Europe (*Fickert et al., 2012*). In general, aggregate tissue engineering represents a versatile tool to form neo-cartilage, both indirectly by forming aggregates for cell differentiation and then dissociating them to form tissues by other methods, and directly by using aggregates to fill defects or assembling them into larger tissue structures. This culture method exhibits some drawbacks such as cell death before cell interaction and coalescence due to lack of substrate contact, or later on in the inner area of the construct. In addition, the cells in the construct cannot proliferate except under specific culture conditions and the constructs usually have uncontrolled and heterogeneous shapes.

- **Self-assembling processes** do not employ external forces to form tissues. To recapitulate the phases of cartilage development, a high-density cell suspension is seeded into a non-adherent mold to ensure that only cellular interactions will drive tissue assembly (*Mesallati et al., 2014*). In this way, cells will coalesce and produce tissue-specific ECM, that will eventually mature and form functional tissue. In contrast to aggregate cultures, self-assembling cartilages are of predictable and repeatable gross appearance, shape and size, as a predetermined number of cells is seeded into a mold with a defined shape. A number of study has shown that articular cartilage and fibrocartilages, such as meniscus and temporomandibular joint disc, can be engineered with physiologically relevant properties using the self-assembling processes (*DuRaine et al., 2014*). However, the cells need to produce large amounts of ECM and survive minimal cell-substrate interactions. Moreover, the self-assembling process requires cell numbers on the order of millions of cells per constructs, and therefore monolayer expansion and subsequent re-differentiation via rotational culture may be necessary. Finally, similarly to other tissue formation techniques, the size of the engineered tissue is limited by diffusion.

6. Novel trends in cartilage tissue engineering: the use of engineered chondrocytes and hMSCs

Preclinical and preliminary clinical studies have shown the benefits of transplanting progenitor cells in human cartilage defects, allowing for the formation of a durable cartilage-like repair tissue (see paragraph 4.2). Although different aspects, including the quality and mechanical features of the newly formed tissue, certainly needs to be improved, these encouraging data have laid a clinical basis for the experimental transplantation of genetically modified cells, as a valuable approach to exploit the full potential of the therapeutic cells (*Madry & Cucchiarini, 2011*). As a consequence, strategies using gene therapy in combination with tissue engineering have become very attractive for developing treatments that could enable durable restoration of joint tissues as cartilage when the degenerative processeses become irreversible. In 1996, Evans and co-workers proposed and implemented the idea of using genetically modified cells for the treatment of arthritis (*Evans et al., 1996*). It was shown that when retrovirally-transduced synovial cells were injected into the metacarpophalangeal joints of patients with rheumatoid arthritis, the active transgene product IL-1Ra was successfully expressed and biologically active (*Evans et al., 2005*). The study confirmed the feasibility of this approach and, since then, considerable progress has been made toward the understanding of the biological and technological requirements for a successful transplantation of genetically modified (or engineered) cells for tissue repair. Specifically, articular chondroctyes and, more recently, hMSCs have been genetically manipulated using viral or non-viral methods. The rationale of this strategy is that, when used in model systems of articular cartilage defects, the engineered cells may not only provide chondrogenic factors selectively stimulating the chondrogenic processes, but also exert specific paracrine effects inducing a regenerative response by the endogenous cell populations. Remarkably, "genetically-enhanced tissue engineering" is also a powerful tool for evaluating potential therapeutic genes, while improving the knowledge of the molecular mechanisms sustaining the degenerative processes of articular cartilage (*Madry & Cucchiarini, 2014*).

Both hMSCs and chondrocytes are permissive to transduction or transfection, and as such are excellent candidates for gene modification to enhance their chondrogenic phenotype and stimulate proliferation, avoiding detrimental cellular differentiation and senescence. hMSCs and chondrocytes have been successfully manipulated to stimulate anabolic pathways by the expression of growth factors and transcription factors, to repress the activation of catabolic pathways, or to address a combination of these effects (*Gurusinghe & Strappe, 2014*).

Viral approaches						
Model	**Gene**	**Method**	**Cells**	**Biomaterial**	**System**	**Ref.**
In vitro	IL-1Ra	Lentivirus	MSC	PCL scaffold	Resistance to inflammation challenge (IL-1)	*(a)*
In vitro	TGF-β	Lentivirus	MSC	PCL scaffold	Cartilage ECM formation	*(b)*
In vivo	Sox trio	Retrovirus	MSC	Fibrin glue	Healing and prevention of degenerative changes in surgically induced OA (rats)	*(c)*

Non-viral approaches								
Model	**Gene**	**Method**	**Cells**	**Biomaterial**	**Animal**	**Joint**	**Defect**	**Ref.**
In vivo	IGF-1	FuGENE 6	CC	Alginate	Rabbit	Knee (patellar groove)	Osteochondral	*(d)*
In vivo	IGF-1/2	FuGENE 6	NIH3T3	Alginate	Rabbit	Knee (patellar groove)	Osteochondral	*(e)*
In vivo	FGF-2	FuGENE 6	CC	Alginate	Rabbit	Knee (patellar groove)	Osteochondral	*(f)*
In vivo	GDF-5	FuGENE 6	MSC	Collagen 1	Rabbit	Knee (patellar groove)	Osteochondral	*(g)*
In vivo	BMP-7	Not reported	CC	Collagen/fibrin	Rabbit	Knee (patellar groove)	Osteochondral	*(h)*
In vivo	TGF-β	Lipofectamine	MSC	PLYS-coated PLA	Rabbit	Knee (patellar groove)	Osteochondral	*(i)*
In vivo	IGF-1	FuGENE 6	CC	PGA	Rabbit	Knee (patellar groove)	Osteochondral	*(j)*

Table 3. *Viral and non-viral approaches for cell manipulation in cartilage repair.* A list of representative studies using viral (top) or non-viral (bottom) approaches to obtain engineered chondrocytes or hMSCs with enhanced chondrogenic properties is reported (adapted from: *Cucchiarini & Madry, 2014; Madry & Cucchiarini, 2014*). References: *(a) Glass et al., 2014, (b) Brunger et al., 2014, (c) Lee et al., 2012, (d) Madry et al., 2005, (e) Orth et al., 2011, (f) Kaul et al., 2006, (g) Katayama et al., 2004, (h) Che et al., 2010, (i) Guo et al., 2006, (j) Madry et al., 2013.*

When planning the transplantation of engineered cells for tissue repair and regeneration, different strategies are possible. Cells are commonly transduced with viral vectors in order to induce a stable expression or silencing of specific molecules that positively affect the chondrogenic process, and some examples are reported (Table 3, top). A variety of viral vectors are available to achieve this goal, each of which has advantages and limitations depending on the biology of the viruses from which they are derived (*Cucchiarini & Madry, 2014*). While most of the viral vectors have been used successfully to transduce the cell populations relevant to the pathogenesis of OA in experimental systems *in vitro*, thus far, only recombinant adeno-associated (rAAV) vectors proved capable of modifying the

cells *in situ*, when they were located in their natural ECM environment. The rAAV vectors are currently the most potent gene delivery vehicles, as they can efficiently and durably transduce articular chondrocytes, hMSCs, synoviocytes and other relevant cell sources constituting the surrounding tissues of cartilage, compared with the relatively less efficient non-viral vectors, the more immunogenic adenoviral vectors, and the retroviral vectors that not only require division and pre-selection of the target cells but also have the ability to integrate into the host genome (*Madry & Cucchiarini, 2011*). In contrast with the literature on focal cartilage defects, few studies have examined the benefits of applying transduced cells combined with a biocompatible scaffold for the treatment of experimentally induced OA. To date, only one study has demonstrated the benefits of injecting hMSCs that had been co-transduced with the Sox trio and combined with fibrin glue to prevent the progression of surgically induced OA in rats (*Lee & Im, 2012*). Indeed, therapeutic approaches for OA *in vivo* have mostly focused on the administration of gene transfer vectors and genetically modified cells in the absence of scaffold matrixes. Nevertheless, there is a large body of evidence showing the benefits of gene therapy for OA, including two clinical trials of administration of TGF-β expressing chondrocytes (*Ha et al., 2012*) and direct delivery of IL-1Ra via rAAV (*Evans et al., 2013*).

Due to the many issues raised by the use of viral methods, virus-free approaches of transient transfection are being widely explored as well (Table 3, bottom). This choice may be convenient not only for safety-related aspects, but also when it is conceivable that the engineered cells might have a less invasive, priming effect on the regeneration process, by triggering the repair mechanisms, as well as stimulating an active and progressive involvement of the host tissues in the repair of the defect (*Abdul Halim et al., 2014*). At the same time, the novel technologies allowing the cultivation of the transfected cells in a 3D microenvironment have greatly increased the duration of transgene expression, which is a well known drawback of transient transfection-based approaches. Among the most relevant examples of gene candidates for non-viral approaches are growth factors, such as insulin-like growth factors (IGFs), fibroblast growth factors (FGFs), bone morphogenetic proteins (BMPs) and transforming growth factors (TGFs), to stimulate anabolic pathways that enhance cell proliferation, differentiation and synthesis of ECM. Madry and co-workers showed that the transplantation of non-virally engineered articular chondrocytes overexpressing IGF-1 into osteochondral defects in rabbits determined enhanced cartilage repair and integration *in vivo* (*Madry et al., 2013*). In another study, the transplantation of TGF-β1-transfected hMSCs into osteochondral defects *in vivo* was associated with improved quality of the cartilage repair tissue (*Guo et al., 2007*). Other important gene

candidates include transcription factors, anti-angiogenic factors, and inhibitors of the catabolic pathways (*Madry & Cucchiarini, 2014*). Bone marrow-derived hMSCs were transfected with a plasmid vector encoding for the master chondrogenic regulator Sox9, and consequently exhibited enhanced chondrogenesis *in vitro* and massive formation of cartilage-like tissue after transplantation into athymic mice (*Tsuchiya et al., 2003*). Another recent study showed that non-viral delivery of the Sox9 gene promoted the chondrogenic differentiation of umbilical cord blood-derived hMSCs (*Wang et al., 2014*). Transfection of primary chondrocytes with a single plasmid encoding IGF-1 and the anti-catabolic cytokine IL-4 suppressed inflammation while promoting cartilage synthesis in an experimental inflammatory model (*Manning et al., 2010*).

Taken together, the current literature highlights the great progress that has been made in developing approaches for the transplantation of genetically modified chondrocytes and hMSCs as a feasible therapeutic option for cartilage repair. Firstly, it is well established that chondrocytes and hMSCs can be conveniently modified using a variety of viral and non-viral approaches and thereafter transplanted into articular cartilage defects *in vivo*, allowing for sustained and clinically relevant effects. Secondly, preclinical studies have shown that the overexpression or silencing of critical factors is effective in enhancing the structural features of the repair tissue of the articular cartilage and subchondral bone, being superior to unmodified cells (*Madry & Cucchiarini, 2011*). It is to be highlighted that there is an urgent need of further efforts in the field, as there is still a scarcity of experimental studies with transplantation of modified cells in models of OA *in vivo*, especially in relation to the use of large animal models.

7. The role of microRNAs in chondrogenesis: chondro-regulatory miRNAs

MicroRNA (miRNAs) are single stranded non-coding RNAs, comprised of 18–22 nucleotides, that are critical in genetic regulation, cell differentiation, development, and pathogenesis. Over the last few years, a plethora of chondro-regulatory miRNAs (chondro-miRs) has been characterized (*Barter et al., 2015*). It has gradually become clear that miRNAs are of paramount importance in the regulation of developmental chondrogenic signalling pathways, chondrocytes growth, senescence, apoptosis and differentiation, and cartilage homeostasis in general (Table 4). Specifically, several microRNAs are involved in the regulation of the different phases of the chondrogenic process, as they target the transcription factors and cytokines that guide the differentiation of the chondro-progenitors.

Cell types	microRNAs	Target genes	Function	Reference
SSCs	miR-146a	SMAD2, SMAD3	N	*(a)*
SFMSCs	miR-23b	PRKACB	P	*(b)*
MSCs	miR-29a	/	N	*(c)*
MSCs	miR-574	Sox9	N	*(d)*
MSCs	miR-375	Cadherin-7	N	*(e)*
MSCs	miR-181b	/	N	*(f)*
MSCs	miR-34a	EphA5	N	*(g)*
MSCs	miR-142	/	N	*(h)*
MSCs	miR-488	/	N	*(i)*
MSCs	miR-221	Mdm2	N	*(j)*
mMSCs	miR-335	ROCK1, Daam1	P	*(k)*
hMSCs	miR-221	/	N	*(l)*
hMSCs	miR-495	Sox9	N	*(m)*
hMSCs	miR-140	RALA	P	*(n)*
hMSCs	miR-10a	KLF4	P	*(o)*
hMSCs	miR-23b	/	P	*(p)*
hMSCs	miR-199a	/	P	*(q)*
hASCs	miR-194	Sox5	N	*(r)*
eCB-MSCs	miR-140	/	P	*(s)*
C3H10T1/2	miR-145	Sox9	N	*(t)*
C3H10T1/2	miR-199a	Smad1	N	*(u)*
articular chondrocytes	miR-558	COX-2	N	*(v)*

Table 4. *Relevant microRNAs related with chondrogenic differentiation.* P = positive effect for chondrocyte differentiation, N = negative effect for chondrocyte differentiation (adapted from: *Chen et al., 2015a*). References: *(a) Cheung et al., 2014, (b) Ham et al., 2014, (c) Guerit et al., 2014, (d) Guerit et al., 2013, (e) Song et al., 2013a, (f) Song et al., 2013b, (g) Kim et al., 2011a, (h) Kim et al., 2011b, (i) Song et al., 2011, (j) Kim et al., 2010, (k) Lin et al., 2014, (l) Lolli et al., 2014, (m) Lee et al., 2014, (n) Karlsen et al., 2014, (o) Li et al., 2013, (p) Ham et al., 2012, (q) Laine et al., 2012, (r) Xu et al., 2012, (s) Buechli et al., 2013, (t) Yang et al., 2011, (u) Lin et al., 2009, (v) Park et al., 2013.*

Accordingly, global reduction of miRNA in chondrocytes by using chondrocyte-specific deletion of Dicer, the essential component for miRNA biogenesis, causes severe skeletal growth defects and premature death of mice (*Hong and Reddi, 2012*). Conditional knockout of Dicer in limb mesenchyme leads to the formation of a smaller limb, while Dicer-null growth plates display a lack of chondrocyte proliferation with enhanced differentiation to post-mitotic hypertrophic chondrocytes (*Le et al., 2013*).

This evidence supports a critical role of miRNAs in maintaining proliferating chondrocytes and inhibiting premature differentiation into hypertrophic chondrocytes in the growth plate, eventually affecting skeletal development. Notably, the emerging body of evidence provided by several studies demonstrates that the intervention of chondro-miRs is tightly connected to every stage of the chondrogenic process, from the mesenchymal condensation to the terminal differentiation of chondrocytes and cartilage calcification (Fig. 6).

The following are some relevant examples of the involvement of specific chondro-miRs in the regulation of the differentiation process. Lin and co-workers demonstrated that the chondrogenesis of C3H10T1/2 stem cells induced by BMP-2 was repressed by the forced expression of miR-199a, with decreased expression of collagen type II, cartilage oligomeric matrix protein (COMP) and Sox9, by targeting Smad1 (*Lin et al., 2009*). On the contrary, miR-675 was shown to up-regulate collagen type II in human articular chondrocytes, and overexpression of miR-675 rescued collagen type II levels in Sox9-depleted cells (*Dudek et al., 2010*). miR-145 is a very relevant microRNA in chondrogenesis, as it has been shown to target Sox9 mRNA directly, resulting in a decrease in cartilage matrix proteins. Accordingly, inhibition of miR-145 was shown to result in elevated expression of Sox9 downstream targets, such as collagen type II, aggrecan and COMP, and enhanced the chondrogenic phenotype in human articular chondrocytes (*Martinez-Sanchez et al., 2012*). Highly specific to cartilage tissue, miR-140 has been extensively studied for its ability to inhibit the expression of chemokine (C-X-C motif) ligand 12 (CXCL12) and A disintegrin and metalloproteinase with thrombospondin motifs 5 (ADAMTS-5) that lead to degradation of articular cartilage in OA (*Buechli et al., 2013*). *In vivo* expression of miR-140 in transgenic mice with the transcript driven by the Col2A1 promoter has shown specific articular cartilage matrix expression and resistance to arthritis. Accordingly, miR-140 knockout mice showed grossly normal skeletal development, but developed age-related OA-like changes, supporting the role of miR-140 in maintaining cartilage tissue homeostasis. Different microRNAs are deeply involved in the regulation of the progression of chondrocytes towards the hypertrophic and terminal stages of differentiation, that anticipate cartilage instability and calcification (*Wu et al., 2014*). miR-1 is the most repressed miRNA following chondrocyte hypertrophy and negatively regulates the expression of aggrecan, although its direct target remains unknown, therefore exerting a role in the maintenance of the integrity of the cartilage tissue.

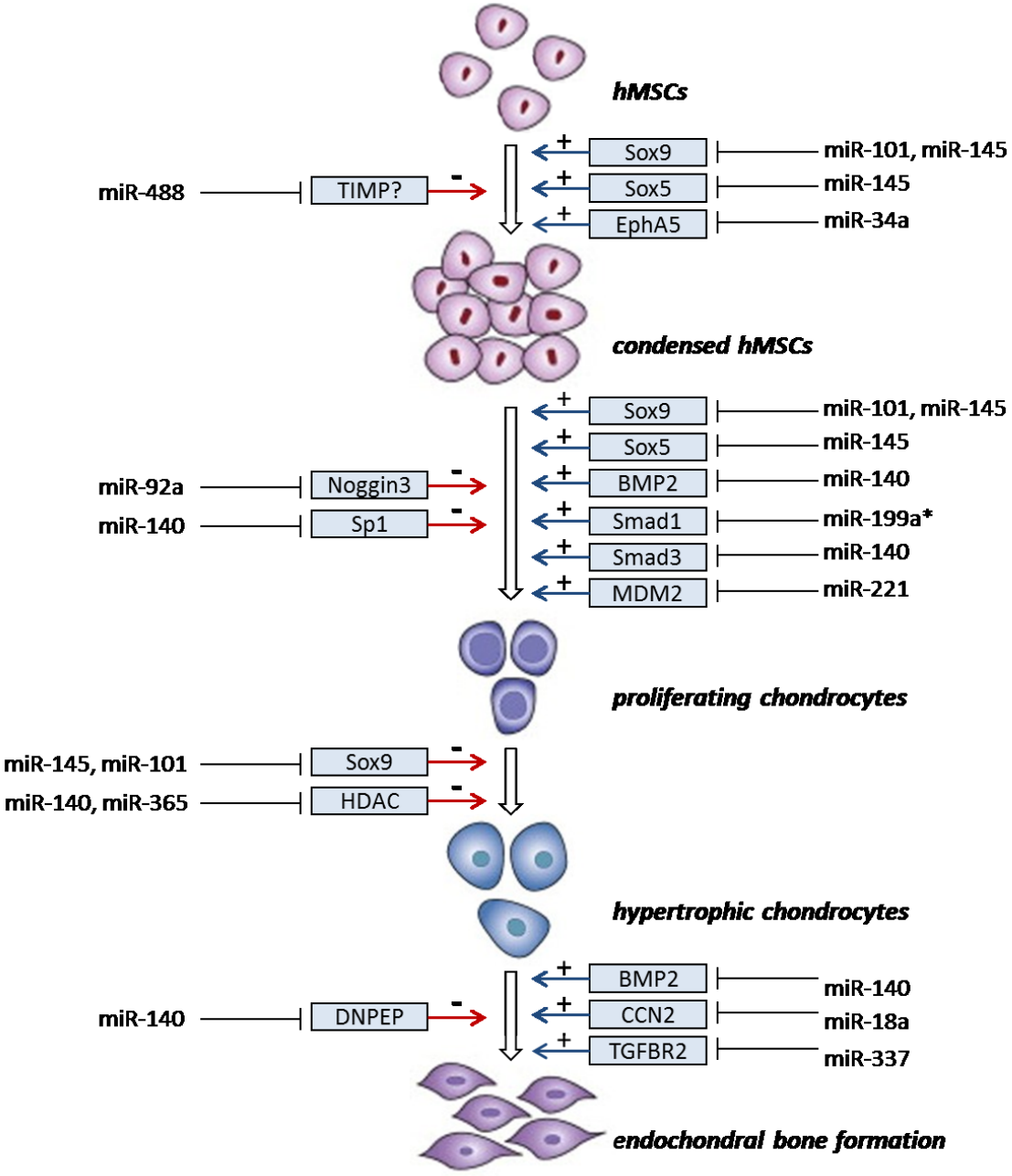

Figure 6. *Influence of microRNAs on the regulation of chondrogenesis.* Specific microRNAs are responsible for the fine-tuning of the expression of key chondro-regulatory molecules (such as transcription factors) that, in turn, tightly control every step of the chondrogenic process (adapted from: *Wu et al., 2014*).

miR-365 is a mechano-responsive microRNA that is highly expressed in the pre-hypertrophic zone to stimulate chondrocyte proliferation and differentiation into hypertrophic cells.Accordingly, miR-365 increases the expression of indian hedgehog (Ihh) and the hypertrophic marker collagen type X, while inhibition of miR-365 blocks the expression of these genes. The expression of miR-337 is strongly downregulated and

almost disappears during the maturation phases of endochondral ossification. Moreover it was found to directly target the TGF-β2 receptor (TGFBR2), that is deeply involved in cartilage development and maturation (*Wu et al., 2014*). As well as being involved in the regulation of chondrogenesis and maturation of articular cartilage, miRNAs also represent relevant targets for cartilage-related diseases and especially OA, as the chondrocyte phenotype and cartilage homeostasis are profoundly affected by the disease (*Hong & Reddi, 2012*). A number of miRNAs, such as miR-140, miR-27b, miR-145, miR-101 and miR-23b, are differentially expressed in osteoarthritic tissues, where they exert a protective or destructive role in relation to the progression of the disease (*Mirzamohammadi et al., 2014*). Accordingly, the manipulation of OA-specific miRNAs has proved to be a feasible strategy to target the pathogenetic mechanisms and therefore slow down the degeneration of the articular tissue, *in vitro* and *in vivo*.

The aforementioned studies represent only a small portion of the wide literature on the involvement of microRNAs in cartilage pathobiology, which has recently pushed research towards the integration of hMSCs-based tissue engineering and miRNAs gene therapy. Nonetheless, the effective application of miRNAs biology in tissue engineering to enhance cell differentiation and tissue regeneration has just begun to bring promising outcomes and much more effort is therefore needed to fully exploit the therapeutic potential of microRNAs for cartilage repair.

Chapter 2

Characterization of novel chondro-regulatory factors: miR-221 and Slug

Outline of the work

In the field of hMSCs-based cartilage tissue engineering there is a need for novel tools to induce reproducible and stable chondrogenesis of the cells, thereby allowing to exploit their full therapeutic potential. In this context, much effort is put into characterizing the differentiation process at a molecular level and identifying novel regulatory circuits that may be targeted to optimize the chondrogenic properties of hMSCs. The experimental work of this section of the project was aimed at elucidating the role of two cell regulators that only recently have been proposed as anti-chondrogenic factors, the microRNA-221 (miR-221) and the zinc-finger transcription factor (TF) Slug. Besides, it was investigated whether the depletion of these molecules by gene silencing techniques could represent a feasible strategy to address hMSCs towards chondrogenesis in the absence of conventional chondrogenic inducers, such as TGF-β. We showed that miR-221 or Slug knockdown in monolayered Wharton's jelly hMSCs was sufficient to induce the expression of chondrogenic ECM proteins, such as collagen type II, and transcription factors, such as Sox9 and TRPS1, in the absence of external cues. Interestingly, the data obtained from gene expression and chromatin immunoprecipitation analysis provided evidence of a novel Slug/miR-221/TRPS1 regulatory circuit that appears to be critical for chondrogenic differentiation. It is therefore conceivable that adequate variations in the expression levels and specific interactions between these chondro-regulatory factors are involved and required for the chondrogenesis of hMSCs. Altogether, our experimental data were relevant both to elucidate yet unidentified regulatory loops with TFs and microRNAs in cartilage biology, and to propose new strategies based on the gene silencing approach for cartilage tissue engineering.

Introduction

The use of hMSCs in the field of tissue engineering for cartilage repair is a very promising tool since these cells are readily expandable and able to differentiate into chondrocytes (*Caplan, 2007; Arthur et al., 2009; Vinatier et al., 2009b*). However, the *in vitro* manipulation of these cells for the production of an implantable construct for cartilage defect healing still presents many challenges. In this regard, several studies are aimed at the development of alternative protocols to obtain chondrogenically differentiated hMSCs with the ability to express the typical proteins required for optimal *in vivo* chondrogenesis. hMSCs proliferation and differentiation are strongly influenced both by exogenous factors present in the culture medium and by intrinsic cell properties, namely the molecular signature of the cells. These aspects need to be taken into account in establishing an appropriate strategy to improve the cell chondrogenic potential and for the maintenance of a chondrocyte-like phenotype that resembles the cells of the articular cartilage (*Vinatier et al., 2009b; Barzilay et al., 2009; Palmer et al., 2005; Oldershaw, 2012; de Crombrugghe et al., 2001; Steinert et al., 2007; Roobrouck et al., 2011*). In an attempt to understand what makes the cells more prone to chondrogenic differentiation and, at the same time, elucidate the network of molecular mechanisms involved in the fate of the osteochondroprogenitors, we adopted the manipulation of gene expression via the siRNA mechanism (*Caplen, 2004; Cheema et al., 2007*). This technology, which turns off a target gene by specific small interfering RNA, is emerging as a powerful tool to drive tissue regeneration through the possibility to control the expression of activators or inhibitors of a specific pathway. At the same time, the gene silencing approach may allow us to better characterize the role of specific genes during a cell differentiation program. Therefore, it is intriguing to use such an approach to guide hMSCs differentiation toward a specific lineage without the addition of differentiating agents.

In order to explore new strategies for the manipulation of hMSCs phenotype and *in vitro* chondrogenic differentiation, we focused on the effects of the downregulation of two negative regulators of chondrogenesis, Slug (SNAI2) transcription factor (TF) and a small non-coding single stranded RNA, miR-221 (*Cobaleda et al., 2007; Garofalo et al., 2012; Seki et al., 2003; Goldring et al., 2006; Kim et al., 2010; Bakhshandeh et al., 2012; Karlsen et al., 2011*). Our interest was to investigate whether the abrogation of the negative role of these molecules could be effective in inducing the chondrogenic differentiation of hMSCs without additional chondrogenic inducers, such as the transforming growth factor β (TGF-β) (*de Crombrugghe et al., 2001*). Slug is a member of the Snail family of zinc-finger transcription factors, which controls key aspects of stem cell function during

development and maintenance of the mesenchymal phenotype (*Cobaleda et al., 2007; Hemavathy et al., 2000*). Slug expression was shown to decrease during chondrogenic differentiation in different experimental models (*Seki et al., 2003; Goldring et al., 2006*). In regards to miR-221, recent studies proposed an involvement of this microRNA in the chondrogenic process, demonstrating, for instance, a reduction of its expression during the chondrogenesis of chick limb mesenchymal cells (*Kim et al., 2010*) and human unrestricted somatic stem cells (USSCs) (*Bakhshandeh et al., 2012*), or an increase in de-differentiated chondrocytes (*Karlsen et al., 2011*). Therefore, our study aimed to the production of hMSCs depleted of negative regulators to be used in cell-based tissue engineering strategies to promote cartilage regeneration. We anticipated that knockdown of Slug or miR-221 could promote an early onset of chondrogenic markers and optimize hMSCs chondrogenesis. Furthermore, since the study of miRNAs–TFs regulatory loops in cartilage biology is just in its infancy (*Karlsen et al., 2011; Hemavathy et al., 2000; Gordeladze et al., 2009; Yang et al., 2011; Hong & Reddi, 2012*), we can take advantage of investigating the characteristics of miR-221- or Slug-silenced hMSCs to study possible correlations between miR-221, Slug, and positive chondrogenic regulators (*Goldring et al., 2006*) such as Sox9, the master regulator of chondrogenesis, and tricho-rhino-phalangeal syndrome type 1 factor (TRPS1), a regulator of chondrocyte proliferation and differentiation.

Materials and Methods

hMSCs cultures

Human umbilical cords (all from natural deliveries) were collected after mothers' consent and approval of the Ethics Committee of the University of Ferrara and S. Anna Hospital. Harvesting procedures of Wharton's jelly from umbilical cord were conducted in full accordance with the Declaration of Helsinki as adopted by the 18th World Medical Assembly in 1964 and successively revised in Edinburgh (2000) and the Good Clinical Practice guidelines. Cords were processed within 4 h and stored in sterile saline until use (*Penolazzi et al., 2010*). Typically, the cord was rinsed several times with sterile phosphate-buffered saline (PBS) before processing and was cut into pieces (2-4 cm in length). Blood and clots were drained from vessels with PBS to avoid any contamination. Single pieces were dissected, after separating the epithelium of each section along its length, to expose the underlying Wharton's jelly. Later, cord vessels (the two arteries and the vein) were pulled away without opening them. The soft gel tissue was then finely

chopped. The same tissue (2-3 mm^2 pieces) was placed directly into a 75 cm^2 flask for culture expansion in 10% Fetal Calf Serum (Euroclone S.p.A., Milan, Italy) Dulbecco's Modified Eagle's Medium (DMEM) low-glucose supplemented with antibiotics (penicillin 100 μg/mL and streptomycin 10 μg/mL), at 37°C in a humidified atmosphere of 5% CO_2. After 5-7 days, the culture medium was removed and then refreshed twice a week. At 70-80% confluence, cells were scraped off by 0.05% trypsin-ethylenediaminetetraaceticacid (EDTA) (Gibco, Grand Island, NE), washed, counted by hemocytometric analysis, assayed for viability, and used thereafter for further *in vitro* experiments (see Fig. S1 for details).

Chondrocyte cultures

Cartilage fragments from nasal septum were obtained from 25 to 60 years old donors that underwent septoplasty surgery procedures after informed consent and approval of the Ethics Committee of the University of Ferrara and S. Anna Hospital. With nasal septum we have the access to abundant healthy tissue by a procedure that is less invasive than removing tissue from specific areas of the joint. It has been recently demonstrated that nasal cartilage exhibits hyaline features and contains differentiated chondrocytes expressing the typical collagens of articular cartilage (*Wachsmuth et al., 2006*). Recent papers revealed that human nasal chondrocytes cultured in a 3D-scaffold were responsive to different physical forces typical of a joint (*Candrian et al., 2008*), and were more potent for cartilage regeneration after subcutaneous implantation (*Pleumeekers et al., 2014*), validating the possibility of using this cell source for articular cartilage repair. Briefly, cartilage fragments were minced into small pieces and rapidly incubated with type VIII Collagenase (Sigma-Aldrich Chemical Co., St. Louis, MO) at 37°C for 16 h (*do Amaral et al., 2012*). Cells were harvested by centrifugation and plated (p0) in 25 cm^2 tissue culture flasks or 8-well culture slides in 50% DMEM high-glucose / 50% DMEM F-12 / 10% Fetal Calf Serum (Euroclone S.p.A., Milan, Italy) supplemented with antibiotics (penicillin 100 μg/mL and streptomycin 10 μg/mL), at 37°C in a humidified atmosphere of 5% CO_2. After 7 days, the culture medium was removed and then refreshed twice a week. At 70-80% confluence, cells were scraped off in 0.05% EDTA (Gibco, Grand Island, NE), washed, plated and allowed to proliferate in standard conditions (50% DMEM high-glucose / 50% DMEM F-12 / 10% Fetal Calf Serum) in order to induce chondrocyte dedifferentiation (until p3).

Flow cytometric analysis

hMSCs from Wharton's jelly were analyzed for the expression of mesenchymal and hematopoietic surface marker molecules, by direct immunofluorescent staining, as previously reported (*Penolazzi et al., 2010*). Briefly, cell pellets were resuspended in PBS and incubated with fluorescein isothiocyanate (FITC)– or phycoerythrin (PE)–conjugated mouse anti-human antibodies CD29-PE, CD34-FITC, CD44-FITC, CD45-PE, CD90-FITC and CD105-PE (DakoCytomation; Dako, Glostrup, Denmark) for 15 min at 4°C. Monoclonal antibodies with no specificity were used as negative control. Antibody-treated cells were then washed with PBS and spinned down. Cell pellets were resuspended in 400 μL of PBS and analyzed by FACS Scan (Becton Dickinson, Franklin Lakes, NJ). For each sample, 20,000 events were acquired and analyzed using the CellQuest software (Becton Dickinson European HQ, ErembodegemAalst, Belgium). The same procedure was used for human chondrocytes at different culture passages (freshly isolated and p3) that were analyzed for the following surface marker molecules: CD14-FITC, CD44-PE, CD73-PE, and CD146-FITC (Becton Dickinson, Franklin Lakes, NJ).

Chondrogenic differentiation of hMSCs

For the induction of chondrogenesis, 2.5 x 10^5 hMSCs (passage 1-3) were seeded in 15 ml polypropylene conical tube and centrifuged to form a 3D-pellet. The supernatant was removed and replaced with chondrogenic inductive media (DMEM high-glucose supplemented with ITS+Premix: 6.25 μg/ml insulin, 6.25 μg/ml transferrin, 5.33 μg/ml linoleic acid and 1.25 μg/ml bovine serum albumin, 100 nM dexamethasone, 50 μg/ml ascorbate-2 phosphate, 1 μM sodium pyruvate, 100 μg/mL penicillin and 10 μg/mL streptomycin) (Sigma, Saint Louis, MO, USA) in the presence of TGF-β3 (10 ng/ml) (Mylteny, Bergisch, Gladbach, Germany). Pellet cultures were maintained at 37°C, 5% CO_2 for 21 days and the medium was refreshed twice a week.

Alcian Blue staining

Glycosaminoglycans (GAGs) accumulation in cultured chondrocytes was assessed by Alcian Blue staining. Cells were rinsed with PBS and fixed in 10% formaldehyde in PBS for 10 min. Cultures were then stained with Alcian Blue pH 2 (1% in 3% acetic acid) (Sigma-Aldrich Chemical Co., St. Louis, MO) overnight at 37°C. The day after, cells were washed with water and observed using a Leitz microscope.

Gene silencing and transfections

hMSCs were transfected with 30 nM antagomiR-221 (Ambion Life Technologies, Grand Island, NY), 30 nM siRNA against Slug (si-Slug) (Invitrogen, Carlsbad, CA), a non-relevant antagomiR (antagomiR-Scr) (Ambion Life Technologies, Grand Island, NY) or a non-relevant siRNA (si-Scr) (Medium GC Stealth RNAi Negative Control Duplex, Invitrogen) (*Lambertini et al., 2009*). For all transfections, Lipofectamine RNAiMAX (Invitrogen, Carlsbad, CA) was used, following the manufacturer's instructions. Briefly, cells were plated the day before transfection in 24-well plates or 8-well culture slides (BD Falcon, Bedford, MA) and transfected twice a week. The transfected cells were grown up to 14 days at 37°C in a humidified atmosphere of 5% CO_2. For hTRPS1 overexpression, hMSCs were transfected with 0.4 μg/cm^2 of pBlight-FLAG-TRPS1 expression vector or with the empty vector (Genentech, San Francisco, USA) for 48 h. Then, total RNA was extracted and stored at -80°C for subsequent quantitative RT-PCR analysis. For immunocytochemical analysis, cells were fixed with methanol and analyzed as indicated below.

Cell viability and proliferation

Viability assay was performed as previously described (*Candrian et al., 2006; Pleumeekers et al., 2014*). For propidium iodide and calcein analysis, cells were visualized under a fluorescence microscope (Nikon, Optiphot-2, Nikon corporation, Japan) using the filter block for fluorescein. Dead cells were stained in red, whereas viable ones appeared in green. The proliferation rate of hMSCs was determined by using the AlamarBlueTM assay (Invitrogen Corporation, Carlsbad, CA). The test is based on the metabolic activity of proliferating cells that results in a chemical reduction of AlamarBlue reagent, previously added to the *in vitro* cultured cells. Briefly, at sequential time points medium containing 5% AlamarBlue was added to the transfected cells, at 37°C and 5% CO_2. After 4 h of incubation, 200 μL samples of culture medium were withdrawn, centrifuged, and subsequently placed on 96-well plates. The visible light absorption of the collected samples was determined at 570 and 620 nm by a Microplate Absorbance Reader (Sunrise, Tecan, Austria). Final values were calculated as the difference in absorbance units between the reduced and oxidized forms of AlamarBlue.

RNA isolation

Total RNA, including the miRNA fraction, was extracted from hMSCs or chondrocytes using the RNeasy Plus Micro Kit (Qiagen, Hilden, Germany), according to the manufacturer's instructions. Total RNA was used for reverse-transcription and stored at -80°C. Briefly, cDNA was synthesized from total RNA (500 ng) in a 20 µl reaction volume using the TaqMan High Capacity cDNA or MicroRNA Reverse Transcription kit (Applied Biosystems) as previously described (*Lambertini et al., 2012*).

Quantitative Real-Time PCR for miRNA and mRNA quantification

Quantification of miR-221 was performed using the TaqMan MicroRNA Assay (Applied Biosystems), followed by detection with the CFX96TM PCR detection system (Bio-Rad, Hercules, CA). The TaqMan MicroRNA Assay for U6 small nuclear RNA (RNUB6) (assay ID: 001973; Applied Biosystems) was used to normalize the relative abundance of miR-221. For the quantification of Slug, Col1A1, Col2A1, Sox9, and TRPS1 mRNA, the appropriate TaqMan probes were purchased from Applied Biosystems (see supplementary Table 1), using glyceraldehyde 3-phosphate dehydrogenase (GAPDH) gene for normalization.

Immunocytochemistry

Immunocytochemical analysis was performed employing the ImmPRESS reagent kit (Vectorlabs, Burlingame, CA). Cells grown in chamber slides were fixed in cold 100% methanol and permeabilized with 0.2% (v/v) Triton X-100 (Sigma-Aldrich Chemical Co., St. Louis, MO) in TBS (Tris-buffered saline). Cells were treated with 0.3% H_2O_2 in TBS, and incubated in 2% normal horse serum (Vectorlabs, Burlingame, CA) for 15 min at room temperature. After the incubation in blocking serum, the different primary antibodies were added and incubated at 4°C overnight: polyclonal antibodies for Col1A1 (rabbit anti-human, 1:200 dilution, Santa Cruz Biotechnology, CA), Col2A1 (mouse anti-human, 1:200 dilution, Abcam, Cambridge, UK), Aggrecan (mouse anti-human, 1:200 dilution, Santa Cruz Biotechnology, CA), Sox9 (rabbit anti-human, Santa Cruz Biotechnology, CA), Slug (rabbit anti-human, 1:400 dilution, Santa Cruz Biotechnology, CA), and TRPS1 (rabbit anti-human, 1:200 dilution, Abcam, Cambridge, UK). Cells were then incubated in Vecstain ABC reagent (Vectorlabs, Burlingame, CA) for 30 min and stained with DAB solution (Vectorlabs, Burlingame, CA). After washing, cells were mounted in glycerol/TBS 9:1 and observed using a Leitz microscope. Quantitative image analysis of immunostained cells was obtained by a computerized video-camera–based image analysis

system (with NIH, USA ImageJ software, public domain available at: http://rsb.info.nih.gov/nih-image/) under brightfield microscopy. Images were grabbed with single stain, without carrying out nuclear counterstaining with hematoxylin. Therefore, in this case colour vector is pure and contains no contribution of other dyes and colour deconvolution of the acquired images wasn't compulsory. Unaltered TIFF images were digitized and converted to black and white picture to evaluate the distribution of relative gray values (i.e. number of pixels in the image as a function of gray value 0–256), which reflected chromogen stain intensity. Images were then segmented using a consistent arbitrary threshold 50% to avoid a floor or ceiling effect, and binarized (black versus white); total black pixels per field were counted and average values were calculated for each sample. Three replicate samples and four fields per replicate were subjected to densitometric analysis. We performed a quantification of pixels per 100 cells and not per area in order to take into account that, as reported in the text, antagomiR-221 and si-Slug treatment slightly affected cell confluence.

Western blotting

For western blot analysis, the cells were washed twice with ice cold PBS and cell lysates were prepared as previously reported (*Lambertini et al., 2009*). Then, 20 μg of each sample were electrophoresed on a 12% SDS-polyacrylamide gel. The proteins were then transferred onto an Immobilon-P PVDF membrane (Millipore, Billerica, MA). After blocking with PBS-0.05% Tween 20 and 5% nonfat dried milk, the membrane was probed with the following antibodies: Slug (mouse anti-human, 1:1000 dilution, Santa Cruz Biotechnology, CA) and actin (mouse anti-human, 1:5000 dilution, Santa Cruz Biotechnology, CA). After washing with PBS-Tween, the membranes were incubated with peroxidase-conjugated anti-mouse (1:2000) (Dako, Glostrup, Denmark) in 5% non-fat dried milk. Immunocomplexes were detected using Supersignal West Femto Substrate (Pierce, Rockford, IL). Actin was used to confirm equal protein loading.

Histological analysis

Cell pellets were rinsed with phosphate buffered solution (PBS), fixed in 4% buffered paraformaldeyde for 24 h at 4°C, embedded in paraffin and cross-sectioned (5-μm thick). For histological evaluation, sections were stained with Alcian blue (Sigma-Aldrich Co., St. Louis, MO) to assess sulphated GAGs content. Furthermore, non-consecutive sections were immunostained with monoclonal antibodies against Col2A1 (Abcam, Cambridge, UK), Sox9, and Slug (Santa Cruz Biotechnology, CA). To this aim, immunohistochemical

sections were deparaffinized, rehydrated, and enzymatically treated with 10 ng/ml of proteinase K, followed by Tris-EDTA high temperature buffer treatment for antigen retrieval. Slides were then processed with 0.3% H_2O_2 in PBS 1X for 5 min and with 2% normal horse serum (Vectorlabs, Burlingame, CA) for 15 min at room temperature. Then the slides were incubated for 1 h with the primary antibody at room temperature, followed by treatment with Vecstain ABC reagent (Vectorlabs, Burlingame, CA) for 30 min. The reactions were developed using DAB solution (Vectorlabs, Burlingame, CA), counterstained with hematoxylin and mounted in glycerol. The sections were observed using a Leitz microscope.

Chromatin Immunoprecipitation (ChIP) assay

Chromatin Immunoprecipitation (ChIP) assays were performed with the ChIP assay kit (Upstate Biotechnology, Lake Placid, NY) as previously described (*Lambertini et al., 2012*). Briefly, hMSCs and p0 chondrocytes were cross-linked with 1% formaldehyde at 37°C for 10 min. The cells were washed in ice-cold PBS, and resuspended in SDS lysis buffer supplemented with 1X protease inhibitor cocktail (Roche Molecular Biochemicals) for 10 min on ice. Samples were sonicated, diluted 10-fold in dilution buffer, and precleared with 80 µl of salmon sperm DNA-coated protein A-agarose beads. The supernatant was used directly for immunoprecipitation with anti-Slug, anti-TRPS1, and anti-acetyl-H3 (Santa Cruz Biotechnology, CA) overnight at 4°C. Immunocomplexes were mixed with 80 µl of DNA-coated protein A-agarose beads followed by incubation for 1 h at 4°C. Beads were collected and sequentially washed 3 times with 1 ml each of the following buffers: low salt wash buffer (0.1% SDS, 1% Triton X-100, 2 mM EDTA, 20 mM Tris-HCl pH 8.1, 150 mM NaCl), high salt wash buffer (0.1% SDS, 1% Triton X-100, 2 mM EDTA, 20 mM Tris-HCl pH 8.1, 500 mM NaCl), LiCl wash buffer (0.25 mM LiCl, 1% IGEPAL-CA630, 1% deoxycholic acid, 1 mM EDTA, 10 mM Tris pH 8.1), and TE buffer. The immunocomplexes were eluted twice by adding a 250 µl aliquot of a freshly prepared solution of 1% SDS, 0.1 M $NaHCO_3$ and the crosslinking reactions were reversed by incubation at 65°C for 4 h. The samples were then digested with proteinase K (10 mg/ml) at 42°C for 1 h and DNA was purified in 50 µL of Tris-EDTA with a PCR purification kit (Qiagen, Valencia, CA) according to the manufacturer's instructions. For PCR analysis, aliquots of chromatin before immunoprecipitation were saved (Input). PCR was performed by using specific primers to amplify different regions of the miR-221 promoter. Each PCR reaction was performed with 5 µl of the bound DNA fraction or 2 µl of the Input. The PCR was performed as follows: pre-incubation at 95°C for 5 min, 30

cycles of 1 min denaturation at 95°C, 1 min annealing at the primers temperature, and 1 min at 72°C. No-antibody negative control was included in each experiment.

Statistical Analysis

Statistical significance was determined by one-way analysis of variance (ANOVA) and Bonferroni post-hoc test if the values followed a normal distribution (paired Student's t-test for single comparison), or by Kruskal-Wallis analysis and Dunn's post-hoc test if the values were not normally distributed (Wilcoxon matched-pairs signed-ranks test for single comparison). Differences were considered statistically significant for p-values ≤ 0.05.

Results

Slug and miR-221 expression increases during chondrocyte de-differentiation

We performed a first analysis aimed at characterizing the de-differentiation process of primary chondrocytes in monolayer cultures, through the analysis of the loss of expression of specific markers (chondrocytes isolation and characterization is described in Fig. S2). As expected, subculturing chondrocytes determined a loss of the cartilaginous phenotype. This was revealed by a decrease in the expression of typical chondrogenic markers, including collagen type II (Col2A1), aggrecan, Sox9, and TRPS1, and an increase in collagen type I (Col1A1). The data reported in Fig. 1A showed that at passage 3 (p3, approximately four population doublings) human chondrocytes may be considered de-differentiated. During monolayer culture cell morphology significantly changed, as chondrocytes lost their round shape and became flattened. As demonstrated by repeated analyses, the expression of the two negative regulators of chondrogenesis under investigation, Slug and miR-221, gradually increased to very high levels in de-differentiated chondrocytes (Fig. 1B).

Slug is upregulated, while miR-221 is decreased, during TGF-β-driven chondrogenesis

Through this type of experiments, as well as data from chondrogenically differentiated hMSCs, we try to shed light on the complex interplay of mechanisms that underlie the maintenance of the chondrocyte phenotype. The debate about how the phenomena observed in hMSCs that are cultured in chondrogenic medium may be informative for the process of chondrogenesis and may help to improve our knowledge of chondrocyte behavior is still open.

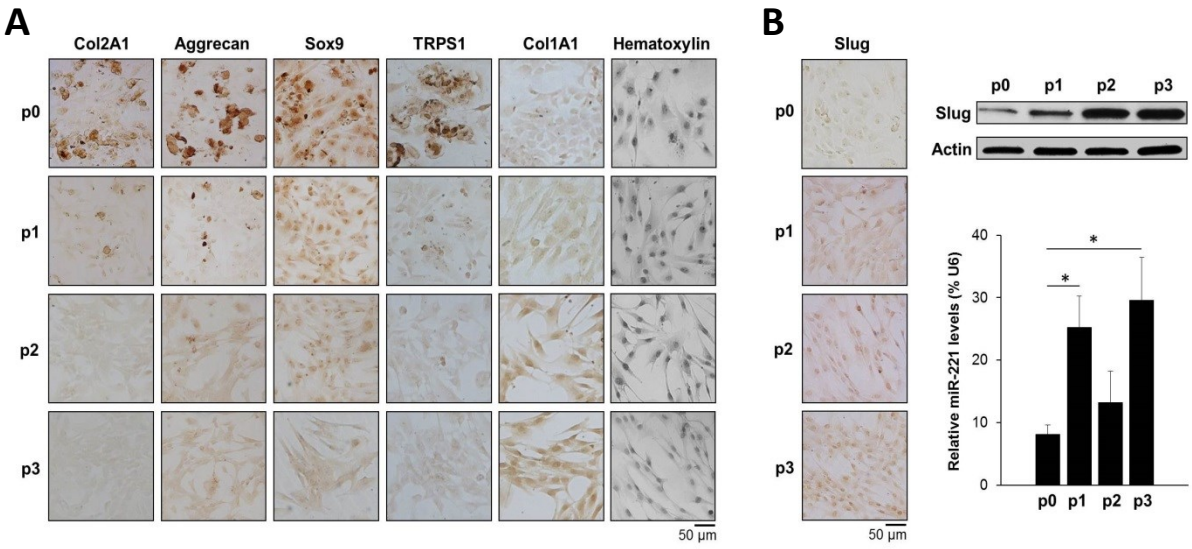

Figure 1. *Expression analysis of chondrogenic markers during monolayer expansion of human chondrocytes.* **(A)** Protein expression of cartilage related genes (Col2A1, Aggrecan, Sox9, TRPS1) and Col1A1 was investigated by immunocytochemistry in human chondrocytes during the de-differentiation process from passage 0 (p0) to passage 3 (p3). Cell morphology was evaluated by Hematoxylin staining. Representative optical photomicrographs are reported. **(B)** Slug protein expression was determined by both immunocytochemistry and western blot analysis; actin was used as loading control. miR-221 expression levels were determined by quantitative RT-PCR. Data are presented as percentage variation from U6 expression level. Results represent means±s.e.m. of three independent experiments (*p≤0.05).

In vitro TGF-β-mediated chondrogenic differentiation is a well accepted system by which hMSCs become chondrocyte-like cells. However, it is taken into account that this is a forced system and, according to recent evidence, it may give rise to unexpected side effects which are worth some attention. In order to investigate this aspect, we cultured hMSCs in pellet in differentiation medium containing transforming growth factor beta 3 (TGF-β3), and monitored chondrogenic marker levels during exposure to the treatment. As expected (Fig. 2A), the cells underwent chondrogenic differentiation, as confirmed by immunostaining for collagen type II and Sox9, and by Alcian Blue staining of proteoglycans. miR-221 expression decreased during induction of chondrogenesis (Fig. 2B), consistently with its very low expression found in primary chondrocytes (Fig. 1B). Conversely, Slug expression, unlike in chondrocytes, increased during hMSCs chondrogenic differentiation. This is the opposite of what we anticipated, since Slug, as well as miR-221, is defined as a negative regulator of chondrogenesis (*Seki et al., 2003; Goldring et al., 2006; Kim et al., 2010; Bakhshandeh et al., 2012; Karlsen et al., 2011*).

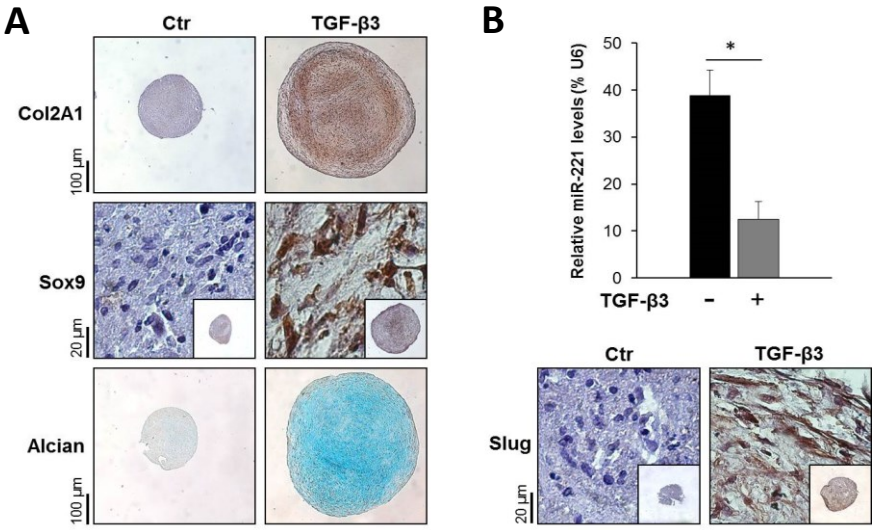

Figure 2. *TGF-β-mediated chondrogenesis of hMSCs from Wharton's jelly cultured for 21 days as pellets in chondrogenic medium.* **(A)** Chondrogenic differentiation was evaluated by immunohistochemical analysis of cartilage markers (Col2A1 and Sox9) and Alcian Blue staining in TGF-β3-treated and control (Ctr) cells. **(B)** miR-221 expression levels were determined by quantitative RT-PCR in hMSCs pellets cultured for 21 days in the presence (+) or absence (−) of TGF-β3. Data are presented as percentage variation from U6 expression level. Results represent means±s.e.m. of three independent experiments (*p≤0.05). Slug expression was determined at protein level by immunohistochemical analysis. Representative optical photomicrographs are reported (inserts: 4X magnification).

However, this result is consistent with the evidence found in other well defined processes, such as embryonic development and tumor progression, where TGF-β3 mediates Slug upregulation (*Medici et al., 2008; Brandl et al., 2010*). Considering the multiple effects of TGF-β treatment on the cells, we wonder how much the fate of hMSCs is modulated by this specific treatment, or whether the differentiation potential of the cells may be weakened by it and therefore underestimated. At the same time, the effect of such a treatment could help us to understand whether a regulatory factor has a predominant role on another one in determining the chondrogenic differentiation. To this purpose, we compared the expression profile of two hMSCs groups, each consisting of four donors, with opposite outcome of chondrogenesis after TGF-β3 treatment. Failure of *in vitro* chondrogenic differentiation is an event that, for different reasons, may occur quite frequently. As reported in Fig. 3, hMSCs samples that failed chondrogenic differentiation, but not those that successfully differentiated towards the chondrogenic phenotype, maintained high miR-221 levels after 21 days in pellet culture.

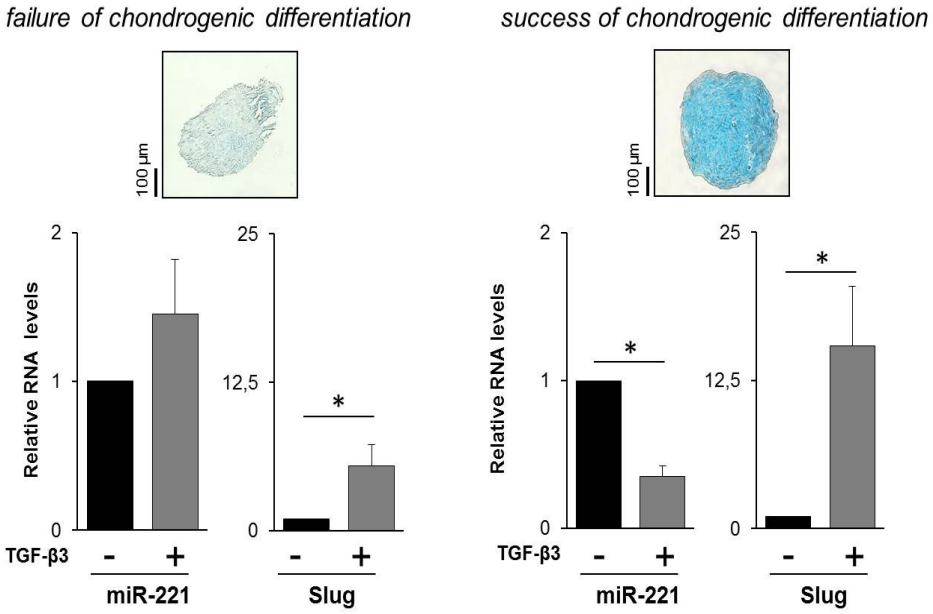

Figure 3. *Comparison of miR-221 and Slug expression in two hMSCs sample groups with opposite outcome of chondrogenesis after TGF-β treatment.* The expression of miR-221 and Slug RNAs was determined in two hMSCs groups, each consisting of four donors, with opposite outcome of chondrogenesis after TGF-β3 exposure for 21 days. Each plot displays the fold changes relative to control (pellets cultured for 21 days in the absence of TGF-β3). Results represent means±s.e.m. (*$p \leq 0.05$). Representative photomicrographs of Alcian Blue stained hMSCs pellets are reported.

This observation suggests a negative role for miR-221 in chondrogenesis. On the contrary, regardless of the effectiveness of TGF-β3 in inducing chondrogenic differentiation, Slug expression increased after TGF-β3 exposure. Therefore, it is likely that in hMSCs, as well in other cells, TGF-β3 positively affects Slug expression.

The effect of Slug and miR-221 knockdown on the chondrogenic potential of hMSCs

It is well accepted that Slug is a negative regulator of chondrogenesis, and its increased expression observed in de-differentiated chondrocytes confirms this assumption (see Fig. 1A). Hence, we wondered whether the well-recognized positive effect of TGF-β on hMSCs chondrogenic induction can be counteracted by the inevitable TGF-β-mediated upregulation of Slug that we reported in Fig. 2B and 3. Therefore, we investigated whether depletion of chondrogenic negative factors, namely Slug and miR-221, was sufficient to specifically drive the chondrogenic differentiation of hMSCs. To this purpose, we performed gene silencing experiments without TGF-β3 (see the scheme in Fig. 4A) on hMSCs grown in conventional 2D culture plates.

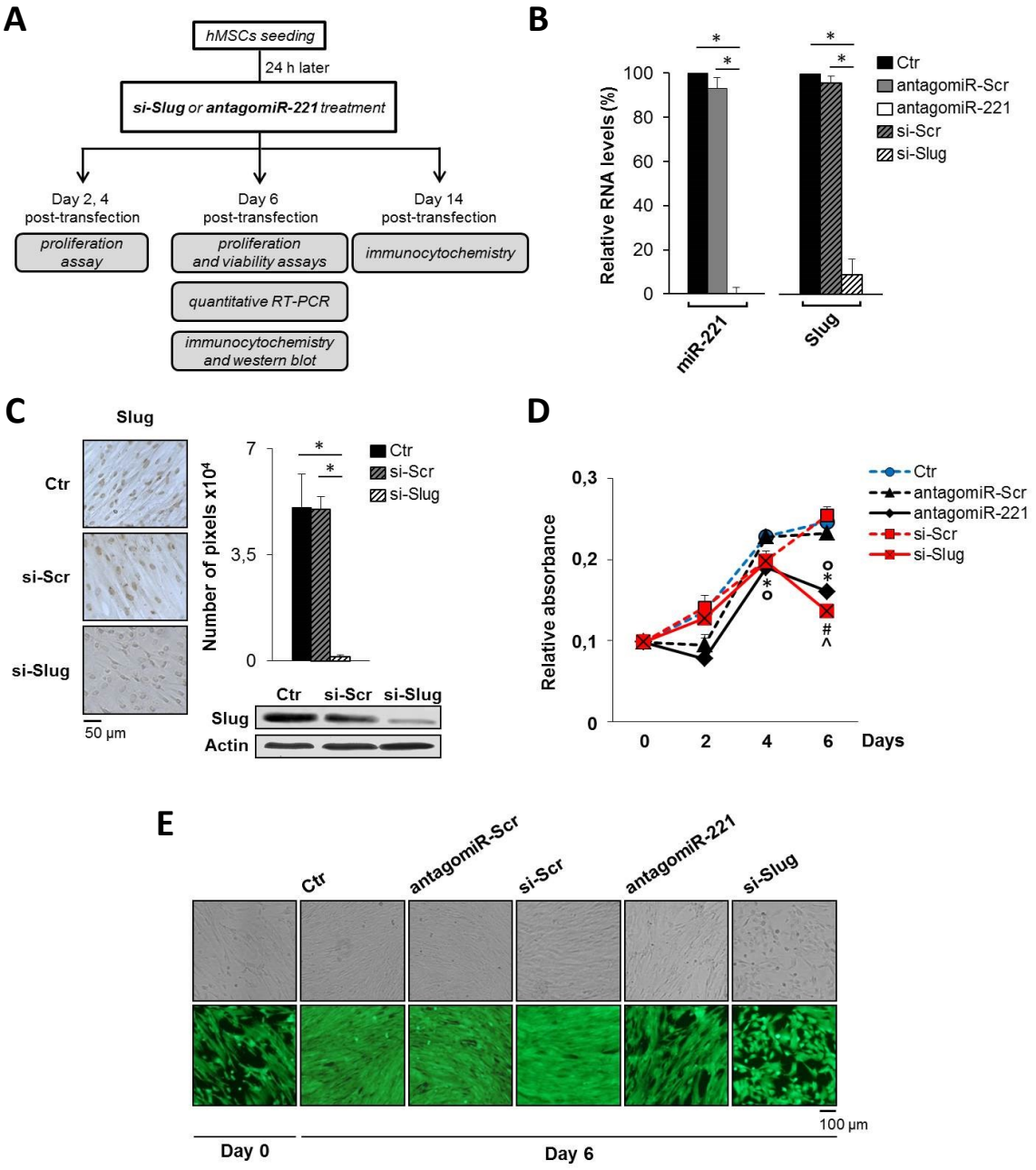

Figure 4. *miR-221 and Slug knockdown in hMSCs.* **(A)** Schematic representation of the experimental strategy for si-Slug or antagomiR-221 treatment. **(B)** The efficiency of miR-221 and Slug knockdown was determined at day 6 post-transfection and revealed by quantitative RT-PCR. Data are presented as percentage variation of expression in comparison to untreated cells (Ctr) (set as 100 % of expression). Results represent means±s.e.m. of three independent experiments (*p≤0.05). **(C)** Slug silencing was confirmed at protein level by immunocytochemistry and western blot analysis. Protein levels were quantified by densitometric analysis of immunocytochemical pictures; four random fields per replicate (three replicates) were captured using ImageJ software (see Material and Methods for details). Data are presented as means of pixels per 100 cells±s.e.m. (*p≤0.05). Two non-relevant control oligos (antagomiR-Scr and si-Scr) were used to verify the specificity of the treatments. **(D)** Proliferation rate of control and treated cells was evaluated up to 6 days using AlamarBlueTM assay. Results represent means±s.e.m. of three independent experiments. Statistical

analysis was performed for cells treated with antagomiR-221 versus untreated cells (Ctr) (indicated as *) or antagomiR-Scr treated cells (o), and si-Slug treated cells versus Ctr (#) or si-Scr treated cells (^) (#, o, ^, *p≤0.05). **(E)** Cell morphology and viability were evaluated before (day 0) and after 6 days of the reported treatments. Fluorescence photomicrographs are representative merged images and show the presence of green fluorescence (calcein-AM)-labelled live cells and the absence of red fluorescence (PI)-labelled dead cells.

Notably, monolayer cell culture is the best condition for transfection, but not for chondrogenic differentiation. As reported in Fig. 4B-C, high knockdown efficiency was obtained both for miR-221 and Slug. After 6 days of antagomiR-221 or si-Slug treatment, hMSCs had slightly reduced proliferation capacity, as showed both by growth curves (Fig. 4D) and microphotographs from double staining with calcein-AM and propidium iodide (Fig. 4E). As shown in Fig. 4E, hMSCs were highly viable and maintained their spindle shaped morphology after antagomiR-221 treatment; on the contrary, Slug knockdown changed the morphology of the cells that became rounded while still remaining viable. Next, we investigated a possible link between Slug and miR-221 functions. By qRT-PCR, western blot, and immunocytochemical analysis (Fig. 5A), we found that miR-221 depletion did not affect the expression of Slug mRNA and protein, even when exposure to antagomiR-221 was prolonged to 14 days. This indicates that Slug is not a direct miR-221 target gene. In contrast, transfection with si-Slug, but not with a non-relevant (scrambled) oligonucleotide sequence, led to a significant down-regulation of miR-221 (Fig. 5B), suggesting that Slug could be a positive regulator of miR-221 expression in hMSCs.

This last evidence prompted us to analyze the *in vivo* recruitment of Slug at the miR-221 promoter by chromatin immunoprecipitation (ChIP) assay. The human genomic DNA sequence belonging to the 5′ regulatory region of the miR-222/221 locus was analyzed for the presence of putative Slug binding sites (E-box motifs, 5′-CACCTG/CAGGTG-3′) by using the Transcription Element Search Software (TESS) for transcription factor search and MatInspector 7.4. As shown in Fig. 6, this analysis identified five potential Slug binding sites in the promoter region, four upstream and one downstream of the transcription start site (+1). Four chromatin subregions were analyzed for E-boxes occupancy, revealing that Slug was recruited at the promoter region in hMSCs but not in p0 chondrocyte chromatin. Specifically, the regions involved in the interaction between Slug and the miR-221 promoter were B and C, whereas no chromatin was immunoprecipitated by the regions A and D. Acetylated histone H3 (Ac-H3), a marker of active chromatin, was highly localized to all these regions in hMSCs.

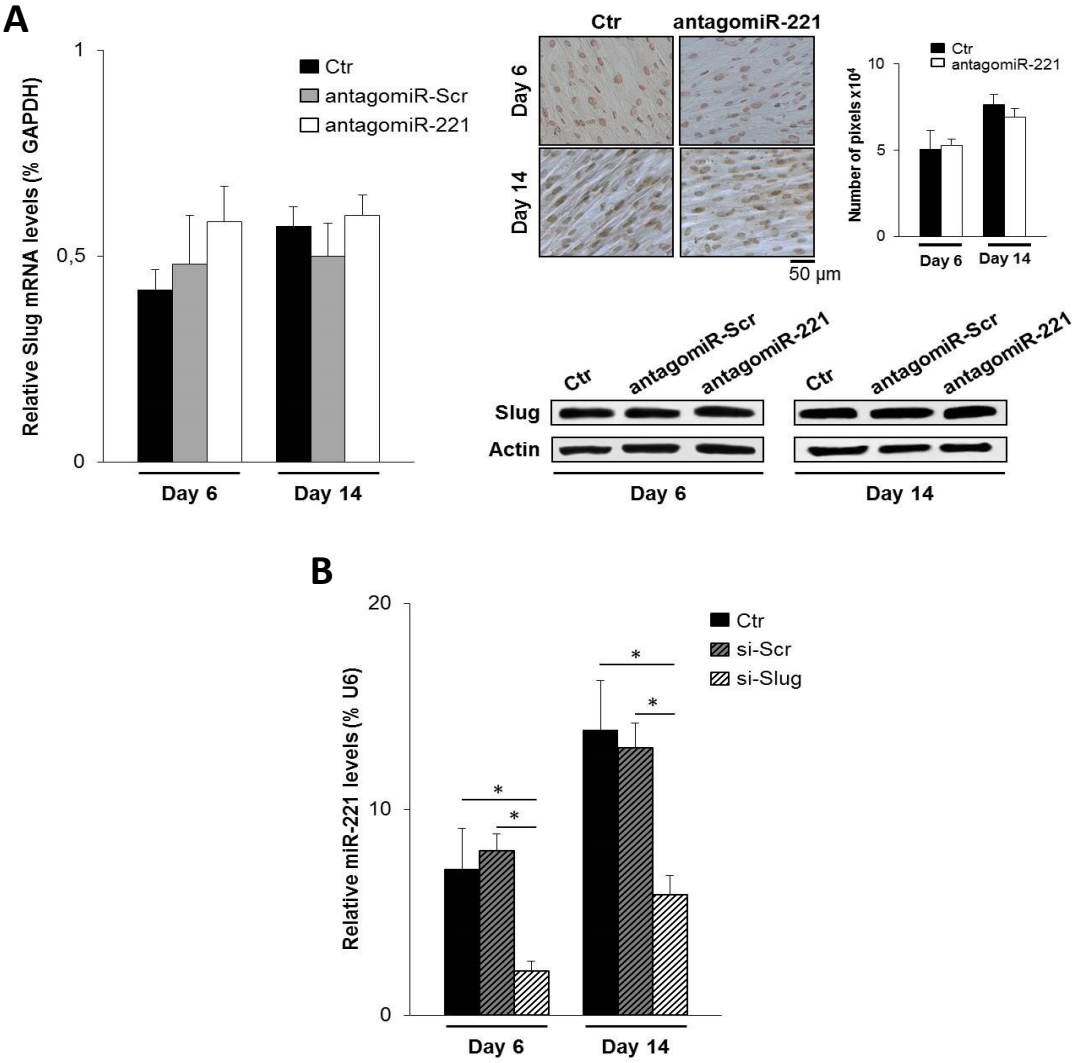

Figure 5. *Relationship between Slug and miR-221.* **(A)** hMSCs were treated up to 14 days with antagomiR molecules (antagomiR-Scr or antagomiR-221). Slug mRNA expression was analyzed by quantitative RT-PCR. Data are presented as percentage variation from GAPDH expression level. Results represent means±s.e.m. of three independent experiments; statistical analysis did not show significant differences between the conditions. Slug protein expression was determined at day 6 or 14 by immunocytochemical analysis and quantified by densitometric analysis of immunocytochemical pictures; four random fields per replicate (three replicates) were captured using ImageJ software (see Material and Methods for details). Data are presented as means of pixels per 100 cells±s.e.m., statistical analysis did not show significant differences between the conditions. Slug expression was also analyzed by western blot; actin was used as loading control. **(B)** Cells were treated for 6 days with siRNA molecules (si-Scr or si-Slug) and miR-221 expression levels were determined by quantitative RT-PCR. Data are presented as percentage variation from U6 expression level. Results represent means±s.e.m. of three independent experiments (*$p \leq 0.05$).

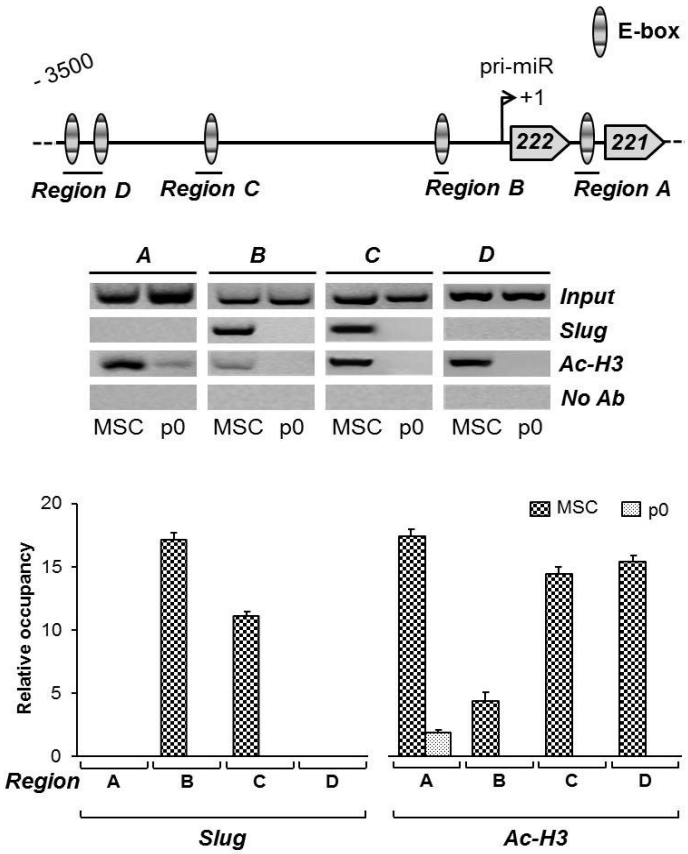

Figure 6. *Analysis of the in vivo recruitment of Slug at the miR-221 promoter by Chromatin Immunoprecipitation (ChIP) assay.* The localization of predicted Slug binding sites (E-box) on the human genomic DNA sequence belonging to the 5′ regulatory region of the miR-222/221 locus (*Di Leva et al., 2010*), is indicated with ovals. Protein-DNA complexes were formaldehyde-cross linked *in vivo* in hMSCs and p0 chondrocytes. Chromatin fragments were subjected to immunoprecipitation with antibodies against Slug and Acetyl Histone H3 (Ac-H3). After cross-link reversal, the co-immunoprecipitated DNA was amplified by PCR using the primers pairs spanning the reported regions of the miR-221 promoter (PCR amplicons are indicated by horizontal bars: region A=155 bp, region B=95 bp, region C=185 bp, region D=289 bp). The input samples, collected before precipitation, were used as normalization control. Chromatin eluted from immunoprecipitation lacking antibody was used as no antibody control (No Ab). Three independent experiments were performed for each ChIP assay and representative results are shown. Bar graphs represent the quantification of the data obtained by densitometric analysis of PCRs from three independent experiments (means±s.e.m.). The intensity of the bands for Slug and Ac-H3 was normalized to input signal and represented as relative occupancy level.

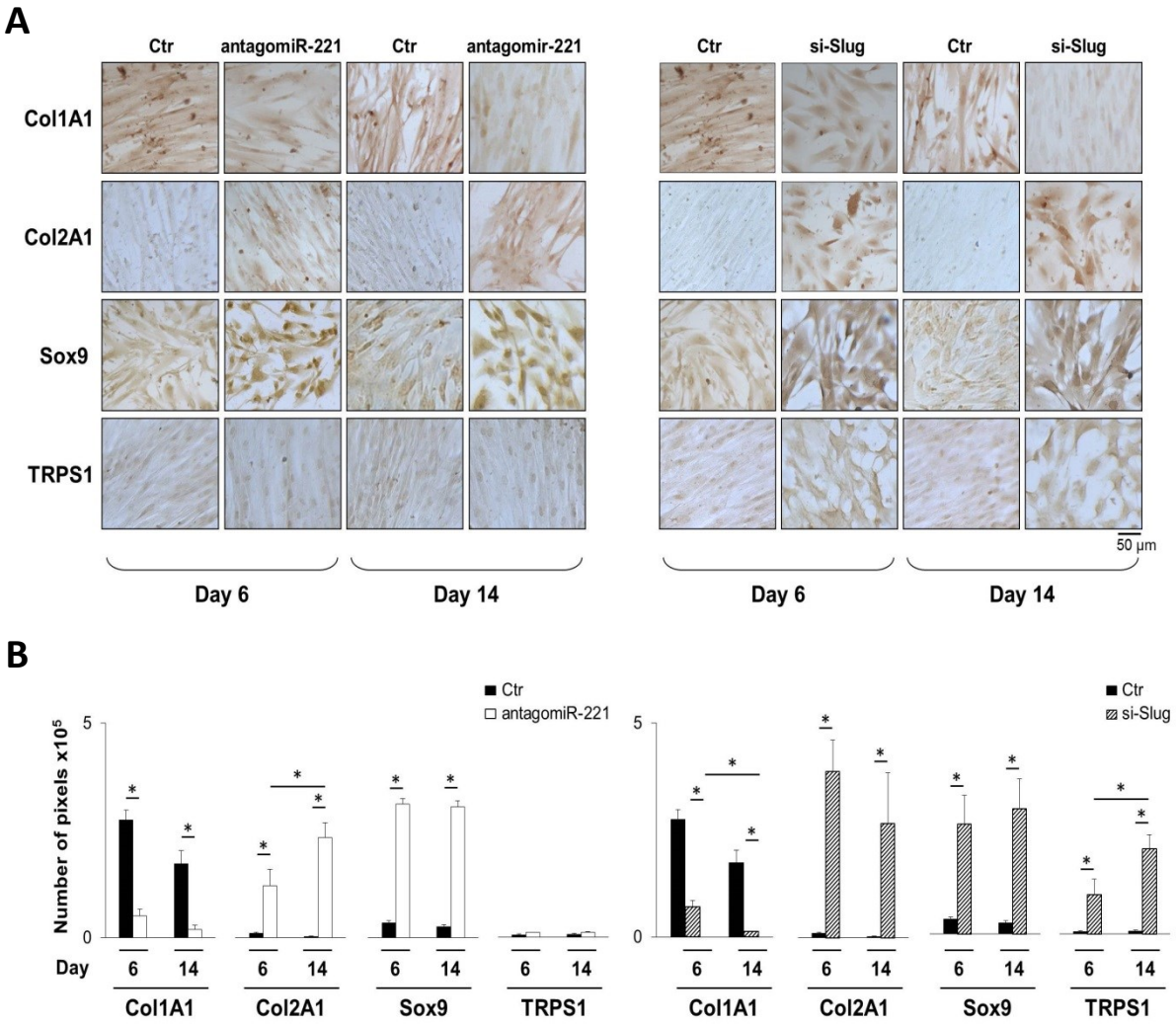

Figure 7. *Effect of miR-221 and Slug knockdown on protein expression.* hMSCs were treated for 6 or 14 days with antagomiR-221, si-Slug, or remained untreated (Ctr). **(A)** The expression of Col1A1 and cartilage-related genes (Col2A1, Sox9, and TRPS1) was investigated by immunocytochemical analysis. Representative optical photomicrographs are reported. **(B)** Pictures of four random fields per replicate (three replicates) were captured for densitometric analysis using ImageJ software (see Material and Methods for details). Data are presented as means of pixels per 100 cells±s.e.m. (*p≤0.05).

This is consistent with the high levels of miR-221 in hMSCs. In contrast, the association of Ac-H3 with this promoter region was significantly reduced in p0 chondrocytes, in agreement with the very low levels of miR-221 found in chondrocytes. Taken together, these results indicate that Slug expression and its presence at the promoter region is required to maintain high levels of miR-221.

Next, we addressed the consequences of miR-221 or Slug knockdown on cell chondrogenic potential by analyzing the expression of specific chondrogenic markers via

immunocytochemical analysis (Fig. 7) and qRT-PCR (Fig. S3). Representative optical photomicrographs (Fig. 7A) and quantification of relative protein levels (Fig. 7B) showed that exposure to both antagomiR-221 and si-Slug strongly reduced the levels of Col1A1 protein, caused the appearance of Col2A1, and strongly increased Sox9, in a time dependent manner. Therefore, Slug depletion, as well as antagomiR-221 treatment, is able to drive hMSCs toward chondrogenesis in the absence of TGF-β treatment, despite unfavorable conditions to chondrogenic differentiation as those represented by the 2D-monolayer culture system. si-Slug transfection, but not antagomiR-221 treatment, also caused an appreciable increase of TRPS1, a protein which plays a pivotal role in promoting chondrogenesis (*Goldring et al., 2006*). This suggests that Slug may act as a repressor of this TF, whose high levels could be an important pre-requisite to predispose the cells to chondrogenesis and support their differentiation. In accordance with this hypothesis, we found that overexpression of TRPS1 strongly inhibited miR-221 expression in hMSCs (Fig. 8), suggesting an involvement of TRPS1 in the regulation of miR-221 levels.

The findings of the ChIP assay shown in Fig. 9 further strengthened this hypothesis. Nine GATA-like consensus sequences for TRPS1 binding (*Malik et al., 2001*) were identified in the 5′ regulatory region of the miR-222/221 locus. In order to investigate TRPS1 recruitment, four chromatin subregions were considered and subjected to PCR. TRPS1 was recruited on the chromatin of p0 chondrocytes, and the regions specifically involved in this interaction were F and G, whereas no chromatin was immunoprecipitated by the regions E and H. hMSCs that express no appreciable levels of endogenous TRPS1 did not show any association of TRPS1 at the miR-221 promoter region. Only hMSCs overexpressing TRPS1 showed a recruitment of this transcription factor to the miR-221 promoter (region F). Taken together, these findings suggest that TRPS1 may act as a direct transcriptional suppressor of miR-221. Therefore, our data indicate that Slug and TRPS1 act, respectively, as negative and positive chondrogenic transcription factors, and this is achieved, at least in part, by directly promoting or inhibiting miR-221 expression. The quantification of mRNA levels of chondrogenic markers after gene silencing is shown in Fig. S3. qRT-PCR analysis revealed that antagomiR-221 treatment caused, already after 6 days, a down-regulation of Col1A1 and an upregulation of Sox9, but had no effect on Col2A1 mRNA expression, that remained undetectable, while expression of TRPS1 (as well as Slug, see Fig. 5) was not significantly altered. The trend of mRNA data was consistent with the immunocytochemical results except for the data on Col2A1. This is not surprising, since Col2A1 is one of those proteins for which discrepancies between mRNA and protein expression are described (*Caron et al., 2012*).

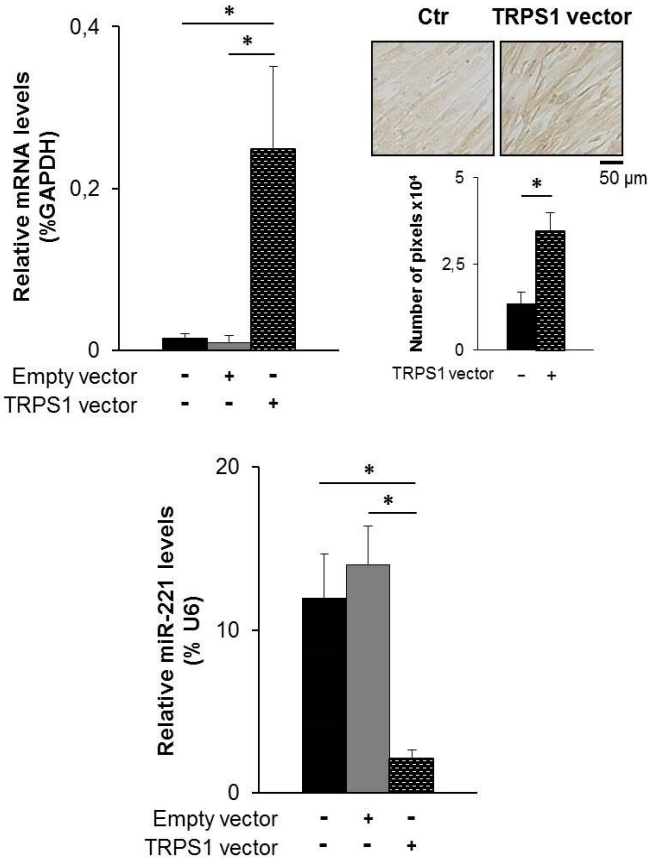

Figure 8. *Effect of the overexpression of human TRPS1 on miR-221 levels in hMSCs.* Cells were transfected with the vector containing the full-length human TRPS1 cDNA or with the empty vector and harvested after 48 h. TRPS1 and miR-221 RNA expression was determined by quantitative RT-PCR. Data are presented as percentage variation from GAPDH and U6 expression levels, respectively. Results represent means±s.e.m. of three independent experiments (*p≤0.05). TRPS1 overexpression was also evaluated at protein level by immunocytochemistry and quantified by densitometric analysis of immunocytochemical pictures; four random fields per replicate (three replicates) were captured using ImageJ software (see Material and Methods for details). Data are presented as means of pixels per 100 cells±s.e.m (*p≤0.05).

In accordance with the immunocytochemical data, Slug knockdown caused a significative upregulation of Sox9 and TRPS1 mRNA expression, in particular after 14 days of treatment, but, also in this case, Col2A1 mRNA remained undetectable. Col1A1 mRNA was not significantly altered upon si-Slug treatment.

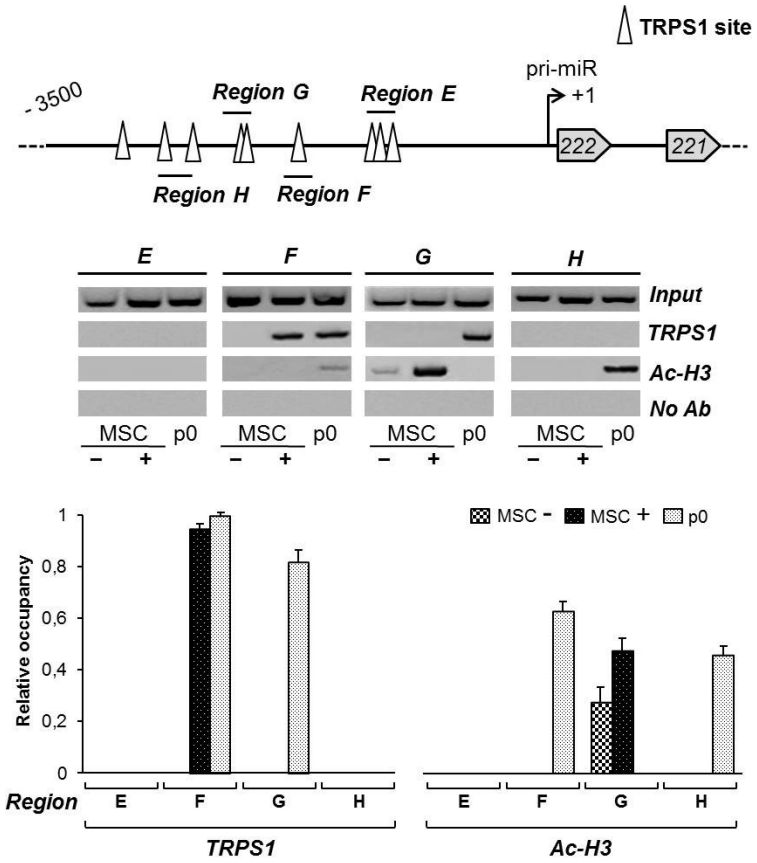

Figure 9. *Analysis of the in vivo recruitment of TRPS1 at the miR-221 promoter by Chromatin Immunoprecipitation (ChIP) assay.* The localization of predicted TRPS1 binding sites (A/T GATA A/G) on the human genomic DNA sequence belonging to 5′ regulatory region of the miR-222/221 locus is indicated with triangles. Protein-DNA complexes were formaldehyde-cross linked *in vivo* in hMSCs previously transfected with the TRPS1 vector (+) or untransfected (−), and p0 chondrocytes. Chromatin fragments were subjected to immunoprecipitation with antibodies against TRPS1 and Acetyl Histone H3 (Ac-H3). After cross-link reversal, the coimmunoprecipitated DNA was amplified by PCR using the primers pairs spanning the reported regions of miR-221 promoter (PCR amplicons are indicated by horizontal bars: region E=159 bp, region F=141 bp, region G=131 bp, region H=196 bp). Three independent experiments were performed for each ChIP assay and representative results are shown. Bar graphs represent the quantification of the data obtained by densitometric analysis of PCRs from three independent experiments (means±s.e.m). The intensity of the bands for TRPS1 and Ac-H3 was normalized to input signal and represented as relative occupancy level.

Discussion

Chondrogenesis is a tightly regulated process in which many factors and mechanisms regulate the different stages of the chondroprogenitor differentiation program, as well as chondrocytes maturation and hypertrophy (*de Crombrugghe et al., 2001; Umlauf et al., 2010; Lefebvre & Smits, 2005*). A better understanding of the mechanisms involved in these processes, and the elucidation of the molecular events underlying cell de-differentiation, is critical for the optimization of cell-based tissue engineering strategies for the treatment of cartilage defects. New perspectives come from recent advancements in understanding the biological functions of transcription factors (TFs) and miRNAs, and in postulating possible regulatory loops between them and their targets (*Hong & Reddi, 2012; Sun et al., 2010; Anokye-Danso et al., 2012*). By targeting specific TFs and miRNAs, we can manipulate their expression levels, and this may result in the enhancement of a specific differentiation process or in the control of cell progression toward a specific lineage (*Caplen, 2004; Cheema et al., 2007; Torreggiani et al., 2012; Handorf & Li, 2011*). This is an interesting new challenge for cartilage, which, unlike most natural tissues, has only limited self-repair capacity and, consequently, even a minor damage can have detrimental effects (*Vinatier et al., 2009b; Steinert et al., 2007; Temenoff & Mikos, 2000*). To date, several biological approaches for cartilage repair have been proposed. These show variable levels of efficacy, due to insufficient cell differentiation, instability of the chondrocyte phenotype, lack of proper ECM secretion, and integration failure (*Vinatier et al., 2009b; Temenoff & Mikos, 2000; Gadjanski et al., 2012; Johnstone et al., 2013; van Beuningen et al., 2000*). These interventions range from the use of Autologous Chondrocyte Implantation (ACI) to various types of three-dimensional scaffolds combined or not with hMSCs, and intra-articular injections of drugs such as TGF-β. A novel contribution for the assessment of chondrogenic differentiation and the formation of artificial cartilage may be offered by molecular tools, including the employment of RNAi technology, to guide the differentiation of chondroprogenitors in the absence of differentiating agents. In this study we have explored this issue without the employment of TGF-β.

The use of traditional exogenous chondrogenic agents is beginning to be questioned for their undesired off-target effects and controversial outcomes. Recent studies demonstrated that the presence of TGF-β during chondrocyte proliferation may be detrimental for the re-differentiation process (*Narcisi et al., 2012a*). Conversely, inhibition of TGF-β signaling increases the chondrogenic re-differentiation ability of articular chondrocytes, or even attenuates osteoarthritis in MSCs in subchondral bone (*Narcisi et al., 2012b; Zhen et al., 2013*).

In the present study, we showed that human mesenchymal stem cells (hMSCs) can acquire a particular potency toward the chondrogenic lineage when cultured in the presence of siRNA against the transcription factor Slug or of antagomiR against miR-221. For the first time, we demonstrated that knockdown of these gene products, which may be defined as anti-chondrogenic factors, induces the differentiation of hMSCs towards the chondrogenic lineage in the absence of external cues. Without a differentiation cocktail, both miR-221- and Slug-silenced hMSCs changed their phenotype and became able to express typical chondrogenic markers such as collagen type 2 and Sox9. Interestingly, only Slug-silenced hMSCs showed a significant increase in the expression of TRPS1, a crucial positive regulator of chondrocyte proliferation and differentiation (*Wuelling et al., 2009*).

The evidence that Slug and TRPS1 expression, both at the mRNA and protein levels, was not affected by miR-221 suggests that these transcription factors are not miR-221 targets in uninduced hMSCs. In contrast, data from gene expression and ChIP analysis suggested that miR-221 is positively regulated by Slug, and this hampers hMSCs chondrogenic differentiation. Moreover, in hMSCs committed towards chondrogenesis through Slug depletion, the chondrogenic potency of TRPS1 contributes to maintaining low miR-221 levels. Similar observations were identified in chondrocytes, whose phenotype and behavior are associated with low levels of Slug. Our results also demonstrated that Slug expression is not influenced by miR-221 or TRPS1 levels. Consistently, TRPS1 overexpression did not affect Slug expression (data not shown).

Therefore, we hypothesized the existence of a regulatory loop in the control of the chondrogenic potential of hMSCs, which directly involves TRPS1 and miR-221, but not Slug. Although further studies are needed, our findings provide a clear evidence of the anti-chondrogenic effects of miR-221 and Slug, as shown by the ability of antagomiR-221 and si-Slug to drive hMSCs toward chondrogenic differentiation. This analysis is part of a broader research interest that focuses on the detection of crucial nodes to control and manipulate hMSCs fate to ultimately improve osteochondral graft generation. A summary of the interpretation of our data is reported in the scheme in Fig. 10. In this tuning model, the correlation among the levels of miR-221, Slug, and TRPS1 points out the similarities between MSCs and dedifferentiated chondrocytes. When adequate changes in the levels of these genes occur, a specific expression profile may be established, and chondrogenic differentiation may proceed.

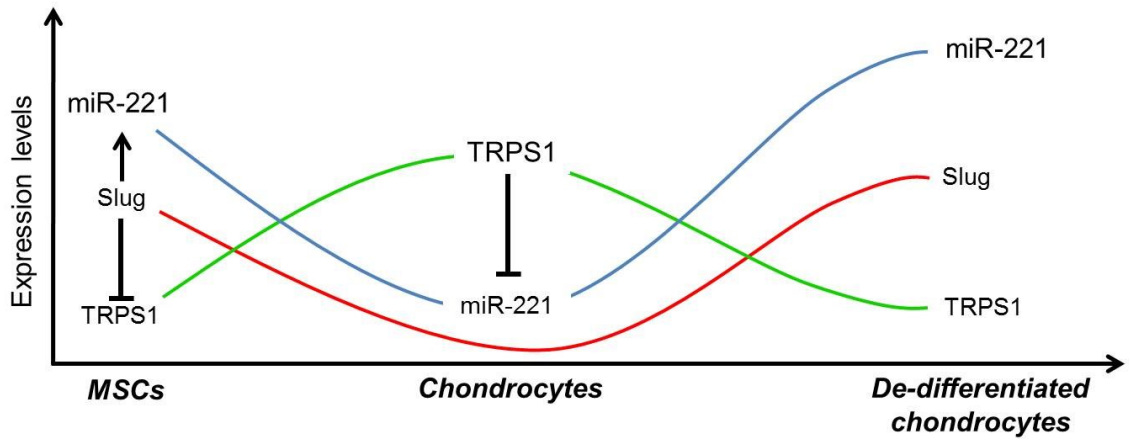

Figure 10. *Schematic representation of the variations in TRPS1, Slug, and miR-221 expression and potential reciprocal regulation in hMSCs, chondrocytes, and de-differentiated chondrocytes.* Slug, present at high levels in hMSCs, positively modulates miR-221 and represses TRPS1. This repression is relieved during chondrogenesis, due to the strong decrease of Slug and other yet unidentified factors. TRPS1 inhibits miR-221, and chondrogenic induction occurs. De-differentiation of chondrocytes is supported by a drop in the levels of TRPS1 and a dramatic upregulation of Slug and miR-221 expression.

Although typical chondrogenic markers, such as collagen type 2 and Sox9, were induced at comparable levels in miR-221- and Slug- silenced cells, and both treatments resulted in a strong decrease of collagen type 1, we did not observe a significant increase in aggrecan expression or Alcian blue staining for glycosaminoglycans (data not shown). This supports the conclusions drawn from previous works (*Umlauf et al., 2010; Johnstone et al., 2013; Tortelli & Cancedda, 2009; Caron et al., 2012*) indicating that cell-cell contact in a 3D-culture system is required for the production of abundant and well organized extracellular matrix (ECM). As the final purpose of cartilage engineering is based on the use of cells that produce an ECM with properties that mimic that of the hyaline cartilage, our strategy needs to be improved. In particular, we will have to test whether the silenced cells we have produced in monolayer conditions represent a cell-based product suitable and sufficient to trigger the process of repair or regenerate damaged cartilage tissue, when implanted in an adequate *in vivo* model. Alternatively, the combination of our silenced-cells with an appropriate scaffold could allow us to obtain subsequent stages of chondrocyte phenotype maturation and lead to the production of the ECM in its correct form in a short time. From this point of view, further research is now ongoing having recently demonstrated that TGF-β-driven chondrogenic differentiation of hMSCs cultured onto a hyaluronan-based

scaffold, HYAFF®-11, was strengthened after cell exposure to siRNA against Slug (*Lisignoli et al., 2014*).

In conclusion, the concepts emerging from our findings allow us to speculate that silencing of those genes that may pose an impediment or a slowdown in the differentiation process may represent a good alternative to conventional pre-implant differentiating strategies for cartilage repair and regeneration (*Mahmoudifa & Doran, 2012*). Once implanted *in vivo*, a group of specifically silenced-hMSCs might be sufficient to trigger a crucial response of the endogenous cellular niche and, consequently, to instruct the cells close to the damaged site to differentiate toward the desired lineage, supporting local tissue repair and improving the clinical outcome.

Supplementary materials

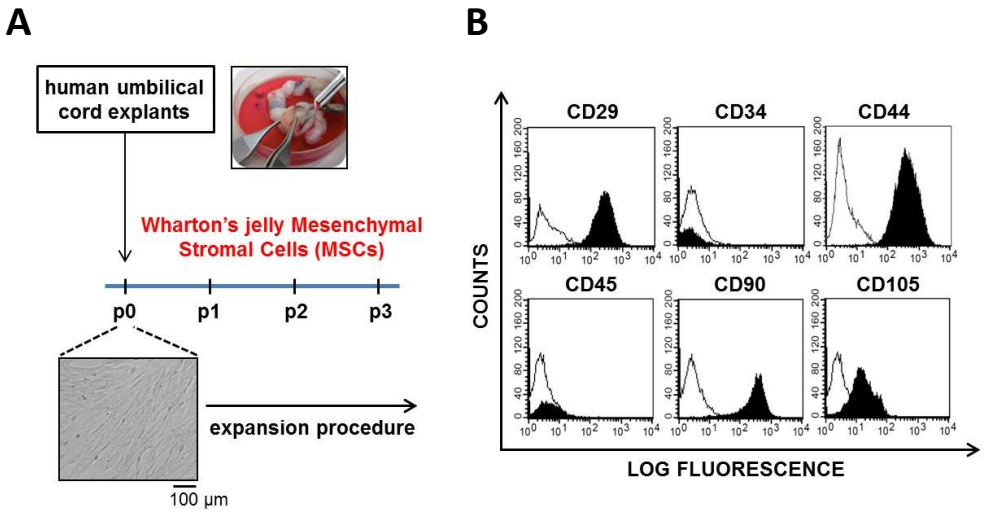

Supplementary figure 1. *Isolation and phenotype characterization of human Wharton's jelly mesenchymal stromal cells.* **(A)** The experimental procedure used to obtain MSCs from the Wharton's jelly of human umbilical cords is schematized. The morphology of the cells grown in monolayer is shown in a representative optical photomicrograph. **(B)** The expression of typical mesenchymal surface markers (CD29, CD44, CD90 and CD105) and hematopoietic markers (CD34 and CD45) was investigated by flow cytometric analysis. Isotype controls are represented by the white curves.

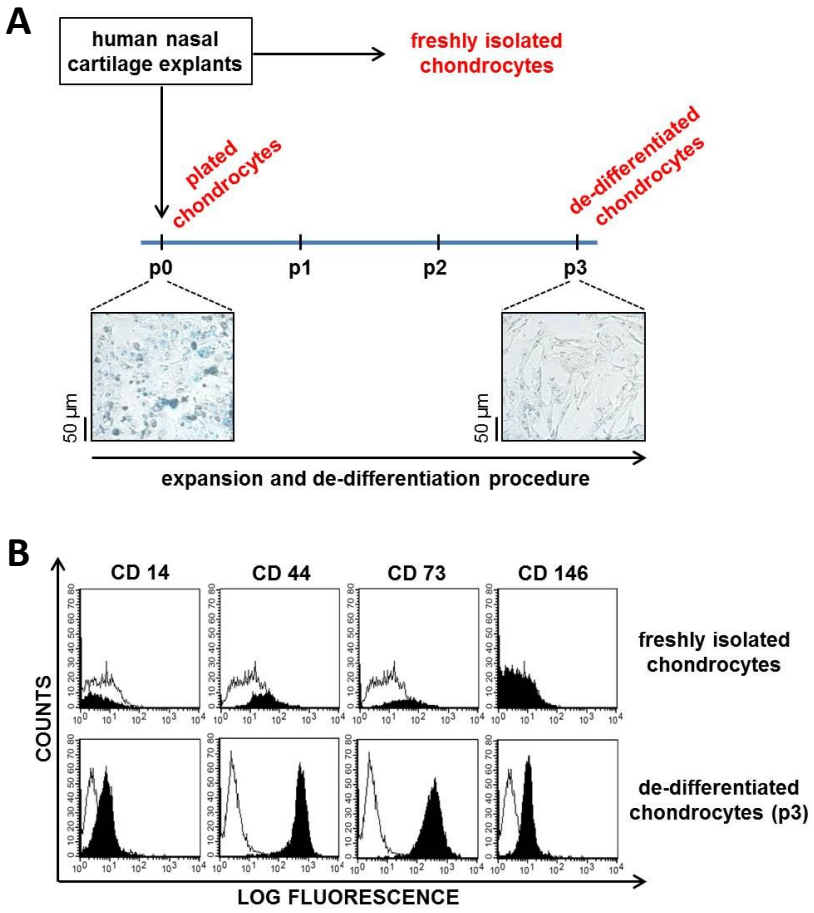

Supplementary figure 2. *Isolation and characterization of human chondrocytes from nasal septum cartilage.* **(A)** The experimental procedure used to obtain chondrocytes and de-differentiated chondrocytes is shown. Human chondrocytes isolated from cartilage explants were directly analyzed or plated and expanded to obtain de-differentiated chondrocytes by monolayer culture. After 7 days, plated cells were considered as p0 chondrocytes. At day 28 plated cells were considered as p3 de-differentiated chondrocytes. p1 and p2 were intermediate passages at day 14 and 21, respectively. Chondrocytes at the different passages were collected and used for the specific analysis (see Fig. 1), including Alcian Blue staining to determine proteoglycans expression, as reported in the figure. **(B)** The expression of surface markers CD14, CD44, CD73 and CD146 was investigated by flow cytometric analysis in freshly isolated and p3 de-differentiated chondrocytes.

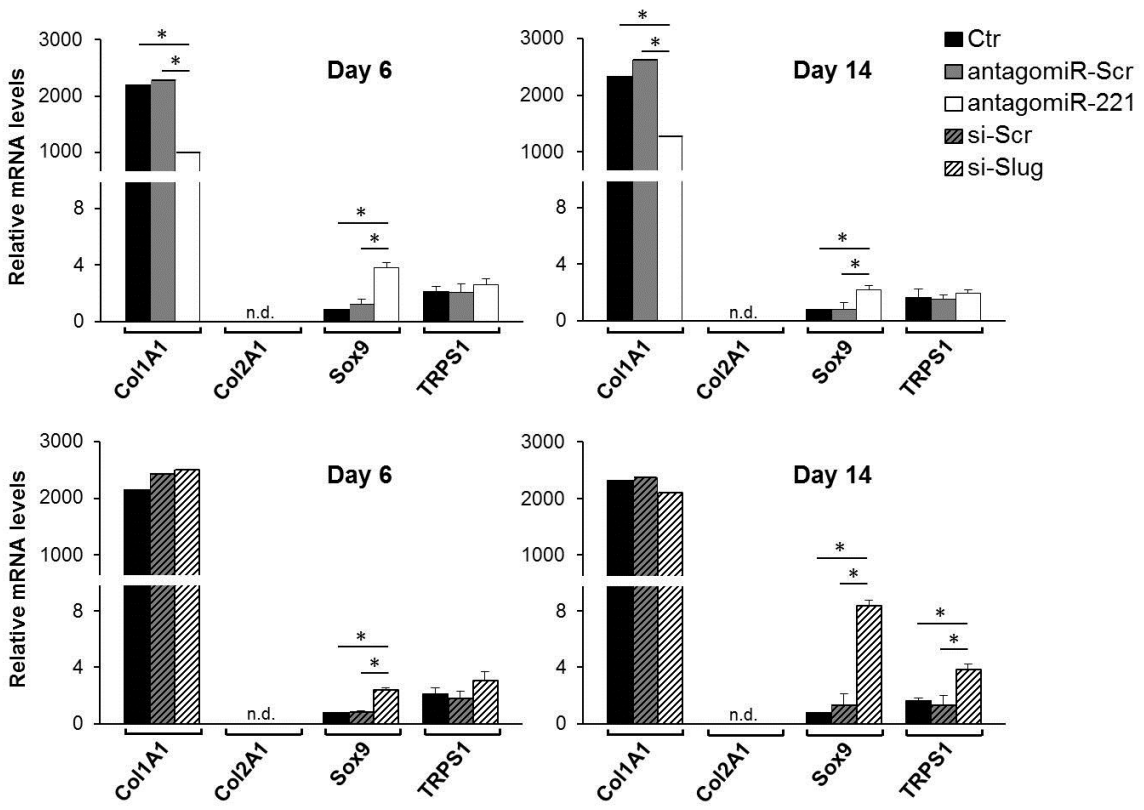

Supplementary figure 3. *Effect of miR-221 and Slug knockdown on mRNA levels of chondrogenic markers.* hMSCs were treated up to 14 days with antagomiR (antagomiR-Scr or antagomiR-221) or siRNA (si-Scr or si-Slug) molecules and mRNA levels of Col1A1, Col2A1, Sox9 and TRPS1 were determined by quantitative RT-PCR. mRNA expression data are presented as fold change respect to the sample with the lowest mRNA expression (Sox9 level in untreated cells). Results represent means±s.e.m. of three independent experiments (*$p \leq 0.05$).

GENE SYMBOL	*GENE NAME*	*TaqMan assay no.*
Col2A1	Collagen type II	Hs00264051_m1
Col1A1	Collagen type I	Hs00164004_m1
Sox9	SRY (sex determining region Y)-box9	Hs00165814_m1
Slug	Snail homolog 2 (Drosophila)	Hs00950344_m1
TRPS1	Trichorhinophalangeal syndrome I	Hs00936363_m1
miR-221	Mature microRNA-221	000524

Supplementary Table 1. *TaqMan gene expression assays used in this study.*

Chapter 3

Correlation between Slug and Lamin B1 in osteoarthritic chondrocytes

Outline of the work

The etiology of osteoarthritis (OA) is particularly complex, with genetic, developmental, biochemical and mechanical factors contributing to the disease process. As a consequence, and despite the tremendous impact of the disease on the world population, our understanding of the pathogenesis of OA is still limited. Recently, mounting evidence has suggested that the processes of cell senescence and de-differentiation may have a crucial role in determining the aberrant phenotype of osteoarthritic chondrocytes. In this context, it has been shown that mutations or altered expression of the nuclear lamins are frequently involved and correlated with cell aging and tissue degeneration. While it is well established that overexpression of lamin A occurs in chondrocytes from OA leading to cellular senescence, the contribution of lamin B remains unexplored. In order to elucidate the molecular mechanisms involved in the loss of the mature and stable chondrocytic phenotype in OA, we investigated the correlation between the nuclear lamina protein lamin B1 and the recently characterized anti-chondrogenic regulator Slug in OA chondrocytes. We demonstrated that lamin B1 and Slug proteins are upregulated in OA cartilage explants and *in vitro* cultured OA chondrocytes. In addition, we found that Slug is recruited *in vivo* at the promoter region of lamin B1, and particularly when chondrocytes undergo de-differentation or OA degeneration. Our data highlight for the first time a potential regulatory role of Slug on the expression of lamin B1 in OA chondrocytes. We speculate that our findings may have important implications for the study of cartilage senescence and degeneration, possibly contributing to the development of novel therapeutic strategies able to target the signals supporting cartilage damage in OA.

Introduction

Lamins (A, B1, B2, C) are nuclear intermediate filament proteins with multifunctional characteristics (*Choi & Worman, 2014)*. They support the structural integrity of the nucleus, and play a key role in a wide range of nuclear functions, including transcription, DNA replication and repair, control of cell cycle and stem cell niche function, cell proliferation and differentiation of specific lineages during development and adult life (*Choi & Worman, 2014; Camozzi et al., 2014*). It has been demonstrated that tissue homeostasis can be disrupted by different mutations or abundance variation in lamins causing a variety of diseases, collectively termed laminopathies, including the premature aging syndrome Hutchinson-Gilford progeria (*Bonne et al., 1999*). In recent years, the study on the lamins contributed to a better understanding of the phenomenon of cellular aging, tissue degeneration and pathogenesis of age-related diseases. Interestingly, changes of A:B lamin stoichiometry is correlated with stiffness, and tissues such as cartilage and bone have a high A:B ratio (*Swift et al., 2013*). Overexpression of lamin A or the presence of its mutant form progerin leads to impaired chondrogenic potential of mesenchymal stem cells (MSCs) (*Mateos et al., 2013*). High levels of lamin A were found in osteoarthritic chondrocytes (*Attur et al., 2012*), whilst the contribution of lamin B remains unexplored. OA is a common degenerative joint disease characterized by cellular senescence, loss of chondrocyte activity and degradation of articular cartilage (*Loeser et al., 2012*). Due to the complexity of these phenomena, there is a limited understanding in OA pathogenesis. The hypothesis to be explored is the possibility that chondrocyte response to various OA inducing conditions converges on de-differentiation and acquisition of stem cell-like properties. This might occur before reentry into the cell cycle or acquisition of the senescent phenotype. Clarifying this issue may be important to devise new approaches for OA prevention and treatment. We recently found that Slug, an anti-chondrogenic transcription factor, is a marker of chondrocyte de-differentiation (*Lolli et al., 2014*). In order to find new Slug target molecules and to explore the participation of lamin B1 in the cartilage damage, we investigated their expression and molecular relationship in OA cartilage explants and *in vitro* dedifferentiated chondrocytes.

Material and Methods

Cartilage explants analysis

Knee cartilage explants from normal subjects (at autopsy, n = 3, age = 55±3 years, sex = male, Mankin score = 0-3) and OA patients (from joint replacement, n = 6, age = 58±7 years, sex = male, Mankin score = 8-10) were fixed in a freshly prepared 9:1 mixture of B5 solution (mercuric-chloride containing fixative) / 40% formaldehyde at room temperature for 2 h, dehydrated and embedded in paraffin as previously described (*Lisignoli et al., 2002*). The slides were then incubated using the following antibodies: β-galactosidase (goat anti-human 1:200) from Santa Cruz Biotechnology (Santa Cruz, CA, USA), Slug (mouse anti-human, 1:300) from Origene (Rockville, MD, USA), Lamin A (rabbit anti-human 1:200) and Lamin B1 (rabbit anti-human 1:200) from Abcam (Cambridge,UK), overnight at 4°C. The slides were then rinsed and incubated with anti-goat- or anti-mouse/rabbit-biotinilated and alkaline phosphatase-conjugated streptavidin (Kit BioGenex, San Ramon, CA, USA) at room temperature for 30 min. The staining was performed using new fast red as substrate and evaluated using a brightfield microscope. Safranin-O staining was also performed. The study was approved by the local ethical committee at the Istituto Ortopedico Rizzoli, Bologna (Italy).

Cell culture, immunofluorescence and gene expression analysis

Normal (n = 3) and osteoarthritic chondrocytes (n = 6) were isolated from articular cartilage by sequential enzymatic digestion as previously described (*Cavallo et al., 2010*). Cells from passage 0 (p0) to passage 2 (p2) grown on glass coverslips were fixed in -20°C methanol for 7 min, blocked in 4% BSA-PBS and incubated with rabbit anti-human Slug (clone H140, 1:10, Santa Cruz Biotechnology) and mouse anti-human Lamin B1 antibodies (clone 8D1, 1:100, Santa Cruz Biotechnology) overnight at 4°C. Coverslips were next washed and incubated with fluorescence-labeled secondary antibodies (Sigma-Aldrich Chemical Co., St. Louis, MO) for 1 h at room temperature. Nuclei were counterstained with DAPI (4,6-diamino-2-phenylindole). Slides were mounted with antifade reagent in glycerol and observed with a Nikon E600 epifluorescence microscope (100X magnification, 1,3 NA - numerical aperture) equipped with a digital camera. Images were processed using Adobe Photoshop (Adobe Systems). Total RNA was extracted from cells at p0 and p2, reverse transcribed and the expression of collagen type I, collagen type II and Sox9 was measured by quantitative qRT-PCR, as previously described (*Cavallo et al., 2010*).

Western blotting

20 µg of whole cell lysates were resolved by SDS-PAGE, transferred to PVDF (Millipore, Billerica, MA, USA) and blocked with PBS 0.05% Tween 20 / 5% NFDM, then probed overnight (4°C) with the following antibodies: Slug (mouse anti-human, clone A-7, 1:1000), Actin (mouse anti-human, clone C-2, 1:5000) from Santa Cruz Biotechnology, and Lamin B1 (rabbit anti-human 1:1500) from Abcam. The membranes were incubated with anti-mouse or anti-rabbit HRP conjugated antibodies (DAKO, Glostrup, Denmark) 1:2000, and signals were detected by Supersignal West Femto Substrate (Pierce, Rockford, IL, USA). Actin was used to confirm equal protein loading.

Chromatin Immunoprecipitation assay (ChIP)

ChIP was performed using a CHIP assay kit (Upstate Biotechnology, Waltham, MA, USA) according to the manufacturer's instructions as previously described (*Lolli et al., 2014*). Chromatin samples from normal or OA chondrocytes were immunoprecipitated with a specific Slug antibody. IgG antibody was used as a negative control (all antibodies were purchased from Santa Cruz Biotechnology). PCR was carried out with three primer sets (Set 1: F= 5'-GTCACCCTCGTCTTGCATTT-3', R= 5'-GCGTTTAGAGGAACGGA GAA-3'; Set 2: F= 5'-GTAGAGACGGGGTTTCACCA-3', R= 5'-TGGATTACCCATCC ACACAA-3'; Set 3: F= 5'-ACGGGGTTTCACTATGTTGG-3' R= 5'-TTGGTTGTGAG ACCCTTTCC-3'), spanning Slug binding sites in the hLMNB1 gene promoter.

Results

Loss of chondrocyte-specific properties was detected in degenerated cartilage tissue from OA patients. As shown in Fig. 1, OA cartilage displayed a low level of Safranin-O staining for sulfated glicosaminoglycans, and increased senescence-associated β-galactosidase and Lamin A immunostaining. This confirmed that a combination of phenomena including deterioration of tissue function and senescence occurs in OA cartilage. In search for new mediators of cartilage damage, we next analyzed tissue sections for the presence of another key player in cellular senescence, Lamin B1, and an anti-chondrogenic molecule, Slug transcription factor. Interestingly, the expression of Lamin B1 was increased in OA cartilage compared to normal samples and Slug colocalized with Lamin B1 (Fig. 2).

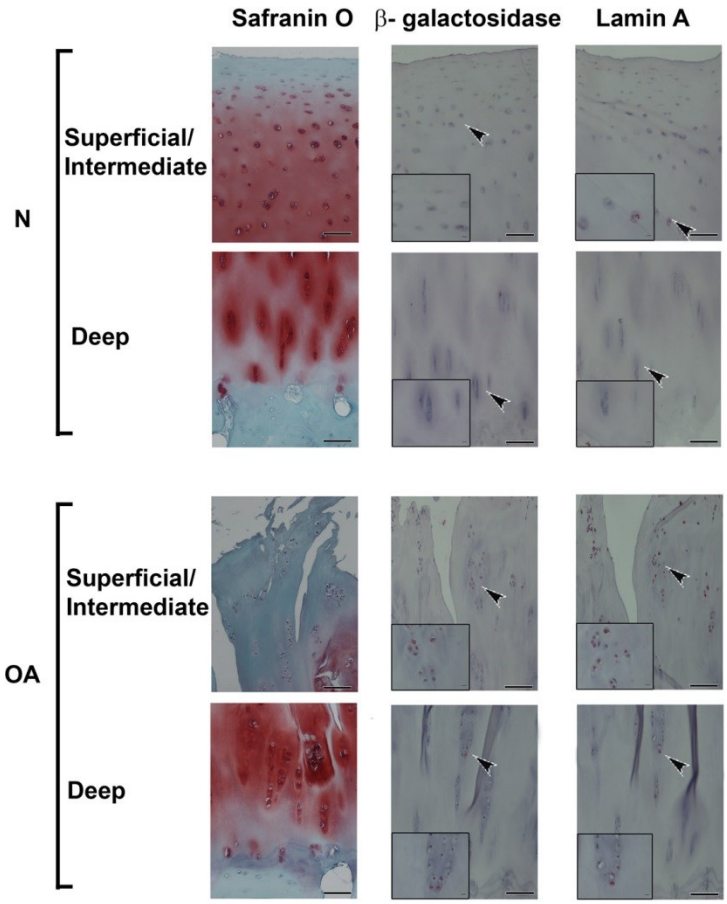

Figure 1. *Histological (Safranin-O) and immunohistochemical (β-galactosidase, Lamin A) characterization of the superficial/intermediate and deep zone of representative normal (N) and OA cartilage.* Bar = 100 µm, insert bar = 10 µm.

Notably, in normal cartilage few Slug-positive cells were present, both in the superficial/intermediate and deep area of the tissue. Conversely, a higher number of Slug-positive cells, located in all cartilage layers, were detected in OA cartilage. As senescence of chondrocytes is inherent to the OA process (*Loeser et al., 2012*), we state that Slug, in addition to being a marker of cell de-differentiation (*Lolli et al., 2014*), can also be associated to senescence.

To further validate this hypothesis, we isolated and cultured normal and OA chondrocytes. The cells were de-differentiated by prolonged passages in monolayer culture. In aggrement with literature (*Cavallo et al., 2010; Ono et al., 2013*), we confirmed a loss of the cartilaginous phenotype associated with the de-differentiation process, as demonstrated by the decrease in the expression of typical chondrogenic markers, including collagen type II and Sox9, and an increase of collagen type I (Fig. 3A).

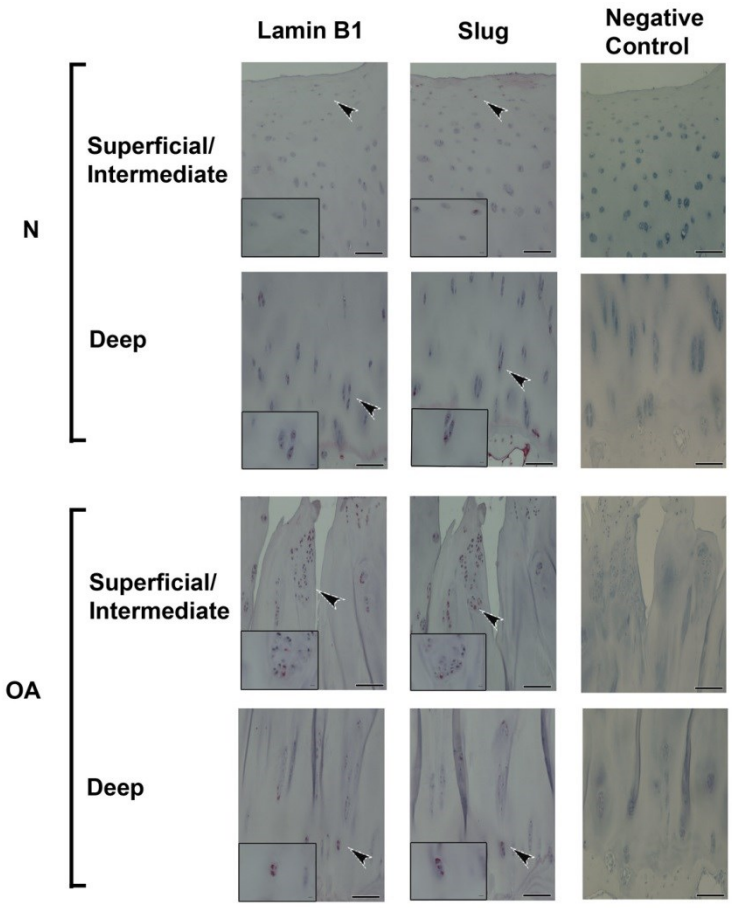

Figure 2. *Immunohistochemical analysis of Lamin B1 and Slug on serial sections of cartilage from normal (N) and OA cartilage.* Bar = 100 µm, insert bar = 10 µm..

As previously demonstrated (*Lolli et al., 2014*), Slug protein gradually increased to very high levels during the de-differentiation process of normal chondrocytes. This phenomenon was observed here, for the first time, also in OA chondrocytes, as shown by the immunoblot analysis reported in Fig. 3A. The same analysis revealed the presence of Lamin B1 in p0 chondrocytes and dedifferentiated p2 chondrocytes from healthy subjects and OA patients. Higher Slug levels were detected in OA samples compared with controls. This was confirmed by immunofluorescence analysis showing that Lamin B1 localized at the nuclear periphery, while Slug was mostly recruited in the nuclear interior (Fig. 3B). These findings prompted us to hypothesize a functional link between Slug and Lamin B1, investigating a possible role of Slug as regulator of Lamin B1 expression during the chondrocyte de-differentiation process. The possibility that Lamin B1 is a direct transcriptional target of Slug was investigated by ChIP assay.

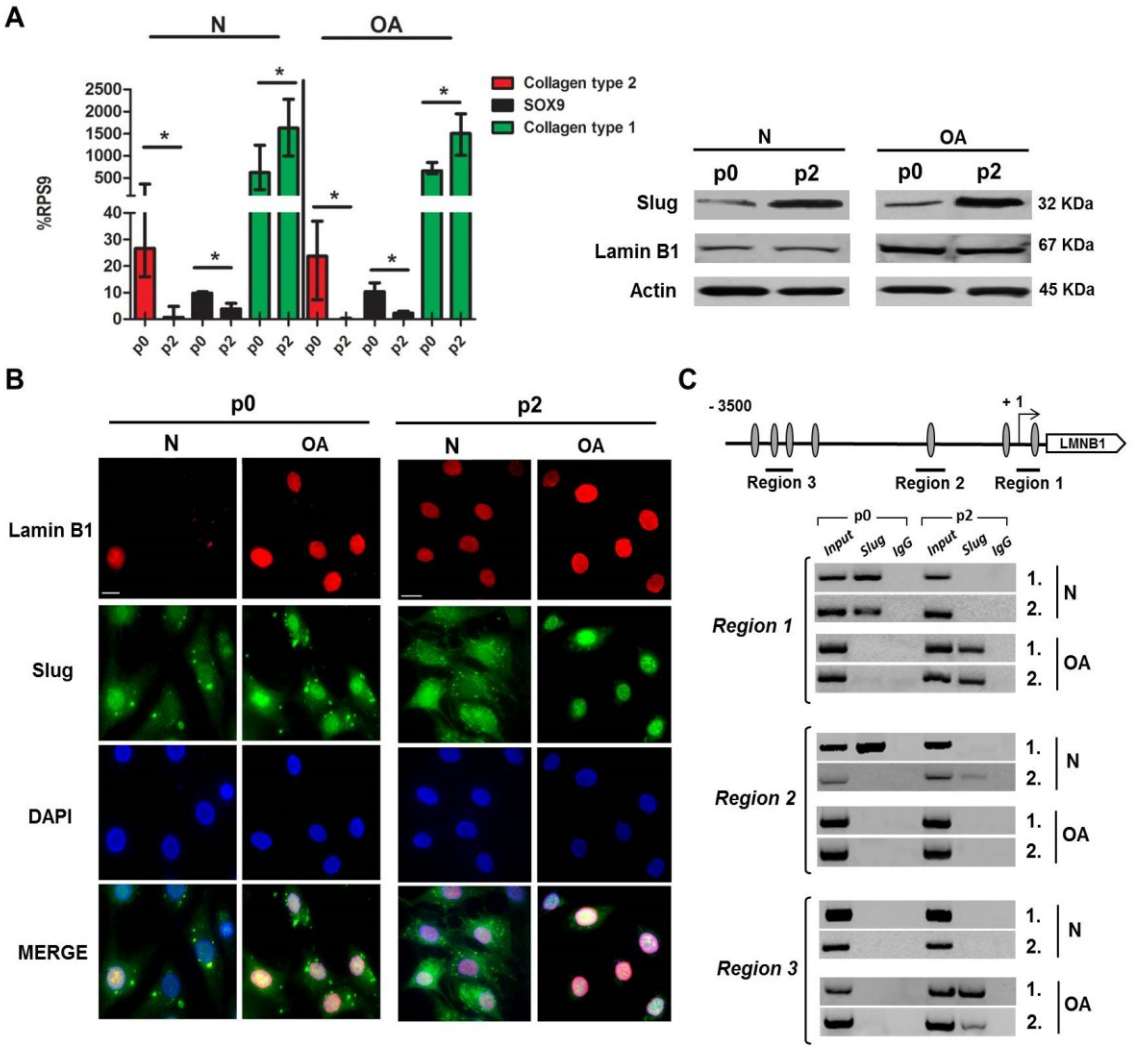

Figure 3. (A) Collagen type II, SOX9 and collagen type I expression levels were determined by qRT-PCR in p0 chondrocytes and p2 de-differentiated chondrocytes from healthy subjects (N) and OA patients. Real time PCR was run in a LightCycler Instrument (Roche Molecular Biochemicals, Mannheim, Germany) using the SYBR Premix Ex Taq (TaKaRa Biomedicals, Tokyo, Japan). For each target gene, mRNA levels were calculated, normalized to RPS9 according to the formula $2^{-\Delta Ct}$ and expressed as a percentage of the reference gene. Statistical analysis was performed comparing p0 to p2 chondrocytes, using non parametric Wilcoxon matched pair test. Significant differences *p< 0.05. Slug and Lamin B1 expression levels were determined by Western blotting in p0 chondrocytes and de-differentiated p2 chondrocytes from healthy subjects (N) and OA patients (OA). 20 µg of each samples were assayed on SDS-PAGE and proteins were visualized by ECL method (PIERCE). Actin was used as loading control. **(B)** Representative immunofluorescence analysis performed on p0 and de-differentiated p2 chondrocytes from healthy subjects (N) and OA patients (OA) using anti-Lamin B1 (red) and Slug (green) antibodies. Nuclei were counterstained with DAPI. Merge contains the combined image of Slug and Lamin B1 immunostaining and DAPI staining. Determinations were performed in triplicate in three independent cell cultures. Bar = 10 µm. **(C)** Schematic representation of the human LMNB1 promoter region; putative Slug binding sites are indicated with grey ovals. ChIP assay of *in vivo* Slug binding to the Lamin B1 proximal promoter was performed. DNA templates were obtained from

p0 chondrocytes and de-differentiated p2 chondrocytes from two healthy subjects (N) and two OA patients (OA). Immunoprecipitation was performed using an anti-Slug antibody or preimmune rabbit IgG. DNA samples of ChIP reactions (Slug, IgG) and Input DNA, collected before precipitation, were used in PCRs with different primer pairs and amplicons are reported: region 1 = 174 bp, region 2 = 189 bp, region 3 = 178 bp. Each PCR reaction was performed with 5 µl of the bound DNA fraction or 2 µl of the Input. PCR fragments were analyzed on 1.5% agarose gel.

By using the Transcription Element Search Software (TESS) for transcription factor search and MatInspector 7.4, we identified seven potential Slug binding sites (E-boxes, 5'-CANNTG/CANNTG-3') in the LMNB1 gene 5' regulatory region, six upstream and one downstream of the transcription start site. We focused on three chromatin subregions of the hLMNB1 promoter for *in vivo* E-box occupancy analysis. We observed Slug binding to regions 1 and 3 in p2 OA chondrocytes, whereas Slug was mostly recruited at region 1 and 2 in p0 normal chondrocytes (Fig. 3C). Concomitant binding of acetylated histone H3 (Ac-H3) confirmed the active transcription of the locus (data not shown).

Discussion

An effective strategy to prevent cartilage loss or treat cartilage diseases is still lacking. Therefore, the search for potential molecular targets that are involved in the mechanisms of pathogenesis represents an important challenge. In this study, we described for the first time the upregulation of Slug and Lamin B1 in both OA cartilage explants and *in vitro* de-differentiated chondrocytes, suggesting the implications of these molecules in two critical phenomena involved in the onset of OA, the loss of cell differentiation and the promotion of cellular senescence. We previously demonstrated that the inhibition of Slug, a transcriptional repressor of cartilage formation (*Goldring et al., 2006*), is effective in inducing chondrogenesis of mesenchymal stem cells (*Lolli et al., 2014*). Our data evidence that Slug is involved in chondrocyte senescence, possibly due to its *in vivo* recruitment at the promoter of the hLMNB1 gene. However, further studies will be needed to dissect the way Slug can accomplish its task. Our results suggest that Slug might drive the loss of chondrocytic phenotype through regulation of Lamin B1 expression and lead us to speculate that Slug inhibition in culture-expanded chondrocytes could prevent the de-differentiation process. Contrasting roles of Lamin B1 in cellular senescence have been described (*Hutchison, 2014*). Reduced levels of Lamin B1 have been observed in HGPS patient-derived fibroblasts and senescent normal fibroblasts *in vitro* (*Hutchison, 2014*).

In one report, Lamin B1 silencing led to apoptosis in HeLa cells (*Harborth et al., 2001*), whereas recent work suggested that inhibition of Lamin B1 causes senescence in WI-38 cells (*Dreesen et al., 2013*). Conversely, Lamin B1 overexpression appeared to enhance proliferation and delay the onset of senescence, whereas a second study showed that elevated levels of Lamin B1 triggered senescence (*Hutchison, 2014*). Our data demonstrate a marked increase of Lamin B1 in OA chondrocytes, in favor of the hypothesis of its association with tissue degeneration and senescence.

Tissue degeneration and senescence involve a plethora of mediators so it is difficult to establish a hierarchy of events. Therefore, the key question is whether Slug and Lamin B1 are upstream or downstream the OA pathogenetic process. However, the proof of the *in vivo* molecular relationship between these two proteins could help to identify potential mechanisms by which catabolic changes in the articular cartilage lead to the onset of OA, and to devise new approaches for the prevention and treatment of OA. Moreover, our findings may be useful to improve cell-based therapies that use chondrocytes, as the issues of cellular senescence and de-differentiation occuring during *in vitro* expansion likely represent the major practical barriers to the clinical application of these cells.

Chapter 4

Chondrogenic potential of Slug-depleted hMSCs

Outline of the work

Tissue engineering constructs for cartilage repair generally consist of a combination of biocompatible scaffolds, bioactive molecules and cells, most frequently chondrocytes and hMSCs, that need to be induced towards the chondrogenic lineage, thus leading to the production of cartilage ECM and tissue repair *in vivo*. The experimental work of this section of the project focused on the possibility to force the chondrogenic differentiation of bone marrow-derived hMSCs cultured onto a hyaluronan-based scaffold (HYAFF-11) by knocking down a negative regulator of chondrogenesis, the transcription factor (TF) Slug. Our data showed that the TGF-β driven chondrogenesis of hMSCs onto HYAFF-11 could be strengthened by treatment with a siRNA against Slug. Indeed, Slug silencing was effective in promoting the expression of the cartilage ECM proteins collagen type II and aggrecan, and the pro-chondrogenic transcription factors Sox9, Lef-1 and TRPS1. Our data showed that the HYAFF-11 scaffold not only is a good candidate for the use of hMSCs in cartilage tissue engineering, but also sustained the combination of TGF-β exposure with Slug silencing for the enhancement of the chondrogenic potential of hMSCs. Remarkably, preliminary results obtained using the hMSCs/HYAFF-11 experimental model here described confirmed that Slug silencing had a pro-chondrogenic effect even in the absence of differentiation supplements, such as TGF-β. Taken as a whole, our findings highlighted the potential use of Slug silencing in combination or as an alternative to TGF-β exposure for the induction of hMSCs chondrogenesis, and the critical role of Slug TF in determining the fate of hMSCs.

Introduction

Different approaches in regenerative medicine often use a combination of scaffolds, bioactive factors, and cells to induce the formation of the desired tissue within a specific defect site. In this scenario, tissue engineering of cartilage presents several challenges (*Mahmoudifar & Doran, 2012; Hollander et al., 2010; Vinatier et al., 2009a; Vinatier et al., 2009b; Anderer & Libera, 2002; Tang et al., 2012*). Indeed, the achievement of effective and sustained cartilage repair mediated by cell-based therapy has several limitations (*Johnstone et al., 2013; Oldershaw, 2012; Satija et al., 2007; Bianco et al., 2001; Johnstone et al., 1998*). These include the loss of the chondrogenic phenotype of *in vitro* cultured chondrocytes from healthy donors, and the phenotypic instability and unwanted premature hypertrophy of chondrogenically induced human mesenchymal stem cells (hMSCs) (*Steinert et al., 2007; Schnabel et al., 2002; Pelttari et al., 2006; Studer et al., 2012*). Therefore, in order to explore new approaches to produce cells useful for cartilage regeneration, we investigated the possibility to enhance the differentiation potential of hMSCs by depleting a transcription factor (TF) with a specific negative role in chondrogenesis. This approach could be effective to guide the differentiation of osteochondroprogenitors toward the chondrogenic lineage merely by delivering short interfering RNA (siRNA) against a specific TF. In particular, we assessed whether exposure of hMSCs to a siRNA against the Slug TF, in combination with TGF-β3, could improve chondrogenic differentiation onto a hyaluronan-based scaffold (HYAFF-11). We used HYAFF-11 as a three-dimensional (3D) structure able to ensure chondrogenic differentiation and to favor cellular transfection. The properties of this biodegradable biomaterial have been extensively described (*Lisignoli et al., 2005; Dehne et al., 2009; Pasquinelli et al., 2008; Fiumana et al., 2013; Cavallo et al., 2013*). HYAFF-11 is already used by clinicians as a scaffold for the reconstruction of cartilage defects in trauma patients (*Marcacci et al., 2002; Pavesio et al., 2003*). In addition, the feasibility of combining HYAFF-11 with hMSCs showed that this scaffold may have important applications for the treatment of early osteoarthritis in humans (*Cavallo et al., 2013; Benedetti et al., 1993; Grigolo et al., 2002; Grigolo et al., 2009*).

We hypothesized that the knockdown of Slug, a negative regulator of chondrocyte differentiation (*Goldring et al., 2006; Seki et al., 2003*), might promote an early onset of chondrogenic markers, thus allowing the optimization of hMSCs chondrogenesis as well as the formation of cells with a potential chondrocyte-like phenotype for transplantation purposes in cartilage defect healing.

In this study we described a 3D-culture system which anticipates and favors the chondrogenic differentiation of hMSCs from bone marrow, by silencing a specific TF such as Slug that is relevant to chondrogenic differentiation.

Materials and Methods

hMSCs isolation

Human bone marrow aspirates (n = 6) were harvested from the iliac crest during orthopedic surgery, after obtaining the patients' informed consent. hMSCs were isolated using Ficoll-Hypaque density gradient (d = 1.077 g/mL). The cells were grown in α-MEM medium supplemented with 15% FBS and penicillin-streptomycin (100 U/mL–100 mg/mL), counted, and plated at a concentration of 3 x 10^6 cells / T150 flask. After 48 h, non-adherent cells were removed and the adherent ones were expanded *in vitro*. The expression of hematopoietic and non-hematopoietic markers was analyzed using monoclonal antibodies anti-CD3, -CD14, -CD31, -CD34, -CD45 (DAKO Cytomation), -CD73, -CD90, -CD146 (Becton Dickinson), and -CD105 (produced from the hybridoma cell line, clone SH2; ATCC) to test the purity of the isolated cells by flow cytometric analysis, as previously described (*Torreggiani et al., 2012*).

Chondrogenic differentiation of hMSCs onto HYAFF-11 scaffold

2.5 x 10^5 hMSCs were seeded on a non-woven hyaluronan-based scaffold (HYAFF-11; Anika Therapeutics S.r.l.) in chondrogenic medium (DMEM high-glucose supplemented with ITS+ Premix: 6.25 µg/mL insulin, 6.25 µg/mL transferrin, 5.33 µg/mL linoleic acid, and 1.25 µg/mL bovine serum albumin (BSA), 100 nM dexamethasone, 50 µg/mL ascorbate-2 phosphate, 1 µM sodium pyruvate, and penicillin-streptomycin (100 U/mL–100 mg/mL) (Sigma) as previously reported (*Lisignoli et al., 2005*). 24 h later (day 0), samples were divided into four groups: (1) chondrogenic medium, (2) chondrogenic medium plus 50 nM siRNA against Slug (siSlug) combined with Lipofectamine RNAiMAX (Life Technology) according to the manufacturer's instructions, (3) chondrogenic medium supplemented with TGF-β3 (10 ng/mL; Miltenyi), and (4) chondrogenic medium with TGF-β3 plus 50 nM siSlug. Cell culture medium was refreshed twice a week. Chondrogenesis was analyzed on days 0, 14, 21, and 28. The nucleotide sequences of the siSlug pair are as follows: sense: 5'-CCCUGGUUGCUUCAAGGACAC AUUA-3', antisense: 5'-UAAUGUGUCCUUGAAGCAACCAGGG-3'. Control pellet

micromasses were prepared as previously described (*Seki et al., 2003*). Briefly, 2.5 x 10^5 hMSCs were suspended in 500 µL chondrogenic medium and centrifuged at 600 g for 5 min in 15-mL polypropylene conical tubes. Pelleted cells were incubated at 37°C under 5% CO_2 with loosened caps to permit gas exchange. Within 24 h of incubation, the sedimented cells formed a spherical aggregate at the bottom of each tube. The medium was refreshed every 3 days and pellets were harvested on day 28.

Human chondrocyte isolation

Human nasoseptal chondrocytes were isolated by enzymatic digestion with 2 mg/mL collagenase (Sigma c-2139) in Dulbecco's modified Eagle's medium (DMEM/F-12) for 12 h. Cell suspensions were filtered (70 mm) and cells were seeded in a 24-well plate (4 x 10^4 cells/well) in DMEM / F-12 supplemented with 10% FCS and penicillin/streptomycin. Cultures were maintained at 37°C in a humid atmosphere with 5% CO_2 and the medium was refreshed every 3 days. The cells were monitored for mRNA expression at the first passage.

Immunohistochemical analysis

The scaffold–cell cultures were fixed in 2% paraformaldehyde in 0.1M PBS buffer (pH 7.4) for 3 h, washed in PBS containing 6.8% sucrose, dehydrated in acetone at 4°C, and embedded in glycometacrylate (Technovit). Sections were dried at room temperature and immunohistochemical procedures were used to evaluate the expression of collagen type 1, type 2, and type 10 and aggrecan. Briefly, for collagen type 1, type 2, and type 10 and aggrecan an enzymatic pretreatment with hyaluronidase 0.1% (Sigma) at 37°C for 10 min was performed. The slides were incubated for 60 min at room temperature with monoclonal anti-human CD73 (Abcam), CD90 (Becton Dickinson), Slug (Origene), collagen type 1, collagen type 2, collagen type 10, and aggrecan (Millipore Corporation) diluted 1:100, 1:100, 1:150, 1:40, 1:20, 1:50, and 1:50, respectively, in PBS containing 1% BSA; rinsed in PBS; and then sequentially incubated at room temperature for 20 min with multilinker biotinylated secondary antibody (Biocare Medical) and alkaline phosphatase-conjugated streptavidin (Biocare Medical). The reactions were developed using fast red substrate (Biocare Medical), counterstained with hematoxylin, and mounted in glycerol gel. The sections were evaluated using a bright-field microscope (Nikon Instruments Europe BV). Negative and isotype-matched controls were performed. For light microscopy analysis, toluidine blue/aggrecan-positive areas located on the border of the scaffolds were analyzed by two independent observers (G.L. and N.Z.). At least four sections from each

of the different thicknesses of the scaffold were analyzed using the Bern score (*Grogan et al., 2006*). At the same time the evaluation considered (1) uniformity and darkness of the staining (0 = no staining, 1 = weak staining of poorly formed matrix, 2 = moderately even staining, 3 = even dark staining), (2) the amount of extracellular matrix (ECM) (0 = high cell density with no matrix, 1 = high cell density with little matrix in between, 2 = moderate cell density with matrix, 3 = low cell density with moderate distance between cells and extensive matrix), and (3) cellular morphologies represented (0 = condensed, necrotic, pycnotic bodies, 1 = spindle fibrous, 2 = mixed spindle/fibrous with rounded chondrogenic morphology, 3 = majority rounded/chondrogenic). The minimum score was 0 and the maximum was 9.

Light and electron microscopy analysis

On days 14, 21 and 28, scaffold–cell cultures were fixed in 2.5% glutaraldehyde in 0.1M cacodilate buffer (pH 7.4) for 3 h, post-fixed with 1% osmium tetroxide, dehydrated in a graded series of ethanol, and embedded in Epon. Cross-sections of each scaffold were cut to allow internal analysis. Semi-thin sections were stained with toluidine blue to define the area that would be analyzed by electron microscopy. Thin sections were stained with tannic acid, uranyl acetate, and lead citrate, and observed with a Zeiss 109 Electron microscope.

Quantitative reverse-transcriptase PCR analysis

Total RNA was extracted on days 0, 14, 21 and 28 using RNA PURE reagent (Euroclone S.p.a.) according to the manufacturer's instructions, and then treated with DNase I (DNA-free Kit; Ambion). Reverse transcription was performed using SuperScript VILO (Invitrogen Life Technologies) reverse transcriptase and random hexamers, following the manufacturer's protocol. Quantitative reverse-transcriptase PCR (qRT-PCR) was carried out using the CFX96^{TM} PCR detection system (Bio-Rad). For quantification of the target genes collagen type 2 (Col2A1), aggrecan, collagen type 1 (Col1A1), MMP-13, Slug, Sox9, LEF1, and TRPS1, the appropriate TaqMan probes were purchased from Life Technologies (see supplementary Table 1). mRNA levels were normalized to GAPDH according to the formula $2^{-\Delta\Delta Ct}$ and scaled relative to day-0 expression levels. Data are shown as average of technical triplicates of six hMSCs samples.

Statistical analysis

Statistical analysis was performed using mainly non-parametric tests since the data did not have a normal and strongly asymmetric distribution (Wilcoxon paired tests calculated with the exact method for small groups). W-Kendall non-parametric test was used to evaluate the trend. Values were expressed as the median and interquartile range or as mean±s.e.m. depending on the distribution. CSS Statistical Software (Statsoft, Inc.) was used for analysis and p-values≤0.05 were considered significant.

Results

Knockdown of Slug in hMSCs grown onto HYAFF-11

Experimental conditions were optimized for hMSCs cultured on HYAFF-11 to ensure both chondrogenic differentiation and cellular transfection. First, we found that hMSCs grown onto HYAFF-11 (indicated as hMSC/HYAFF-11) were not able to differentiate as a mere effect of scaffold biological/physical factors. In fact, as reported in Fig. 1A, only in the presence of TGF-β3 the cells onto HYAFF-11 (indicated as hMSC/HYAFF-11/TGF-β3) were able to produce sulfated glycosaminoglycans (GAGs), a major component of cartilage matrix, as well as in standard pellet cell culture. Second, Slug TF expression was evaluated and, consistent with the authors' previous studies (*Torreggiani et al., 2012*), it was maintained consistently high in undifferentiated hMSCs (Ctr) from day 0 to 28. In hMSC/HYAFF-11/TGF-β3, Slug expression decreased to levels that were comparable to those of chondrogenically induced hMSCs in the pellet (Fig. 1B). However, in both cases a substantial level of Slug expression was found in comparison with that present in chondrocytes (Fig. 1B). This suggested that TGF-β3 exposure of hMSCs was not sufficient to fully abolish the expression of a negative regulator of chondrogenesis like Slug. This observation led us to perform Slug knockdown, in order to exploit the full differentiation potential of the cells, and explore a new approach to improve chondrogenic differentiation of hMSCs. To this purpose, Slug silencing was performed on both hMSC/HYAFF-11 and hMSC/HYAFF-11/TGF-β3 by using a specific siRNA against Slug (siSlug). As shown in Fig. 1C, at day 28 of culture a high efficiency of Slug silencing was achieved (about 85%). Immunostaining for Slug confirmed a strong decrease of the protein in silenced cells (Fig. 1D).

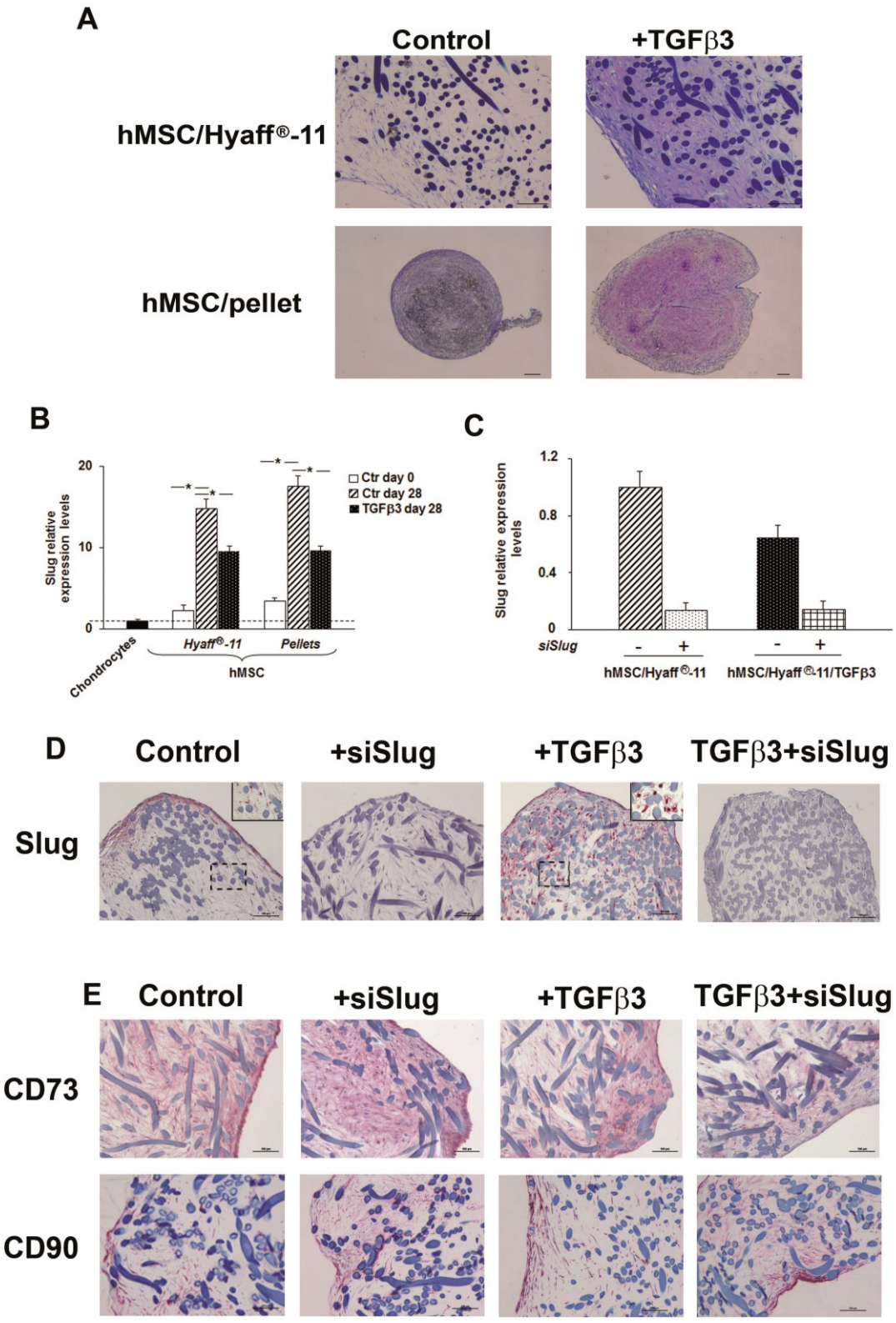

Figure 1. *hMSCs chondrogenic differentiation and Slug expression.* **(A)** hMSCs were cultured onto HYAFF-11 scaffold or in pellets in chondrogenic medium supplemented or not with TGF-β3 for 28 days. Toluidine blue staining of glycometacrylate-embedded sections revealed GAGs production (scale bar = 100 μm). **(B)** qRT-PCR analysis of Slug mRNA expression on freshly isolated chondrocytes and chondrogenically induced hMSCs cultured onto HYAFF-11 or in pellets. Results are expressed as fold change with respect to Slug

levels in human chondrocytes. Data are shown as mean±s.e.m. of four samples (*p≤0.05). **(C)** Efficiency of Slug knockdown on hMSCs grown onto HYAFF-11 scaffold. hMSCs were treated with 50 nM siSlug for 28 days in the presence or absence of TGF-β3. Slug mRNA levels were measured by qRT-PCR, normalized to GAPDH and expressed as fold change with respect to hMSC/HYAFF-11 untreated cells. **(D)** Immunohistochemical analysis of Slug on hMSCs cultured onto HYAFF-11 scaffold in chondrogenic medium supplemented or not with TGF-β3, with or without siSlug treatment for 28 days. Fibers and negative cells display a blue staining whereas positive cells display a red staining. Scale bars = 100 μm. The rectangles indicate the area shown at higher magnification (inset, scale bars = 10 μm). **(E)** Immunohistochemical analysis of CD73 and CD90 markers of stemness on hMSCs cultured onto HYAFF-11 scaffold in chondrogenic medium supplemented or not with TGF-β3, with or without siSlug treatment for 28 days. Fibers and negative cells display a blue staining whereas positive cells display a red staining. Scale bars = 100 μm.

In all conditions (Control, si-Slug, TGF-β3, and TGF-β3+siSlug), the analysis of CD90 and CD73 expression at the end point of culture (Fig. 1E) revealed some cell positivity, indicating that a stem cell phenotype is partly retained. This suggests that a reservoir of cells that are potentially responsive to differentiating stimuli is maintained.

Effect of Slug knockdown on hMSCs chondrogenic differentiation

We then compared the chondrogenic differentiation ability of the cells cultured in the presence of TGF-β3 or TGF-β3 and siSlug by analyzing their morphological features. As previously reported (*Lisignoli et al., 2005*), Toluidine blue staining performed on glycometacrylate-embedded thin sections revealed that hMSCs arranged mainly at the border of the scaffold, assumed a rounded chondrocyte-like cell morphology, and underwent chondrogenic differentiation (Fig. 2A), as confirmed by the positive red proteoglycan area mainly in TGF-β3+siSlug-treated cells. Electron microscopic analysis showed that cell differentiation induced the secretion of an extensive ECM, which assembled around the cells (Fig. 2B). Interestingly, ECM production was particularly abundant when TGF-β3 exposure was combined with Slug knockdown.

Slug knockdown differently modulates chondrogenic, fibrotic, and hypertrophic markers

We investigated the effect of Slug silencing on TGF-β3-mediated hMSCs chondrogenesis by analyzing the modulation of the expression of aggrecan, collagen types 2, 1, and 10, as typical chondrogenic, fibrotic, and hypertrophic markers, respectively. Toluidine blue staining and immunohistochemical analysis helped us identify the protein expression in the areas displaying cells with a specific chondrocyte-like morphology.

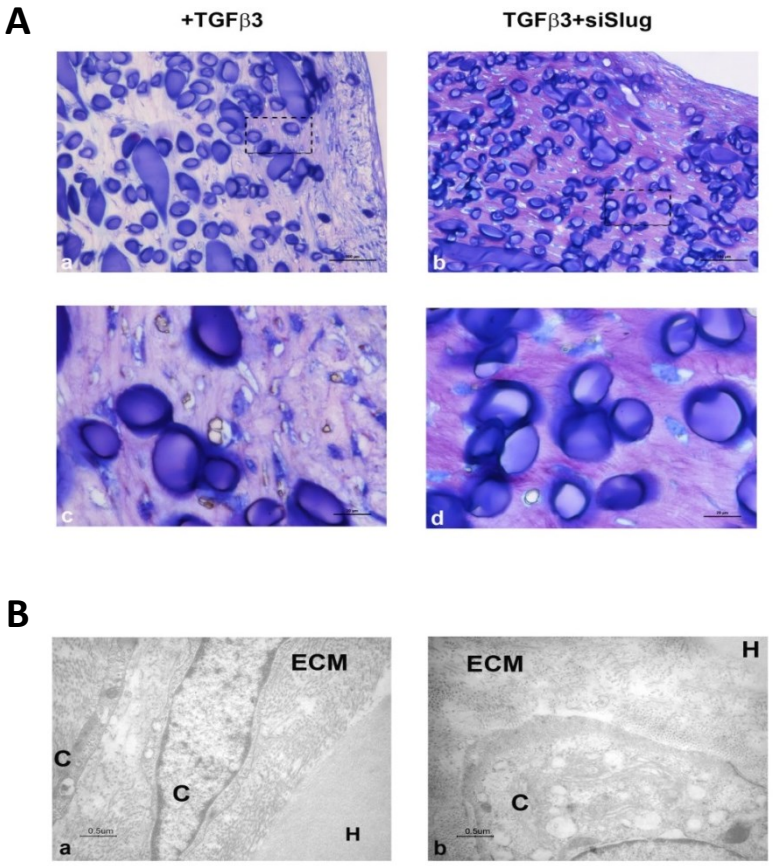

Figure 2. *Effects of Slug silencing on chondrogenesis of hMSCs grown onto HYAFF-11 scaffold.* **(A)** Toluidine blue-stained sections of hMSCs grown onto HYAFF-11 scaffold in the presence of TGF-β3, with or without siSlug treatment for 28 days. Cells with a chondrocyte-like morphology were observed mainly in the TGF-β3+siSlug condition. Pictures are shown at two different magnifications (scale bars = 100 µm, a, b; a rectangle indicates the area shown at a higher magnification, scale bars = 20 µm, c, d). **(B)** Electron microscopy showed cells with a round morphology surrounded by extracellular matrix (ECM), at day 28. ECM was particularly abundant for TGF-β3+siSlug-treated cells (b) than in TGF-β3-induced cells (a). Scale bars = 0.5 µm. C = cells, H = HYAFF-11.

A semiquantitative analysis on the toluidine blue/aggrecan-positive areas, using the Bern scoring system, showed that Slug silencing significantly accelerated hMSCs chondrogenesis, thus increasing the accumulation of sulfated proteoglycans starting from day 14 until day 28 ($p = 0.02$) (Fig. 3A). In particular, TGF-β3 exposure associated with Slug silencing caused, in each sample analyzed, a more positive staining for both aggrecan and collagen type 2 with respect to the TGF-β3 only condition (Fig. 3B). Conversely, chondrogenically differentiated areas were almost completely negative to collagen types 1 and 10. Therefore, despite the heterogeneity of the cell population among the donors, the hMSC samples showed a very similar trend of response to treatment.

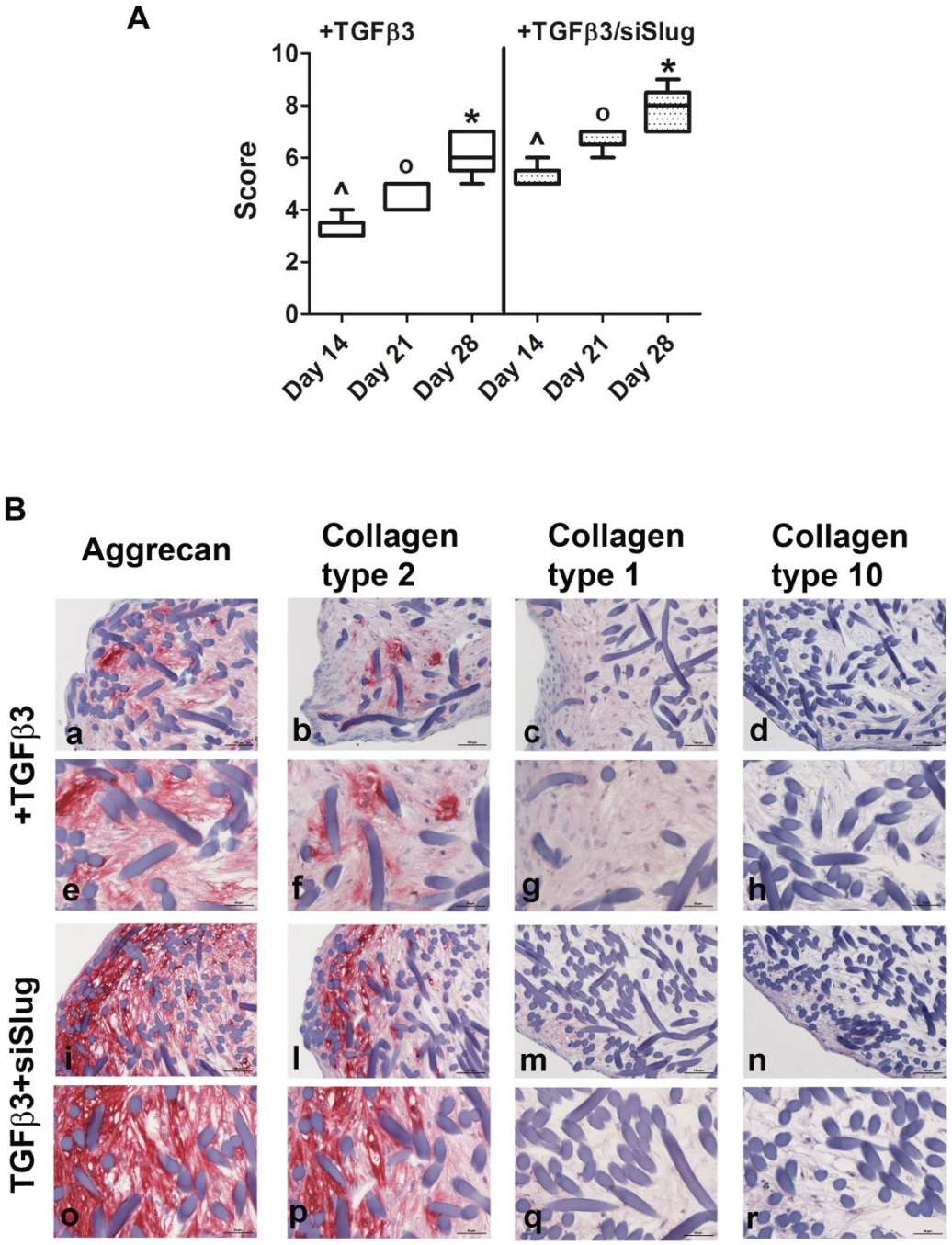

Figure 3. *Effects of Slug silencing on chondrogenic, fibrotic, and hypertrophic markers.* **(A)** Semiquantitative analysis of toluidine blue/aggrecan-positive area using the Bern scoring system on six hMSCs samples cultured onto HYAFF-11 scaffold in the presence of TGF-β3, with or without siSlug treatment for 14, 21, and 28 days. Data are shown as median and interquartile range. Significant differences between untreated and siSlug-treated hMSCs at day 14 (^p = 0.02), day 21 (^{o}p = 0.02), and day 28 (*p = 0.02). **(B)** Immunohistochemical analysis of aggrecan (a, e, i, o), collagen type 2 (b, f, l, p), type 1 (c, g, m, q), and type 10 (d, h, n, r) on hMSCs cultured onto HYAFF-11 scaffold in the presence of TGF-β3, with or without siSlug treatment for 28 days. Fibers and negative cells show a blue staining, whereas positive cells show a red staining. Pictures are shown at two different magnifications (Scale bars = 100 µm (a, b, c, d, i, l, m, n), 50 µm (e, f, g, h, o, p, q, r)).

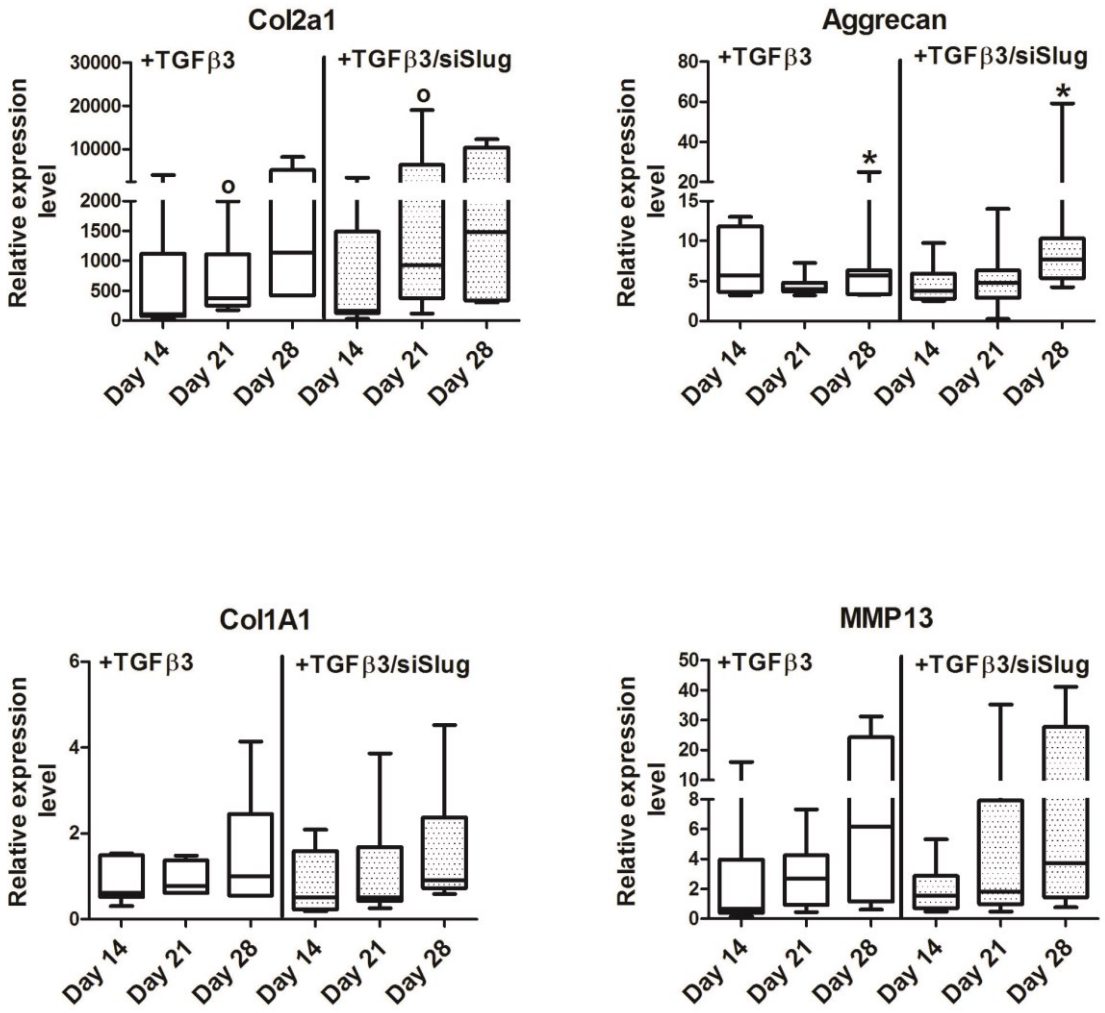

Figure 4. qRT-PCR analysis of Col2A1, aggrecan, Col1A1, and MMP13 mRNA expression during chondrogenesis of hMSCs cultured on HYAFF-11 scaffold in the presence of TGF-β3, with or without siSlug treatment for 14, 21, and 28 days. Gene expression levels were scaled relative to day-0 expression levels. Data are shown as median and interquartile range. Significant differences between untreated and siSlug-treated hMSCs at day 21 (op = 0.01) and day 28 (*p = 0.04).

This was confirmed at mRNA level by qRT-PCR. As shown in Fig. 4, the combination of TGF-β3 exposure and Slug silencing was particularly effective at increasing the expression of aggrecan and Col2A1. In particular, the combined statistical analysis of chondrogenic marker (Col2A1 and aggrecan) trends showed a significant increase for TGF-β3+siSlug-treated samples on days 21 ($p = 0.01$) and 28 ($p = 0.04$), respectively. Interestingly, the mRNA levels of a hypertrophic marker like MMP13, a key collagen degrading-matrix metalloproteinase, decreased after Slug knockdown.

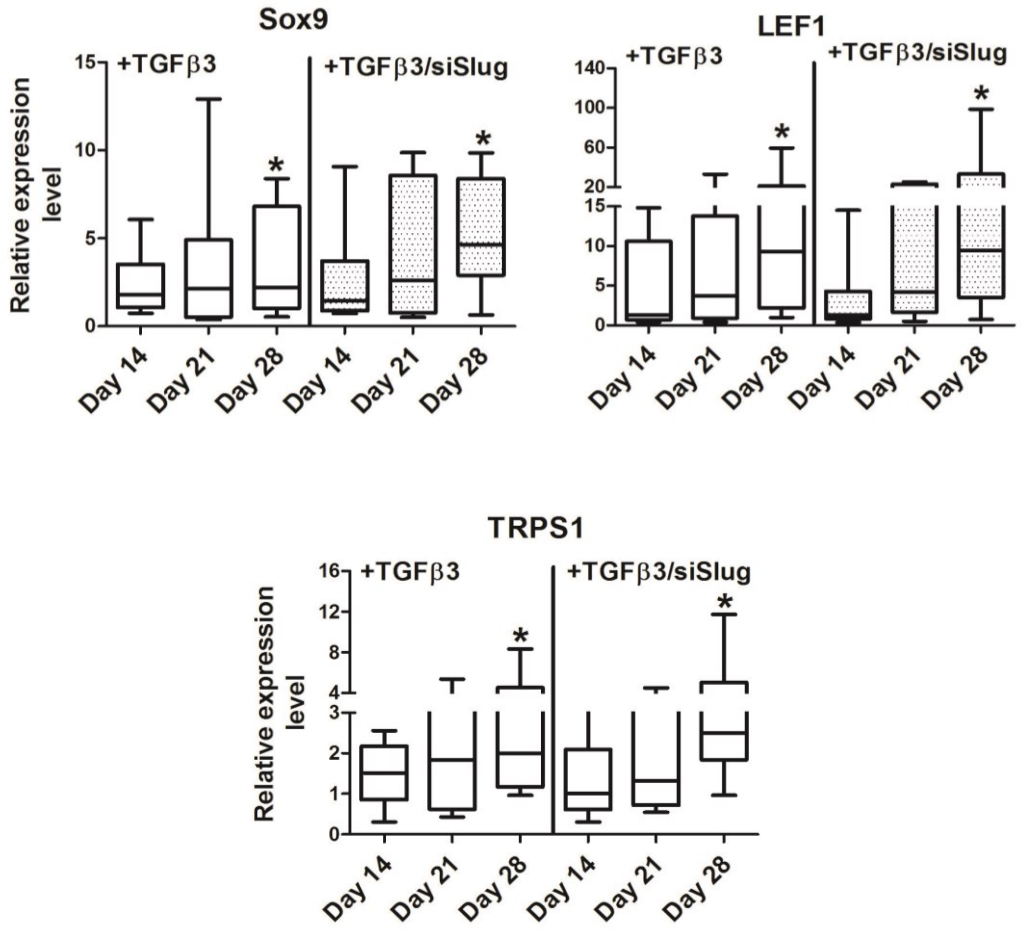

Figure 5. *Effects of Slug silencing on specific transcription factors involved in chondrogenesis.* qRT-PCR analysis of Sox9, LEF1, and TRPS1 mRNA expression during chondrogenesis of hMSCs cultured on HYAFF-11 scaffold in the presence of TGF-β3, with or without siSlug treatment for 14, 21, and 28 days. Gene expression levels were scaled relative to day-0 expression levels. Data are shown as median and interquartile range. Significant differences between untreated and siSlug-treated hMSCs at day 28 (*p = 0.03).

Slug knockdown affects TFs involved in chondrogenesis

The analysis then focused on the effect of Slug silencing on the expression of those TFs that are responsible for the regulation of the previously investigated chondrogenic markers. These include Sox9, the master regulator of some of the key genes in chondrogenesis; lymphoid enhancer-binding factor-1 (LEF1), a positive regulator for Col2A1 expression during the normal process of chondrocyte differentiation; and tricho-rhino-phalangeal syndrome type 1 factor (TRPS1), a regulator of chondrocyte proliferation and differentiation.

As shown in Fig. 5, the combination of TGF-β3 exposure and Slug silencing generally promoted the expression of these TFs, thus suggesting that the effect of Slug silencing in enhancing chondrogenesis is mediated by the depletion of an upstream negative effect exerted by Slug on chondro-stimulatory regulators. Combined statistical analysis of Sox9, LEF1, and TRPS1 trends showed a significant increase ($p = 0.03$, 0.03, and 0.05, respectively) for TGF-β3+siSlug-treated samples at day 28.

Slug knockdown guides hMSCs toward chondrogenesis in the absence of TGF-β3

Finally, in order to specifically assess the role of Slug in the chondrogenic differentiation of hMSCs, the effect of siRNA-mediated knockdown of Slug was analyzed after 28 days of culture without TGF-β3. Detectable phenotypic evidence of chondrogenesis was observed in cells that received siSlug only. Toluidine blue staining of glycometacrylate-embedded sections revealed a greater cellularity and rounded chondrocyte-like cells after siSlug treatment, in comparison with untreated cells (Fig. 6A), and a positive staining for proteoglycans could be appreciated. The differentiation grade, evaluated by the Bern scoring system, showed a significant ($p = 0.03$) efficacy of siSlug treatment in inducing the accumulation of aggrecan also in the absence of TGF-β3 (Fig. 6B) from days 14 to 28, suggesting that anticipation of matrix production and deposition may be favored by Slug knockdown. Gene expression analysis by qRT-PCR (Fig. 6C, D) revealed that Slug knockdown alone induced a significant upregulation of Col2A1 ($p = 0.013$), Sox9 ($p = 0.015$), and LEF1 ($p = 0.039$), thus providing important evidence of chondrogenic differentiation at mRNA level. siSlug treatment alone did not affect aggrecan, Col1A1, MMP13, or TRPS1 mRNA levels. Altogether, the present findings suggest that the transition from an undifferentiated hMSCs status to chondrogenic commitment may be influenced by Slug knockdown, and that Slug depletion may be sufficient to direct the cells toward the chondrogenic lineage.

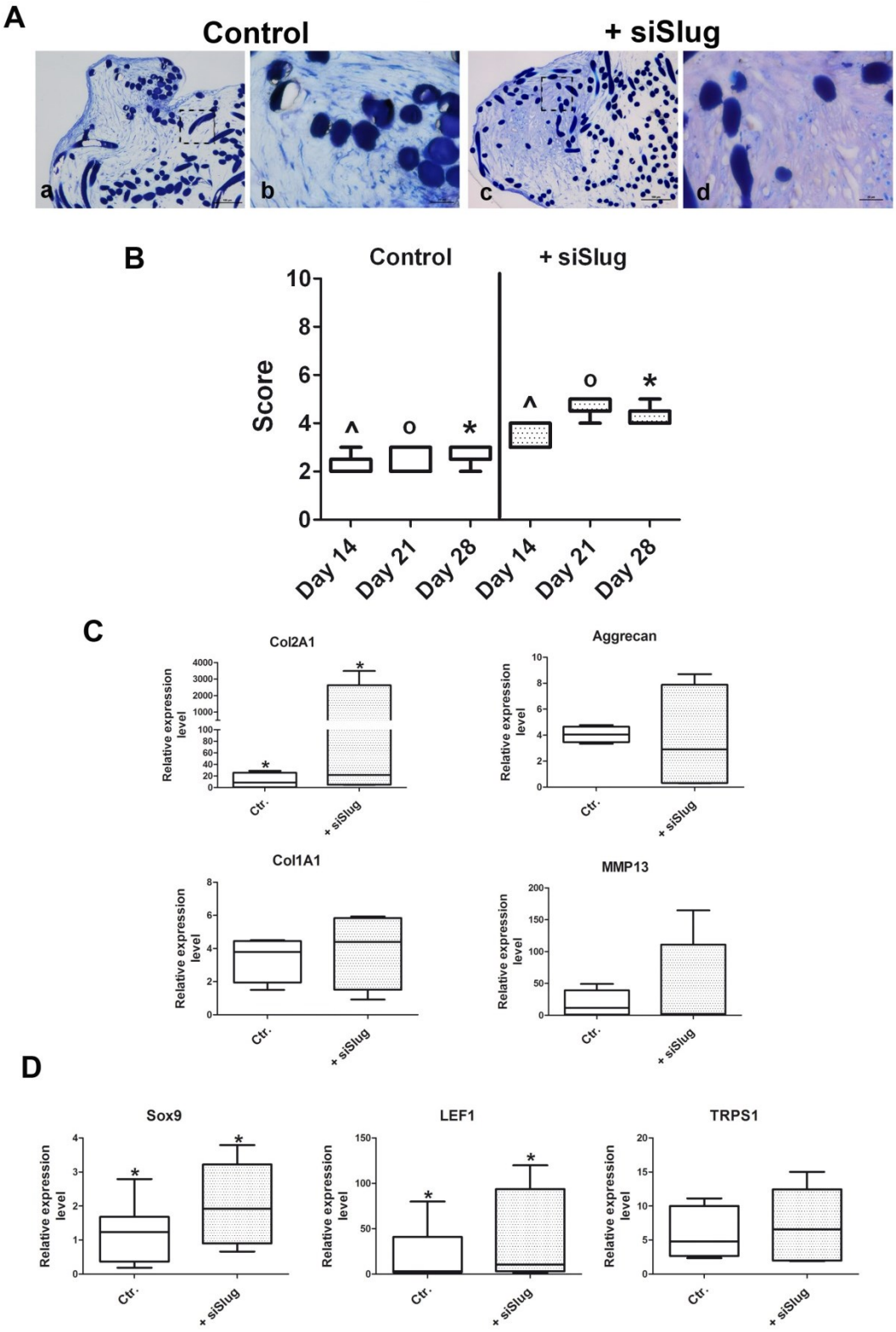

Figure 6. *Slug-silenced hMSCs grown onto HYAFF-11 in the absence of TGF-β3*. **(A)** Toluidine blue staining of sections of hMSCs grown onto HYAFF-11 scaffold with (+siSlug, c, d) or without (Control, a, b) siSlug treatment, in the absence of TGF-β3 for 28 days. Cells with a chondrocyte-like morphology were observed after siSlug treatment. Pictures are shown at two different magnifications (scale bars = 100 µm (a, c); a rectangle indicates the areas shown at a higher magnification, scale bars = 20 µm (b,d)). **(B)** Semiquantitative analysis of aggrecan-positive areas using the Bern scoring system on six hMSCs samples

cultured onto HYAFF-11 scaffold with (+siSlug) or without (Control) siSlug treatment, in the absence of TGF-β3 for 14, 21, and 28 days. Data are shown as median and interquartile range. Significant differences between untreated and siSlug-treated hMSCs at day 14 (^p = 0.03), day 21 (^{o}p = 0.03), and day 28 (*p = 0.03). Expression analysis of the chondrogenic markers Col2A1, aggrecan, Col1A1, and MMP13 **(C)** and the transcription factors Sox9, LEF1 and TRPS1 **(D)**. mRNA levels were assessed by qRT-PCR in hMSCs cultured onto HYAFF-11 scaffold with (+siSlug) or without (Ctr.) siSlug treatment for 28 days. mRNA levels were scaled relative to day-0 expression levels. Data are shown as median and interquartile range. Significant differences between untreated and siSlug-treated hMSCs for Col2A1 (*p = 0.013), Sox9 (*p = 0.015), and LEF1 (*p = 0.039).

Discussion

In the field of hMSCs-based cartilage tissue engineering, several approaches have been proposed to improve and optimize the chondrogenic potential of hMSCs. These include (1) well-defined media containing soluble factors, e.g. TGF-β, BMPs, IGF1, and FGF-2 (*Penick et al., 2005; Huang et al., 2008*); (2) mechanical stimulation (*Palomares et al., 2009*); (3) hypoxia (*Xu et al., 2007; Lee et al., 2013*); (4) transfection of hMSCs with growth factor genes (*Guo et al., 2007; Palmer et al., 2005*); (5) co-culture techniques of hMSCs and chondrocytes (*Fischer et al., 2010; Bian et al., 2011*); and (6) the employment of different types of porous scaffolds and biofunctional constructs (*Seo & Na, 2011*). Although promising, the outcomes are not always satisfactory and the induced chondrogenic differentiation often exhibits some drawbacks, including instability of the chondrocytic phenotype and lack of proper ECM secretion. To date, unique systems able to address both "cartilage damage" and "cartilage degeneration" have not been found. Recently, alternative cell differentiation protocols based on RNAi technology and aimed at downregulating the expression of specific TFs or microRNAs have been proposed (*Palmer et al., 2005; Handorf & Li, 2011; Ríos et al., 2012; Bobick et al., 2010; Wang et al., 2010; Zhang et al., 2010; Gordeladze et al., 2008; Gibbons et al., 2013; Barzilay et al., 2009*). To explore this strategy, we tried to guide the differentiation of hMSCs by a siRNA against the Slug TF, a negative regulator of chondrogenesis (*Goldring et al., 2006; Seki et al., 2003*). We chose to test our hypothesis on hMSCs seeded onto HYAFF-11 scaffold, because the hMSC/HYAFF-11 construct previously proved to be efficient in supporting cell survival, proliferation, and differentiation in the presence of specific inducers that promote the production of an ECM rich in collagen and proteoglycans (*Lisignoli et al., 2005; Vindigni et al., 2009*). In addition, the cells are able to adhere to the fibers of the scaffold and are arranged on the biomaterial in a way that may make them more easily

transfectable. Indeed, cells cultured in a standard pellet or micromass are usually hard to transfect, and this may lead to a highly heterogeneous cell response. On the contrary, using this experimental approach based on hMSC/HYAFF-11 constructs, we were able to obtain an efficient siRNA-mediated gene knockdown during the progression of chondrogenesis up to 28 days, thus showing that TGF-β3 exposure associated with Slug silencing improves the chondrogenic potential of hMSCs.

These data supported the concept that a low Slug expression is an important pre-requisite for chondrogenic induction, and strengthens our hypothesis about the pro-chondrogenic effect of Slug silencing, as we previously suggested for two dimensional (2D)-cultured hMSCs (*Lisignoli et al., 2005; Lambertini et al., 2009*). However, in the previous studies, we failed to show a clear differentiation potential of such treatment in hMSCs grown in 2D. On the other hand, using TGF-β3-induced hMSCs combined with HYAFF-11 scaffold, we showed that 3D culture exposed the cells to Slug knockdown with an increase of (1) the expression of an early pivotal TF in chondrogenesis, Sox9, and (2) the expression of Col2A1 and aggrecan, the major structural proteins of cartilage. Moreover, we showed that typical hypertrophic (collagen type 10) and fibrotic markers (collagen type 1) were not expressed in the chondrogenic area, thus confirming that Slug silencing may better induce hMSCs chondrogenic differentiation.

Although currently we have no data on the levels of protein expression due to the reduced number of histological sections available, the preliminary data regarding the effect of si-Slug treatment alone led to an important observation. In fact, as shown in Fig. 6, Slug silencing alone without TGF-β3 had a pro-chondrogenic effect in hMSCs. This evidence supports the critical role of the Slug TF in determining hMSCs fate, and the potential use of siSlug as an alternative strategy to TGF-β exposure. Interestingly, we also previously found that Slug expression was not completely abolished in hMSCs induced toward chondrogenesis by TGF-β3 supplementation (*Brini et al., 2013*). These data raise questions about the relationship between TGF-β signaling and Slug during chondrogenic differentiation. In fact, it is well established that TGF-β plays a key role in inducing chondrogenic differentiation in hMSCs cultured in a 3D system, by stimulating the expression of chondrogenic markers. However, at the same time, TGF-β signaling highly increases Slug expression in well-defined processes, such as embryonic development and tumor progression (*Yang & Weinberg, 2008*). Hence, it is necessary to investigate in further detail the TGF-β/Slug relationship in chondrogenesis, considering that the TGF-β positive effect on chondrogenic differentiation can be counteracted by the TGF-β-mediated upregulation of Slug that, conversely, slows down chondrogenesis. These preliminary data

suggest that undifferentiated hMSCs are able to undergo chondrogenesis when depleted of Slug. At this point it becomes critical to understand which strategy, TGF-β exposure or Slug silencing, may be more effective at promoting chondrogenesis and enhancing the differentiation potential of hMSCs *in vivo*, and further experiments need to be performed.

Taken together, the present findings may be relevant in the field of siRNA technology as a tissue engineering tool to directly modulate the bone/cartilage regenerative process (*Palmer et al., 2005; Ríos et al., 2012; Wang et al., 2010; Zhang et al., 2010; Gordeladze et al., 2008; Gibbons et al., 2013; Barzilay et al., 2009; Jash et al., 2012; Nooeaid et al., 2012; Piersanti et al., 2010*).

In particular, the quality of the generated ECM suggests that Slug silencing could replace TGF-β in producing cartilaginous tissue, and that Slug-silenced hMSCs/HYAFF-11 without differentiating agents may be proposed for tissue regeneration in bone disorders where the recruitment or differentiation potential of hMSCs is compromised. However, additional work will be needed to fully characterize the combination Slug-silenced hMSCs/HYAFF-11 as a valid alternative approach to differentiated chondrocytes for cartilage repair and regeneration. In particular, we are pursuing an in-depth study of the characteristics of the HYAFF-11 scaffold as a nucleic-acid-based drug delivery system, and its effectiveness in healing focal cartilage defects *in vivo*.

Supplementary materials

Gene symbol	*Gene name*	*TaqMan assay no.*
Col2A1	Type II collagen	Hs00264051_m1
Col1A1	Type I Collagen	Hs00164004_m1
ACAN	Aggrecan	Hs00153936_m1
MMP13	Matrix metallopeptidase 13	Hs00233992_m1
Sox9	SRY (sex determining region Y)-box9	Hs00165814_m1
Slug	Snail homolog 2 (Drosophila)	Hs00950344_m1
TRPS1	Trichorhinophalangeal syndrome I	Hs00936363_m1
Lef1	Lymphoid enhancer-binding factor 1	Hs01547250_m1

Supplementary Table 1. *TaqMan gene expression assays used in this study*.

Chapter 5

A 3D-dynamic osteoblasts-osteoclasts co-culture model to simulate the jawbone microenvironment in vitro

Outline of the work

The research on bone diseases and osteochondral lesions highlights the need for reliable experimental models that may faithfully recapitulate *in vitro* the bone microenvironment, thereby providing a platform for the development of novel strategies for tissue regeneration. Taking into account that, at its simplest level, the production of bone mineralized tissue requires the presence of osteoblasts (hOBs) and osteoclasts (hOCs) enclosed in a structured matrix, much effort is focused on the set-up of specific simplified *in vitro* hOBs/hOCs co-culture systems. Here we aimed to establish a 3D hOBs/hOCs co-culture system requiring limited amounts of human primary cells and that could serve as a platform to 1. recapitulate an "oral bone microenvironment" in healthy or pathological conditions, and 2. produce potentially implantable cell constructs for regeneration of jawbone which can be negatively affected by bisphosphonates. To this aim, hOBs from healthy bone or jawbone of patients taking BPs (hnOBs) were co-cultured with monocytes (hMCs) either in static (3D-C) or dynamic (3D-DyC) condition using the RCCS-4™ bioreactor. We showed that hOBs supported the formation of mature osteoclasts (hOCs), without requiring differentiating agents or exogenous scaffolds. 3D-DyC condition associated with a ground based condition (Xg) rather than modeled microgravity (μXg) produced aggregates exhibiting features of mineralized bone matrix. Importantly, hnOBs co-cultured with monocytes in 3D-Dyc/Xg condition generated OPN- and mineral matrix-positive aggregates as well. As a whole, we optimized a 3D co-culture system with a limited amount of cells preserving viability and functionality of bone cellular components and generating bone-like aggregates even using cells from jawbone necrotic tissue. We postulate that the feasibility to obtain viable cells from sites of bone degeneration and form aggregates by co-culture with hMCs will support the development of autologous implantable constructs to overcome jawbone deficiency in patients, such as in the case of MRONJ (Medication-Related Osteonecrosis of the Jaws).

Introduction

A plethora of three-dimensional (3D) co-culture systems have been developed during the last decade in the effort to recreate the physiological cellular microenvironment of a specific tissue, and extend cell culture longevity and functionality (*Kaji et al., 2011; Knight & Przyborski, 2014; Sekine et al., 2013*).

Regarding the bone tissue, several *in vitro* co-culture systems based on bone-forming cells (osteoblasts, OBs) and bone-resorbing cells (osteoclasts, OCs) have been proposed (*Bloemen et al., 2009; Gamblin et al., 2014; Heinemann et al., 2011; Jones et al., 2009; Kuttenberger et al., 2013; Widbiller et al., 2015*), with the aim of creating the Basic Multicellular Unit (BMU). Different parameters such as cell sources and culture conditions may influence the establishment of the complex interactions and intimate crosstalk that naturally occur *in vivo* between OBs, OCs and their precursors (*Sims & Martin, 2014; Tortelli et al., 2009; Papadimitropoulos et al., 2011; Halai et al., 2014*). To make the results of these studies the most informative and reproducible, the majority of the evidence were so far obtained using a substantial number of cells that could guarantee the formation of an appreciable cellular aggregate. For this reason cell lines, such as MC3T3-E1, MG63 and SaOS-2 for the osteoblastic lineage, and RAW264.7 for the osteoclast lineage are widely used. However, cell lines often fail to mimic the primary counterparts.

Considering the osteoclastic lineage, peripheral blood mononuclear cells (PBMCs), bone marrow and spleen-derived cell populations are good options for the obtainment of an adequate amount of primary OCs (*Zhang & Huang, 2012; Jacome-Galarza et al., 2013*). Setting up abundant primary cultures of OBs from human tissues is more challenging. In many cases a limited number of precursors or mature cells from a given source can be obtained with a noninvasive procedure and, consequently, few cells are available for *in vitro* or *in vivo* experiments. This occurs when the cells are harvested from atrophic tissue, with insufficient bone quality and volume, or in sites lacking of stem and progenitor cells due to extensive trauma, radiation therapy, or medications such as bisphosphonates (BPs) anti-resorptive drugs. BPs promote proliferation and differentiation of OBs and inhibit OCs (*Reszka & Rodan, 2003*). Sometimes these conditions hesitate in adverse non-healing lesions, such as Medication-Related Osteonecrosis of the Jaws (MRONJ), a condition of exposed bone in the maxillofacial region compromising the quality of life with significant morbility (*Rosini et al., 2015; Ruggiero et al., 2014*). The optimal treatment strategy for MRONJ is still to be established. BPs treatment cessation is not sufficient to restore the reparative process and, therefore, targeted interventions of regenerative medicine could be an attractive option (*Cardemil et al., 2015; Huang et al., 2015; Albanese et al., 2013;*

Gonzálvez-García et al., 2013). In this context, the replacement of healthy bone in necrotic lesions represents an important challenge for bone tissue engineering (*Devaki et al., 2012; Barba-Recreo et al., 2015*).

These considerations led us to study the minimal combination of OBs/OCs able to promote cell aggregation and differentiation, mimicking a bone microenvironment in a 3D static or dynamic co-culture system. Different culture conditions with limited amounts of human primary bone cells in a perfusion bioreactor (*Clarke et al., 2013; Vecchiatini et al., 2015*) are being explored in order to set up a protocol exportable to critical situations. Specifically, the possibility to obtain vital bone specimens from jaw bone of patients taking BPs was evaluated, in order to investigate the potential of cells from such a compromised tissue area, assuming that the approach here described could be helpful to generate an autologous implantable construct.

Materials and Methods

Cell culture and harvesting procedure

Human normal osteoblasts (hOBs) were obtained from nasal septum. Bone fragments from nasal septum (*Torreggiani et al., 2011*) were harvested from healthy donors (25-60 years old) undergoing septoplasty surgery procedures after informed consent and approval of the Ethics Committee of the University of Ferrara and S. Anna Hospital. Briefly, bone chips were dissected into smaller pieces and plated in T-25 culture flasks in 50% DMEM high-glucose / 50% DMEM F-12 / 20% Fetal Calf Serum (FCS) (Euroclone S.p.A., Milan, Italy), supplemented with 1 mM L-Glutamine and antibiotics (penicillin 100 μg/mL, streptomycin 10 μg/mL) at 37°C in a humidified atmosphere of 5% CO_2. At 70-80% of confluence, cells were scraped off by treatment with 0.05% trypsin-ethylenediaminetetraaceticacid (EDTA) (Sigma-Aldrich, St. Louis, MO, USA), washed, plated and allowed to proliferate in standard conditions (10% FCS DMEM high-glucose). hOBs (p0) were characterized for the presence of alkaline phosphatase activity (ALP Leukocyte kit; Sigma-Aldrich). Osteopontin (OPN) and RUNT-related transcription factor 2 (Runx2) expression was assessed by immunostaining. For osteogenic differentiation, hOBs were cultured up to 21 days in osteogenic medium consisting of 10% FCS DMEM high-glucose supplemented with 10 mM β-glycerophosphate, 100 nM dexamethasone and 100 μM ascorbate (Sigma-Aldrich). The osteogenic medium was refreshed twice a week

and the extent of mineralized matrix in the plates was determined by Alizarin Red S staining (ARS; Sigma-Aldrich). For co-culture experiments, hOBs were used until p3.
Human osteoblasts from the jawbone of patients taking BPs at risk for "necrotic" lesions (hnOBs) were obtained as described below. Harvesting procedures of autogenous bone were conducted in full accordance with the "Declaration of Helsinki", as adopted by the 18th World Medical Assembly in 1964 and revised in Edinburgh (2000) and the Good Clinical Practice guidelines. Before surgery, each subject provided an informed consent. All surgical extractions and treatments were performed by the same clinician, according to standard surgical and anesthetic protocols of the Dental Clinic at the University of Ferrara.

Bone specimens were harvested from the alveolar process during planned surgical treatments in different patients:
- patients previously treated with anti-resorptive agents, such as Zoledronate or Alendronate, for metastatic disease or osteoporosis, undergoing routinary tooth extraction;
- patients previously treated with anti-resorptive agents, such as Zoledronate or Alendronate, for metastatic disease or osteoporosis, undergoing surgical treatment of MRONJ.

There was no history of radiation therapy to the head and neck region in any of these patients. Before surgical treatment, 3% mepivacaine was locally administered, as needed. Buccal flaps were raised, lingual tissues were retracted and protected. After tooth extraction, buccal and distal alveolar bone was harvested with a bone scraper (Safescraper® Twist Cortical Bone Collector, Meta, Italy).
Considering the risk for MRONJ onset, each patient received the same standard pre-operative therapy (1 g amoxicillin twice a day and 250 mg metronidazole thrice a day starting 3 days before surgery) and post-operative instructions for non-steroidal anti-inflammatory drugs (NSAIDs) and antibiotics prescription (1 g amoxicillin twice a day for 10 days; 80 mg ketoprofen thrice a day for day 1, 2 and 3). 0.2% Chlorhexidine mouth rinses were prescribed from day 2 until day 14. A post-operative meeting was scheduled for day 7 and day 10, to check swelling and primary wound closure. During the second meeting sutures were removed.
During surgical treatment of MRONJ, bone specimen were collected with the use of a Modified Trephine Bur n.TRE040M (Hu-Friedy Mfg. Co., LLC). As proposed by Cardemil and coworkers (*Cardemil et al., 2015*), the alveolar bone samples were collected some distance away from exposed necrotic bone (Fig. 7A), within the considered boundary bone. The boundary of the MRONJ lesion was defined as the region where vital, light, and bleeding jawbone replaced grayish, brittle, and necrotic bone (*Cardemil et al., 2015*).

Considering the presence of MRONJ, each patient received the same standard pre-operative therapy (1 g amoxicillin twice a day starting 6 days before surgery; 250 mg metronidazole thrice a day starting 3 days before surgery) and post-operative instructions for non-steroidal anti-inflammatory drugs (NSAIDs) and antibiotics prescription (1 g amoxicillin twice a day and 250 mg metronidazole thrice a day for 10 days; 80 mg ketoprofen thrice a day for day 1, 2 and 3). 0.2% Chlorhexidine mouth rinses were prescribed from day 2 until day 14. A post-operative meeting was scheduled for day 7 and day 10, to check swelling and primary wound closure. During the second meeting sutures were removed.

After specimens collections, in all cases the surgical area was treated with piezo-electric surgery, and it was cleaned with either a diamond (piezo) or a round diamond-burr drill, at low speed and with generous saline irrigation, leaving dense, highly mineralized bone. Finally the wound space was thoroughly debrided and closed with interrupted sutures (Vicryl 4-0, Ethicon Spa, Pomezia, Italy), to achieve a primary closure, as appropriate.

The samples were dissected into smaller pieces, plated and cultured in T-25 culture flasks as already described. The culture medium for hnOBs was further supplemented with a higher concentration of antibiotics (penicillin 500 μg/mL and streptomycin 50 μg/mL, gentamicin 50 μg/mL) and antimycotic (fungizone 10 μg/mL). We adopted these conditions given the derivation of the samples and the consequent possibility of contaminations. hnOBs were characterized by immunocytochemical analysis for OPN and Runx2 and ARS staining after osteogenic induction, as already described.

Human monocytes (hMCs) were obtained from peripheral blood (PB) of healthy volunteers (different from the hOBs donors) after informed consent (median age 37.5 years, range 25-50, approximately the same age range of the hOBs donors). PB mononuclear cells (PBMCs) were obtained from diluted peripheral blood (1:2 in Hanks solution), separated by Histopaque®-1077 (Sigma-Aldrich). hMCs were purified from PBMCs by adhesion selection on polystyrene plates: 1 x 10^6 PBMCs/cm^2 were plated in T-25 culture flasks, allowed to settle for 4 h at 37°C and the flasks were then rinsed to remove non-adherent cells (lymphocytes, platelets, red blood cells, polymorphonuclear cells) (*Piva et al., 2005*). The purity of hMCs population was verified by cytofluorimetric analysis. Briefly, 1 x 10^5 cells were resuspended in phosphate-buffered saline (PBS) and incubated with fluorescein isothiocyanate (FITC)-conjugated anti-human CD14 antibody (ImmunoTools GmbH, Friesoythe, Germany) for 15 min at 4°C. A monoclonal antibody with no specificity was used as negative control. Cells were then washed and resuspended in 400 μL of PBS. The fluorescence levels were measured using the FACS Scan flow

cytometer (Becton Dickinson, Franklin Lakes, NJ, USA) and CELLQUEST software (Becton Dickinson European HQ, Erembodegem Aalst, Belgium). Only the samples that after FACS analysis were $CD14^{+}\geq 95\%$ were used. In order to confirm the ability of isolated hMCs to differentiate into mature osteoclasts (hOCs), M-CSF (25 ng/mL) and RANKL (30 ng/mL) (PeproTech EC Ltd, London, UK) were added to the culture medium. After 7-10 days, TRAP staining (*Piva et al., 2005*) was carried out with the Acid Phosphatase Leukocyte (TRAP) Kit no. 386 (Sigma-Aldrich), according to the manufacturer's protocol. The expression levels of the osteoclast-specific markers MMP-9 and Cathepsin K were assessed by immunocytochemistry. In order to verify the resorbing capacity, hMCs were plated into a calcium phosphate-coated OAAS (OAAS, Osteoclast Activity Assay Substrate, Oscotect Inc., Seoul, Korea) at the density of 1×10^6 cells/well, and maintained in the same culture conditions indicated previously. After 7 days, when TRAP-positive hOCs appeared, the cells were removed with a solution of 5% sodium hypochlorite. Bone resorption activity was measured by direct observation under phase contrast microscopy.

Indirect hOBs/hOCs co-culture system

1.5×10^5 hOBs were pre-cultured on polystyrene 24-well plates until confluence, then 0.45 μm cell culture inserts (Becton Dickinson, NJ, USA) seeded with hMCs (0.5×10^5, hOBs/hMCs 3:1 cell ratio) were added. Cells were cultured in 10% FCS DMEM high-glucose in the absence of osteoclastogenic inducers (M-CSF and RANKL). This method established a co-culture condition with the two cell types not coming into contact, but allowing the interaction with the soluble factors produced by the cells. Co-cultures exposed to M-CSF (25 ng/mL) and RANKL (30 ng/mL) were used as positive control, while hMCs cultured in the absence of hOBs were employed as negative control. After 7 days, TRAP staining and immunocytochemistry analysis for Cathepsin K were carried out on cells cultured in the upper chamber, in order to verify the presence of mature osteoclasts (hOCs). After 14 day of osteogenic induction, the expression levels of OPN, OSX and Runx2, the ALP activity and the presence of mineralized matrix deposition (ARS staining) were evaluated. Each individual experiment was entirely performed with hMCs obtained from PBMCs from the same donor.

hOBs/hOCs three-dimensional (3D) co-culture systems

hOBs/hOCs aggregates were generated in the absence of exogenous scaffolds by using two different experimental approaches: 3D co-culture system obtained in static condition (3D-C) or in dynamic condition (3D-Dyc).

For 3D-C condition, 0.5-1 x 10^6 hMCs were incubated with 1-2 x 10^6 hOBs in agarose coated polystyrene 6-well plate, in 2 mL of 10% FCS DMEM high-glucose at 37°C (humidified atmosphere, 5% CO_2), with the medium being refreshed twice a week. After 24 h, the presence of spheroids with a diameter >500 μm was observed. After 7 days, a first set of aggregates were collected, fixed in 4% formalin, embedded in paraffin, sectioned and processed for TRAP analysis. 3D-C aggregates were maintained in osteogenic medium for further 14 days of co-culture. The aggregates were then fixed, embedded in paraffin, sectioned and processed for histochemisty.

The 3D-DyC condition was set up by using the RCCS-4^{TM} bioreactor (Synthecon™, Inc., Houston, TX, USA), with a High Aspect Ratio Vessel (HARV^{TM}; Synthecon™, Inc., Houston, TX, USA). The HARV vessel consists of a horizontally rotated culture chamber, where the cells are suspended, and a perfusion system with media continuously flowing through the culture chamber. The culture chamber can rotate in the X-axis at certain speeds (rpm): higher rpm are associated to a lower gravity. 0.5-1 x 10^6 hMCs and 1-2 x 10^6 hOBs were inoculated in 2 mL HARV vessels filled with 10% FCS DMEM high-glucose and all air bubbles were removed from the culture chamber. The HARV vessels were then inserted into the RCCS-4 rotary bioreactor and placed in an incubator at 37°C, for the indicated times, in a humidified atmosphere with 5% CO_2. After 7 days, a first set of aggregates were collected for TRAP assay and the others were maintained for further 14 days in osteogenic medium. The rotation speed used for the bioreactor was 4 rpm for the Ground Based dynamic culture at 1 x g (Xg) and 14-16 rpm for the Modeled Microgravity condition (μXg), where the aggregate floated in suspension. Medium was refreshed twice a week. At the end-point of co-culture (21 days), the aggregates were collected, fixed in 4% formalin and embedded in paraffin for further analysis. All the tested experimental conditions are reported in Fig. 3.

hnOBs/hMCs aggregates were obtained by incubation of 0.5 x 10^6 hMCs and 1 x 10^6 hnOBs, inoculated in 2 mL HARV vessels, inserted into the RCCS-4 rotary bioreactor (37°C, humidified atmosphere, 5% CO_2), cultured under Modeled Microgravity (3D-DyC/Xg condition) and collected after 21 days (of which 14 days in osteogenic medium) for viability and histological analysis.

Cell viability

Viability of the cells was analyzed by double staining with propidium iodide (PI) and Calcein-AM assay (Sigma-Aldrich), according to the manufacturer's instructions. Cells were observed under a fluorescence microscope (Nikon, Optiphot-2; Nikon Corporation, Tokyo, Japan) using the filter block for fluorescein. Dead cells were stained in red, whereas viable ones appeared in green.

Immunocytochemistry and histology

Immunocytochemistry analysis was performed using the ImmPRESS (Vectorlabs, Burlingame, CA) or 4plus AP universal (Biocare Medical, Concord, CA) detection kit. Briefly, cells grown in 12-wells plate or from indirect co-culture were fixed in cold 100% methanol and permeabilized with 0.2% (v/v) Triton X-100 (Sigma-Aldrich) in TBS 1X (Tris-buffered saline). Cells were treated with 3% H_2O_2 in TBS and incubated in 2% normal horse serum (Vectorlabs, Burlingame, CA) for 15 min at room temperature. After incubation in blocking serum, the different primary antibodies were added and incubated at 4°C overnight: polyclonal antibodies for MMP-9 (H-129), OPN (LF-123), Runx2 (M-70), OSX (M-15), Cathepsin K (E-7) (rabbit anti-human, 1:200 dilution, Santa Cruz Biotechnology, Dallas TX USA). Cells were then incubated in Vecstain ABC (Vectorlabs, Burlingame, CA) or Universal AP detection (Biocare Medical, Concord, CA) reagents for 30 min and stained, respectively, with DAB solution (Vectorlabs, Burlingame, CA) or Vulcan Fast Red chromogen kit (Biocare Medical, Concord, CA). After washing, cells were mounted in glycerol and observed using the Nikon Esclipse 50i optical microscope.
Histological sections (5 µm) of 3D-C and 3D-Dyc aggregates were subjected to immunohistochemistry. To this aim, non-consecutive sections were immunostained with a primary antibody against Cathepsin K (E-7), OPN (LF-123), OSX (M-15), Runx2 (M-70) (rabbit anti-human, 1:100 dilution, Santa Cruz Biotechnology). Histological sections were deparaffinized, rehydrated and enzymatically treated with 1 mg/mL pronase and 10 mg/ml hyaluronidase (Sigma-Aldrich) for antigen retrieval and permeabilization. Slides were then incubated overnight with the primary antibody in a humid chamber at 4°C. An alkaline phosphatase-labeled secondary antibody was used (4plus Universal AP Detection, Biocare Medical, Concord, CA, USA) in combination with the Vulcan Fast Red Chromogen Kit (Biocare Medical, Concord, CA, USA), resulting in a red staining. The sections were counterstained with hematoxylin, mounted in glycerol and observed using the Nikon Esclipse 50i optical microscope. TRAP staining was carried out with the Acid Phosphatase Leukocyte (TRAP) Kit no. 386 (Sigma-Aldrich), according to the manufacturer's protocol

as already reported (*Reszka & Rodan, 2003*). For Alizarin Red S staining, cells cultured in monolayer or 3D aggregates (3D-C and 3D-Dyc) were fixed in 4% formalin, and then stained with 40 mM Alizarin Red S solution (pH 4.2) at room temperature for 10 min. Samples were rinsed five times with distilled water and three times with PBS on an orbital shaker at 40 rpm for 5 min each, to reduce non-specific binding.

The stainings were quantified by a computerised video camera-based image analysis system (NIH, USA ImageJ software, public domain available at: http://rsb.info.nih.gov/nih-image/) under brightfield microscopy (Nikon Eclipse 50i; Nikon Corporation, Tokyo, Japan). For the analysis of sections obtained from 3D-C and 3D-Dyc aggregates, the positive immunostaining was expressed as % of positive area (five sections per replicate; three replicates per donors; n = 3).

Statistical analysis

Statistical significance was analysed by one-way analysis of variance (ANOVA) and Bonferroni post-hoc test if the values followed a normal distribution, or by Kruskal-Wallis analysis (nonparametric one-way ANOVA) and Dunn's post-hoc test if the values were not normally distributed. For all statistical analysis, differences were considered statistically significant for p-values ≤ 0.05.

Results

Phenotypical characterization of hOBs and hOCs monotype cell cultures

hOBs were characterized for their osteogenic potential, in terms of alkaline phosphatase activity (ALP), osteopontin (OPN) and Runx2 expression and deposition of mineral matrix after 21 days of culture (Fig. 1A). Monocytes (hMCs) from human peripheral blood were used as the source of osteoclast progenitors. hMCs purification by adhesion selection on polystyrene plates (4 h, 37°C) allows the removal of contaminating blood cells (lymphocytes, platelets, red blood cells, polymorphonuclear cells), as confirmed by microscopic observations and flow cytometric characterization. As shown in Fig. 1B we obtained more than 95% of purified hMCs, as calculated on the basis of forward and side light scatter profiles and cell surface display pattern (CD14).

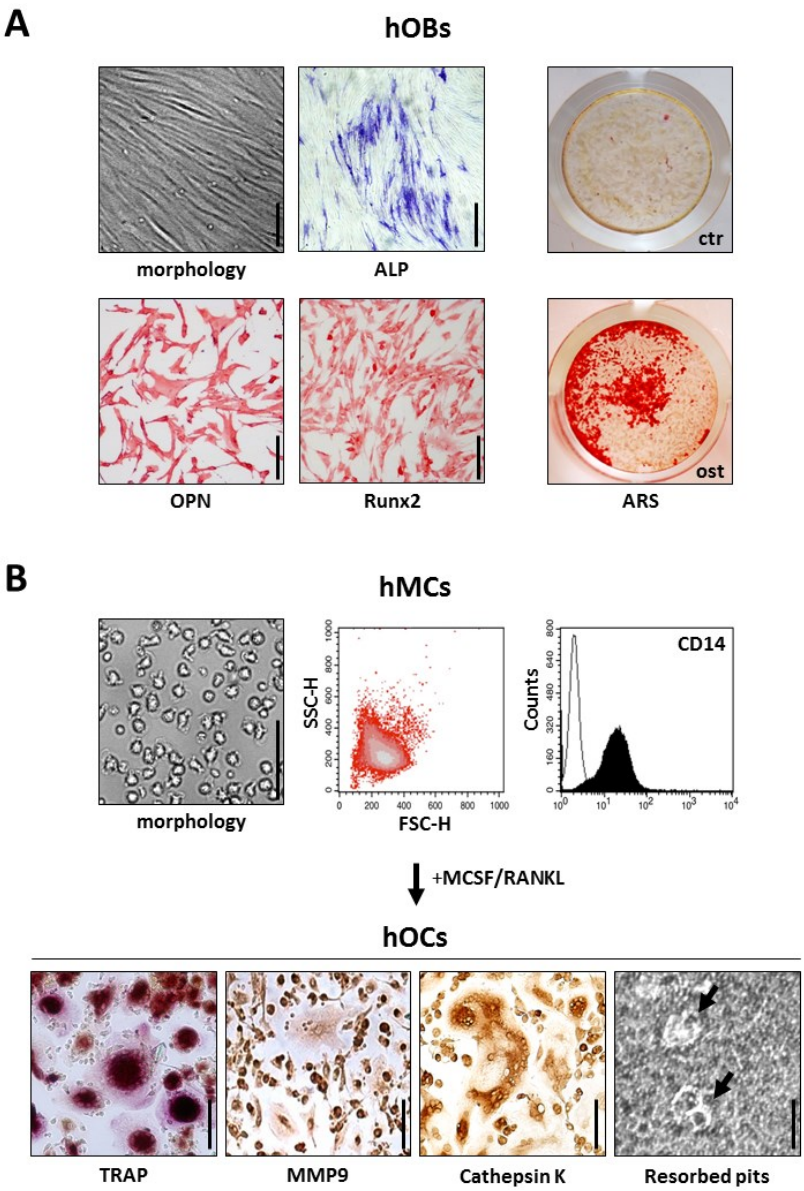

Figure 1. *Isolation and characterization of human osteoblasts and monocytes for the co-culture system.* **(A)** Human primary osteoblasts (hOBs) were isolated from bone specimens and characterized in terms of morphology, ALP activity and expression of OPN and Runx2 by immunocytochemistry. hOBs were assayed for mineralization capacity by Alizarin Red S (ARS) staining after culture in osteogenic medium (ost) for 21 days (ctr = cells cultured in basal medium). **(B)** Human primary monocytes (hMCs) were isolated from peripheral blood and characterized in terms of morphology and CD14 expression by FACS analysis (CD14 positive cells≥95%). The ability of hMCs to differentiate into mature osteoclasts (hOCs) was confirmed in terms of TRAP-positivity, MMP9 and Cathepsin K expression after stimulation with M-CSF (25ng/mL) and RANKL (30 ng/mL) for 7 days. Bars: 250 µm. The pit formation ability of hOCs is also reported. Bars: 20 µm.

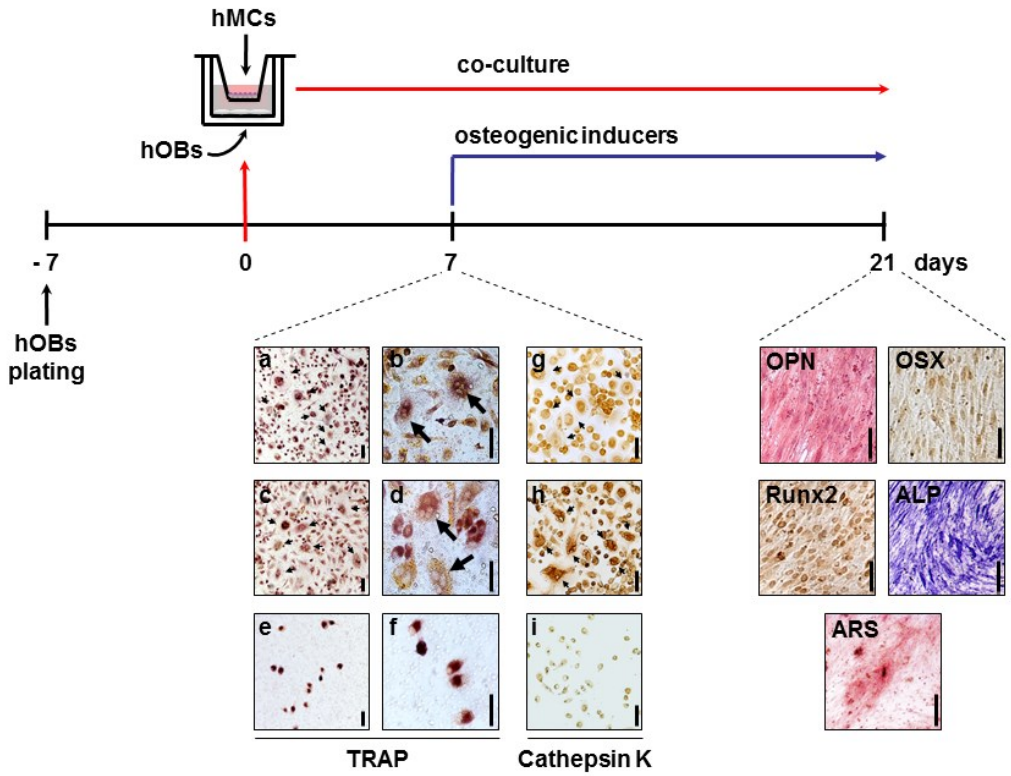

Figure 2. *Experimental set-up of the in vitro hOBs/hMCs co-culture system.* In order to establish a hOBs/hMCs co-culture system, hOBs were plated and after 7 days hMCs were seeded on the apical side of culture plate inserts (day 0). At day 7 of co-culture, the presence of differentiated hOCs (indicated by arrows) was evaluated by TRAP assay (a, b) and Cathepsin K expression (g). The analysis was also performed after stimulation with M-CSF/RANKL (c, d, h: positive control) and in the absence of hOBs (e, f, i: negative control). Bars: 50 µm. Afterwards, osteogenic differentiation of hOBs was induced by replacing the basal medium with osteogenic medium. At day 21 of co-culture, the presence of osteogenic markers was assessed by immunostaining for OPN, OSX, Runx2, ALP activity and ARS staining for mineralized bone matrix. Bars: 20 µm.

The ability of the purified hMCs to differentiate into mature multinucleated osteoclasts (hOCs) after exposure to osteoclastogenic inducers (M-CSF and RANKL) was confirmed, by evaluating the positivity for the tartrate resistant acid phosphatase (TRAP), immunostaining for the osteoclast-specific matrix metalloproteinase-9 (MMP-9) and Cathepsin K, and the pit formation ability.

Indirect hOBs/hOCs co-culture system

An indirect hOBs/hMCs co-culture system was used to validate the cell differentiation potential in our experimental model, prior to the establishment of three-dimensional (3D) co-culture conditions. The ability of hOBs to support osteoclastogenesis was investigated

seeding hMCs on polystyrene culture plate inserts in the simultaneous presence of hOBs (lower chamber) and without any osteoclastogenic inducers. We found that 1:3 hMCs/hOBs ratio was the optimal seeding condition allowing the induction of a high percentage of mature TRAP and Cathepsin K positive multinucleated osteoclasts (hOCs), already detectable after 7 days of culture (Fig. 2, panels a, b, g). The hOCs formation observed in these conditions was comparable to that found when osteoclastogenic inducers were added in the medium (Fig. 2, panels c, d, h). On the contrary, when hOBs were omitted no hOCs were generated (Fig. 2, panels e, f, i). With the progression of culture in osteogenic medium the expression of OPN, OSX, Runx2, ALP activity and the deposition of mineralized matrix were observed at day 21, indicating that the conventional 2D indirect co-culture system also supported osteoblast maturation.

hOBs/hOCs three-dimensional (3D) co-culture systems

Two different types of 3D microenvironments were then used comparing the effect of static culture (3D-C) and dynamic flow (3D-DyC) conditions on the co-culture system (Fig. 3A). 3D-C condition was obtained by direct combination of hMCs and hOBs in agarose coated polystyrene wells, while 3D-DyC by growing the same cells in the horizontally rotated culture chamber High Aspect Ratio Vessels (HARV) applied to the Rotary Cell Culture System (RCCS-4). In 3D-DyC, the cells were maintained up to 21 days in controlled microgravity condition - Modeled Microgravity (μXg) - where the aggregate floated in suspension (14-16 rpm), or in 1 x g condition - Ground Based dynamic culture (Xg) - where the aggregate was in continuous falling rotation close to the bottom of the vessel (4 rpm). To evaluate the optimal condition to generate spontaneously cellular aggregates, the tests reported in the insert of Fig. 3A were performed. These included the variation of i. cell number and ratio; ii. exposure to differentiating agents (M-CSF and RANKL); iii. rotation rate and modeled microgravity; and iiii. days in culture. While it is difficult to characterize the aggregation process, microscopic observations revealed an initial formation of cell assemblies that over time formed spherical aggregates both in 3D-C and 3D-DyC condition, mostly when 3 x 10^6 cells/mL were used. Cell ratio had no effect for 3D-C, but appeared relevant for 3D-DyC condition where cell aggregation process was favored by 1:2 hMCs/hOBs ratio. The presence of inducers (M-CSF/RANKL) was not necessary for the osteoclastogenic process. Interestingly, already after 7 days of culture, the 3D-DyC condition supported the formation of a functional aggregate exhibiting TRAP positivity (Fig. 3B). Altogether, these findings suggest that the tested microenvironments could allow aggregate formation.

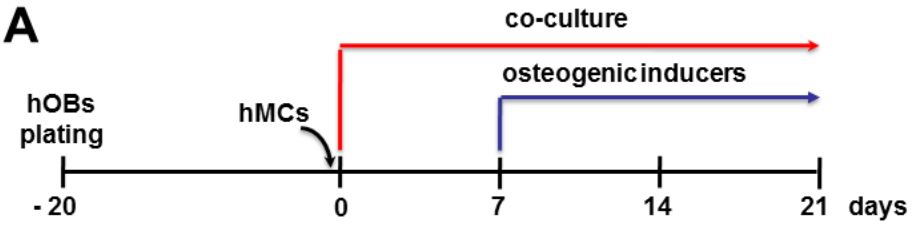

Co-culture system	Cell number	hMCs/hOBs ratio	MCSF/ RANKL	Rpm	Days
3D-C					
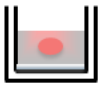	$3x10^6$	1:2	-	-	7
	$3x10^6$	1:2	-	-	21
	$3x10^6$	1:3	-	-	21
	$2x10^6$	1:2	-	-	21
	$2x10^6$	1:2	+	-	21
3D-DyC					
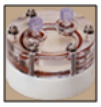	$3x10^6$	1:2	-	14 (µXg)	7
	$3x10^6$	1:2	+	14 (µXg)	21
	$3x10^6$	1:2	-	14 (µXg)	21
	$3x10^6$	1:3	-	14 (µXg)	21
	$2x10^6$	1:2	-	14 (µXg)	21
	$2x10^6$	1:2	-	4 (Xg)	21
	$3x10^6$	1:2	-	4 (Xg)	21

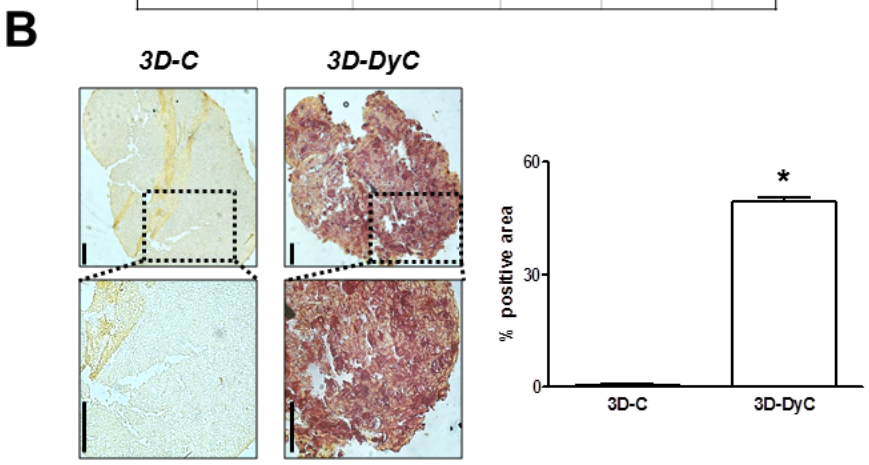

Figure 3. *Establishment of three-dimensional (3D) hOBs/hMCs co-culture models.* **(A)** After expansion in monolayer, hOBs were trypsinized and seeded with hMCs (day 0) in agarose-coated wells (3D static condition = 3D-C) or inoculated in HARV culture vessels with the dynamic RCCS-4 bioreactor culture system (3D dynamic condition = 3D-DyC) (n = 3). All the tested experimental conditions are reported in the insert as cell number and ratio (hOBs/hMCs), exposure to differentiating agents (M-CSF/RANKL), rotation rate (rpm) and presence or not of controlled microgravity (µXg - modelled microgravity), days of co-culture. **(B)** At day 7 of co-culture, the presence of mature hOCs was evaluated by TRAP assay in 3D-C and 3D-DyC conditions. Higher magnification fields are reported. Bars: 50 µm. TRAP activity was quantified by densitometric analysis using ImageJ software and expressed as percentage of positive area. Data are presented as means±sem. Statistical analysis was performed: *= $p \leq 0.0001$.

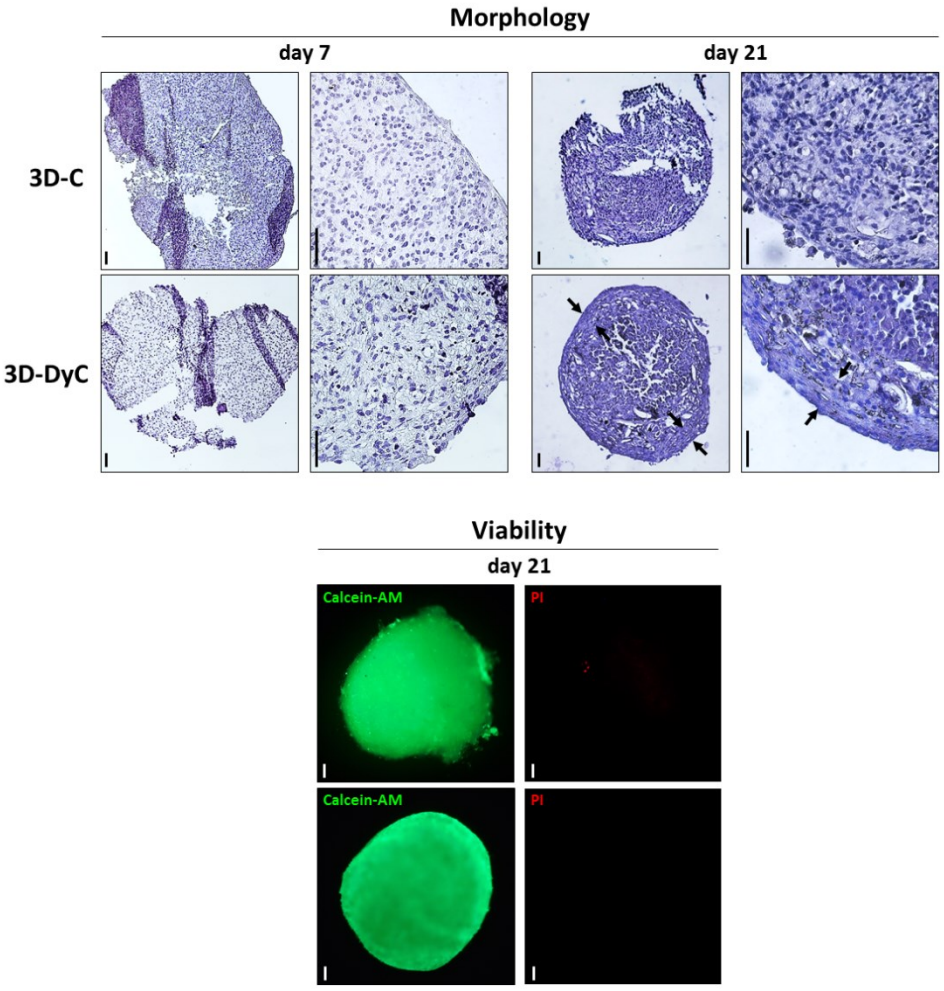

Figure 4. *Morphological features and viability of 3D-C and 3D-DyC aggregates at day 7 and 21 of co-culture.* As shown by the haematoxylin staining, only 3D-DyC constructs at day 21 displayed a noticeable cellular organization in three different cell layers: an outer region (arrows) surrounding the construct, an intermediate region with a trabecular-like structure and an inner region. Representative Calcein-AM fluorescence images of live cells and Propidium iodide (PI) fluorescence images of dead cells at day 21 of co-culture are reported. Bars: 50 μm.

Functionality of the cells within 3D-C and 3D-DyC aggregates

Considering that the overall function of the aggregate depends on the architecture that it achieves in culture, the next analysis were performed at day 21 of culture, when the cells were better organized within the aggregate. Before processing for histological analysis, aggregates were subjected to Calcein AM/Propidium Iodide (PI) double staining for cell viability assessment. As shown in Fig. 4, both 3D-C and 3D-DyC conditions generated aggregates that appeared intact and highly viable at a comparable level, up to 21 days of culture.

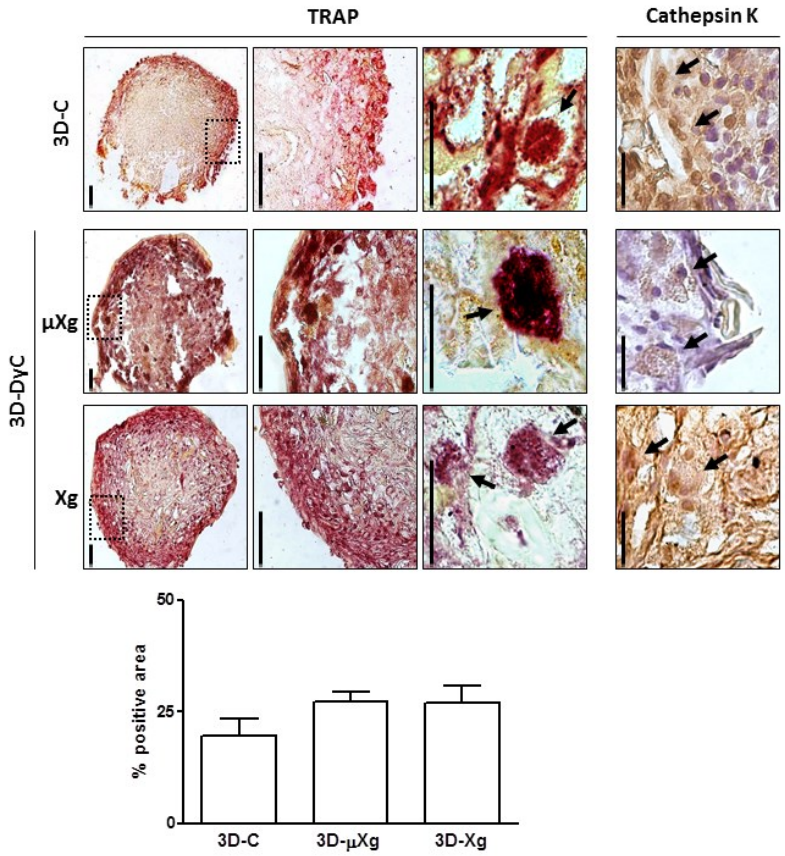

Figure 5. *Histochemical characterization of the osteoclastic component in 3D-C and 3D-DyC aggregates, cultured under Modeled Microgravity (µXg) or Ground Based dynamic culture (Xg).* The aggregates were characterized to determine hOCs activity by TRAP assay and Cathepsin K expression. Higher magnification fields are indicated by the boxed areas and reported in the right column. Bars: 50 µm. Multinucleated mature hOCs are arrowed. The stainings were quantified by ImageJ software and expressed as % of positive area (means±s.e.m., n = 3).

In both conditions, after 21 days of culture the mass appeared more compact when compared with the cellular aggregate at day 7. Interestingly, haematoxylin staining of the histological sections revealed an appreciable difference in the organization of the aggregates at day 21. This suggests that the intercellular crosstalk, cell-stroma interactions and arrangement of the cells change over time, promoting the formation of a cell aggregate that is progressively better organized. However, in comparison with 3D-DyC, cells within aggregates from 3D-C culture appeared poorly organized. In fact, 3D-DyC aggregates displayed a layered structure with an appreciable cellular organization: an outer region (arrows) surrounding the aggregate, an intermediate region with a trabecular-like structure and an inner region with different morphological characteristics (Fig. 4). The functional properties of the cells within the aggregates were then investigated.

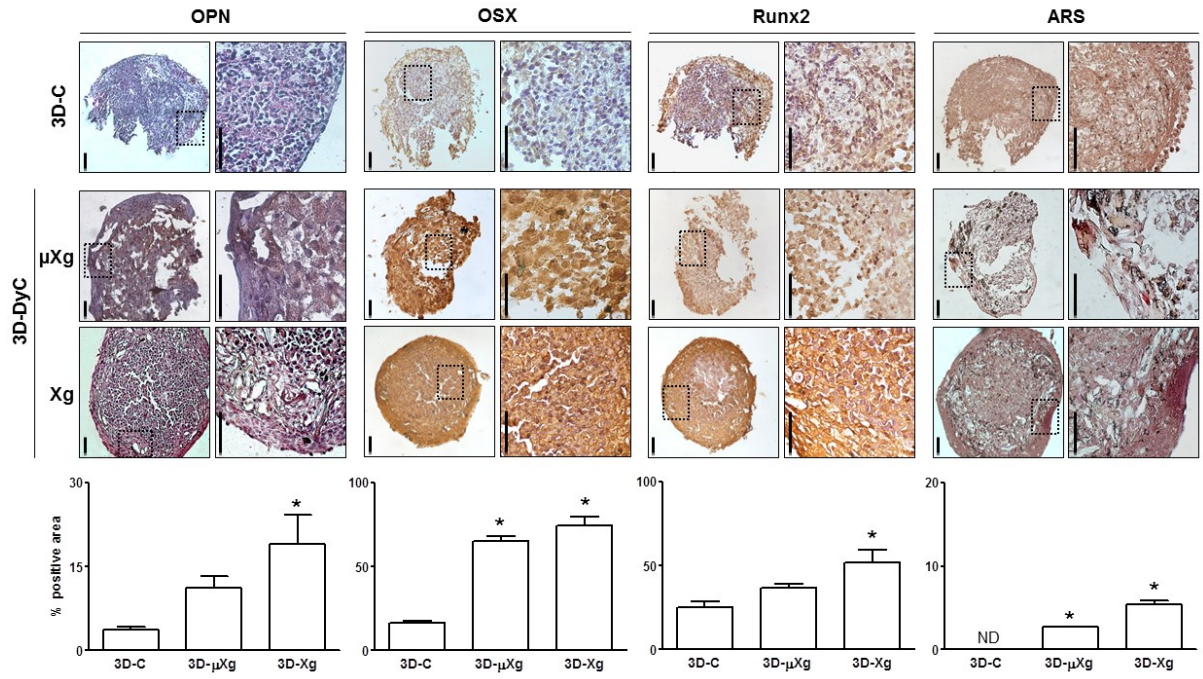

Figure 6. *Histochemical characterization of the osteoblastic component in 3D-C and 3D-DyC aggregates, cultured under Modeled Microgravity (µXg) or Ground Based dynamic culture (Xg).* The aggregates were characterized to determine hOBs activity by the analysis of OPN, OSX and Runx2 expression levels and ARS staining. Higher magnification fields are indicated by the boxed areas and reported in the right column. Bars: 50 µm. The stainings were quantified by ImageJ software and expressed as % of positive area (means± s.e.m., n = 3). ND: not detectable, *p<0.05 vs 3D-C.

As shown in Fig. 5, 3D-C and 3D-DyC conditions revealed substantial TRAP and Cathepsin K positivity demonstrating the presence of functional osteoclasts in the aggregates. Concerning the osteoblastic cellular component (Fig. 6), 3D-C aggregates clearly exhibited a low expression of OPN, OSX and Runx2 and a faint ARS staining compared to 3D-DyC aggregates. Detailed analysis of 3D-DyC conditions revealed that functionality of the hOBs grown in Xg seems to be better that those maintained in µXg. Xg condition induced a more solid cellular organization with numerous osteogenic markers-positive, compared to what was found in 3D-DyC aggregates subjected to Modeled Microgravity. The presence of hMCs in the co-cultures was found to be critical for the formation of a functional aggregate, as 3D-monocultures of hOBs alone failed to organize an intact cellular aggregate, as well as to deposit mineral matrix even in the most favorable condition (3D-DyC Xg) (Fig. S1).

Sample	Age	Gender	BP	Treatment indication	Drug Administration	Therapy duration	Co-morbidities	Indication for referral	Jaw	ONJ onset (within 12 months)	Cell attachment	Cell proliferation
1	73	F	ALN[a]	osteoporosis	oral	10 yrs	none	surgical extraction	mand[a]	none	+	-
2	80	F	ZOL[a]	Multiple myeloma	i.v.[a]	24 months	none	surgical extraction	mand[a]	none	+	contaminated
3	70	F	ALN[a]	osteoporosis	Oral	5 yrs	Takotsubo Syndrome	surgical extraction	mand[a]	none	-	-
4	64	F	ALN[a]	osteoporosis	Oral	5 yrs	Type I diabetes	surgical extraction	mand[a]	none	+	contaminated
5	70	F	ZOL[a]	Multiple myeloma	i.v.[a]	4 months	Osteoporosis Type I diabetes Former smoker	surgical treatment of MRONJ	mand[a]	Complete healing within 2 months	+	+
			CLODR[a]		i.m.[a]	6 months						
6	67	F	ALN[a]	osteoporosis	Oral	7yrs	Type I diabetes smoker	surgical extraction	mand[a]	none	+	+

Table 1. *Clinical parameters of the patients included in the study.* [a]ALN: alendronate; ZOL: zoledronate; CLODR: clodronate; i.v.: intravenous; i.m.: intramuscular; mand: mandible.

Human primary osteoblasts from jawbone of patients taking BPs with or without MRONJ lesions (hnOBs)

After demonstrating the feasibility of producing a construct mimicking the bone microenvironment with limited numbers of cells, we investigated the possibility to apply the same approach to cells from critical anatomic conditions. As a first step, we investigated if a suitable, although low, number of osteoblasts could be obtained from the jawbone of patients taking BPs (hnOBs). Bone chips were collected from 6 patients undergoing oral surgery for different reasons (see Table 1 for clinical parameters). Regarding donors, they were all female subjects, as a reflection of the higher prevalence of BPs prescription in the female population due to the indication of BPs treatment for specific diseases (i.e. osteoporosis, breast cancer, multiple myeloma) (*Ruggiero et al., 2014*). Recently, co-morbid conditions among cancer patients were inconsistently reported to be associated with an increased risk for MRONJ, including anemia and diabetes. Regarding the anatomic factors, all samples were harvested from the mandible, while one sample was harvested during MRONJ surgical treatment. Nowadays, limited new information concerning anatomic risk factors for MRONJ is available. MRONJ is more likely to appear in the mandible (73%) than the maxilla (22.5%), but can affect both jaws (4.5%) (*Ruggiero et al., 2014*).

Once harvested, bone chips were maintained in basal medium condition without supplementation of growth factors for the time required (at least 30 days) for the cells to spread out and grow as small clusters until confluence. We observed that these cells required a higher expansion time than hOBs. One donor out of six failed to give cells in culture. With the remaining five donors, the cells spread out, attached to the plastic surface and assumed a spindle-shape morphology. However, due to the peculiarity of the source, cells from two donors encountered bacterial contamination, while cells from one donor did not proliferate. Therefore, positive outcomes were achieved from two donors (5 and 6), which gave rise to proliferating and viable cells. These cells were characterized as hnOBs, since they exhibited high OPN and Runx2 expression levels, as revealed by immunocytochemical analysis (Fig. 7A). Furthermore, the positive staining for extracellular calcium deposition at day 21 of culture in osteogenic medium demonstrated the functional ability of hnOBs to deposit mineral matrix. Despite the limitations related to the number and quality of the cells, we combined hnOBs from donor 5 and 6 with hMCs in the most favorable 3D culture condition, namely 3D-DyC in Xg. An intact aggregate consisting of viable cells was formed in both cases (Fig. 7B).

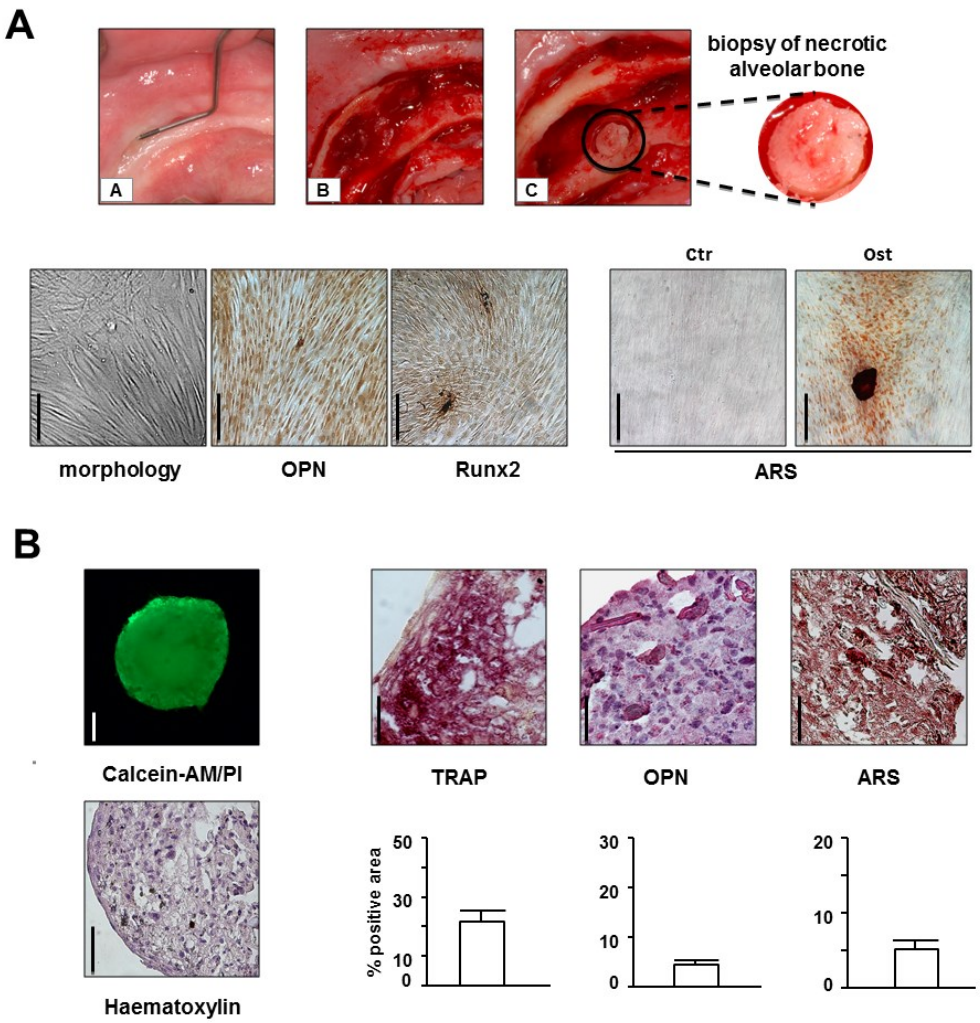

Figure 7. *Isolation and characterization of human primary osteoblasts obtained from alveolar bone samples of patients taking BPs (hnOBs).* **(A)** Bone chips were harvested from patients with a potential diagnosis of MRONJ (A, B, C) and cultured as described. The cells were characterized in terms of morphology, and expression of OPN and Runx2 by immunocytochemistry. hnOBs were assayed for mineralization capacity by ARS staining after culture in osteogenic medium (ost) for 21 days (ctr = cells cultured in basal medium). **(B)** Viability and histochemical characterization of hnOBs/hMCs 3D-DyC aggregates generated after 21 days in Xg condition (4 rpm). The fluorescence photomicrograph is a representative merged image showing the presence of Calcein-AM-labelled live cells and the absence of PI-labelled dead cells. Analysis of the histological sections confirmed the presence of TRAP-positive multinucleated osteoclasts. OPN and ARS positive stainings suggested the presence of functional osteoblasts. TRAP activity and OPN/ARS staining were quantified by ImageJ software and expressed as % of positive area (means±s.e.m., n = 2). Bars: 50 µm.

Therefore, even if the cells were derived from a tissue of poor quality, hnOBs were able to interact with hMCs, generating a whole aggregate characterized by TRAP positive areas associated with osteoblasts expressing OPN and producing Alizarin Red-positive small noduli.

Discussion

To date, several *in vitro* experimental models have been proposed for basic research aimed to investigate bone diseases and bone repair. A great opportunity comes from 3D co-culture systems of different cells in combination with natural or synthetic scaffolds, generating cell-based constructs that potentially resemble the bone microenvironment *in vitro* (*Hayden et al., 2014; Heinemann et al., 2013*). To be easily handled and well characterized, cell aggregates need to be formed by a substantial number of cells, and, for this reason, most of the evidence in the literature refers to human or murine cell lines (*Nishi et al., 2011; Li et al., 2009*). As a consequence, while this approach may be useful to standardize and optimize culture conditions, it is hardly exportable to human primary cells. On the other hand, the use of cells obtained from the patient is an essential step towards a better elucidation of the pathogenetic mechanisms and the development of novel treatments inspired by the principle of "personalized medicine".

In the present study, we aimed to establish an *in vitro* 3D hOBs/hOCs co-culture model requiring a minimal amount of cells, and therefore particularly suitable for the use of primary bone cells that cannot be obtained in a large amount, since harvested from compromised tissue areas such as osteonecrotic jawbone. In order to establish culture conditions that could be as close as possible to the *in vivo* microenvironment, we used a rotational culture bioreactor as a physiological stimulus to promote cell aggregation and interaction. Importantly, it has been shown that this strategy may be efficiently employed to induce the production of bone-like matrix in the cell aggregates (*Clarke et al., 2013*) without exogenous scaffolds, the use of which may not always be desired since affecting cell metabolism and response to stimuli. The scaffold-free system we developed has therefore the advantage to allow the investigation of the endogenous features of the cells. Besides being one step closer to the *in vivo* microenvironment, the culture system here adopted may also facilitate a fine tuning of the biophysical, biochemical and biomechanical cues, while allowing the monitoring of different parameters and the measurement of soluble factors.

Notably, we showed that co-culturing hOBs and osteoclast progenitors (hMCs) in 3D dynamic flow condition (3D-DyC) using the RCCS bioreactor led to the formation of cell aggregates that preserved cell viability and exhibited a well-defined structure over the entire period of culture. On the contrary, the 3D static condition (3D-C) was less favorable for the generation of structured cell aggregates, confirming that the mechanical forces induced by rotational culture are important to promote and maintain the integrity and organization of the aggregates, especially under Xg condition.

Indeed, the application of Modeled Microgravity (μXg) did not allow the osteoblastic component to reach the levels of differentiation displayed by cellular aggregates cultured in Xg. This is supported by the expression levels of Osteopontin, Osterix and Runx2, as well as the production of bone mineral matrix at day 21 of culture. This is an interesting aspect that deserves to be investigated in more detail, in order to determine the signaling pathways or bioactive molecules that are responsible for this phenomenon. Regardless the level of osteoblastic maturation, the histochemical and functional analysis confirmed the presence of mature multinucleated hOCs in all the different 3D co-culture models considered, in the absence of exogenous osteoclastogenic inducers (M-CSF/RANKL). This observation is relevant as it highlights the potency of the osteoblastic cellular component, supporting the hypothesis of a potential use of this system *in vivo* to prime endogenous repair phenomena and bone remodeling process in its entirety. As a whole, these preliminary data demonstrate the feasibility of establishing a 3D dynamic co-culture model that preserves the viability and functionality of the cellular components (hOBs and hMCs-hOCs), despite the low number of cells. Importantly, such a system produced intact cell aggregates exhibiting active matrix remodeling and potentially implantable without requiring the presence of a scaffold.

Next, we aimed to adopt the same conditions to recreate an *in vitro* "oral bone microenvironment" with hOBs from jawbone necrotic area. To the best of our knowledge, an experimental model with this specific purpose is still lacking. In this regards, one of the major challenges that must be overcome is the obtainment of vital and expandable cell populations from compromised tissues such as jawbone of patients taking BPs. For this reason, we tried to isolate osteoblasts from alveolar bone specimens of BPs-treated patients, harvested from either boundary bone during surgical treatment of MRONJ lesion or during teeth extraction (hnOBs). Despite the extremely poor quality of the biological specimens, as demonstrated by the relatively high incidence of sample contamination or insufficient cell growth (see Table 1), we showed that it is possible to obtain a sufficient number of primary hnOBs able to form an aggregate in combination with hMCs. We hypothesize that optimization of the culture conditions could help to further improve the isolation of hnOBs from the bone chips, in terms of cell number and growth potential. Nevertheless, we confirmed by immunocytochemical analysis that hnOBs prior and after 3D co-culture condition maintained the osteogenic potential, as suggested by the production of a typical bone protein such as OPN and synthesis of mineral matrix.

Our findings, together with previous reports, highlight the need for further studies on the primary cells that can be isolated from the affected tissues of patients treated with anti-

resorptive agents, such as BPs. Indeed, this would allow a better investigation of the specific roles of each cell type in MRONJ onset and development. The pathophysiology of MRONJ is still not fully understood and only few clinical studies have addressed the influence of anti-resorptive agents on the cellular mechanisms involved in bone tissue healing/lack of healing in the human oral cavity (*Ruggiero et al., 2014; Otto et al., 2012*). Intravenous administration of a single dose of BPs leads on the other hand to rapid accumulation of the drug in the bone tissue, approximately 60% in 1 h (*Lin et al., 1994*). Once incorporated into the bone, BPs are released again only when the bone is resorbed, possibly never again, due to the compromised bone turnover (*Lin, 1996*). Although the length of exposure seems to be a crucial risk factor for MRONJ development, early cases were reported also after few doses (*Bamias et al., 2005; Barasch et al., 2011*). Barasch and coworkers showed that the risk for development of MRONJ begins within 2 years of treatment, for both cancer and non-cancer patients, and that even the less potent BPs are linked to MRONJ after a relatively short period of treatment (*Barasch et al., 2011*).

Considering the clinical conditions of the patients involved in this study, limitations are represented by the small group of patients, the different indications for treatment with anti-resorptive agents, the different ways of administration, and the fact that specimens were harvested from different sites in the mandible during different surgical procedures. Another confounding factor is the large number of other medicines taken by such patients. Generally, the risk for developing MRONJ after oral treatment has to be carefully considered for patients with osteoporosis or oncologic diseases and severely compromised tissues. However, while our findings must be cautiously interpreted, they provide evidence of a potential cell-based tissue engineering approach that could be associated with surgical procedures for the treatment or prevention of MRONJ. To confirm our evidence, further studies with a large number of patients are urgently needed. At the same time, we speculate that our data will be useful for the *in vitro* development of smart cell-based constructs with regenerative properties, and therefore potentially able to trigger and promote oral tissue repair once implanted in the site of the defect.

Conclusions

In conclusion, we demonstrated the feasibility of a 3D co-culture system with limited amounts of cells that preserves viability and functionality of bone cellular components, and also allows the generation of bone-like aggregates using cells isolated from compromised jawbone sites. The approach here described will allow the future development of a

platform useful both to study the molecular mechanisms sustaining the osteonecrosis and test drugs potentially able to revert the aberrant phenotype of bone cells. Nonetheless, depending on the cell populations chosen for the co-culture system, such a tool could be exploited not only for diseases affecting the alveolar bone but also other tissues of the oral cavity, such as the jaw muscles or the temporomandibular joint.

Supplementary materials

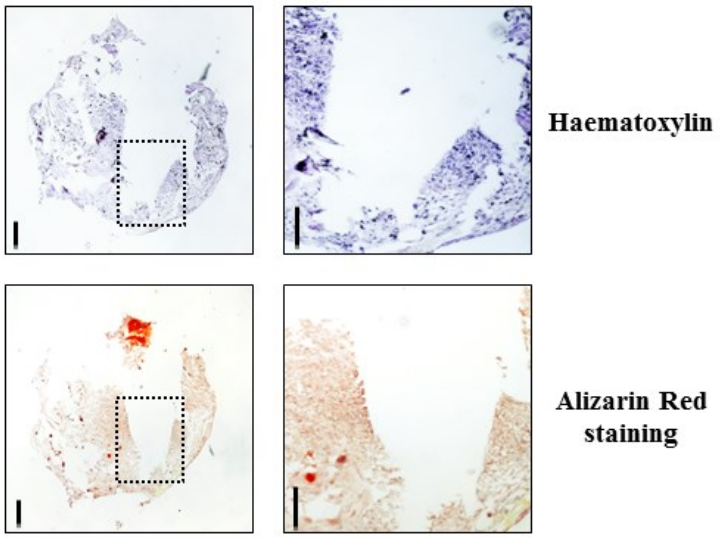

Supplementary figure 1. After expansion in monolayer, 3 x 10^6 hOBs were trypsinized and inoculated in HARV culture vessels using the dynamic RCCS-4 bioreactor setting Ground Based dynamic condition (Xg, 4 rpm). After 21 days in osteogenic medium, the partially smashed aggregates that were retrieved revealed a poor cellular organization (haematoxylin) and a very limited mineral matrix deposition (Alizarin Red staining). Bars: 50 µm.

Chapter 6

Silencing of miR-221 improves cartilage repair in vivo

Outline of the work

We have previously demonstrated that the silencing of miR-221 in monolayered hMSCs is effective and sufficient to address the cells towards the acquisition of a chondrocyte-like phenotype, without requiring supplementation with growth factors. Based on this first evidence, this section of the project was aimed at exploring the possibility to influence the chondrogenic/regenerative potential of hMSCs by miR-221 depletion, *in vitro* and *in vivo*. Indeed, current tissue engineering-based regenerative strategies make use of hMSCs that are implanted in a cartilage defect, but the control of hMSCs differentiation towards the chondrogenic lineage as well as the maintenance of a stable chondrocytic phenotype are still objectives to be achieved. We investigated the chondrogenic features of miR-221 depleted hMSCs first in conventional 3D-pellet culture and then using an *in vivo* model of osteochondral defect. In pellet cultures, we observed that miR-221 depleted hMSCs underwent spontaneous chondrogenic differentiation, in the absence of TGF-β or other inducers. The engineered hMSCs were then encapsulated in alginate and seeded in a simulated cartilage defect in an osteochondral biopsy. Following subcutaneous implantation of the biopsies in nude mice, we found that the silencing of miR-221 strongly enhanced cartilage repair *in vivo*, compared to the control conditions (defects filled with untreated hMSCs or alginate only). Importantly, miR-221 silenced hMSCs led to the production of a cartilage-like matrix with no sign of collagen type X deposition, a marker of undesired hypertrophic and terminal maturation, both *in vitro* and *in vivo*. Altogether, our data demonstrate that the silencing of miR-221 has a pro-chondrogenic effect *in vivo*, opening new possibilities for the use of hMSCs for cartilage repair.

Introduction

Adult articular cartilage does not heal spontaneously after injury and surgical repair remains a significant clinical challenge with few and sub-optimal therapeutic options (*van Osch et al., 2009*). Mesenchymal stromal cells (hMSCs) have been identified as an attractive cell source for cartilage regeneration due to their chondrogenic potential (*Gordeladze et al., 2011; Johnstone et al., 2013; Demoor et al., 2014; Xian & Foster, 2006*). Many studies demonstrating that cartilage tissue can be created from hMSCs have paid special attention to growth factors that are involved in promoting chondrogenesis. These growth factors, particularly the members of the transforming growth factor beta (TGF-β) family, induce hMSCs to acquire a chondrogenic phenotype, and synthesize specific extracellular matrix proteins such as collagen type II and aggrecan (*Mackay et al., 1998; Liao et al., 2014; de Crombrugghe et al., 2001*).

The use of TGF-β, however, revealed contradictory findings and undesired off-target effects on the synthesis and functionality of cartilage matrix components. In fact, during chondrogenesis release of high levels of TGF-β may drive progenitor cells to become hypertrophic or induce fibrosis (*Hellingman et al., 2011; van Beuningen et al., 2000*). The presence of TGF-β during chondrocyte proliferation may be detrimental for the re-differentiation process and may promote the rapid and undesirable differentiation into fibroblast-like cells (*Narcisi et al., 2012a*). Additionally, recent studies have demonstrated that TGF-β signaling plays a critical role in chondrocytes, MSCs and synovial lining cells during the development and progression of osteoarthritis (OA), one of the most common joint diseases (*Baugé et al., 2014*). This emerging body of evidence has stimulated researchers to pay special attention to feasible alternatives, including inhibition of specific TGF-β signaling pathways, to achieve sustained and long-term repair, or reduce degeneration of articular cartilage (*Hellingman et al., 2011; Narcisi et al., 2012b; Scharstuhl et al., 2002; Blaney et al., 2007; Zhen et al., 2013*).

Alternatively, cartilage regeneration protocols may rely on deploying morphogenetic signals of developmental pathways or removing potentially anti-chondrogenic factors. As part of this effort, we previously demonstrated that silencing of two anti-chondrogenic regulators, Slug transcription factor and miR-221, induced the expression of chondrogenic markers in hMSCs cultured in monolayer without TGF-β (*Lolli et al., 2014*). This prompted us to investigate whether these silenced cells, when properly organized in a three-dimensional environment, could be suitable to trigger the repair process of damaged cartilage tissue *in vivo*. The aim of this study was to evaluate the chondrogenic potential of miR-221 silenced hMSCs in a three dimensional environment, without exposure to

chondrogenic induction media containing TGF-β. The efficacy of miR-221 depletion to induce neocartilage formation and prevent terminal differentiation was investigated in conventional 3D *in vitro* culture and in an *in vivo* system represented by a well-established osteochondral culture model (*de Vries-van Melle et al., 2012; de Vries-van Melle et al., 2014a; de Vries-van Melle et al., 2014b*). The experimental approach based on miR-221 silencing is in accordance with recent literature demonstrating the effectiveness of the direct targeting of chondrogenic regulators to induce cartilage repair or prevent cartilage degeneration (*Madry et al., 2005; Im et al., 2011; Diekman et al., 2015; Pi et al., 2015; Guérit et al., 2014; Seidl et al., 2016*).

We found that silencing of miR-221 promoted chondrogenesis in 3D pellets cultured without TGF-β, a condition that normally does not lead to cartilage formation. Moreover, we demonstrated that miR-221 depleted hMSCs guided the formation of cartilage tissue *in vivo*, and had a reduced tendency to undergo terminal differentiation. This demonstrates that miR-221 silencing can be sufficient to promote chondrogenesis of hMSCs *in vitro* and *in vivo*, thereby having potential for therapeutic applications.

Material and methods

hMSCs cultures

hMSCs were isolated from two sources, Wharton's jelly of umbilical cords and bone marrow. Human umbilical cords (all from natural deliveries) were collected after mothers' consent and approval of the Ethics Committee of the University of Ferrara and S. Anna Hospital (protocol approved on November 19, 2006). Cords were processed within 4 h and stored in sterile saline until use (*Penolazzi et al., 2012*). Typically, the cord was rinsed several times with sterile phosphate-buffered saline (PBS) before processing and cut into pieces (2-4 cm in length). Blood and clots were drained from vessels with PBS to avoid any contamination. Single pieces were dissected, after separating the epithelium of each section along its length, to expose the underlying Wharton's jelly. Subsequently, cord vessels were pulled away and the soft gel tissue was finely chopped. The same tissue (2-3 mm^2 pieces) was placed directly into 75 cm^2 flasks in expansion medium (10% Fetal Calf Serum (Euroclone S.p.A., Milan, Italy), Dulbecco's Modified Eagle's Medium (DMEM) low-glucose supplemented with 100 µg/mL penicillin and 10 µg/mL streptomycin), at 37°C in a humidified atmosphere of 5% CO_2. After 5-7 days, the culture medium was

removed and then changed twice a week. At subconfluence, cells were trypsinized, and thereafter expanded and used at passage 3 or 4 for *in vitro* experiments of pellet culture.
hMSCs from bone marrow were obtained from femoral biopsies of donors (age 50-78 years) undergoing total hip replacement, after signed informed consent and with approval of the local ethical committees (Erasmus MC number MEC-2004-142; Albert Schweizer Hospital number 2011.07). Cells from bone marrow aspirates were seeded at a density of approximately 50,000 nucleated cells/cm^2 in expansion medium (10% Fetal Calf Serum, alpha-MEM (GIBCO, Rockville, MD, USA) supplemented with 1 ng/mL FGF2 (AbD Serotec, Oxford, UK), 25 μg/mL ascorbic acid-2-phosphate (Sigma-Aldrich, Saint Louis, MO, USA), 1.5 μg/mL fungizone, and 50 μg/mL gentamicin). Non-adherent cells were washed off after 24 h, and adherent cells were further expanded. At subconfluence, hMSCs were trypsinized and replated at a density of 2,300 cells/cm^2. Medium was refreshed twice a week and expanded cells at passage 3 or 4 were used for the experiments.

Transfections

hMSCs from Wharton's jelly or bone marrow were transfected with 10 nM antagomiR-221 or a non-relevant antagomiR (antagomiR-Scr). For all transfections, Lipofectamine RNAiMAX reagent (Invitrogen, Carlsbad, CA, USA) was used as delivering agent, by combination with the oligonucleotides for 20 min at RT. Monolayered hMSCs were transfected twice, the day after the plating and again after 3 days. The transfected cells were cultured in expansion medium without FGF2, at 37°C in a humidified atmosphere of 5% CO_2, then detached and used for *in vitro* or *in vivo* experiments.

Pellet culture of hMSCs

To provide a suitable microenvironment for chondrogenic differentiation, 2.5 x 10^5 hMSCs from the Wharton's jelly of three different donors were transfected with antagomiR-221 or antagomiR-Scr, seeded in 15 ml-polypropylene conical tube, and centrifuged to form a 3D pellet. The supernatant was removed and replaced with DMEM high-glucose supplemented with ITS+Premix: 6.25 μg/mL insulin, 6.25 μg/mL transferrin, 5.33 μg/mL linoleic acid, 1.25 μg/mL bovine serum albumin, 100 nM dexamethasone, 50 μg/ml ascorbate-2 phosphate, 1 mM sodium pyruvate, 100 μg/mL penicillin and 10 μg/mL streptomycin (Sigma-Aldrich), in the absence of conventional chondrogenic inducers (TGF-β). Simultaneously, untransfected hMSCs were cultured as pellets as described above, with or without 10 ng/mL TGF-β3 (Miltenyi, Bergisch, Gladbach, Germany): these conditions were named "TGF-β" and "untreated", respectively. All pellet cultures were

maintained at 37°C, 5% CO_2 up to 21 days and the medium was refreshed twice a week. At the chosen time-points (see Fig. 1A), pellets were either disrupted with a pellet pestle and processed for RNA isolation or fixed in 4% PFA, embedded in paraffin, sectioned and processed for immunohistochemistry.

Osteochondral culture model

Osteochondral defects were created in bovine osteochondral biopsies, as previously described by de Vries-van Melle and colleagues (*de Vries-van Melle et al., 2012*). Osteochondral biopsies that were 8 mm in diameter and 5 mm in length were produced using a diamond-coated trephine drill (Synthes, Oberdorf, Switzerland) from the four proximal sesamoid bones of fresh metacarpal phalangeal joints of 3 to 8 month-old calves. Biopsies were incubated overnight in 10% Fetal Calf Serum DMEM high-glucose supplemented with 1.5 µg/mL fungizone and 50 µg/mL gentamicin to verify sterility. Using a 6 mm-diameter dermal biopsy punch (Stiefel Laboratories, Durham, NC, USA) and a scalpel, osteochondral defects were created: the cartilage and calcified cartilage layers were removed completely and parts of the subchondral bone were damaged by scraping the surface with the scalpel. To prevent outgrowth of cells from the subchondral bone, biopsies were placed in 2% low-gelling agarose (gelling temperature 37-39°C; Eurogentec, Liege, Belgium) in physiological saline solution, in such a way that the bone was surrounded by the agarose and the cartilage was above the agarose surface.

Culture of hMSCs in the osteochondral model *in vitro*

To combine the use of transfected hMSCs with the osteochondral model, a specific protocol was optimized. Monolayered hMSCs from bone marrow of three different donors were transfected with antagomiR-221 or antagomiR-Scr as described above, then trypsinized at day 7 and resuspended in 1.2% low viscosity alginate (Keltone, San Diego, CA, USA) in physiological saline solution, at a density of 12.5 x 10^6 cells/mL. Simultaneously, 40 µL of alginate cell suspension and 60 µL of 102 mM CaCl2 were added to the simulated osteochondral defects, enabling in-situ gelation. To evaluate a possible effect of alginate entrapment and the osteochondral microenvironment on cell viability and efficiency of gene silencing, the hMSCs/alginate constructs were maintained *in vitro* in the presence or absence of the osteochondral biopsies for 4 weeks. The alginate constructs were then harvested and assayed for cell viability. Alternatively, the constructs were dissolved in 450 µL of 55 mM sodium citrate (Sigma-Aldrich) in 20 mM ethylene diamintetraacetate (EDTA, Sigma-Aldrich), incubated at 4°C and subsequently

centrifuged. The supernatant was removed, the samples were washed twice with PBS and then processed for RNA isolation as reported below.

In vivo implantation of osteochondral biopsies with hMSCs

hMSCs from bone marrow of three donors, either left untreated or transfected with antagomiR-221, were resuspended in 1.2% low viscosity alginate (Keltone) at a density of 25 x 10^6 cells/mL, and the cells suspension was solidified in the osteochondral defects, as described above. Alginate without cells was solidified in osteochondral defects as negative control condition. Biopsies were cultured overnight to allow stabilization of the system. The osteochondral biopsies were implanted subcutaneously on the back of 10 to 14 week old female NMRI nu/nu mouse (Charles River, Wilmington, MA, USA) under isofluorane anesthesia. For each hMSCs donor, three osteochondral biopsies per mice were implanted (duplicate samples, hence two mice per donor) in such a way that the three different conditions (alginate, untreated hMSCs and antagomiR-221 treated hMSCs) were present in the same animal. The osteochondral biopsies were covered using an 8 mm-diameter Neuro-Patch membrane (Braun, Melsungen, Germany) to prevent in-growth of host cell/tissue. Before surgery and 6 h after surgery, mice received 0.05 mg/Kg bodyweight of Temgesic (Reckitt Benckiser, Slough, UK). During surgery, mice received 9 mg/Kg bodyweight of Ampi-dry (Dopharma, Raamsdonksveer, The Netherlands). After 12 weeks, mice were euthanized by cervical dislocation and the osteochondral biopsies were explanted and fixed in 4% formalin. After 1 week of fixation, biopsies were decalcified using 10% formic acid for 2 weeks and subsequently embedded in paraffin, sectioned and subjected to histological evaluation. Animal experiments were conducted in the animal facility of the Erasmus MC with approval of the local animal ethics committee (under protocol number 116-14-02) according to the national animal act (EMC 2429).

Cell viability

A viability assay was performed by double staining with calcein-AM and propidium iodide (PI) using the LIVE/DEAD® Viability/Cytotoxicity Kit (Invitrogen), according to the manufacturer's instructions. The cells were visualized under a fluorescence microscope: dead cells were stained in red, whereas viable ones appeared in green. For the evaluation of cell viability, calcein-AM- and PI-positive cells in representative hMSCs/alginate and hMSCs/alginate/plug constructs were counted, and viability was expressed as % of living cells in the constructs (five fields per replicate, two replicates).

RNA isolation and Quantitative Real-Time PCR analysis

Total RNA, including miRNAs, was extracted from hMSCs using the RNeasy Micro Kit (Qiagen, Hilden, Germany), according to the manufacturer's instructions. RNA concentration and quality was measured using a NanoDrop ND1000 UV-VIS spectrophotometer (Isogen Life Science, de Meern, the Netherlands). cDNA was synthesized from total RNA in a 20 µl reaction volume using the TaqMan MicroRNA Reverse Transcription kit (Life Technologies, Carlsbad, CA, USA) for analysis of microRNAs, or the TaqMan High Capacity cDNA Reverse Transcription kit (Life Technologies) for analysis of mRNAs. Quantification of miR-221-3p and miR-222-3p was performed using the TaqMan MicroRNA Assays (Life Technologies), using U6 snRNA for normalization. For the quantification of collagen type X, alkaline phosphatase (ALP) and matrix metalloproteinase 13 (MMP13) mRNA, the appropriate TaqMan Assays were purchased (Life Technologies); for the quantification of lubricin mRNA, the primers reported in (*Das et al., 2008*) were used. Glyceraldehyde 3-phosphate dehydrogenase (GAPDH) gene was used for normalization of mRNA abundances. Polymerase chain reactions were performed with the TaqMan Universal PCR MasterMix (Applied Biosystems) or SYBR Green MasterMix (Fermentas), and using the CFX96TM PCR detection system (Bio-Rad, Hercules, CA, USA). Relative gene expression was calculated using the comparative $2^{-\Delta Ct}$ method.

Histology and immunohistochemistry

Histological sections of hMSCs osteochondral constructs (6 µm) were stained with 0.4% thionine solution (Sigma-Aldrich) in demineralized water to detect glycosaminoglycans (GAGs). Sections of hMSCs pellets (5 µm) or osteochondral constructs were subjected to immunohistochemistry. To this aim, non-consecutive sections were immunostained with primary antibodies against the cartilage matrix proteins collagen type II (mouse anti-human, 1:100 dilution, Abcam, Cambridge, UK; mouse anti-human, 1:100 dilution, II-II/II6B3, Developmental Studies Hybridoma Bank, University of Iowa) and collagen type X (mouse anti-human, 1:25 dilution; Quartett, Germany), or the chondro-regulatory transcription factors Sox9 (rabbit anti-human, 1:100 dilution; Santa Cruz Biotechnology, CA, USA), TRPS1 (rabbit anti-human, 1:100 dilution; Abcam) and Slug (mouse anti-human, 1:100 dilution; OriGene, Rockville, MD, USA). Histological sections were deparaffinized, rehydrated and enzymatic treated with 1 mg/mL pronase (Sigma-Aldrich) in PBS 1X or 0.1% pepsin (Boehringer Mannheim, Germany) in 0.5 M acetic acid pH 2.0 for collagen type X, followed by treatment with 10 mg/mL hyaluronidase (Sigma-Aldrich)

in PBS 1X for antigen retrieval. In the case of the staining for collagen type II of the sections of the osteochondral constructs, the primary antibody was pre-incubated overnight with a goat anti-mouse biotin-conjugated antibody (#115-066-062; Jackson ImmunoResearch Europe, Amsterdam, The Netherlands) to prevent cross-reaction with mouse antigens. Excessive primary antibody was captured by addition of 0.1% normal mouse serum prior to the overnight incubation at 4°C with the sections. Alternatively, slides were incubated overnight with the primary antibodies at 4°C and with the secondary antibody (link; 4plus Universal AP Detection, Biocare Medical, Concord, CA, USA) for 10 min at RT. Alkaline phosphatase-labeled antibodies were then used (HK321-UK, Biogenex, Fremont, CA, USA; 4plus Universal AP Detection, Biocare Medical) in combination with the Vulcan Fast Red Chromogen Kit (Biocare Medical) or Neu Fuchsine substrate, resulting in a red staining. An isotype IgG1 monoclonal antibody was used as negative control. The sections were counterstained with hematoxylin and eosin and mounted in glycerol. The stainings were quantified by a computerised video camera-based image analysis system (NIH, USA ImageJ software, public domain available at: http://rsb.info.nih.gov/nih-image/) under brightfield microscopy (Nikon Eclipse 50i; Nikon Corporation, Tokyo, Japan). For the analysis of sections obtained from hMSCs pellets, the positive immunostaining was expressed as % of positive area of the pellet (three replicates per donor were acquired; n = 3). For the analysis of sections obtained from the osteochondral samples, thionine positivity and immunostaining for matrix proteins (collagen type II, collagen type X) in the area of the defect was expressed as % of positive area of the osteochondral defect (two replicates per donor; n = 3 for thionine and collagen type II, n = 2 for collagen type X); for the analysis of transcription factors (Sox9, TRPS1), positive cells in the area of the defect were counted and protein levels were expressed as % of positive nuclei (five fields per replicate, two replicates per donor; n = 3).

Statistical analysis

The normal distribution of data was verified using the Kolmogorov-Smirnov test. In the case of single comparison, statistical significance was determined by paired Student's t-test for normally distributed data and Wilcoxon matched-pairs signed-ranks test for non-normally distributed data. In the case of multiple comparisons, statistical significance was analyzed by one-way analysis of variance (ANOVA) and Bonferroni post hoc test if the values followed a normal distribution, or by Kruskal–Wallis analysis (non-parametric one-way ANOVA) and Dunn's post hoc test if the values were not normally distributed. For all statistical analysis, differences were considered statistically significant for p-values ≤ 0.05.

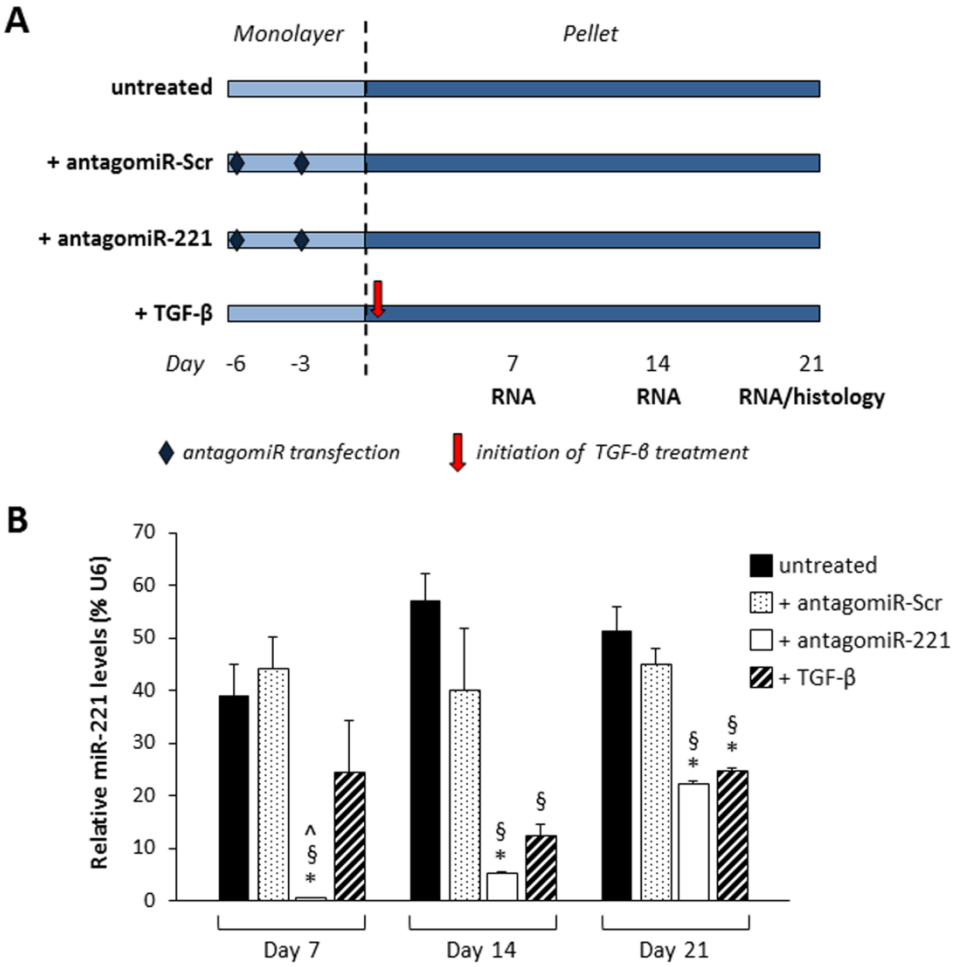

Figure 1. *3D-pellet culture of antagomiR-221 treated hMSCs.* **(A)** Monolayered hMSCs from Wharton's jelly were transfected with antagomiR-221 or a scrambled oligonucleotide (antagomiR-Scr) at the indicated times, and then transferred to 3D-pellet culture for 21 days in the absence of TGF-β. Simultaneously, untransfected hMSCs were cultured as pellets, either untreated or treated with TGF-β. hMSCs pellets were harvested for RNA isolation and processed for histology at the indicated times. **(B)** The expression levels of miR-221 were measured at day 7, 14 or 21 in hMSCs pellets by quantitative RT-PCR. Data are presented as percentage variation from U6 expression levels and results represent means±s.e.m. (three donors). Statistical analysis was performed versus untreated cells (§) and antagomiR-Scr (*) or TGF-β (^) treated hMSCs. $p \leq 0.05$ were considered statistically significant.

Results

miR-221 silenced hMSCs spontaneously undergo chondrogenesis in pellet culture

The effect of miR-221 silencing on chondrogenic potential was evaluated in pellets formed by hMSCs from Wharton's jelly in the absence of the chondrogenic inducer TGF-β for 21 days (Fig. 1A). We confirmed here the previous evidence about the downregulation of miR-221 by TGF-β (*Lolli et al., 2014*) (Fig. 1B).

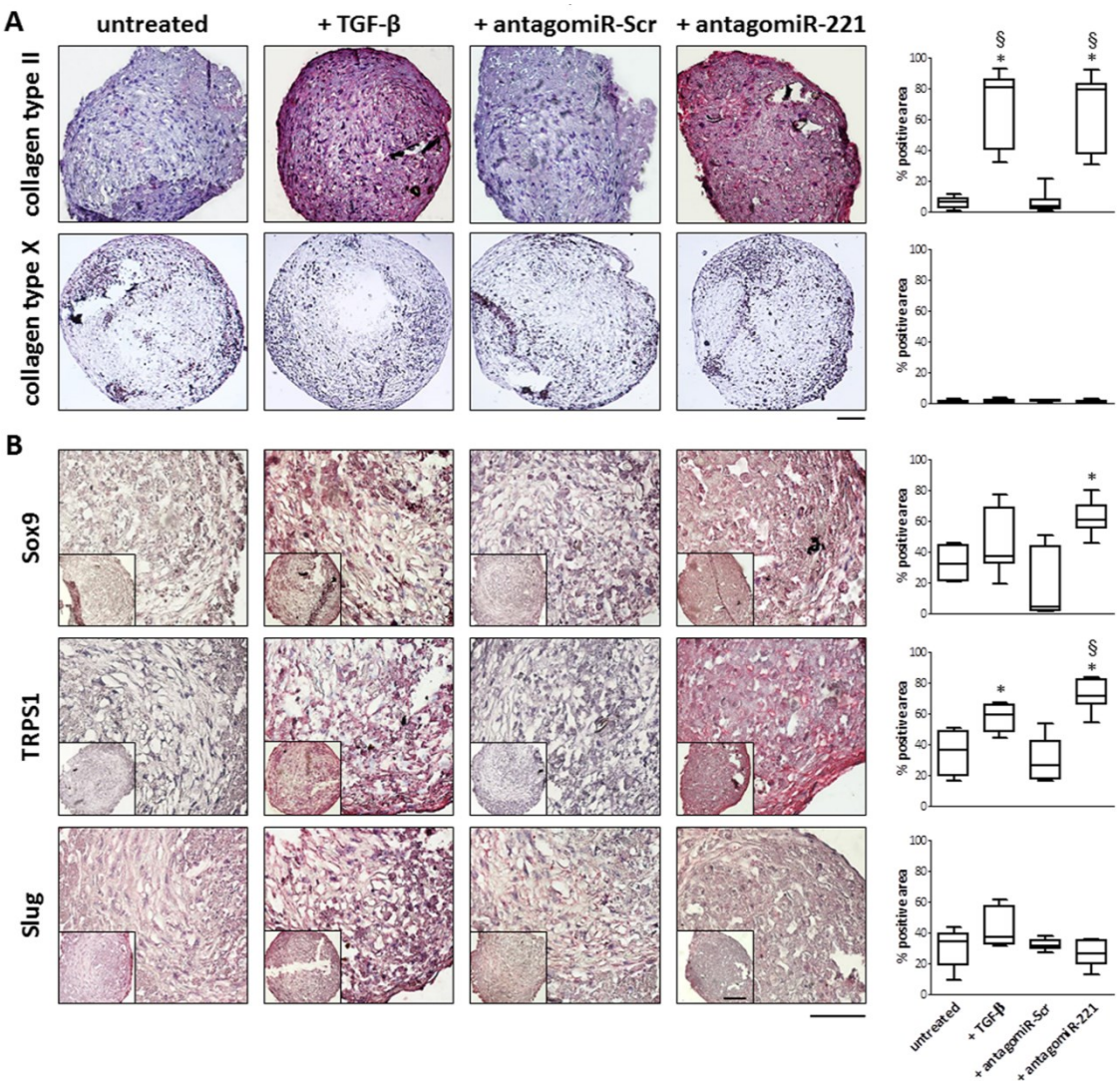

Figure 2. *Evaluation of the in vitro chondrogenic potential of antagomiR-221 treated hMSCs from Wharton's jelly.* At day 21 of culture, hMSCs pellets were immunostained for the matrix proteins collagen type II and collagen type X **(A)** and for the chondroregulatory transcription factors Sox9, TRPS1 and Slug **(B)**. Representative optical photomicrographs are reported. Scale bars correspond to 100 μm and insert bar in (B) corresponds to 200 μm. Protein levels were quantified by densitometric analysis of immunohistochemical pictures using ImageJ software and expressed as % of positive area of the pellet (three replicates per donor, three donors). Data are presented as median and interquartile range. Statistical analysis was performed versus untreated cells (§) and antagomiR-Scr (*) or TGF-β (^) treated hMSCs ($p \leq 0.05$).

Interestingly, antagomiR-221 treatment was highly effective in miR-221 knockdown up to 14 days of pellet culture, achieving >95% inhibition of miR-221 expression with respect to untreated cells. After 21 days of pellet culture, the effect of antagomiR-221 was still appreciable (~60% silencing), with a residual level of miR-221 comparable to the TGF-β treated cells. This evidence allowed us to compare the effects of two different stimuli that

lead to a comparable down-regulation of miR-221 expression. Considering that miR-221 is a paralog of miR-222, the effect of antagomiR-221 on miR-222 levels was also evaluated (Fig. S1). Before pellet formation (day 0), we observed a significant down-regulation of miR-222 by antagomiR-221 treatment. However, the residual levels of miR-222 were higher than those of miR-221, with a ~450-fold difference (4.51% vs 0.01%). At day 7 of pellet culture, the expression of miR-222, unlike miR-221, was strongly recovered (38.41% vs 1.46%), while at day 21 miR-222 was unaffected by antagomiR-221 treatment (Fig. S1). Overall, these data indicate that the effects due to a long exposure to the treatment can be mainly attributed to the silencing of miR-221.

Histological analysis performed on sections from day-21 pellets revealed a comparable positive staining for collagen type II in the antagomiR-221 treated and TGF-β treated cells, (Fig. 2A), and, accordingly, a strong Alcian Blue staining for GAGs (data not shown). Collagen type X was not detectable on immunohistochemistry (Fig. 2A) nor on mRNA expression (data not shown), indicating that these cells in the pellets were not prone to undergo hypertrophic differentiation. Notably, antagomiR-221 treatment was more effective than TGF-β in inducing the expression of the pro-chondrogenic Sox9 and TRPS1 transcription factors (Fig. 2B) (*de Crombrugghe et al., 2001*). In agreement with previous data (*Lolli et al., 2014*), antagomiR-221 treatment, unlike TGF-β, maintained Slug protein at very low levels, a favorable condition for the chondrogenic process (Fig. 2B). These results indicate that miR-221 silencing in hMSCs in pellet culture is effective and sufficient to induce chondrogenesis, in the absence of exogenously added growth factors. The effect of antagomiR-221 treatment was also confirmed in hMSCs from bone marrow (Fig. S2 and S3), allowing us to strengthen the starting hypothesis about the effectiveness of silencing miR-221 on chondrogenic induction. Interestingly, in this case the known TGF-β dependent up-regulation of collagen type X was avoided by antagomiR-221 treatment, as revealed by immunohistochemistry (quantification of the positive area: 24.0% vs 1.8% at day 21, and 64.5% vs 2.8% at day 28) and qRT-PCR analysis. Two additional hypertrophic markers, alkaline phosphatase (ALP) and matrix metalloproteinase 13 (MMP13), were found downregulated, further confirming the reduced tendency of miR-221 depleted hMSCs to undergo hypertrophy.

miR-221 silenced hMSCs are effective in regenerating cartilage *in vivo*

To validate the anti-chondrogenic role of miR-221 *in vivo*, hMSCs were cultured in an osteochondral microenvironment using a cartilage defect model (*de Vries-van Melle et al., 2012; de Vries-van Melle et al., 2014a; de Vries-van Melle et al., 2014b*) (Fig. 3A).

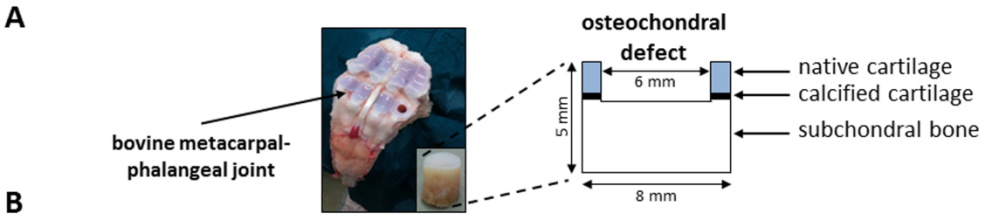

construct	condition	time point	viability of embedded cells: untreated	viability of embedded cells: antagomiR-221	miR-221 levels: treatment	$2^{-\Delta Ct}$	%
hMSCs/alginate	*in vitro*	4 weeks	91.52 %	88.53 %	-	0.213	100.00
					antagomiR-Scr	0.258	121.25
					antagomiR-221	**0.037**	**17.30** *§
hMSCs/alginate/plug	*in vitro*	4 weeks	91.04 %	85.89 %	-	0.139	100.00
					antagomiR-Scr	0.110	79.15
					antagomiR-221	**0.022**	**15.73** *§
hMSCs/alginate/plug	*in vivo*	12 weeks	implantation scheme: donor 1, donor 2, donor 3		alginate only; untreated hMSCs; hMSCs + antagomiR-221		

Figure 3. *Establishment of an in vivo experimental model of cartilage defect to test the chondrogenic potential of miR-221 silenced hMSCs.* **(A)** Osteochondral plugs were harvested from the sesamoid bones of young calves (3-8 months) after exposure of the metacarpal-phalangeal joint. Osteochondral defects with a diameter of 6 mm were produced. **(B)** hMSCs/alginate and hMSCs/alginate/plug constructs were cultured *in vitro* for 4 weeks in order to evaluate the effect of culture conditions on cell viability and silencing efficiency. Cell viability was assessed by double staining with calcein-AM/propidium iodide and representative merged photomicrographs are reported (scale bars: 50 μm). Viability was expressed as percentage of Calcein-AM-positive (green fluorescence) living cells in the constructs. The levels of miR-221 were measured by quantitative RT-PCR and data are presented as $2^{-\Delta Ct}$ or percentage variation from miR-221 expression in untreated hMSCs, taken as 100%. Statistical analysis was performed versus untreated cells (§) and antagomiR-Scr (*) treated hMSCs ($p \leq 0.05$, three donors). For the *in vivo* experiments, hMSCs/alginate/plug constructs were implanted subcutaneously in nude mice as duplicate samples (two mice per donor, three donors), as outlined in the implantation scheme. After 12 weeks, the constructs were harvested and processed for histological characterization. In case of donor 3, the constructs could be retrieved from one animal only as the second one had to be sacrificed early due to illness.

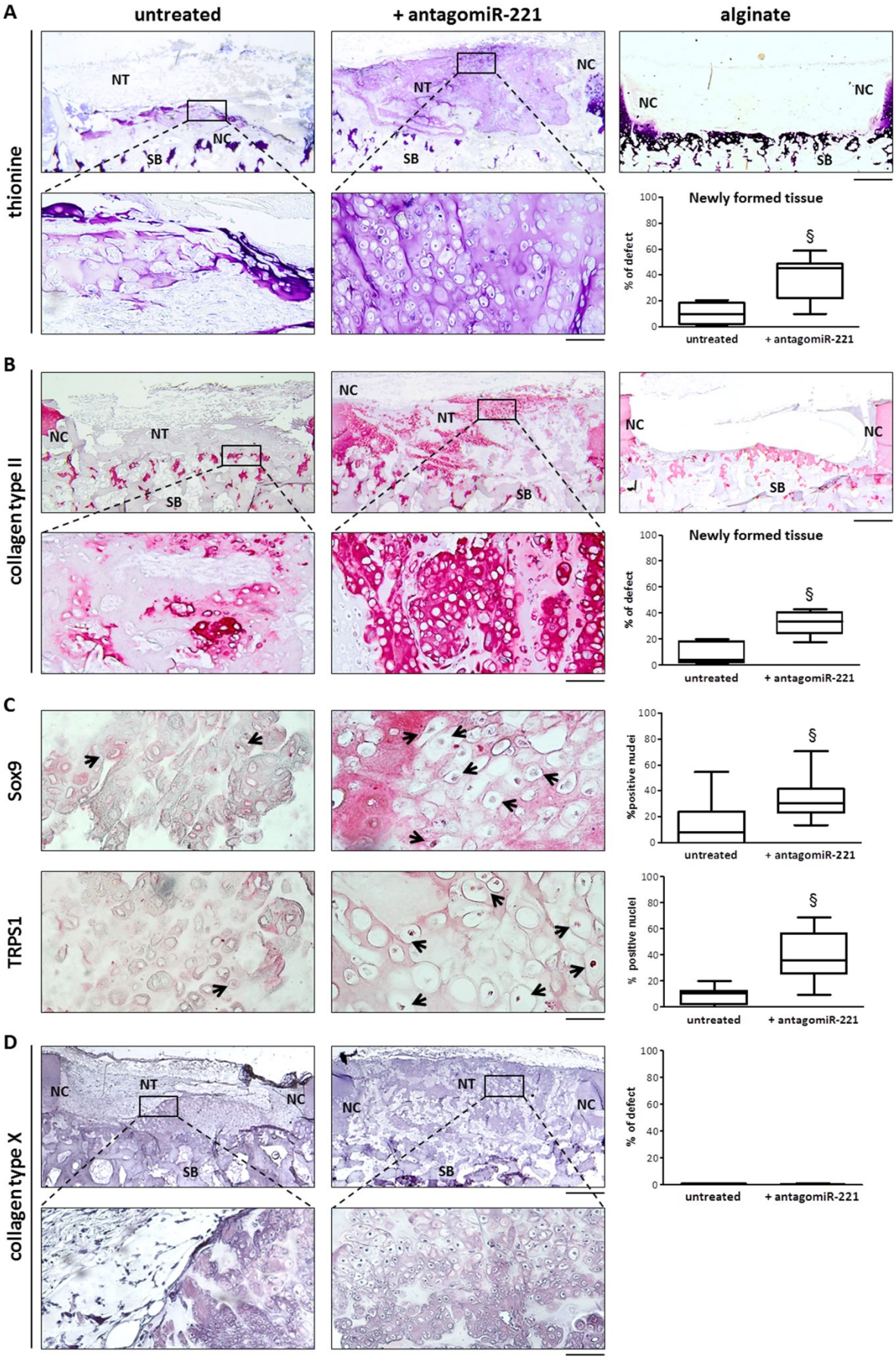
A
untreated
+ antagomiR-221
alginate
thionine
NT
NC
SB
Newly formed tissue
% of defect
§
untreated
+ antagomiR-221
B
collagen type II
C
Sox9
%positive nuclei
TRPS1
% positive nuclei
D
collagen type X

Figure 4. *Evaluation of the ability of miR-221 depleted hMSCs to stimulate cartilage repair in vivo.* Representative sections of hMSCs/alginate constructs in simulated cartilage defects implanted subcutaneously in nude mice for 12 weeks are reported (two replicates per donor, three donors). Cartilage formation was assessed by thionine staining **(A)** and immunostaining for collagen type II matrix protein **(B)**. The organization of the newly formed matrix is shown at different magnifications. Osteochondral defects filled with alginate without cells were used as negative control condition. Scale bars correspond to 1 mm and 70 μm for the lower and higher magnification photomicrographs, respectively. **(C)** The expression of Sox9 and TRPS1 by the cells in the defect area is shown by representative immunohistochemical pictures (positive cells are indicated with arrows). Scale bar corresponds to 30 μm. **(D)** The newly formed matrix was immunostained for the hypertrophic marker collagen type X. The absence of collagen type X positive area is shown at different magnifications. Scale bars correspond to 1 mm and 70 μm for the lower and higher magnification photomicrographs, respectively. Protein levels were quantified by densitometric analysis using ImageJ software and expressed as % of defect for thionine and matrix proteins staining or as % of positive nuclei for transcription factors. Data are presented as median and interquartile range. Statistical analysis was performed versus untreated cells (§) ($p \leq 0.05$). (NT = newly formed tissue, NC = native cartilage, SB = subchondral bone)

We first evaluated whether the osteochondral model could influence cell viability and silencing efficiency, by culturing hMSCs/alginate and hMSCs/alginate/plug constructs *in vitro* (Fig. 3B). We showed that cell viability was not affected for at least 4 weeks, as demonstrated by the high percentage (>85%) of Calcein-AM-positive cells in the constructs. Furthermore, antagomiR-221 treated cells maintained very low levels of miR-221 expression in both conditions (~75% silencing with respect to untreated cells), thereby demonstrating that our experimental setting was suitable for culturing miR-221 depleted hMSCs *in vivo*. For *in vivo* experiments, hMSCs/alginate/plug constructs with miR-221 depleted or untreated cells were then implanted subcutaneously in nude mice (Fig. 3B). After 12 weeks, miR-221 silenced hMSCs generated a tissue characterized by extensive production of glycosaminoglycans, as evidenced by the presence of a large thionine positive area throughout the entire region of the defect (~37% compared to 12% in control condition; Fig. 4A). This was different from the newly formed tissue localized in small spots observed when untreated hMSCs were used, and the absence of cartilage formation in defects that were filled with alginate without hMSCs (Fig. 4A). Consistent with these observations, immunohistological analysis revealed a significantly stronger staining for the chondrogenic markers collagen type II (matrix protein), Sox9 and TRPS1 (transcription factors) in the osteochondral defects filled with miR-221 silenced hMSCs, compared to the osteochondral defects filled with untreated hMSCs (Fig. 4B, C and Table 1).

	Treatment	% positive area			% positive nuclei	
		thionine	collagen type II	collagen type X	Sox9	TRPS1
Donor 1	-	19.3	3.9	ND*	8.5	1.7
	antagomiR-221	53.6	33.5	ND*	29.1	50.2
Donor 2	-	1.9	2.0	0.5	14.8	9.6
	antagomiR-221	44.9	22.1	0.9	31.1	27.4
Donor 3	-	15.2	18.9	0.6	19.9	13.5
	antagomiR-221	13.0	41.5	0.3	43.9	41.0
Average	-	12.1	8.3	0.6	14.3	8.9
	antagomiR-221	37.2	32.4	0.6	33.6	39.7

Table 1. *Densitometric values obtained by the quantification analysis of the stained histological sections with ImageJ software.* *ND = not determined.

The expression of collagen type X was close to detection limit in two out of three hMSCs donors (Fig. 4D and Table 1). These data confirmed the *in vitro* results, showing again that an increased deposition of collagen type II is not correlated with an increased deposition of collagen type X after antagomiR-221 treatment.

Discussion

Repair of damaged cartilage remains a major clinical challenge that may rely upon the development of innovative technologies, including regenerative strategies based on the use of hMSCs. Different hMSCs application modalities have been described, some in combination with bio-inspired smart biomaterials and growth factors, to provide better targeted tissue regeneration. However, the optimal strategy has not yet been identified. Much remains to be investigated, such as which hMSCs molecular signaling supports chondrogenic potential, and which culture methods improve hMSCs chondrogenic differentiation before implantation. In the present study, we demonstrated that miR-221 depleted hMSCs are able to spontaneously undergo chondrogenesis in pellet culture *in vitro* and form cartilage *in vivo*, without requiring growth factor supplementation. We showed that maintaining low levels of a negative factor by silencing is an effective alternative to induce chondrogenic differentiation, compared to standardized procedures primarily based on TGF-β treatment.

In recent years, many researchers are moving to investigate specific sets of culture conditions which attempt to resemble the physiological environment. In the natural milieu, chondrogenesis goes through a complex differentiation program with production of specific matrix components, due to exposure to a combination of factors with a tight spatiotemporal regulation. Previous molecular studies have shown that mesenchymal progenitors can be stimulated to adopt a chondrogenic fate by TGF-βs (*Xian & Foster, 2006; Mackay et al., 1998*). We here confirmed our previous observation that one of the effects of TGF-β is the down-regulation of miR-221, but not its complete suppression (*Lolli et al., 2014*). Therefore, the pro-chondrogenic activity of TGF-β may be counteracted by anti-chondrogenic factors such as miR-221, that still persist in the TGF-β enriched environment. Conversely, hMSCs cultured with antagomiR-221 are able to undergo chondrogenesis avoiding the expression of undesired proteins such as Slug or collagen type X. Therefore, our findings suggested the silencing of miR-221 as a new tool to repair a cartilage defect.

We used an *in vivo* approach with subcutaneous implantation in mice of a recently developed osteochondral defect model (*de Vries-van Melle et al., 2012; de Vries-van Melle et al., 2014a; de Vries-van Melle et al., 2014b*). This tool proved the enhanced potential of engineered hMSCs to regenerate articular cartilage in a microenvironment similar to that found in damaged cartilage. Previously, implantation of osteochondral biopsies containing hMSCs in osteochondral defects demonstrated the importance of the subchondral bone for the synthesis of cartilage repair tissue, and the contribution of soluble factors others than those of the TGF-β family (*de Vries-van Melle et al., 2012; de Vries-van Melle et al., 2014a; de Vries-van Melle et al., 2014b*). In the present work, the results obtained *in vitro* were validated by the *in vivo* experiments. Indeed, implantation of osteochondral biopsies with miR-221 silenced hMSCs resulted in significantly more cartilaginous repair tissue compared to the use of non-engineered hMSCs. miR-221 depleted hMSCs promoted a differentiation program that led to the expression of genes required for hyaline chondrogenesis, such as collagen type II and the transcription factors Sox9 and TRPS1. Moreover, one of the most interesting aspect of our results was the observation that the newly formed *in vivo* tissue was characterized by an ECM that was negative for collagen type X. It is well known that the expression of collagen type X, a marker for chondrocyte hypertrophy and apoptotic death, is an undesired outcome, and remains an unresolved issue in the cell-based approach for cartilage regeneration (*Steinert et al., 2007; Roelofs et al., 2013*). Therefore, the ability of miR-221 depleted hMSCs to downregulate collagen type X, as well as other hypertrophic genes such as ALP and MMP13, represents a crucial event

during the formation of cartilaginous repair tissue, and a promising approach for the application of hMSCs in the repair of articular cartilage defects.

An unequivocal characterization of the participation of donor cells in the neoformation/repair tissue is technically challenging, raising the question about the kind of phenomenon that supports the formation of neo-cartilage in our *in vivo* model. Several explanations on the regeneration process we observed *in vivo* may be postulated: i. at an early stage, the silenced hMSCs produce cartilage-like matrix which subsequently guides the resident cells towards chondrogenic differentiation and production of cartilage components; ii. the chondrogenic properties of the silenced hMSCs are maintained over time thanks to a sort of autocrine circuit; iii. our 3D *in vivo* setting provides a favorable microenvironment to promote the survival and maintenance of the chondrogenic phenotype of individual or groups of silenced hMSCs; iv. pro-chondrogenic growth factors are expressed endogenously by the resident cells in response to trophic factors secreted by the implanted cells (paracrine effect). Although the exact mechanism cannot be deduced from our current experiments, the cartilage formation process observed after implantation of miR-221 silenced hMSCs is very promising for further research and applications.

It is important to underline that silencing experiments in pellet cultures were here conducted initially with hMSCs from Wharton's jelly, to validate our hypothesis with the same cell source previously used in monolayer culture (*Lolli et al., 2014*). Due to the need for a higher number of cells for the *in vivo* experiments, we then moved to the use of hMSCs from bone marrow. By doing so, we further confirmed the pro-chondrogenic effect of miR-221 silencing, and we also showed that antagomiR-221 treatment was able to induce the expression of the cartilage ECM protein lubricin (*Jay et al., 2000*). In general, the use of hMSCs from different sources allowed us to prove the validity of our hypothesis, concerning the key role of miR-221 as an anti-chondrogenic factor involved in a common regulatory pathway associated with cell fate.

Currently, validated data on the role and mechanism of action of miR-221 during the chondrogenic process, as well as in diseased cartilage, are limited. Putative targets of miR-221 have been recently proposed by a miRNA signature which regulates the chondrogenic mechanism in unrestricted somatic stem cells (*Bakhshandeh et al., 2012*). miR-221 has been also postulated to be a mechanically responsive miRNA in chondrocytes, being highly expressed in weight bearing compared with non-weight bearing regions of bovine articular cartilage (*Dunn et al., 2009; Noren Hooten et al., 2010*). Moreover, miR-221 expression has been correlated with age, and its low levels have been associated with an increase in phosphatidylinositol 3-kinase signaling, a pathway shown to be implicated in

OA (*Hong & Reddi, 2013*). Within the group of the main predicted and experimentally validated targets of miR-221 and its paralog miR-222, we highlighted the genes known to have a role in cartilage-related pathways, and thus worth pursuing as potential miR-221/222 chondro-targets (supplementary Table 1). These two miRNAs are encoded by a gene cluster, have the same seed sequence and thus share common predicted target genes. miR-221, as many other miRNAs, can control cellular differentiation and may function through different mechanisms depending on the tissue microenvironment. Therefore, it is not surprising that the list in supplementary Table 1 includes genes such as TIMP, FOXO3, DKK2, DVL2, MEOX2, PGC1α, SEMA3B, STMN1, MDM2, TRPS1, RECK, ICAM1, FOS, DICER1, ETS1, and ESR1, which are involved in chondrogenesis and cartilage biology. Among these genes, only cyclin-dependent kinase inhibitor 1B (p27) and mouse double-minute 2 homolog (MDM2) have been experimentally validated as relevant miR-221 chondro-targets (*Yang et al., 2015; Kim et al., 2010*). In fact, in bovine cartilage and isolated chondrocytes, Yang and coauthors demonstrated that miR-221 mimic suppressed the expression of p27 leading to the stimulation of chondrocyte proliferation (*Yang et al., 2015*). Down-modulation of MDM2 by miR-221 prevented the degradation of Slug protein, which negatively regulates the proliferation of chondroprogenitors during chondrogenesis of chick limb mesenchymal cells (*Kim et al., 2010*). Consistent with this last evidence, we demonstrated here a very low level of Slug protein in antagomiR-221 treated hMSC cultures, supporting the hypothesis that miR-221 may act through MDM2 to prevent cartilage ECM synthesis. Hypothesized mechanisms for miR-221 action in the chondrogenic process have been illustrated in Fig. 5 and S4. We suggest that antagomiR-221 treatment promotes chondrogenic processes since it leads to a weakening of the negative control that Slug exerts on chondrogenic factors, such as Sox9 and TRPS1, and cartilage ECM proteins, such as collagen type II and aggrecan (Fig. 5). Although Slug is not a direct target of miR-221 (*Lolli et al., 2014*), it might act as an effector in a circuit that we hypothesize to end with a reciprocal negative regulation between TRPS1 and miR-221. Accordingly, we demonstrated here an increase in TRPS1 expression after miR-221 depletion and, previously, the ability of TRPS1 to strongly inhibit miR-221 expression (*Lolli et al., 2014*). Since TRPS1 acts as a repressor of Runx2 function (*Napierala et al., 2008*), the increased TRPS1 expression may contribute to repress the Runx2-mediated transactivation of genes associated with cartilage hypertrophy and ECM degradation, such as collagen type X, alkaline phosphatase (ALP) and matrix metalloproteinases (MMPs).

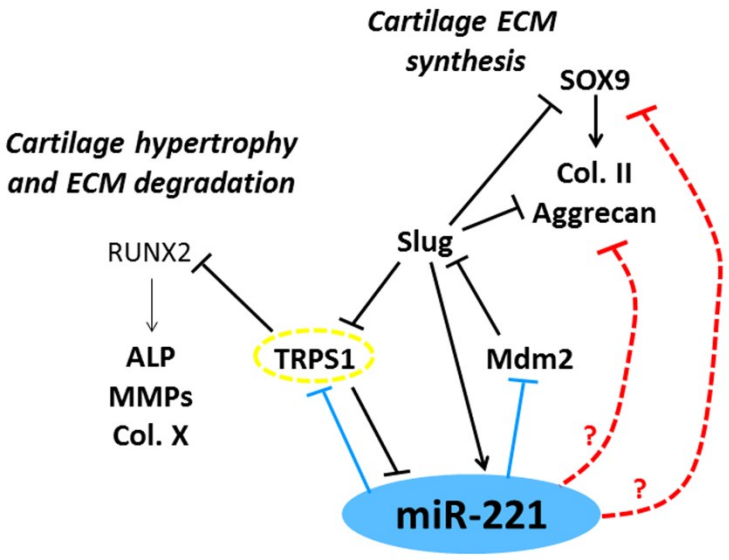

Figure 5. *Schematic representation of miR-221-dependent regulatory interplays potentially mediating its effects on chondrogenesis.* miR-221 targets (blue lines) and putative downstream interactions that are hypothesized to be more directly involved in the remodeling of cartilage ECM are outlined. Common targets of miR-221 and miR-222 are circled in yellow. We speculated that miR-221 might block cartilage synthesis mainly by targeting MDM2 and TRPS1, while sustaining cartilage hypertrophy and degradation by promoting the Runx2-mediated transactivation of ALP, MMPs and collagen type X. Moreover, miR-221 might exert further anti-chondrogenic effects via a direct inhibition of Sox9 transcription factor and the cartilage ECM proteins collagen type II and aggrecan (dashed red lines), in a manner to be explored (see Discussion for a detailed explanation).

It is also conceivable that Sox9, collagen type II and aggrecan are direct miR-221 targets. These genes do not show sequences homologous to miR-221 seed region in their 3'-UTR. However, increasing evidence demonstrates that targeting can also be mediated through sites others than the 3'-UTR, and that seed region base pairing is not necessarily required (*Thomson et al., 2011*). Accordingly, a high throughput screening of a human 3'-UTR library has recently shown that Sox9 is indeed a candidate target gene of miR-221 (*Kotagama et al., 2015*). In addition, the roles of TGF and Wnt signaling in regulating cell fate during differentiation (*Hellingman et al., 2011; Narcisi et al., 2015*) suggest other scenarios possibly correlated with miR-221 action (Fig. S4). Specific modulation of those factors lead to the production of a stable cartilage phenotype, where hypertrophy is repressed. In light of the results herein reported, we postulate that molecules involved in the TGF/Wnt pathways and regulators of cell cycle/proliferation might be targets of miR-221, thereby affecting the cell fate and the ECM produced by the chondrocytes (Fig. S4).

Novel insight onto the mechanisms by which miR-221 works and its interplay with regulatory networks may come from microarray analysis and non-invasive technologies, such as *in vivo* molecular imaging, that could be applied to our model (*Kim et al., 2008; Kim et al., 2009*). In this perspective, our results demonstrating for the first time the critical role of miR-221 in the control of chondrogenesis *in vivo*, strengthens the need to further investigate miR-221 targets, and offers a new model to apply the aforementioned techniques. We are aware that the demonstration of the effectiveness of silencing anti-chondrogenic factors in MSCs for cartilage repair, does not solve the challenges of creating an environment conducive for long term tissue survival, or restoring functional cartilage. For this purpose, future experiments will also be aimed at assessing the mechanical properties of our constructs, to better define the quality of neo-cartilage that has been formed following the approach herein described. In any case, our results provide a proof of concept for developing experiments which would allow measurement of function restoration, using large animal models of critical size osteochondral defects.

Conclusions

The work outlined above demonstrates the effectiveness of an innovative approach based on transient transfection of an antagomiRNA as a non-integrative means of direct lineage differentiation. In addition to demonstrating that the expression of miR-221 is a hindrance or major delayer of chondrogenic differentiation, this study showed how knockdown of this molecular regulator is sufficient to enable hMSCs to repair an osteochondral defect. More generally, the modulation of endogenous molecular cues in directed differentiation strategies will enable greater efficiency and leverage in the generation of target cell types for basic research and regenerative medicine applications.

Supplementary materials

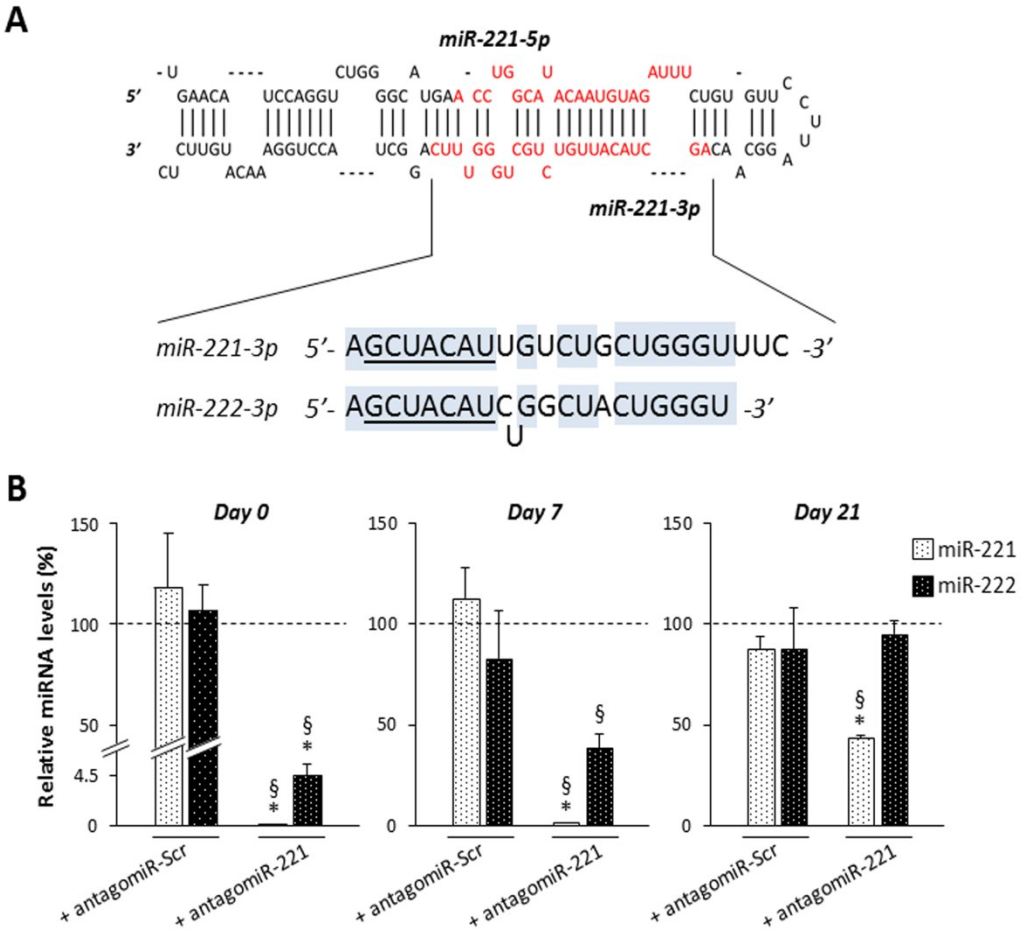

Supplementary figure 1. *Effect of antagomiR-221 treatment on the expression of miR-222 in Wharton's jelly hMSCs pellet cultures.* **(A)** Schematic representation of the stem-loop structure of the primary transcript of the miR-222/221 cluster (pri-miR-222/221) containing miR-221-5p and miR-221-3p (red nucleotides; source: miRBase.org). As highlighted in the scheme, mature miR-221-3p and miR-222-3p are highly homologous miRNAs, sharing the same "seed-region" (underlined nucleotides) and consequently several targets. **(B)** The expression levels of miR-221-3p and miR-222-3p were measured before pellet formation (day 0), and at day 7 and 21 of pellet culture, by quantitative RT-PCR. Data are presented as percentage variation of expression in comparison to untreated cells at the same time-point (set as 100% of expression), and results represent means±s.e.m. Statistical analysis was performed versus untreated cells (§) and antagomiR-Scr (*) treated hMSCs ($p \leq 0.05$).

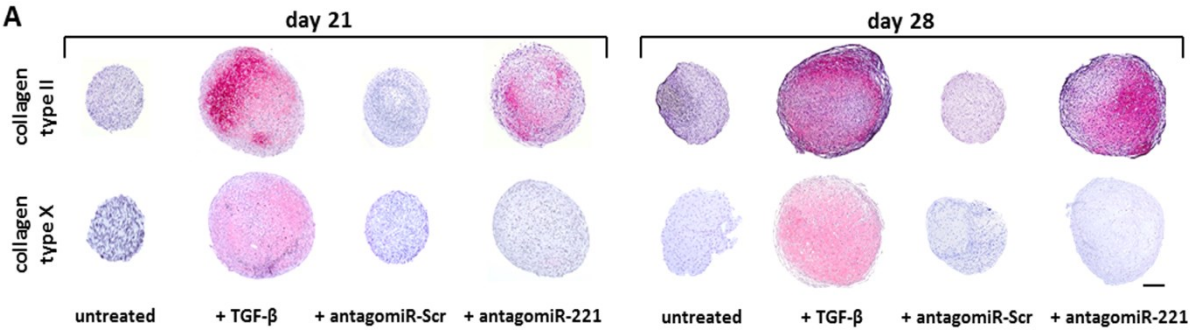

B

Treatment	% positive area				
	coll. II		coll. X		thionine (GAGs)
	day 21	day 28	day 21	day 28	day 28
untreated	0.5 ±0.3	0.5 ±0.2	0.7 ±0.6	0.6 ±0.4	0.2 ±0.1
+ TGF-β	32.4 ±18.8	53.9 ±2.8	24.0 ±13.8	64.5 ±7.1	48.9 ±9.2
+ antagomiR-Scr	0.2 ±0.1	0.5 ±0.2	0.6 ±0.4	0.4 ±0.1	0.5 ±0.3
+ antagomiR-221	16.7 ±9.7	48.9 ±7.1	1.8 ±1.3	2.8 ±2.3	35.4 ±8.3

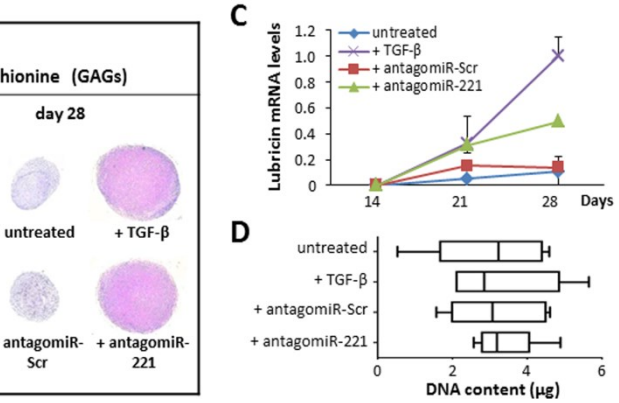

Supplementary figure 2. *Evaluation of the in vitro chondrogenic potential of antagomiR-221 treated hMSCs from bone marrow* (three replicates per time-point; n = 2). **(A)** hMSCs pellets were immunostained for collagen type II and X at day 21 and 28. The red staining represents positivity for collagen type II or collagen type X. The sections were counterstained with hematoxylin and eosin (scale bar: 200 µm). **(B)** Protein levels were quantified by densitometric analysis of immunohistochemical pictures. GAGs content was measured by quantification of thionine staining (a representative staining is reported). Data were quantified using ImageJ software and expressed as % of positive area of the pellet. Average densitometric values ± s.e.m. are reported. The data demonstrated that collagen type II and GAGs are similarly induced in TGF-β and antagomiR-221 treated cells, while collagen type X expression is markedly reduced following antagomiR-221 treatment. **(C)** mRNA quantification of the cartilage marker lubricin. Results represent means±s.e.m. and are presented as fold change respect to TGF-β treated cells at day 28. Interestingly, an appreciable level of lubricin mRNA was detected both in TGF-β and antagomiR-221 treated cells. **(D)** Measurement of DNA content in hMSCs pellets at day 28 of culture. Data are presented as median and interquartile range. Since no differences in DNA content were detected, the increase in size of TGF-β and antagomiR-221 treated pellets is to be attributed mainly to matrix production (see collagen type II and thionine staining) rather than variation of the proliferation rates.

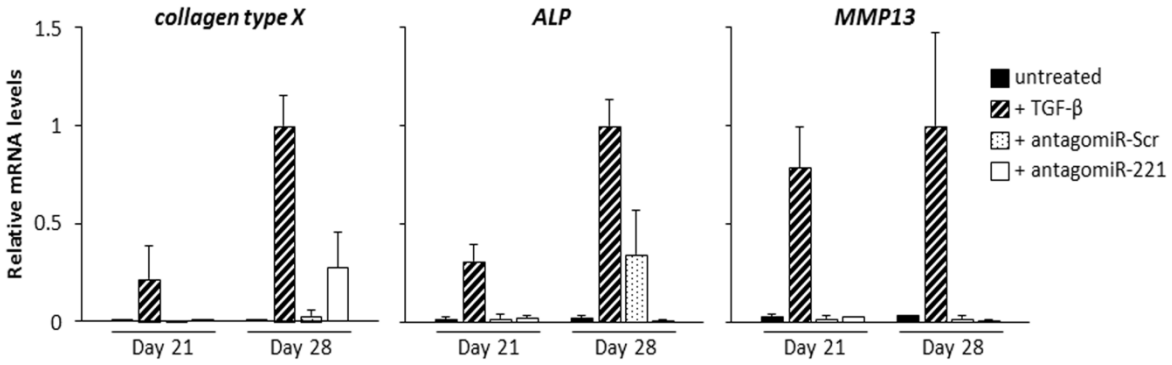

Supplementary figure 3. *Effect of antagomiR-221 on the expression of hypertrophic markers in hMSCs pellet cultures.* The mRNA levels of collagen type X, ALP and MMP13 were measured at day 21 and 28 of pellet culture of bone marrow-derived hMSCs. Results represent means±s.e.m. and are presented as fold change respect to TGF-β treated cells at day 28.

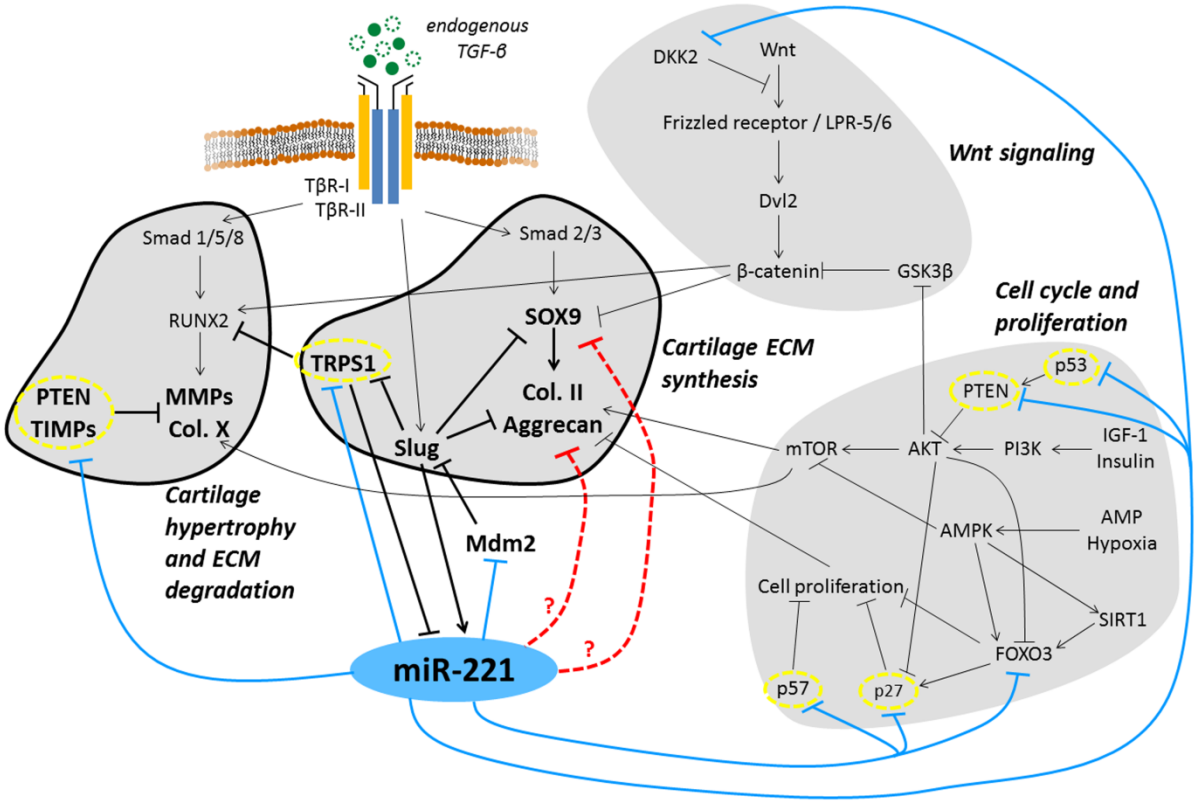

Supplementary figure 4. *General overview of miR-221 targets and downstream effects potentially affecting the synthesis and maintenance of cartilage ECM.* Four possible scenarios have been considered: cartilage hypertrophy and ECM degradation, cartilage ECM synthesis, Wnt signaling, cell cycle and proliferation (see supplementary Table 1 for the references). Among the experimentally validated targets of miR-221 (blue lines) are transcription factors and regulators involved in signaling pathways that directly or indirectly affect cartilage ECM remodeling. Common targets of miR-221 and miR-222 are circled in yellow. Based on our experimental evidence, we specifically focused on the two pathways circled in black and detailed in Fig. 5 and Discussion.

Target gene	Cell signaling pathway	References
validated targets of miR-221 (strong evidence*)		
TIMP2	Oncogenesis	[1]
BCL2L11	Apoptosis	[2]
DDIT4	Oncogenesis/Apoptosis	[3]
BMF	Apoptosis	[4]
FOXO3	Oncogenesis/Apoptosis	[5]
HMGXB4	Embryogenesis	[3]
ARIH2	Embryogenesis/Inflammation	[3]
USP18	Inflammation	[3]
BRAP	Oncogenesis	[3]
CREBZF	Oncogenesis	[3]
DKK2	WNT signaling	[3]
MYBL1	Oncogenesis	[3]
TBK1	Oncogenesis/Inflammation	[3]
BNIP3L	Apoptosis	[3]
BNIP3	Apoptosis/Autophagy	[3]
NAIP	Apoptosis	[6]
TICAM1	Inflammation	[7]
FMR1	Embryogenesis	[8]
DVL2	WNT signaling	[9]
POU3F2	Embryogenesis	[9]
HOXC10	Morphogenesis	[10]
MEOX2	EMT/Embryogenesis	[10]
ZEB2	EMT	[10]
PGC1α	Energy metabolism	[11]
SEMA3B	Oncogenesis	[12]
STMN1	EMT	[13]
ATXN1	EMT	[14]
MDM2	Cell cycle	[15]
validated targets of miR-221/miR-222 (strong evidence*)		
CDKN1B	Oncogenesis	[16]
STAT5	Oncogenesis	[17]
KIT	Oncogenesis	[18]
TMED7	Oncogenesis	[3]
CDKN1C	Cell cycle	[19]

TIMP3	Oncogenesis	[20]
RECK	Oncogenesis	[21]
BBC3	Apoptosis	[22]
PTEN	Cell cycle	[23]
ICAM1	Cell adhesion	[24]
FOS	Oncogenesis	[25]
CORO1A	Oncogenesis/Cell cycle	[26]
DICER1	Cell cycle/miRNA biogenesis	[27]
ETS1	Oncogenesis	[28]
DIRAS3	Oncogenesis	[29]
TNFSF10	Apoptosis	[30]
ESR1	Cell cycle/Sexual development	[31]
SELE	Cell adhesion	[24]
TP53	Cell cycle	[26]
TCEAL1	Cell cycle	[26]
TRPS1	EMT	[32]
CERS2	Cell cycle	[33]

targets of miR-221 validated by NGS:

PDIK1L, ABHD3, NDUFB5, SPTSSA, CSTF2T, NR2C2AP, APOL2, TDRP, GTF2E1, TMEM168, TUB, ZNF652, EIF2AK1, TNIP1, KLF9, TOMM20, TMEM64, GID8, ZNF571, CASP3, ATL2, E2F3, PTBP3, CXorf38, ARID1A, NHSL1, HIVEP1, WDR61, TRPC3, SLC6A9, TMEM245, RNF20, PHF12, WEE1, NUFIP2, LYSMD1, NDFIP1, TIPARP, GPR107, LHFPL2, STAMBP, HNRNPD, UBE2N, ELAVL2, ACSL3, RNF4, ASXL3, CTNNB1, PLOD2, RNF44, LIMS1, ZNF275, TMEM132B, CCSAP, BRD1, AGAP1, FBXO28, TFAP2A, PANK3, ZKSCAN8, HNRNPA0, UBE2J1, MIDN, CYP1B1, ATXN1, POGZ, PPP1R15B, HECTD2, RUNDC3B, TRAF4, YWHAE, C15orf40, RBM33, CROT, ACTB, HIST2H2AC, USP28, PALB2, CCT3, YY1, PLP2, PXN, SMCHD1, RPS24, TSN, HIST1H3D, AMMECR1L, PSMD4, PELO, LGTN, XRCC6, FSCN1, HIST2H3D, MTSS1L, EEF1A1, NOP58, TUBA1C, DDAH1, TMEM248, RAB5C, RPL15, VPS53, LPHN2, DYNC1H1, TIAM1, ASXL2, UTP14A, B4GALT2, HSPA1B, PEX19, PITPNM1, AP2A1, KIF16B, SEPHS1, KPNA6, SF1, RHOA, RBM39, HIST1H2AE, FLNA, CCDC142, ZYX, KLHL8, TLE4, MDFIC, NME2, EIF4G3, UBC, UQCR10, ADD1, HECTD1, FUS, CNOT1, HIST1H2AC, RPL21, WDR34, NT5DC2, LRP6, AP3B1, EVL, NCL, GLYR1, PEG10, ANKRD28, TMEM183A, LDHB, TRIM28, NUP210, YWHAB, PEX1, MKI67, SRP68, NUF2, FARSA, CHCHD2, CLIC1, UHRF1, NFYC, PHF21A, TSC22D2, PKM, CENPT, DHX15, LAMTOR5, MIEN1, RPS7, NABP2, IQCE, RPLP0, YOD1, CDC25C, TOB2, MBNL1, RACGAP1, SPAG5, TNKS2, SGTA, SAPCD2, NFYA, KHSRP, AMOT, POLG, SKI, FBN3, SPRYD3, ACIN1, BAG3, ATP6V1E1, PRDM16, GCN1L1, UNC13B, ERK1, SF3B3, GATAD2B, ARHGEF18, PTPRF, SLC30A7, ARHGAP42, DDX3Y [34]

*strong evidence: reporter assay, western blot and qPCR
NGS = next generation sequencing
= target genes involved in cartilage-related pathways

Supplementary table 1. *Experimentally validated targets of miR-221/miR-222.*

References (Supplementary table 1):

[1] Xu Q, Li P, Chen X, Zong L, Jiang Z, Nan L, Lei J, Duan W, Zhang D, Li X, Sha H, Wu Z, Ma Q, Wang Z. ”miR-221/222 induces pancreatic cancer progression through the regulation of matrix metalloproteinases.” Oncotarget. 2015; 6(16):14153-64.

[2] Sehgal M, Zeremski M, Talal AH, Ginwala R, Elrod E, Grakoui A, Li QG, Philip R, Khan ZK, Jain P. “IFN-α-induced downregulation of miR-221 in dendritic cells: implications for HCV pathogenesis and treatment.” J Interferon Cytokine Res. 2015; 35(9):698-709

[3] Pineau P, Volinia S, McJunkin K, Marchio A, Battiston C, Terris B, Mazzaferro V, Lowe SW, Croce CM, Dejean A. “miR-221 overexpression contributes to liver tumorigenesis.” Proc Natl Acad Sci U S A. 2010; 107(1):264-9.

[4] Gramantieri L, Fornari F, Ferracin M, Veronese A, Sabbioni S, Calin GA, Grazi GL, Croce CM, Bolondi L, Negrini M. “MicroRNA-221 targets Bmf in hepatocellular carcinoma and correlates with tumor multifocality.” Clin Cancer Res. 2009; 15(16):5073-81.

[5] Garofalo M, Quintavalle C, Romano G, Croce CM, Condorelli G. “miR221/222 in cancer: their role in tumor progression and response to therapy.” Curr Mol Med. 2012; 12(1):27-33.

[6] Hu G, Gong AY, Liu J, Zhou R, Deng C, Chen XM. “miR-221 suppresses ICAM-1 translation and regulates interferon-gamma-induced ICAM-1 expression in human cholangiocytes.” Am J Physiol Gastrointest Liver Physiol. 2010; 298(4):G542-50.

[7] Gong AY, Hu G, Zhou R, Liu J, Feng Y, Soukup GA, Chen XM. “MicroRNA-221 controls expression of intercellular adhesion molecule-1 in epithelial cells in response to Cryptosporidium parvum infection.” Int J Parasitol. 2011; 41(3-4):397-403.

[8] Zongaro S, Hukema R, D'Antoni S, Davidovic L, Barbry P, Catania MV, Willemsen R, Mari B, Bardoni B. “The 3' UTR of FMR1 mRNA is a target of miR-101, miR-129-5p and miR-221: implications for the molecular pathology of FXTAS at the synapse.” Hum Mol Genet. 2013; 22(10):1971-82.

[9] Zheng C, Yinghao S, Li J. “miR-221 expression affects invasion potential of human prostate carcinoma cell lines by targeting DVL2.” Med Oncol. 2012; 29(2):815-22.

[10] Chen Y, Banda M, Speyer CL, Smith JS, Rabson AB, Gorski DH. “Regulation of the expression and activity of the antiangiogenic homeobox gene GAX/MEOX2 by ZEB2 and microRNA-221.” Mol Cell Biol. 2010; 30(15):3902-13.

[11] Xue Y, Wei Z, Ding H, Wang Q, Zhou Z, Zheng S, Zhang Y, Hou D, Liu Y, Zen K, Zhang CY, Li J, Wang D, Jiang X. “MicroRNA-19b/221/222 induces endothelial cell dysfunction via suppression of PGC-1α in the progression of atherosclerosis.” Atherosclerosis. 2015; 241(2):671-81.

[12] Cai G, Qiao S, Chen K. “Suppression of miR-221 inhibits glioma cells proliferation and invasion via targeting SEMA3B.” Biol Res. 2015; 48:37.

[13] Liu J, Cao J, Zhao X. “miR-221 facilitates the TGFbeta1-induced epithelial-mesenchymal transition in human bladder cancer cells by targeting STMN1.” BMC Urol. 2015; 15:36.

[14] Ke J, Zhao Z, Hong SH, Bai S, He Z, Malik F, Xu J, Zhou L, Chen W, Martin-Trevino R, Wu X1, Lan P, Yi Y6, Ginestier C, Ibarra I, Shang L, McDermott S, Luther T, Clouthier SG, Wicha MS, Liu S. “Role of microRNA221 in regulating normal mammary epithelial hierarchy and breast cancer stem-like cells.” Oncotarget. 2015; 6(6):3709-21.

[15] Kim D, Song J, Jin EJ. “MicroRNA-221 regulates chondrogenic differentiation through promoting proteosomal degradation of slug by targeting Mdm2.” J Biol Chem. 2010; 285(35):26900-7.

[16] Galardi S, Mercatelli N, Giorda E, Massalini S, Frajese GV, Ciafrè SA, Farace MG. “miR-221 and miR-222 expression affects the proliferation potential of human prostate carcinoma cell lines by targeting p27Kip1.” J Biol Chem. 2007; 282(32):23716-24.

[17] Dentelli P, Traversa M, Rosso A, Togliatto G, Olgasi C, Marchiò C, Provero P, Lembo A, Bon G, Annaratone L, Sapino A, Falcioni R, Brizzi MF. “miR-221/222 control luminal breast cancer tumor progression by regulating different targets.” Cell Cycle. 2014; 13(11):1811-26.

[18] Felli N, Fontana L, Pelosi E, Botta R, Bonci D, Facchiano F, Liuzzi F, Lulli V, Morsilli O, Santoro S, Valtieri M, Calin GA, Liu CG, Sorrentino A, Croce CM, Peschle C. “MicroRNAs 221 and 222 inhibit normal erythropoiesis and erythroleukemic cell growth via kit receptor down-modulation.” Proc Natl Acad Sci U S A. 2005; 102(50):18081-6.

[19] Fornari F, Gramantieri L, Ferracin M, Veronese A, Sabbioni S, Calin GA, Grazi GL, Giovannini C, Croce CM, Bolondi L, Negrini M. “miR-221 controls CDKN1C/p57 and CDKN1B/p27 expression in human hepatocellular carcinoma.” Oncogene. 2008; 27(43):5651-61.

[20] Garofalo M, Di Leva G, Romano G, Nuovo G, Suh SS, Ngankeu A, Taccioli C, Pichiorri F, Alder H, Secchiero P, Gasparini P, Gonelli A, Costinean S, Acunzo M, Condorelli G, Croce CM. “miR-221&222 regulate TRAIL resistance and enhance tumorigenicity through PTEN and TIMP3 downregulation.” Cancer Cell. 2009; 16(6):498-509.

[21] Qin J, Luo M. “MicroRNA-221 promotes colorectal cancer cell invasion and metastasis by targeting RECK.” FEBS Lett. 2014; 588(1):99-104.

[22] Zhang C, Zhang J, Zhang A, Wang Y, Han L, You Y, Pu P, Kang C. “PUMA is a novel target of miR-221/222 in human epithelial cancers.” Int J Oncol. 2010; 37(6):1621-6.

[23] Garofalo M, Di Leva G, Romano G, Nuovo G, Suh SS, Ngankeu A, Taccioli C, Pichiorri F, Alder H, Secchiero P, Gasparini P, Gonelli A, Costinean S, Acunzo M, Condorelli G, Croce CM. “miR-221&222 regulate TRAIL resistance and enhance tumorigenicity through PTEN and TIMP3 downregulation.” Cancer Cell. 2009; 16(6):498-509.

[24] Suárez Y, Wang C, Manes TD, Pober JS. “Cutting edge: TNF-induced microRNAs regulate TNF-induced expression of E-selectin and intercellular adhesion molecule-1 on human endothelial cells: feedback control of inflammation.” J Immunol. 2010; 184(1):21-5.

[25] Kameswaran V, Bramswig NC, McKenna LB, Penn M, Schug J, Hand NJ, Chen Y, Choi I, Vourekas A, Won KJ, Liu C, Vivek K, Naji A, Friedman JR, Kaestner KH. “Epigenetic regulation of the DLK1-MEG3 microRNA cluster in human type 2 diabetic islets.” Cell Metab. 2014; 19(1):135-45.

[26] Yang CJ, Shen WG, Liu CJ, Chen YW, Lu HH, Tsai MM, Lin SC. “miR-221 and miR-222 expression increased the growth and tumorigenesis of oral carcinoma cells.” J Oral Pathol Med. 2011; 40(7):560-6.

[27] Cochrane DR, Cittelly DM, Howe EN, Spoelstra NS, McKinsey EL, LaPara K, Elias A, Yee D, Richer JK. “MicroRNAs link estrogen receptor alpha status and Dicer levels in breast cancer.” Horm Cancer. 2010; 1(6):306-19.

[28] Wu YH, Hu TF, Chen YC, Tsai YN, Tsai YH, Cheng CC, Wang HW. “The manipulation of miRNA-gene regulatory networks by KSHV induces endothelial cell motility.” Blood. 2011; 118(10):2896-905.

[29] Li Y, Liu M, Zhang Y, Han C, You J, Yang J, Cao C, Jiao S. “Effects of ARHI on breast cancer cell biological behavior regulated by microRNA-221.” Tumour Biol. 2013; 34(6):3545-54.

[30] Garofalo M, Quintavalle C, Di Leva G, Zanca C, Romano G, Taccioli C, Liu CG, Croce CM, Condorelli G. “MicroRNA signatures of TRAIL resistance in human non-small cell lung cancer.” Oncogene. 2008; 27(27):3845-55.

[31] Zhao JJ, Lin J, Yang H, Kong W, He L, Ma X, Coppola D, Cheng JQ. “MicroRNA-221/222 negatively regulates estrogen receptor alpha and is associated with tamoxifen resistance in breast cancer.” J Biol Chem. 2008; 283(45):31079-86.

[32] Stinson S, Lackner MR, Adai AT, Yu N, Kim HJ, O'Brien C, Spoerke J, Jhunjhunwala S, Boyd Z, Januario T, Newman RJ, Yue P, Bourgon R, Modrusan Z, Stern HM, Warming S, de Sauvage FJ, Amler L, Yeh RF, Dornan D. “miR-221/222 targeting of trichorhinophalangeal 1 (TRPS1) promotes epithelial-to-mesenchymal transition in breast cancer.” Sci Signal. 2011; 4(186):pt5.

[33] Yu B, Zhou S, Wang Y, Qian T, Ding G, Ding F, Gu X. “miR-221 and miR-222 promote Schwann cell proliferation and migration by targeting LASS2 after sciatic nerve injury.” J Cell Sci. 2012; 125(Pt 11):2675-83.

[34] from http://www.mirbase.org.

Supplementary methods:

Pellet culture of hMSCs from bone marrow

2 x 10^5 hMSCs from bone marrow of two donors were centrifuged to form 3D-pellets. antagomiR-221 or antagomiR-Scr treated hMSCs were cultured in DMEM high-glucose supplemented with GlutaMAX+ (GIBCO), 1:100 insulin, transferrin, and selenous acid (ITS+; BD Biosciences, San Jose, CA, USA), 40 µg/mL L-proline (Sigma-Aldrich), 1 mM sodium pyruvate (GIBCO), 100 nM dexamethasone (Sigma-Aldrich), 25 µg/mL ascorbic acid-2-phosphate (Sigma-Aldrich), 1.5 µg/mL fungizone and 50 µg/mL gentamicin, in the absence of conventional chondrogenic inducers (TGF-β). Pellets formed with untransfected hMSCs were cultured as described above, and supplemented or not with 10 ng/mL TGF-β1 (R&D Systems, Minneapolis, MN, USA) ("TGF-β" and "untreated" condition, respectively). All pellet cultures were maintained at 37°C, 5% CO_2 up to 28 days and the medium was refreshed twice a week. Pellets were processed for DNA/RNA isolation or fixed in 4% formalin, embedded in paraffin, sectioned and processed for immunohistochemistry (as described in the materials and methods section).

DNA quantification

hMSCs pellets were digested with 300 µl of proteinase K solution (1 mg/mL proteinase K, 50 mM Trizma base, 1 mM EDTA, 1 mM iodoacetamide, 10 µg/ml pepstatin [pH 7.6]; all from Sigma-Aldrich) for 16 h at 60°C. After digestion, proteinase K was inactivated for 10 min at 105°C. Samples were loaded in technical triplicate on an ice-cold 96-well plate. After incubation with heparin (8.3 U/mL in PBS; Leo Pharma) and RNase solution (0.05 mg/mL in PBS; Sigma-Aldrich), 50 µl of ethidium bromide (25 µg/mL in PBS; GIBCO) were added to each sample. Using the Wallac 1420 VICTOR2 (PerkinElmer) apparatus, the ratio between the absorbance at 340 nm (extinction filter) and the absorbance at 590 nm (emission filter), corrected by the background (wells loaded with PBS only), was calculated. Purified calf thymus DNA (Sigma-Aldrich) was used to set the standard curve.

Chapter 7

Discussion

Age-related cartilage disorders represent a major cause of morbidity globally and result in enormous costs for health and social care systems (*Musumeci et al., 2015*). Unfortunately, it is conceivable that the increase in life expectancy will further exacerbate this burden in future years. It is predicted that the number of total knee replacements will jump from 700,000 to 3.48 million annually by the year 2030 (*Green et al., 2015*). As a consequence, there is an acute and urgent need both for lifestyle interventions that can prevent these disorders and novel pharmacological and biological therapies that can effectively treat them. To date, these objectives are still far from being achieved. Since surgical approaches have shown a number of limitations and relatively high failure rates, basic and clinical research have gradually moved towards cell-based therapies. These strategies aim at a cell-driven regeneration of the articular tissue, and offer a number of advantages when compared with conventional techniques, mainly in terms of the quality of the repair tissue that is to be produced. Indeed, cell therapy is aimed at not only filling the cartilage lesions with a cartilage-like substitute, but also reconstituting the structure, the physico-chemical properties and the functionality of the hyaline matrix. Cell-based therapy has been used for the treatment of osteoarticular lesions for over two decades, in the form of autologous chondrocyte implantation (ACI). While this approach has proved effective in slowing down the progression of osteoarthritis (OA) and delay partial or total joint replacement surgery, currently used procedures are associated with the risk of serious adverse events and cannot be considered overall satisfying.

Due to these limitations, experimental therapies using undifferentiated cell sources, and specifically hMSCs, are receiving an increasing amount of scientific and public interest. The extraordinary potential offered by hMSCs application in cartilage tissue engineering and regenerative medicine is unquestionable. Besides, this does not apply exclusively to human beings, as there is a growing interest in the application of stem cells in the veterinary field, which is evolving rapidly both experimentally and clinically, for instance

for the treatment of musculoskeletal injures in dogs and race horses (*Fortier & Travis, 2011*).

The preclinical and clinical studies using adult hMSCs have demonstrated encouraging results, although more cases and long-term observations are now being performed for reaching a conclusion about the efficacy. Usually, hMSCs-based treatments are carried out by intraarticular injection (more practicable for generalized OA) or surgical arthrotomy with cell transplantation at the site of the lesion (for focal defects) (*Frisch et al., 2015*). Nevertheless, a number of hurdles still need to be addressed before hMSCs-based approaches might evolve into first-line therapies for cartilage repair (see Chapter 1 for a comprehensive analysis). Indeed, much more research is needed to gain a complete knowledge concerning the processes of hMSCs commitment and differentiation and the behavior of hMSCs upon transplantation, as well as the mechanisms of their interaction with the diseased microenvironment. In this context, the major challenge that basic research has to deal with is likely the control of cell differentiation. While hMSCs have proven able to reform cartilage, the microenvironmental conditions needed to induce a stable mature chondrocytic phenotype, as well as a sufficient production of cartilage matrix, are not defined (*Demoor et al., 2014*). The nature of the medium, the amount of oxygen, the presence of pro-chondrogenic biochemical and mechanical stimuli, the use of different biomaterials, and the gene manipulation strategies are all parameters that are being considered to stabilize the hMSCs differentiated phenotype.

1. Characterization of novel chondro-regulators: miR-221 and Slug

It is widely accepted that cell-based regeneration techniques should recapitulate, at least in part, the main steps naturally occurring *in vivo* at a developmental stage (*Richardson et al., 2015*). As a consequence, understanding the regulation of "natural" chondrogenesis is of paramount importance and a pre-requisite for the development of novel and more effective tools in cartilage regenerative medicine. To date, many biological regulators of chondrogenesis have been characterized, thereby providing various ways to induce differentiation of hMSCs and progenitor cells. Current research suggests that among the many growth factors implicated to have a regulatory effect on chondrogenesis, TGF-β proteins are the most potent biological inducers. In contrast, other growth factors, including IGFs, FGFs, and PDGFs, appear to mediate chondrocytic physiology to a greater extent than they promote chondrogenesis in hMSCs. Unfortunately, from a translational

standpoint, the use of molecules such as TGF-β1 and TGF-β3 raises a number of issues, mainly related to their side effects *in vivo* and involvement in the pathogenesis of OA. It has become gradually clear that a "gross" stimulation of such a wide and complex signalling as the TGF-β pathway will not only induce chondrogenic differentation, but also activate cell processes that are not desirable, thereby limiting the therapeutic value of this approach. Accordingly, we have recently confirmed that TGF-β treatment in hMSCs sustains or even induces the expression of anti-chondrogenic regulators, that may counteract the pro-chondrogenic stimulus (*Lolli et al., 2014; Lisignoli et al., 2014*). In search of alternative differentiation protocols, it has been hypothesized that a precise modulation of crucial down-stream regulators could be still sufficient to induce differentiation, while avoiding or reducing the unwanted side effects. In light of this, much effort is now being put into characterizing the chondrogenic process at a molecular level, and identifying critical factors to be targeted to induce hMSCs to acquire a chondrogenic phenotype.

Remarkably, it has been shown that chondrogenesis and production of cartilage matrix by hMSCs can be achieved by activation of precise morphogenetic signals of developmental pathways or removing potentially anti-chondrogenic factors (*Madry et al., 2005; Im et al., 2011; Guérit et al., 2014; Diekman et al., 2015; Pi et al., 2015; Seidl et al., 2016*). As part of this effort, we focused on two cell regulators that in recent years have been proposed as potential anti-chondrogenic factors, the microRNA-221 (miR-221) and the zinc-finger transcription factor Slug. While these molecules were thought to exert a role during the chondrogenic process, there was a lack of studies concerning the underlying molecular mechanisms and the possibility to manipulate these factors to influence the chondrogenic potential of hMSCs. As outlined in **Chapter 2**, we demonstrated not only a precise involvement of miR-221 and Slug in the acquisition (or loss) of the chondrogenic phenotype, but also the existence of a functional correlation between them, with Slug being recruited at the miR-221 promoter to stimulate its expression. Remarkably, we showed that miR-221 or Slug silencing in hMSCs induces the commitment towards a chondrocyte-like phenotype, as demonstrated by the expression of cartilage ECM proteins (collagen type II) and chondrogenic transcription factors (Sox9, TRPS1). Notably, this was achieved in the absence of TGF-β and by 2D-monolayer culture, which is a favorable condition for transfection but a major hindrance for chondrogenesis.

An *in vitro* model of OA chondrocytes, described in **Chapter 3**, further allowed us to strengthen the hypothesis concerning the key role of the transcription factor Slug in cartilage homeostasis. We showed that Slug, besides regulating chondrogenesis, takes part

in the processes of chondrocyte senescence and de-differentation. As mounting evidence suggests that these phenomena may be responsible for the aberrant phenotype of chondrocytes in OA, there is a need to identify molecular targets that may account for the instability of the chondrocytic phenotype. We demonstrated that Slug can be indeed considered an anti-chondrogenic pro-senescent marker, possibly *via* a direct regulation of lamin B1, a nuclear protein that appears to have a role in the cell senescent phenotype and in laminopathies. It is particularly relevant that the same transcription factor, Slug, might be possibly manipulated both to induce chondrogenic differentiation and to counteract OA-related aberrant mechanisms, hence supporting its importance for the maintenance of a stable chondrogenic phenotype.

Taken as a whole, these data highlighted the need to further characterize miR-221 and Slug as candidate cell regulators to be targeted to enhance the chondrogenic potential of hMSCs. Consistently with recent literature, this first phase of the project supported the silencing of anti-chondrogenic factors, and the manipulation of specific TF-miRNA interplays, as a pre-implantation strategy alternative to the use of growth factors for the use of hMSCs in cartilage tissue engineering.

2. From 2D- to 3D-models: towards the establishment of an osteochondral-like microenvironment *in vitro*

Experimental models using conventional 2D-culture conditions, such as those reported above, are extremely useful to gain novel insights into basic processes, such as regulation of gene expression and response of the cells to controlled changes of the microenvironment. Besides, these techniques are easy to handle and significantly less cost- and time-consuming compared to more complex approaches. However, it cannot be ignored that cell culture on 2D-plastic or substrates represents a major limit, as these conditions completely fail to capture the 3D-spatial interactions that are crucial for cell functionality *in vivo*, possibly resulting in controversial or misleading conclusions. Based on this concept, it is essential for researchers to develop specific *in vitro* 3D-culture systems that might be a step closer to the *in vivo* microenvironment. Particularly in the field of bone and cartilage biology, this effort has led to the establishment of cutting-edge models that, besides producing much more informative results, also enable a fine-tuning of the biophysical, biochemical and biomechanical cues, while allowing their monitoring.

The second phase of the project focused on the establishment of specific 3D-culture systems displaying a different degree of complexity, and that could be useful to validate

our data in contexts more similar to the *in vivo* osteochondral microenvironment. Specifically, the work described in **Chapters 4-6** involved (i) the combination of hMSCs with biocompatible scaffolds supporting cell culture and differentiation (scaffold-based tissue engineering), (ii) the employment of 3D-pellet culture and co-culture aggregate techniques (scaffold-less aggregate tissue engineering), and (iii) the use of osteochondral models with simulated tissue defects. From a technical standpoint, these studies were useful to establish culture systems that will serve as platforms to test different approaches to optimize the differentiation/therapeutic ability of hMSCs, or assess their response to novel drugs. As a proof of principle, such an approach allowed us to validate in complex 3D-microenvironments the silencing of the anti-chondrogenic factors miR-221 and Slug as a feasible strategy to enhance the chondrogenic potential of hMSCs.

The study outlined in **Chapter 4** involved the culture of hMSCs onto HYAFF-11, a biocompatible scaffold that, besides being already in clinical use, also provides a microenvironment where the cells are easier to transfect compared with standard 3D-culture systems. Here we showed that a strong inhibition of Slug TF was effective in enhancing the chondrogenesis and production of cartilage ECM by TGF-β-induced hMSCs. Notably, Slug silencing alone was itself sufficient to address hMSCs towards chondrogenesis, without requiring supplementation with TGF-β or other growth factors. This evidence validated the concept that Slug silencing could replace TGF-β in producing cartilaginous tissue, and that Slug depleted hMSCs/HYAFF-11 constructs could be developed for cartilage tissue regeneration, especially in contexts where the recruitment or differentiation potential of endogenous hMSCs is compromised.

According to the traditional paradigm of cartilage tissue engineering, a bioactive construct requires three elements, namely cells, a scaffold matrix and pro-chondrogenic agents, e.g. growth factors and gene vectors (Fig. 1, panel D). Taking into account that any exogenous agent will affect the target tissue and likely produce side effects *in vivo*, the inclusion of each component in the construct must be carefully evaluated. Based on this concept, the "dogma" of tissue engineering has been overcome, and approaches based on alternative constructs have been developed (Fig. 1), being already at a preclinical or clinical stage. Particularly, the development of scaffold-less tissue engineering (Fig. 1, panel B) has provided novel scaffold-independent techniques, such as those based on the formation of cell-sheets and aggregates, that also allow to better mimic the developmental processes. With this in mind, we evaluated the possibility to chondrogenically differentiate hMSCs within a 3D-environment by gene silencing only, and in the absence of any external cues or scaffolds, using the pellet culture system (**Chapter 6**).

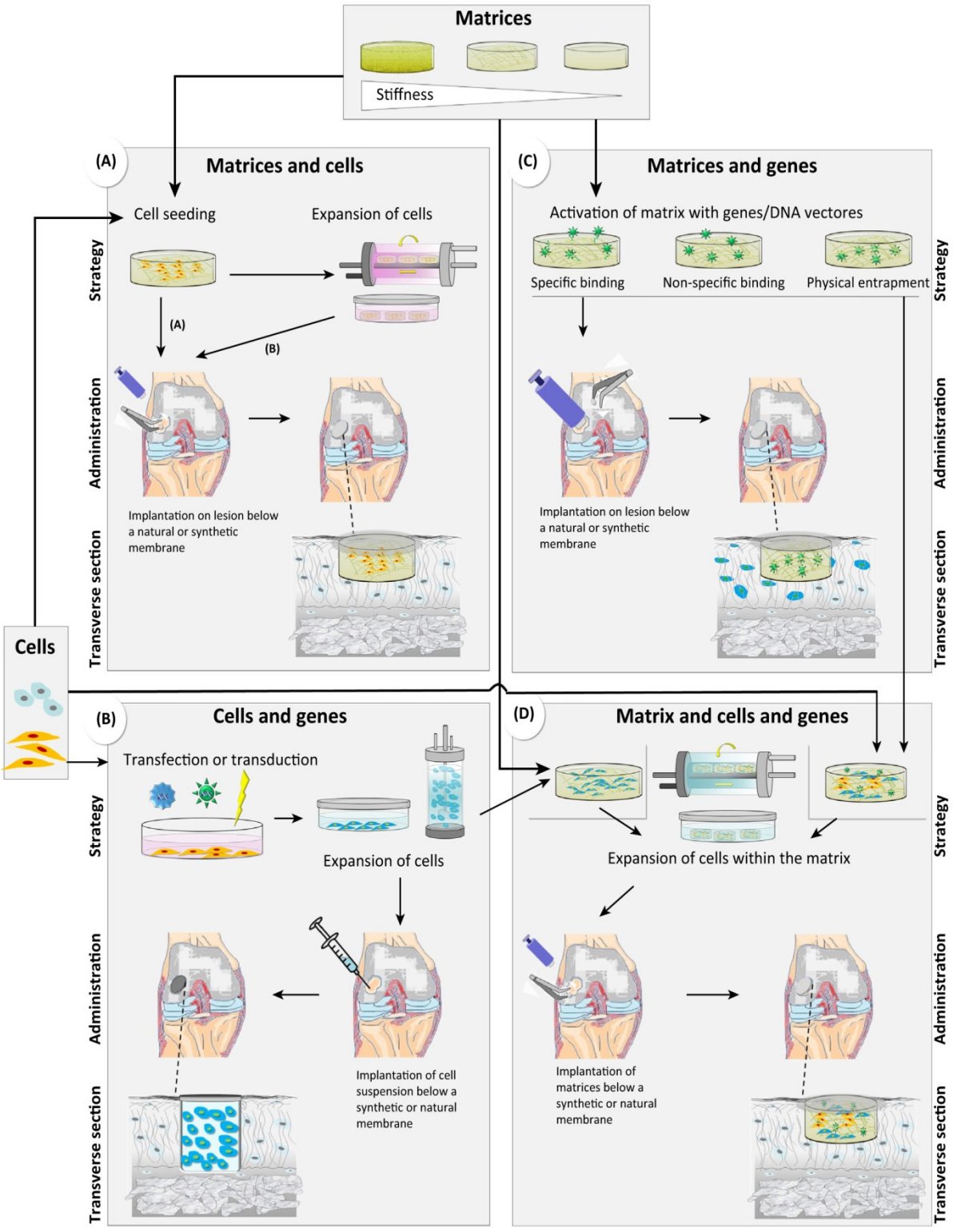

Figure 1. *Combination strategies currently under investigation in preclinical and clinical studies for cartilage regeneration (Madeira et al., 2015).*

We demonstrated that miR-221 depleted hMSCs in pellet culture spontaneously differentiated into chondrocyte-like cells, that expressed specific pro-chondrogenic TFs and synthesized cartilage ECM proteins and GAGs. It is particularly relevant that these results were obtained using a culture system which is a major hindrance both for cell transfection and for matrix production in the absence of stimulation with growth factors. Importantly, these findings were confirmed using hMSCs derived from different sources, namely Wharton's jelly of umbilical cord and bone marrow, further strengthening the validity of our data.

The evidence that miR-221 silencing was sufficient to induce the accumulation of a cartilage-like ECM matrix that could both maintain an intact cell construct and preserve the survival/differentiation of hMSCs was very encouraging. Indeed, this was the premise for the use of miR-221 depleted hMSCs to repair a cartilage defect *in vivo*.

3. An osteochondral culture model to study the chondrogenic potential of engineered hMSCs *in vivo*

For the *in vivo* studies of this project, we used an experimental model based on bovine osteochondral biopsies, that allowed us to culture our engineered hMSCs in simulated tissue defects (*de Vries-van Melle et al., 2014a*) (**Chapter 6**). This strategy has been recently developed and validated by de Vries-van Melle and co-workers, in order to study cartilage repair mechanisms in a well characterized osteochondral microenvironment. This model is particularly relevant and informative to gain insights into the chondrogenic/therapeutic potential of cell populations, especially when compared to more conventional *in vitro* systems, such as alginate constructs or cartilage-only explants. Specifically, these advantages are related to:

- the presence of both cartilage and subchondral bone, whose strict interactions are known to be essential for the physiology of the joint;
- the possibility to produce controlled cartilage/bone defects of different nature, depth and size;
- the possibility to serve either as a platform for cell culture *in vitro* or as an implantable construct;
- the ease of handling and the possibility to establish a relatively controlled environment, something which is not possible when using conventional *in vivo* models of chondral defects.

Interestingly, it was initially proved that hMSCs, when cultured in the simulated osteochondral defects, were able to spontaneously undergo chondrogenesis *in vitro* and led to a partial repair of the defect *in vivo*. Based on our previous work, we hypothesized that this repair process could be improved or accelerated by a proper manipulation of the molecular signature of the cells, and specifically by silencing of the anti-chondrogenic miR-221. Interestingly, the possibility to exploit the osteochondral model to assess the differentiation potential of manipulated hMSCs was still unexplored. Therefore, we cultured miR-221 depleted hMSCs in the simulated osteochondral defects. An approach of transient transfection was used, similarly to the *in vitro* experiments, even if this technique cannot be expected to guarantee a stable silencing of the target molecule. However, this is convenient when the engineered cells might have a less invasive, priming effect on the regeneration process, by triggering the repair mechanisms, as well as stimulating a progressive involvement of the host tissues in the repair of the defect (*Abdul Halim et al., 2014*). It is conceivable that, compared to the treatment of chronic/genetic diseases where likely a lifelong expression or silencing is required, musculoskeletal repair might offer a different opportunity for a clinical application of gene therapy, as it may only require a transient and localized expression or silencing of specific genes (*Steinert et al., 2008*).

We first confirmed that our system did not only preserve the viability of the engineered hMSCs, but also the efficiency of silencing for a convenient period of time (at least 4 weeks). This is very relevant, as the scarce duration of transgene expression or silencing is a serious drawback of transient transfection-based approaches, especially under 3D-culture conditions. Hence, our experimental setting was suitable for culturing miR-221 depleted hMSCs *in vivo*. We then demonstrated that implantation of osteochondral biopsies with miR-221 depleted hMSCs-alginate constructs resulted in significantly more cartilaginous repair tissue after 12 weeks than what was found in defects containing non-engineered hMSCs. This newly-formed tissue displayed extensive production of GAGs, cartilage ECM proteins (collagen type II), and chondro-transcription factors (Sox9, TRPS1). To the best of our knowledge, ours was the first study demonstrating that the silencing of miR-221 is a feasible strategy not only to improve the chondrogenic properties of hMSCs, but to strengthen their ability to repair a cartilage defect *in vivo*.

In the context of our work, the use of engineered hMSCs *in vitro* and *in vivo* was crucial for the characterization of the anti-chondrogenic role of miR-221. Nevertheless, it should be considered that the depletion of miR-221 *in vivo* might be sufficient on its own to promote a healing response. Indeed, among the different combination strategies that have been proposed for cartilage tissue engineering are also cell-free approaches (Fig. 1, panel

C). This kind of strategy offers different advantages, such as avoiding the issues related to the use of exogenous cells and a more direct involvement of the host tissues in the repair process. In this regard, an interesting option is the implantation of a 3D-matrix pre-loaded with a gene/miRNA delivery vehicle ("gene-activated matrix") into the defect, allowing infiltrating endogenous cells to acquire the vector and trigger the regenerative response. Hence, it should be also evaluated whether endogenous hMSCs could be induced to repair a cartilage damage by targeted administration of a miR-221 inhibitor into the joint, possibly with the aid of a suitable 3D-matrix or hydrogel.

While our *in vivo* findings are very promising in view of a potential application of miR-221 depleted hMSCs for cartilage regeneration, it is to be considered that the experimental setting was not specifically aimed at determining the quality of the repair tissue. Indeed we defined it as "cartilage-like tissue", on the basis of the histomorphological appearance, expression of cartilage-specific ECM proteins and transcriptional regulators. However, it remains to be established if miR-221 depleted hMSCs are in fact capable of producing true hyaline cartilage, which is the ultimate goal in this field. In basic research, repair tissue is all too often designated as being "hyaline-like" on insufficient grounds, while it needs to be subjected to a rigorous analysis: its maturation status should be defined, so, too, should its architectonic and ultrastructural features, including the degree of anisotropy and the long-term stability. While the osteochondral model is exploitable as a platform to gain insights into molecular mechanisms or novel targets involved in cartilage repair, a meticulous assessment of the quality and stability of the newly synthesized ECM requires a different experimental approach. Firstly, our model lacks of a controlled and measurable mechanical loading, which is known to be an essential factor both for the production and the maintenance of fully functional cartilage. Secondly, an unequivocal characterization of the participation of donor cells in tissue repair is technically challenging, as the engineered hMSCs are likely to interact simultaneously with mouse and bovine host tissues. As a consequence, large animal models of chondral defects would be the natural and suitable choice for a follow-up project aimed at the evaluation of the biomechanical and physical properties of the ECM produced by miR-221 depleted hMSCs.

Beside the hyaline nature of the repair tissue, a second aspect must be necessarily taken into account, namely its hypertrophic features. This is a general issue that likely represents the real limit of the available approaches for cartilage regeneration, and that is related to their inability to induce the formation of permanent cartilage. Both articular cartilage and growth plate cartilage are indeed of hyaline nature, but the difference is substantial.

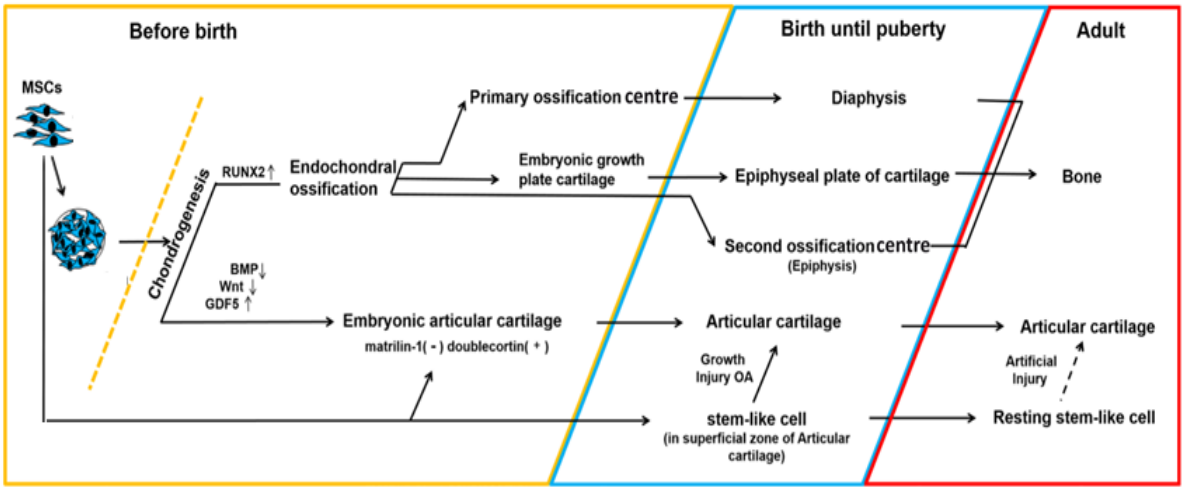

Figure 2. *Schematic representation of the different stages of chondrogenesis and endochondral ossification.* At the embryonic stage, hMSCs chondrogenesis occurring in the developing bone may either lead to the formation of bone via endochondral ossification (at the primary and secondary centres of ossification, and in the growth plate) or to stable hyaline cartilage.

While the former is permanent cartilage that maintains its function throughout life, the latter is cartilage that transitionally exists serving as a skeletal template in the process of endochondral ossification (Fig. 2). Hence, if the regenerated tissue has indeed transient cartilage features, and this is usually the case, chondrocytes will undergo hypertrophy and will eventually be replaced by bone, making the approach *de facto* inefficient for cartilage reconstruction. During embryonic development, the permanent articular cartilage and the transient hypertrophic cartilage both arise from the same cartilaginous anlage. However, specific sets of stimuli drive these two hyaline cartilages into distinct differentiation programs. Attempts to identify the required stimuli to drive the formation of permanent articular cartilage have been largely unsuccessful to date. Chondrogenically differentiated hMSCs, particularly when induced with TGF-β and regardless of the source and expansion conditions, appear to be prone to undergo endochondral ossification, and display signs of terminal differentiation and mineralization *in vitro* and *in vivo* (*Hellingman et al., 2011*). To date, many strategies aiming to inhibit the terminal differentiation of hMSCs have been tested, but the results are still not satisfying.

In light of this issue, we investigated the tendency of miR-221 depleted hMSCs to undergo hypertrophic maturation, by measuring the expression of collagen type X protein both in chondrogenic pellets and in the cartilage-like repair tissue produced *in vivo*. Remarkably, the expression of collagen type X was not or barely detectable after pellet culture of miR-

221 depleted hMSCs up to 28 days, suggesting that the silencing of miR-221 was more effective than TGF-β in inducing chondrogenesis without stimulating overt hypertrophic maturation. Accordingly, the same trend was observed for two additional hypertrophic markers, alkaline phosphatase (ALP) and matrix metalloproteinase 13 (MMP13). These results were validated *in vivo*, as no sign of collagen X expression could be detected even in the osteochondral constructs implanted in mice for 12 weeks. We are aware that our findings needs to be further confirmed, using more complex *in vivo* models and possibly measuring the expression of a panel of hypertrophic and mineralization markers. However, the ability of miR-221 depleted hMSCs to downregulate hypertrophic genes represents a crucial event during the formation of cartilaginous repair tissue, and is very promising for potential applications in regenerative medicine.

It is worth mentioning that the intrinsic tendency of hMSCs to undergo hypertrophic maturation, while being a serious hindrance for cartilage regeneration, represents an opportunity for bone repair. Bone tissue engineering normally relies on direct differentiation of progenitor cells and hMSCs towards the osteogenic lineage and production of mineralized matrix in attempting to accelerate tissue recovery. However, this approach still suffers from major limitations. Since the development of long bones does not involve direct osteogenic commitment of hMSCs (intramembranous ossification), it has been suggested that bone substitutes should be generated by phenocopying the steps of endochondral ossification, with the production of a cartilage template ("developmental engineering") (*Tonnarelli et al., 2014*). Based on this concept, different studies have succeeded in recapitulating the pathway of endochondral ossification for the production of bone constructs using hMSCs (*Scotti et al., 2010; Farrell et al., 2011; Scotti et al., 2013*). In such a context, the combined use of miR-221 depletion and treatment with TGF-β or BMPs would be worthy of investigation. Indeed, this could allow to further accelerate the synthesis of the cartilage template, while still allowing the newly formed cartilage to undergo hypertrophy and endochondral ossification.

4. Molecular basis for the anti-chondrogenic properties of miR-221

The work of this thesis provides novel insights into the chondrogenic features of miR-221 depleted hMSCs for cartilage tissue engineering purposes. Importantly, a molecular explanation for this phenomena is still lacking. In this regards, it is to be investigated which of the known or yet uncharacterized targets of miR-221 might mediate the pro-

chondrogenic effects that are observed following miR-221 silencing. In **Chapter 6**, we tried to give a measure of this complex scenario by assembling a list of the validated targets of miR-221, and highlighting those that are known to be involved in the process of chondrogenic differentiation. This screening of the literature, coupled with our experimental evidence, allows us to hypothesize a number of potential regulatory mechanisms supporting the anti-chondrogenic role of miR-221, that will be worth pursuing as follow-up of the work. Specifically, this can be summarized as follows:

- *Inhibition of cartilage ECM synthesis*. By targeting the ubiquitin ligase MDM2, miR-221 may prevent the degradation and therefore lead to sustained expression of Slug protein, that is known to directly inhibit the pro-chondrogenic transcription factors Sox9 and TRPS1, and the cartilage ECM proteins collagen type II and aggrecan. Consistently, we detected very low levels of Slug protein in miR-221 depleted hMSCs, supporting the hypothesis that miR-221 may act through MDM2 to prevent cartilage ECM synthesis. Our previous evidence that Slug is directly recruited at the miR-221 promoter to stimulate its expression (*Lolli et al., 2014*) supports the existence of such a miR-221/Slug circuit able to prevent chondrogenic differentiation. This interplay may be further reinforced by a reciprocal negative regulation between TRPS1 and miR-221. Accordingly, we demonstrated previously the ability of TRPS1 to strongly inhibit miR-221 expression (*Lolli et al., 2014*), and here an increase in TRPS1 expression after miR-221 depletion.
- *Stimulation of cartilage ECM degradation.* Since TRPS1 acts as a repressor of Runx2 activity, the targeting of TRPS1 by miR-221 may promote the Runx2-mediated transactivation of genes associated with cartilage hypertrophy and ECM degradation, such as collagen type X, alkaline phosphatase (ALP) and matrix metalloproteinases (MMPs). In agreement with this hypothesis, the expression of these genes in miR-221 depleted hMSCs was reduced, and these cells were shown to be less prone to undergo terminal differentiation. Targeting of anti-catabolic mediators by miR-221, such as phosphatase and tensin homolog (PTEN) and tissue inhibitor of metalloproteinases (TIMPs), may further sustain the degradation of cartilage ECM.

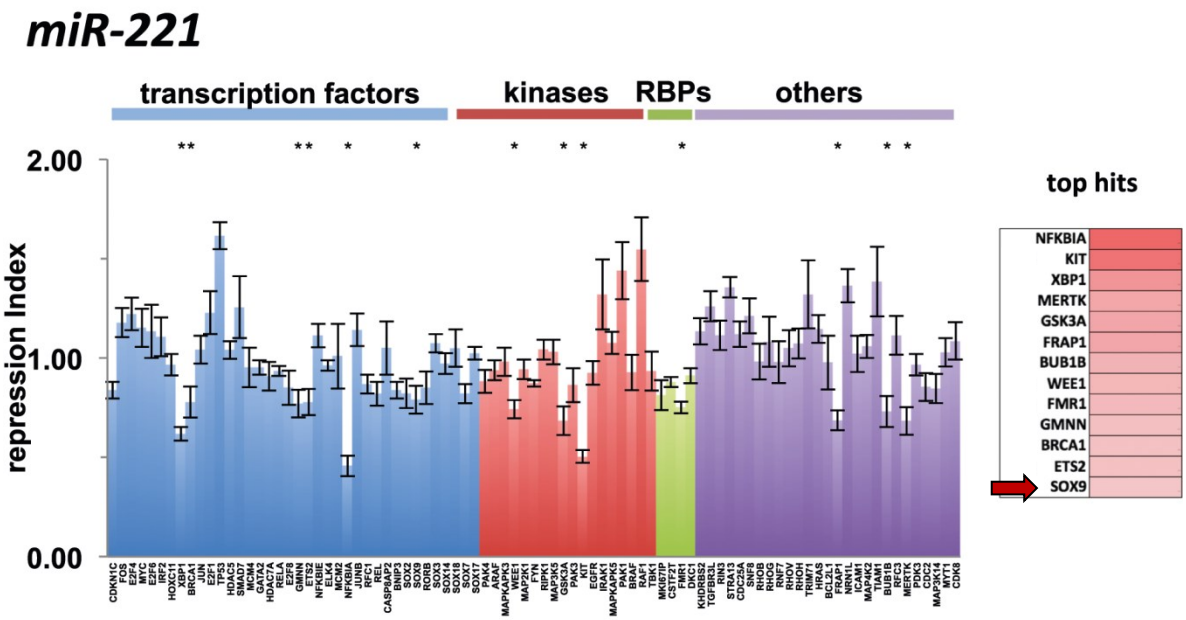

Figure 3. *High-throughput screening of a 3'-UTR library for the identification of novel targets of miR-221.* A dual luciferase assay (3'LIFE) screening was performed on 87 human 3'-UTRs extracted from the h3'-UTRome v1 library, to identify cell regulators that are targeted by miR-221. The top hits are displayed as a heat map on the right panel. Interestingly, 13 top hits (miR-221 targets) were identified, and among them is the transcription factor Sox9 (*Kotagama et al., 2015*).

- *Non-canonical targeting of chondrogenic regulators and ECM proteins.* It is conceivable that miR-221 might directly target the master chondro-regulator Sox9 and collagen type II, as their expression becomes upregulated following miR-221 knockdown in all examined conditions. While these genes do not display conventional conserved miR-221 "seed-match" sites in their 3'-UTRs, it is well established that miRNA targeting can also be mediated by unconserved sequences, or mechanisms that differ from the canonical seed/3'-UTR pairing (*Thomson et al., 2011*). Accordingly, a high-throughput screening of a human 3'-UTR library (h3'UTRome v1) has recently shown that Sox9 is indeed a candidate target of miR-221 (Fig. 3) (*Kotagama et al., 2015*). Hence, the relevance of these non-canonical miRNA-target interactions in the chondrogenic context should be experimentally investigated.
- *Modulation of pathways linked with cartilage homeostasis.* The previous mechanisms require a direct regulation by miR-221 of crucial regulators and ECM molecules that are responsible for the maintenance of the chondrocytic phenotype. Alternatively (or simultaneously), miR-221 might exert its chondro-inhibitory effects by targeting mediators of different pathways, such as TGF or Wnt signalling (e.g. DKK2). Indeed, a

specific modulation of these factors could lead to the production of a stable cartilage phenotype, where collagen type II and aggrecan are strongly stimulated while hypertrophy is repressed. It is also relevant that among the validated targets of miR-221 are regulators of cell cycle and proliferation, such as p27, p57, PTEN and p53. As a strict regulation of the proliferation of chondrogenic cells is required, it is conceivable that targeting of these regulators by miR-221 may have an impact on specific phases or phenotypic transitions that are essential for chondrogenesis.

- *Modulation of the epigenetic machinery.* miR-221 has been recently shown to directly modulate the expression of different regulators of the epigenetic machinery, such as the histone deacetylase HDAC6 and the DNA methyltransferase DNMT3B (*Bae et al., 2015; Roscigno et al., 2015*). This might in turn influence chondrogenesis, as it is well established that most of the cartilage-specific genes (e.g. Sox9, collagen type II, aggrecan, collagen type X) are susceptible of epigenetic regulation (*Furumatsu & Ozaki, 2010; Miranda-Duarte, 2015*).

In order to gain preliminary evidence concerning candidate target genes of miR-221, we are currently planning a microarray analysis to detect variations in the mRNA expression profile following the silencing of miR-221 in hMSCs. This will provide novel insights onto the downstream signals and targets that are modulated by miR-221 in hMSCs, and allow us to determine which of our hypothesis are more likely to be true. The validation of the newly identified targets by a reporter assay, and their manipulation in a 3D microenvironment (such as the osteochondral biopsy), will then be the natural follow-up of this work. Additionally, useful information concerning the miR-221-mediated regulatory mechanisms could be obtained by laser capture microdissection (LCM) techniques. In this way, it would be possible to isolate from histological samples the cell populations that are specifically responsible for cartilage ECM synthesis after miR-221 knockdown, thereby performing targeted expression and functional analysis (quantitative RT-PCR, western blot, ChIP and reporter assays). Finally, novel non-invasive technologies such as molecular imaging techniques could be applied as well to elucidate the putative mechanisms by which miR-221 works *in vivo*, and its interplays with complex gene networks.

Our experimental work aimed at the characterization of miR-221-3p, which is considered the mature miR-221 (guide strand). According to the traditional view, while the guide strand is selected and loaded onto RISC, the passenger strand is discarded and eventually degraded, being a non-functional side product of miRNA biogenesis. Despite this general consensus, recent publications have provided evidence that the relevance of miRNA passenger strands have been underestimated, as they display important functions both in

physiology and disease. This might apply also to miR-221-5p, as it has been recently shown to play a critical role in colitis and inhibit the expression of crucial factors such as TNFα, CXCL10 and collagen type II (*Fang et al., 2015*). Due to this recent evidence, the expression and relevance of miR-221-5p in chondrogenesis will be worth of investigation.
In this scenario, the contributions of miR-222-3p and -5p should be explored as well. Indeed, miR-221 and miR-222 are highly homologous miRNAs, encoded by the same gene cluster and having the same seed sequence, thus sharing many predicted and validated targets and often regulating the same cellular pathways. It is therefore possible that miR-221 and miR-222 might have a similar anti-chondrogenic activity. If that is the case, silencing both miRNAs would have a synergic effect on chondrogenesis, likely further promoting differentiation and synthesis of cartilage matrix.
As a whole, these molecular studies will be useful to define yet uncharacterized miRNA-mediated circuits in chondrogenesis, and to identify novel targets to be properly manipulated in the effort to strictly control and stabilize the chondrogenic phenotype of differentiated hMSCs.

5. RNA interference-based therapeutics: current challenges and opportunities

The elucidation of the mechanisms of RNAi, and specifically those related to siRNAs and miRNAs, has offered researchers the chance to alter the paradigm of medical therapeutics. Although our understanding of these RNA molecules represents perhaps only the tip of the iceberg, with the rapid development of molecular biotechnology they are continuously found to have far more important functions than previously recognized (*Lam et al., 2015*). Notably, new classes of non-coding RNAs such as piwi-like RNAs (piRNAs) are still being found, and need to be properly characterized as their functions remain largely unknown. With the ability to selectively suppress the function of a gene, RNAi not only provides a powerful tool for molecular studies, but also for the development of novel therapeutics aimed at inhibiting crucial gene products involved in disease or mechanisms responsible for tissue dysfunction (*Battistella & Marsden, 2015*). To date, pharmaceutical industry is looking forward to investigating the diagnostic and therapeutic potentials of nucleic acid-based drugs including RNAi-based tools. Indeed, siRNAs and miRNAs offer the advantages of being highly potent and able to act on “non-druggable” targets, e.g. proteins which lack an enzymatic function or have a conformation that is inaccessible to

traditional drugs. Most importantly, these molecules can be designed to affect virtually any gene of interest.

RNAi in the form of siRNAs and miRNAs is a relatively simple technique to specifically manipulate gene function *in vitro*. In the field of cartilage repair, as well as every area of biomedical research, countless studies have been and are being performed, providing critical insights into tissue-specific regulatory mechanisms and novel targets to induce tissue reconstruction. Importantly, a number of early proof-of-principle studies in animal models and early phase clinical trials have supported the use of RNAi as a therapeutic agent without significant toxicity. However, there are different issues that still need to be addressed before RNAi can really enter into routine clinical use. These criticisms are essentially related to the need to design molecules exhibiting both potency and negligible off-target effects, and to the *in vivo* delivery.

The first crucial step for successful RNAi therapy is the design of a sequence that is potent and specific to the intended mRNA or miRNA, to minimize any off-target effect. siRNAs and miRNAs have specific characteristics in binding to their targets, and our current limited knowledge of these aspects cause unwanted effects, e.g. non-specific silencing of genes, dose-dependent immune response and saturation of the RNAi machinery. As a general rule, prediction of susceptible off-target domains that can influence silencing efficiency and outcome is required. This can be partly achieved by the assistance of bioinformatic tools, as well as a careful evaluation of the different parameters that can affect the RNAi/target interaction, such as the spatiotemporal gene expression pattern of the target tissue. In this context, several strategies are being explored, such as using the lowest possible siRNA/miRNA concentrations, the pooling of multiple RNAi molecules directed to the same target, and a proper design and modification of the sequence. Specifically, chemical modification of the phosphodiester backbone (phosphorothioate, boranophosphate, phosphonoacetate), the ribose 2'-OH group (2'-OMe, 2'-F, 2'-O-MOE, LNA) and the ribose ring (thio, hydroxy, iodo) are widely employed to improve stability, potency and specificity of RNAi therapeutics (*Borna et al., 2014*).

The *in vivo* delivery of RNAi therapeutics to target cells at effective concentrations remains the most significant challenge in translating these molecules into the clinic. siRNAs and miRNAs have an intracellular site of action, but their intrinsic properties, (hydrophilic nature, negative charge, high molecular weight), render them poorly permeable across membranes. As a consequence, a number of delivery systems have been developed, both to protect the nucleic acids from premature nuclease degradation and to improve the efficiency and specificity of the cellular uptake (*Lam et al., 2015*).

Delivery system	Disease	miRNA/siRNA	Animal model	Route of administration
Unmodified PEI				
PEI	Asthma	siRNA targeting IL-13	Mouse sensitized and challenged with ovalbumin	Intravenous
	Sepsis	siRNA targeting IL-6 and TNFα	Mouse with polymicrobial sepsis induced by cecal ligation and puncture	Intravenous; intraperitoneal
	Colon cancer	miRNA-145; miRNA-33a	Mouse xenograft tumor	Intratumoral; intraperitoneal
Modified PEI				
SA-PEI-CNT	Melanoma	siRNA targeting Braf	*In situ* mouse melanoma model	Topical
PU-PEI	Lung cancer	miRNA-145	Mouse xenograft tumor	Intratumoral
	Gliobastoma	miRNA-145	Mouse xenograft tumor	Intratumoral
Dendrimers				
PAMAM	Ovarian cancer	siRNA targeting Akt	Mouse xenograft tumor	Intratumoral
	Drug-resistant prostate cancer	siRNA targeting Hsp27	Mouse xenograft tumor	Intratumoral
PAMAM-folic acid	Glioma	miRNA-7	Mouse xenograft tumor	Intratumoral; intravenous
	Ovarian cancer	siRNA targeting CD44	Mouse xenograft tumor	Intraperitoneal
Natural polymers				
Glycol chitosan	Drug-resistant breast cancer	siRNA targeting P-glycoprotein	Mouse xenograft tumor	Intravenous
Hyaluronic acid-chitosan	Breast cancer	miRNA-34a	Mouse xenograft tumor	Intravenous
Atelocollagen	Prostate cancer	siRNA targeting Bcl-xL	Mouse xenograft tumor	Intravenous
	Muscular dystrophy	siRNA targeting Mst	Genetically modified mouse with limb-girdle muscular dystrophy	Intramuscular
	Metastatic prostate cancer	miRNA-16	Mouse xenograft tumor	Intravenous
PLGA				
PLGA microspheres with PEI	Sarcoma	siRNA targeting VEGF	Mouse xenograft tumor	Intratumoral
	Joint inflammation	siRNA targeting FcγRIII	Rat with temporomandibular inflammation induced by Complete Freund's Adjuvant injection	Intra-articular
PLGA nanoparticles with PEI	Lung cancer	siRNA targeting STAT3	Mouse with lung cancer induced by carcinogen	Intraperitoneal
Other nanoparticles				
Tf-targeted nanoparticles of CDP	Subcutaneous tumor	siRNA targeting RRM2	Mouse with subcutaneous tumor of murine neuroblastoma cells	Intravenous
Mesoporous silica nanoparticles with pDMAEMA	Cervical cancer	siRNA targeting PLK1	Mouse xenograft tumor	Intravenous
Mesoporous silica nanoparticles with KALA peptide-PEG-PEI	Ovarian cancer	siRNA targeting VEGF	Mouse xenograft tumor	Intravenous
Porous silica nanoparticles with GD2 antibody	Neuroblastoma	miRNA-34a	Mouse xenograft tumor	Intravenous
Lipoplexes				
Cationic liposomes	Melanoma with lung metastasis	siRNA targeting Mcl1	Mouse with lung cancer induced by intravenous injection of murine melanoma or lung carcinoma cells	Intrapulmonary
PEG-cationic liposomes	Prostate and pancreatic cancer	siRNA targeting PKN3	Mouse xenograft tumor	Intravenous
	Drug-resistant renal cancer	siRNA targeting PLK1	Mouse xenograft tumor	Intravenous
RGD peptide -PEG-cationic liposomes	Melanoma with lung metastasis	siRNA targeting c-Myc, MDM2 and VEGF	Mouse with lung cancer induced by intravenous injection of murine melanoma cells	Intravenous
Peptides-modified PEG-cationic liposomes	Glioma	siRNA targeting VEGF	Mouse xenograft tumor	Intratumoral; Intravenous
Cationic liposomes (Lipofectamine™)	Colon cancer	miRNA-143	Mouse xenograft tumor	Intratumoral; Intravenous
Cationic liposomes DOTMA/cholesterol/TPGS	Non–small-cell lung cancer	miRNA-29b	Mouse xenograft tumor	Intravenous
Neutral lipid emulsion (RNALancerII)	Non–small-cell lung cancer	miRNA-34a, *let-7*	Mouse xenograft tumor	Intravenous
Lipid-based nanoparticles (SNALPs, SLNs and LPH nanoparticles)				
SNALP	Ebola infection	siRNA targeting polymerase of Ebola virus	Guinea pigs infected with Ebola virus	Intraperitoneal
SLN	Lung cancer	miRNA-34a	Mouse xenograft tumor	Intravenous
	Melanoma with lung metastasis	miRNA-34a	Mouse with lung cancer induced by intravenously injection of murine melanoma cells	Intravenous
LPH with single chain antibody fragment	Melanoma with lung metastasis	Combined miRNA-34a and siRNA targeting MDM2, c-myc and VEGF	Mouse with lung cancer induced by intravenously injection of murine melanoma cells	Intravenous
Lipopolymer				
StA-PEI	Melanoma	siRNA targeting STAT3	Mouse xenograft tumor	Intratumoral
DA-PEI	Colorectal cancer	siRNA targeting XIAP	Mouse xenograft tumor	Intratumoral
	Myocardial infarction	siRNA targeting RAGE	Rat subjected to ischemic-reperfusion injury by transient coronary artery ligation	Intra-myocardial
Cholesterol-PEI	Prostate cancer	siRNA targeting VEGF	Mouse xenograft tumor	Intratumoral

Table 1. *Selected examples of non-viral delivery systems for RNAi therapeutics (Lam et al., 2015).*

As previously mentioned (see Chapter 1, par. 6), delivery systems are normally categorized as viral and non-viral. Viruses that are more commonly employed include lentiviruses, adenoviruses and adeno-associated viruses (AAVs). They are extremely efficient in transferring RNAi-encoding vectors into the nucleus of mammalian cells to ensure stable expression of RNA. Nevertheless, due to safety concerns and the high production costs of viral vectors, virus-free systems have become attractive alternatives, despite their inferior transfection efficiency. A plethora of non-viral delivery systems have been developed, including cationic peptides, cationic polymers, liposomes, dendrimers, nanoparticles, aptamers, bio-conjugates and bacteria-derived cells (minicells). A detailed list of the main non-viral systems currently under investigation for RNAi delivery in animal and preclinical studies is reported in Table 1.

The first clinical trial of siRNA therapeutics was initiated in 2004, only 6 years after the discovery of RNAi. To date, around 30 siRNA candidates have reached various stages of clinical trials for the treatment of different diseases (Table 2, top). On the other hand, the clinical development of miRNA as therapeutics is lagging behind, as the first miRNA therapeutic trial began only in 2013. The relatively slow progress of miRNA therapeutics could be due to the yet uncertain mechanism of action and specificity, as well as the diverse potential applications of miRNA (e.g. as drug target and biomarkers). Importantly, miRNAs have a crucial advantage over siRNAs, as with their ability to inhibit the expression of a number of target genes, which often work together as a network within the same cellular pathway, a whole disease phenotype can potentially be changed by a single miRNA sequence. To date, a few miRNA therapeutics, indicated for the treatment of cancer or HCV infection, are registered for clinical testing (Table 2, bottom). Nevertheless, many tumor suppressor miRNAs, such as miR-7 and the members of the let-7 families, have proven effective in downregulating oncogenes, and are currently in preclinical stage and ready to enter phase 1 trials. While clinical studies have demonstrated that siRNA therapeutics are generally well-tolerated by the patients, miRNA therapeutics is still in its infancy and more trials are required before conclusions about safety can be drawn. In any case, the promising new findings suggest that both siRNAs and miRNAs now offer hope for *in vivo* use in humans, and that we may soon be able to harness this robust and specific gene silencing mechanism as a therapeutic tool. Specifically, it is expected that by overcoming the delivery barrier, and achieving a better understanding of the effects and the duration of gene silencing, siRNAs and miRNAs will become practical therapeutics in the clinic in the near future.

Targets	Drug	Indications	Developers	Developmental stage
CTNNB (encodes β-catenin)	CEQ508	Familial adenomatous polyposis	Marina Biotech	Phase II
N gene of RSV	ALN-RSV01	Respiratory syncytial virus	Alnylam Pharma	Phase II
TTR	ALN-TTR02	TTR-mediated amyloidosis	Alnylam Pharma	Phase II
TP53	QPI-1002	Acute kidney injury; delayed graft function	Quark	Phase II
KSP, *VEGF*	ALN-VSP	Liver cancers	Alnylam Pharma	Phase I
DDIT4	PF-04523655	Age-related macular degeneration)	Pfizer/Quark	Phase II
FURIN	FANG vaccine	Solid tumours	Gradalis	Phase II
PCSK9	ALN-PCS	Hypercholesterolaemia	Alnylam Pharma	Phase I
PLK1	TKM-PLK1	Advanced solid tumours	Tekmira	Phase II
CTGF	RXI-109	Scar prevention	RXi Pharma	Phase II
CASP2	QPI-1007	Ocular neuroprotection; non-arteritic anterior ischaemic optic neuropathy	Quark	Phase I
STMN1	pbi-shRNA STMN1 lipoplex	Advanced and/or metastatic cancer	Gradalis	Phase I
Not disclosed	ARC-520	Hepatitis B virus infection	Arrowhead Research Corporation	Phase I
PCSK9	SPC5001	Hypercholesterolaemia	Santaris Pharma	Phase I
APOB	SPC4955	Hypercholesterolaemia	Santaris Pharma	Phase I
PSMB8, *PSMB9* and *PSMB10*	NCT00672542	Metastatic melanoma vaccine	Duke University	Phase I
PKN3	Atu027	Solid tumours	Silence Therapeutics	Phase I
Ebola virus	TKM-Ebola	Zaire species of Ebola virus	Tekmira	Phase I

APOB, apolipoprotein B; CASP2, caspase 2; CTGF, connective tissue growth factor; DDIT4, DNA-damage-inducible transcript 4; KSP, kinesin spindle protein; PCSK9, proprotein convertase subtilisin kexin 9; PKN3, protein kinase N3; PLK1, polo-like kinase 1; PSMB, proteasome subunit beta type; RNAi, RNA interference; RSV, respiratory syncytial virus; STMN1, stathmin 1; TP53, tumour suppressor p53; TTR, transthyretin; VEGF, vascular endothelial growth factor.

MicroRNA	Oligonucleotide format	Indications	Companies	Developmental stage
miR-122	LNA-modified antisense inhibitor	HCV infection	Santaris Pharma	Phase II
miR-122	GalNAc-conjugated antisense inhibitor	HCV infection	Regulus Therapeutics	Phase I
miR-34	miRNA mimic replacement	Liver cancer or metastasized cancer involving liver	miRNA Therapeutics	Phase I
Let-7	miRNA mimic replacement	Cancer (details undisclosed)	miRNA Therapeutics	Preclinical
miR-21	2′-F and 2′-MOE bicyclic sugar modified antisense inhibitor	Cancer, fibrosis	Regulus Therapeutics	Preclinical
miR-208	Antisense inhibitor	Heart failure, cardiometabolic disease	miRagen/Servier	Preclinical
miR-195 (miR-15 family)	Antisense inhibitor	Post-myocardial infarction remodelling	miRagen/Servier	Preclinical
miR-221	Antisense inhibitor	Hepatocellular carcinoma	Regulus Therapeutics	Preclinical
miR-103/105	Antisense inhibitor	Insulin resistance	Regulus Therapeutics	Preclinical
miR-10b	Antisense inhibitor	Glioblastoma	Regulus Therapeutics	Preclinical

2′-F, 2′-fluoro; 2′-MOE, 2′-*O*-methyoxyethyl; GalNAc, *N*-acetylgalactosamine; HCV, hepatitis C virus; LNA, locked nucleic acid; miRNA, microRNA.

Table 2. *Selected RNAi therapeutics currently in preclinical or clinical development (Li & Rana, 2014).*

Conclusions and perspectives

The project of this thesis may be considered relevant in the field of cartilage tissue engineering due to the experimental design of novel strategies based on the use of hMSCs depleted of negative regulators of differentiation to enhance the repair of a tissue defect. Besides, the employment of molecular and functional analysis allowed us to unveil novel regulatory interplays involved in chondrogenesis, the knowledge of which is the prerequisite for the development of targeted and more efficient tool to induce cartilage reconstruction. Our work was mainly focused on the anti-chondrogenic regulators miR-221 and Slug, and demonstrated that their silencing is sufficient to address hMSCs towards chondrogenesis *in vitro*. To validate our evidence, we established and optimized specific 3D-culture systems, that will also serve as platforms to test the differentiation/therapeutic potential of manipulated hMSCs, being one step closer to the *in vivo* microenvironment and thereby producing more informative results. In the effort to confer a translational value to our work, we assessed and proved that the silencing of miR-221 is indeed a promising strategy to induce hMSCs to differentiate into chondrocytes *in vivo* and produce cartilage ECM in the context of an osteochondral defect.

The follow-up of this work will mainly pursue two objectives. First, we plan to employ tissue engineering constructs with miR-221/Slug depleted hMSCs (or miR-221/Slug inhibitors) to induce the repair of "critical-size" cartilage defects *in vivo*. At the same time, it will be necessary to achieve a deep understanding of the network of regulatory interplays that sustain the anti-chondrogenic roles of miR-221 and Slug in cartilage cell populations.

In conclusion, we speculate that novel approaches based on the modulation of endogenous molecular cues, such as ours, will soon allow to obtain cell populations displaying a higher differentiation and therapeutic potential. This will lay the basis for important applications in basic research and regenerative medicine.

Chapter 8

References

Peer-reviewed journal articles

Abdul Halim NS, Fakiruddin KS, Ali SA, Yahaya BH. *A comparative study of non-viral gene delivery techniques to human adipose-derived mesenchymal stem cell.* Int J Mol Sci. 15, 15044–15060 (2014).

Ahmed TA & Hincke MT. *Mesenchymal stem cell-based tissue engineering strategies for repair of articular cartilage.* Histol Histopathol. 29, 669–689 (2014).

Albanese A, Licata ME, Polizzi B, Campisi G. *Platelet-rich plasma (PRP) in dental and oral surgery: from the wound healing to bone regeneration.* Immun Ageing. 10, 23 (2013).

Anderer U & Libera J. *In vitro engineering of human autogenous cartilage.* J Bone Miner Res. 17, 1420–1429 (2002).

Angelozzi A, Penolazzi L, Miotto M, Mazzitelli S, Bottaro E, Lambertini E, Keanec TJ, Badylak SF, Piva R, Nastruzzi C. *De-differentiated chondrocytes encapsulated in composite microfibers as tool for cartilage repair.* Submitted.

Anokye-Danso F, Snitow M, Morrisey EE. *How microRNAs facilitate reprogramming to pluripotency.* J Cell Sci. 125, 4179–4187 (2012).

Arthur A, Zannettino A, Gronthos S. *The therapeutic applications of multipotential mesenchymal/stromal stem cells in skeletal tissue repair.* J Cell Physiol. 218, 237–245 (2009).

Attur M, Ben-Artzi A, Yang Q, Al-Mussawir HE, Worman HJ, Palmer G, Abramson SB. *Perturbation of nuclear lamin A causes cell death in chondrocytes.* Arthritis Rheum. 64, 1940–1949 (2012).

Babur BK, Ghanavi P, Levett P, Lott WB, Klein T, Cooper-White JJ, Crawford R, Doran MR. *The interplay between chondrocyte redifferentiation pellet size and oxygen concentration.* PLoS One. 8, e58865 (2013).

Badekas T, Takvorian M, Souras N. *Treatment principles for osteochondral lesions in foot and ankle.* Int Orthop. 37, 1697–1706 (2013).

Bae HJ, Jung KH, Eun JW, Shen Q, Kim HS, Park SJ, Shin WC, Yang HD, Park WS, Lee JY, Nam SW. *MicroRNA-221 governs tumor suppressor HDAC6 to potentiate malignant progression of liver cancer.* J Hepatol. 63, 408–419 (2015).

Bakhshandeh B, Soleimani M, Paylakhi SH, Ghaemi N. *A microRNA signature associated with chondrogenic lineage commitment.* J Genet. 91, 171–182 (2012).

Bamias A, Kastritis E, Bamia C, Moulopoulos LA, Melakopoulos I, Bozas G, Koutsoukou V, Gika D, Anagnostopoulos A, Papadimitriou C, Terpos E, Dimopoulos MA. *Osteonecrosis of the jaw in cancer after treatment with bisphosphonates: incidence and risk factors.* J Clinical Oncol. 23, 8580–8587 (2005).

Barasch A, Cunha-Cruz J, Curro FA, Hujoel P, Sung AH, Vena D, Voinea-Griffin AE; CONDOR Collaborative Group, Beadnell S, Craig RG, DeRouen T, Desaranayake A, Gilbert A, Gilbert GH, Goldberg K, Hauley R, Hashimoto M, Holmes J, Latzke B, Leroux B, Lindblad A, Richman J, Safford M, Ship J, Thompson VP, Williams OD, Yin W. *Risk factors for osteonecrosis of the jaws: a case-control study from the CONDOR dental PBRN*. J Dent Res. 90, 439–444 (2011).

Barba-Recreo P, Del Castillo Pardo de Vera JL, Georgiev-Hristov T, Ruiz Bravo-Burguillos E, Abarrategi A, Burgueño M, García-Arranz M. *Adipose-derived stem cells and platelet-rich plasma for preventive treatment of bisphosphonate-related osteonecrosis of the jaw in a murine model*. J Craniomaxillofac Surg. 43, 1161–1168 (2015).

Barter MJ, Tselepi M, Gómez R, Woods S, Hui W, Smith GR, Shanley DP, Clark IM, Young DA. *Genome-Wide MicroRNA and Gene Analysis of Mesenchymal Stem Cell Chondrogenesis Identifies an Essential Role and Multiple Targets for miR-140-5p.* Stem Cells. 33, 3266–3280 (2015).

Barzilay R, Melamed E, Offen D. *Introducing transcription factors to multipotent mesenchymal stem cells: making transdifferentiation possible.* Stem Cells. 27, 2509–2515 (2009).

Battistella M & Marsden PA. *Advances, nuances, and potential pitfalls when exploiting the therapeutic potential of RNA interference.* Clin Pharmacol Ther. 97, 79–87 (2015).

Baugé C & Boumédiene K. *Use of adult stem cells for cartilage tissue engineering: current status and future developments.* Stem Cells Int. 438026 (2015).

Baugé C, Girard N, Lhuissier E, Bazille C, Boumédiene K. *Regulation and role of TGF-β signaling pathway in aging and osteoarthritis joints.* Aging Dis. 5, 394–405 (2014).

Benedetti L, Cortivo R, Berti T, Berti A, Pea F, Mazzo M, Moras M, Abatangelo G. *Biocompatibility and biodegradation of different hyaluronan derivatives (Hyaff) implanted in rats.* Biomaterials. 14, 1154–1160 (1993).

Bhosale AM & Richardson JB. *Articular cartilage: structure, injuries and review of management.* Br Med Bull. 87, 77–95 (2008).

Bian L, Zhai DY, Mauck RL, Burdick JA. *Coculture of human mesenchymal stem cells and articular chondrocytes reduces hypertrophy and enhances functional properties of engineered cartilage.* Tissue Eng Part A. 17, 1137–1145 (2011).

Bianco P, Riminucci M, Gronthos S, Robey PG. *Bone marrow stromal stem cells: nature, biology, and potential applications.* Stem Cells. 19, 180–192 (2001).

Bittencourt RA, Pereira HR, Felisbino SL, Ferreira RR, Guilherme GR, Moroz A, Deffune E. *Chondrocyte cultures in tridimensional scaffold: alginate hydrogel.* Acta Ortop Bras. 17, 242–246 (2009).

Blaney Davidson EN, van der Kraan PM, van den Berg WB. *TGF-beta and osteoarthritis.* Osteoarthritis Cartilage. 15, 597–604 (2007).

Bloemen V, Schoenmakerv T, de Vries TJ, Everts V. *Direct cell-cell contact between periodontal ligament fibroblasts and osteoclast precursors synergistically increases the expression of genes related to osteoclastogenesis*. J Cell Physiol. 222, 565–573 (2009).

Bobick BE, Matsche AI, Chen FH, Tuan RS. *The ERK5 and ERK1/2 signaling pathways play opposing regulatory roles during chondrogenesis of adult human bone marrow-derived multipotent progenitor cells.* J Cell Physiol. 224, 178–186 (2010).

Bonne G, Di Barletta MR, Varnous S, Bécane HM, Hammouda EH, Merlini L, Muntoni F, Greenberg CR, Gary F, Urtizberea JA, Duboc D, Fardeau M, Toniolo D, Schwartz K. *Mutations in the gene encoding lamin A/C cause autosomal dominant Emery-Dreifuss muscular dystrophy.* Nat Genet. 21, 285–288 (1999).

Borna H, Imani S, Iman M, Azimzadeh Jamalkandi S. *Therapeutic face of RNAi: in vivo challenges.* Expert Opin Biol Ther. 15, 269–285 (2015).

Brandl M, Seidler B, Haller F, Adamski J, Schmid RM, Saur D, Schneider G. *IKK(α) controls canonical TGF(ß)-SMAD signaling to regulate genes expressing SNAIL and SLUG during EMT in panc1 cells.* J Cell Sci. 123, 4231–4239 (2010).

Brini A, Niada S, Lambertini E, Torreggiani E, Arrigoni E, Lisignoli G, Piva R. *Chondrogenic potential of human mesenchymal stem cells and expression levels of Slug transcription factor.* J Tissue Eng Regen Med. 9, 740–744 (2013).

Brittberg M, Lindahl A, Nilsson A, Ohlsson C, Isaksson O, Peterson L. *Treatment of deep cartilage defects in the knee with autologous chondrocyte transplantation.* N Engl J Med. 331, 889–895 (1994).

Buechli ME, Lamarre J, Koch TG. *MicroRNA-140 expression during chondrogenic differentiation of equine cord blood-derived mesenchymal stromal cells.* Stem Cells Dev. 22, 1288–1296 (2013).

Bush JR & Beier F. *TGF-β and osteoarthritis--the good and the bad.* Nat Med. 19, 667–669 (2013).

Caldwell KL & Wang J. *Cell-based articular cartilage repair: the link between development and regeneration.* Osteoarthritis Cartilage. 23, 351–362 (2015).

Callaghan JJ, Martin CT, Gao Y, Pugely AJ, Liu SS, Goetz DD, Kelley SS, Johnston RC. *What can be learned from minimum 20-year follow-up studies of knee arthroplasty?* Clin Orthop Relat Res. 473, 94–100 (2015).

Camozzi D, Capanni C, Cenni V, Mattioli E, Columbaro M, Squarzoni S, Lattanzi G. *Diverse lamin-dependent mechanisms interact to control chromatin dynamics: focus on laminopathies.* Nucleus. 5, 427–440 (2014).

Candrian C, Vonwil D, Barbero A, Bonacina E, Miot S, Farhadi J, Wirz D, Dickinson S, Hollander A, Jakob M, Li Z, Alini M, Heberer M, Martin I. *Engineered cartilage generated by nasal chondrocytes is responsive to physical forces resembling joint loading.* Arthritis and Rheum. 58, 197–208 (2008)

Caplan AI. *Adult mesenchymal stem cells for tissue engineering versus regenerative medicine.* J Cell Physiol. 213, 341–347 (2007).

Caplen NJ. *Gene therapy progress and prospects. Downregulating gene expression: the impact of RNA interference.* Gene Ther. 11, 1241–1248 (2004).

Cardemil C, Thomsen P, Wexell CL. *Jaw Bone Samples From Bisphosphonate-Treated Patients: A Pilot Cohort Study.* Clin Implant Dent Relat Res. Suppl 2, e679–691 (2015).

Caron MM, Emans PJ, Coolsen MM, Voss L, Surtel DA, Cremers A, van Rhijn LW, Welting TJ. *Redifferentiation of dedifferentiated human articular chondrocytes: comparison of 2D and 3D cultures.* Osteoarthritis Cartilage. 20, 1170–1178 (2012).

Cavallo C, Desando G, Columbaro M, Ferrari A, Zini N, Facchini A, Grigolo B. *Chondrogenic differentiation of bone marrow concentrate grown onto a hylauronan scaffold: rationale for its use in the treatment of cartilage lesions.* J Biomed Mater Res A. 101, 1559–1570 (2013).

Cavallo C, Desando G, Facchini A, Grigolo B. *Chondrocytes from patients with osteoarthritis express typical extracellular matrix molecules once grown onto a three-dimensional hyaluronan-based scaffold.* J Biomed Mater Res A. 93, 86–95 (2010).

Cheema SK, Chen E, Shea LD, Mathur AB. *Regulation and guidance of cell behavior for tissue regeneration via the siRNA mechanism.* Wound Repair Regen. 15, 286–295 (2007).

Chen J, Qiu M, Dou C, Cao Z, Dong S. *MicroRNAs in bone balance and osteoporosis.* Drug Dev Res. 76, 235–245 (2015). (a)

Chen S, Fu P, Cong R, Wu H, Pei M. *Strategies to minimize hypertrophy in cartilage engineering and regeneration.* Genes Dis. 2, 76–95 (2015). (b)

Choi JC & Worman HJ. *Nuclear envelope regulation of signaling cascades.* Adv Exp Med Biol. 773, 187–206 (2014).

Clarke MS, Sundaresan A, Vanderburg CR, Banigan MG, Pellis NR. *A three-dimensional tissue culture model of bone formation utilizing rotational co-culture of human adult osteoblasts and osteoclasts.* Acta Biomater. 9, 7908–7916 (2013).

Cobaleda C, Pérez-Caro M, Vicente-Dueñas C, Sánchez-García I. *Function of the zinc-finger transcription factor SNAI2 in cancer and development.* Annu Rev Genet. 41, 41–61 (2007).

Cucchiarini M & Madry H. *Use of tissue engineering strategies to repair joint tissues in osteoarthritis: viral gene transfer approaches.* Curr Rheumatol Rep. 16, 449 (2014).

Da H, Jia SJ, Meng GL, Cheng JH, Zhou W, Xiong Z, Mu YJ, Liu J. *The impact of compact layer in biphasic scaffold on osteochondral tissue engineering.* PLoS One. 8, e54838 (2013).

Das RH, Jahr H, Verhaar JA, van der Linden JC, van Osch GJ, Weinans H. *In vitro expansion affects the response of chondrocytes to mechanical stimulation.* Osteoarthritis Cartilage. 16, 385–391 (2008).

De Ceuninck F, Lesur C, Pastoureau P, Caliez A, Sabatini M. *Culture of chondrocytes in alginate beads.* Methods Mol Med. 100, 15–22 (2004).

de Crombrugghe B, Lefebvre V, Nakashima K. *Regulatory mechanisms in the pathways of cartilage and bone formation.* Curr Opin Cell Biol. 13, 721–727 (2001).

de Vries-van Melle ML, Mandl EW, Kops N, Koevoet WJ, Verhaar JA, van Osch GJ. *An osteochondral culture model to study mechanisms involved in articular cartilage repair.* Tissue Eng Part C Methods. 18, 45–53 (2012).

de Vries-van Melle ML, Narcisi R, Kops N, Koevoet WJ, Bos PK, Murphy JM, Verhaar JA, van der Kraan PM, van Osch GJ. *Chondrogenesis of mesenchymal stem cells in an osteochondral environment is mediated by the subchondral bone.* Tissue Eng Part A. 20, 23–33 (2014). (a)

de Vries-van Melle ML, Tihaya MS, Kops N, Koevoet WJ, Murphy JM, Verhaar JA, Alini M, Eglin D, van Osch GJ. *Chondrogenic differentiation of human bone marrow-derived mesenchymal stem cells in a simulated osteochondral environment is hydrogel dependent.* Eur Cell Mater. 27, 112–123 (2014). (b)

Dehne T, Karlsson C, Ringe J, Sittinger M, Lindahl A. *Chondrogenic differentiation potential of osteoarthritic chondrocytes and their possible use in matrix-associated autologous chondrocyte transplantation.* Arthritis Res Ther. 11, R133 (2009).

Demoor M, Ollitrault D, Gomez-Leduc T, Bouyoucef M, Hervieu M, Fabre H, Lafont J, Denoix JM, Audigié F, Mallein-Gerin F, Legendre F, Galera P. *Cartilage tissue engineering: molecular control of chondrocyte differentiation for proper cartilage matrix reconstruction.* Biochim Biophys Acta. 1840, 2414-2440 (2014).

Devaki VN, Balu K, Ramesh SB, Arvind RJ, Venkatesan P. *Pre-prosthetic surgery: mandible.* J Pharm Bioallied Sci. 4, S414–416 (2012).

Dewan AK, Gibson MA, Elisseeff JH, Trice ME. *Evolution of autologous chondrocyte repair and comparison to other cartilage repair techniques.* 272481 (2014).

Di Leva G, Gasparini P, Piovan C, Ngankeu A, Garofalo M, Taccioli C, Iorio MV, Li M, Volinia S, Alder H, Nakamura T, Nuovo G, Liu Y, Nephew KP, Croce CM. *MicroRNA cluster 221–222 and estrogen receptor alpha interactions in breast cancer.* J Natl Cancer Inst. 102, 706–721. (2010).

Diekman BO, Thakore PI, O'Connor SK, Willard VP, Brunger JM, Christoforou N, Leong KW, Gersbach CA, Guilak F. *Knockdown of the cell cycle inhibitor p21 enhances cartilage formation by induced pluripotent stem cells.* Tissue Eng Part A. 21, 1261–1274 (2015).

do Amaral RJ, Pedrosa Cda S, Kochem MC, Silva KR, Aniceto M, Claudio-da-Silva C, Borojevic R, Baptista LS. *Isolation of human nasoseptal chondrogenic cells: a promise for cartilage engineering.* Stem Cell Res. 8, 292–299 (2012).

Dreesen O, Chojnowski A, Ong PF, Zhao TY, Common JE, Lunny D, Lane EB, Lee SJ, Vardy LA, Stewart CL, Colman A. *Lamin B1 fluctuations have differential effects on cellular proliferation and senescence.* J Cell Biol. 200, 605–617 (2013).

Dudek KA, Lafont JE, Martinez-Sanchez A, Murphy CL. *Type II collagen expression is regulated by tissue-specific miR-675 in human articular chondrocytes.* J. Biol Chem. 285, 24381–24387 (2010).

Dunn W, DuRaine G, Reddi AH. *Profiling microRNA expression in bovine articular cartilage and implications for mechanotransduction.* Arthritis Rheum. 60, 2333–2339 (2009).

DuRaine GD, Brown WE, Hu JC, Athanasiou KA. Emergence of scaffold-free approaches for tissue engineering musculoskeletal cartilages. Ann Biomed Eng. 43, 543–554 (2014).

Evans CH, Ghivizzani SC, Robbins PD. *Arthritis gene therapy and its tortuous path into the clinic.* Transl Res. 161, 205–216 (2013).

Evans CH, Robbins PD, Ghivizzani SC, Herndon JH, Kang R, Bahnson AB, Barranger JA, Elders EM, Gay S, Tomaino MM, Wasko MC, Watkins SC, Whiteside TL, Glorioso JC, Lotze MT, Wright TM. *Clinical trial to assess the safety, feasibility, and efficacy of transferring a potentially anti-arthritic cytokine gene to human joints with rheumatoid arthritis.* Hum Gene Ther. 7, 1261–1280 (1996).

Evans CH, Robbins PD, Ghivizzani SC, Wasko MC, Tomaino MM, Kang R, Muzzonigro TA, Vogt M, Elder EM, Whiteside TL, Watkins SC, Herndon JH. *Gene transfer to human joints: progress toward a gene therapy of arthritis.* Proc Natl Acad Sci U S A. 102, 8698–8703 (2005).

Fang K, Sideri A, Man-Law IK, Bakirtzi K, Polytarchou C, Iliopoulos D, Pothoulakis C. *Identification of a novel substance P (SP)-neurokinin-1 receptor (NK-1R) microRNA-221-5p inflammatory network in human colonic epithelial cells.* Cell Mol Gastroenterol Hepatol. 1, 503–515 (2015).

Farrell E, Both SK, Odörfer KI, Koevoet W, Kops N, O'Brien FJ, Baatenburg de Jong RJ, Verhaar JA, Cuijpers V, Jansen J, Erben RG, van Osch GJ. *In-vivo generation of bone via endochondral ossification by in-vitro chondrogenic priming of adult human and rat mesenchymal stem cells.* BMC Musculoskelet Disord. 12, 31 (2011).

Fibel KH, Hillstrom HJ, Halpern BC. *State-of-the-art management of knee osteoarthritis.* World J Clin Cases. 3, 89–101 (2015).

Fickert S, Gerwien P, Helmert B, Schattenberg T, Weckbach S, Kaszkin-Bettag M, Lehmann L. *One-year clinical and radiological results of a prospective, investigator-initiated trial examining a novel, purely autologous 3-dimensional autologous chondrocyte transplantation product in the knee.* Cartilage. 3, 27–42 (2012).

Fischer J, Dickhut A, Rickert M, Richter W. *Human articular chondrocytes secrete parathyroid hormone-related protein and inhibit hypertrophy of mesenchymal stem cells in coculture during chondrogenesis.* Arthritis Rheum. 62, 2696–2706 (2010).

Fiumana E, Pasquinelli G, Foroni L, Carboni M, Bonafè F, Orrico C, Nardo B, Tsivian M, Neri F, Arpesella G, Guarnieri C, Caldarera CM, Muscari C. *Localization of mesenchymal stem cells grafted with a hyaluronan-based scaffold in the infarcted heart.* J Surg Res. 179, e21–29 (2013).

Fortier LA & Travis AJ. *Stem cells in veterinary medicine.* Stem Cell Res Ther. 2, 9 (2011).

Frisch J, Venkatesan JK, Rey-Rico A, Madry H, Cucchiarini M. *Current progress in stem cell-based gene therapy for articular cartilage repair.* Curr Stem Cell Res Ther. 10, 121–131 (2015).

Furukawa KS, Imura K, Tateishi T, Ushida T. *Scaffold-free cartilage by rotational culture for tissue engineering.* J Biotechnol. 133, 134–145 (2008).

Furumatsu T & Ozaki T. *Epigenetic regulation in chondrogenesis.* Acta Med Okayama. 64, 155–161 (2010).

Gadjanski I, Spiller K, Vunjak-Novakovic G. *Time-dependent processes in stem cell-based tissue engineering of articular cartilage.* Stem Cell Rev. 8, 863–881 (2012).

Gamblin AL, Renaud A, Charrier C, Hulin P, Louarn G, Heymann D, Trichet V, Layrolle P. *Osteoblastic and osteoclastic differentiation of human mesenchymal stem cells and monocytes in a miniaturized three-dimensional culture with mineral granules.* Acta Biomater. 10, 5139–5147 (2014).

Gardner OF, Archer CW, Alini M, Stoddart MJ. *Chondrogenesis of mesenchymal stem cells for cartilage tissue engineering.* Histol Histopathol. 28, 23–42 (2013).

Garofalo M, Quintavalle C, Romano G, Croce CM, Condorelli G. *miR221/222 in cancer: their role in tumor progression and response to therapy.* Curr Mol Med. 12, 27–33 (2012).

Gibbons MC, Foley MA, Cardinal KO. *Thinking inside the box: keeping tissue engineered constructs (in vitro) for use as preclinical models.* Tissue Eng Part B Rev. 19, 14–30 (2013).

Glyn-Jones S, Palmer AJ, Agricola R, Price AJ, Vincent TL, Weinans H, Carr AJ. *Osteoarthritis.* Lancet. 386, 376–387 (2015).

Goldring MB & Berenbaum F. *Emerging targets in osteoarthritis therapy.* Curr Opin Pharmacol. 22, 51–63 (2015).

Goldring MB & Marcu KB. *Epigenomic and microRNA-mediated regulation in cartilage development, homeostasis, and osteoarthritis.* Trends Mol Med. 18, 109–118 (2012).

Goldring MB, Tsuchimochi K, Ijiri K. *The control of chondrogenesis.* J Cell Biochem. 97, 33–44 (2006).

Gonzálvez-García M, Rodríguez-Lozano FJ, Villanueva V, Segarra-Fenoll D, Rodríguez-González MA, Oñate-Sánchez R, Blanquer M, Moraleda JM. *Cell therapy in bisphosphonate-related osteonecrosis of the jaw.* J Craniofac Surg. 24, e226–228 (2013).

Gordeladze JO, Djouad F, Brondello JM, Noël D, Duroux-Richard I, Apparailly F, Jorgensen C. *Concerted stimuli regulating osteo-chondral differentiation from stem cells: phenotype acquisition regulated by microRNAs.* Acta Pharmacol Sin. 30, 1369–1384 (2009).

Gordeladze JO, Noël D, Bony C, Apparailly F, Louis-Plence P, Jorgensen C. *Transient down-regulation of cbfa1/Runx2 by RNA interference in murine C3H10T1/2 mesenchymal stromal cells delays in vitro and in vivo osteogenesis, but does not overtly affect chondrogenesis.* Exp Cell Res. 314, 1495–1506 (2008).

Grande DA, Singh IJ, Pugh J. *Healing of experimentally produced lesions in articular cartilage following chondrocyte transplantation.* Anat Rec. 218, 142–148 (1987).

Green JD, Tollemar V, Dougherty M, Yan Z, Yin L, Ye J, Collier Z, Mohammed MK, Haydon RC, Luu HH, Kang R, Lee MJ, Ho SH, He TC, Shi LL, Athiviraham A. *Multifaceted signaling regulators of chondrogenesis: Implications in cartilage regeneration and tissue engineering.* Genes Dis. 2, 307–327 (2015).

Grigolo B, Lisignoli G, Desando G, Cavallo C, Marconi E, Tschon M, Giavaresi G, Fini M, Giardino R, Facchini A. *Osteoarthritis treated with mesenchymal stem cells on hyaluronan-based scaffold in rabbit.* Tissue Eng Part C Methods. 15, 647–658 (2009).

Grigolo B, Lisignoli G, Piacentini A, Fiorini M, Gobbi P, Mazzotti G, Duca M, Pavesio A, Facchini A. *Evidence for redifferentiation of human chondrocytes grown on a hyaluronan-based biomaterial (HYAFF11): molecular, immunohistochemical and ultrastructural analysis.* Biomaterials. 23, 1187–1195 (2002).

Grigolo B, Roseti L, Fiorini M, Fini M, Giavaresi G, Aldini NN, Giardino R, Facchini A. *Transplantation of chondrocytes seeded on a hyaluronan derivative (hyaff-11) into cartilage defects in rabbits.* Biomaterials. 22, 2417–2424 (2001).

Grogan SP, Barbero A, Winkelmann V, Rieser F, Fitzsimmons JS, O'Driscoll S, Martin I, Mainil-Varlet P. *Visual histological grading system for the evaluation of in vitro-generated neocartilage.* Tissue Eng. 12, 2141–2149 (2006).

Guérit D, Brondello JM, Chuchana P, Philipot D, Toupet K, Bony C, Jorgensen C, Noël D. *FOXO3A regulation by miRNA-29a controls chondrogenic differentiation of mesenchymal stem cells and cartilage formation.* Stem Cells Dev. 23, 1195–1205 (2014).

Guo CA, Liu XG, Huo JZ, Jiang C, Wen XJ, Chen ZR. *Novel gene-modified-tissue engineering of cartilage using stable transforming growth factor-beta1-transfected mesenchymal stem cells grown on chitosan scaffolds.* J Biosci Bioeng 103, 547–556 (2007).

Gurusinghe S & Strappe P. *Gene modification of mesenchymal stem cells and articular chondrocytes to enhance chondrogenesis.* Biomed Res Int. 369528 (2014).

Ha CW, Noh MJ, Choi KB, Lee KH. *Initial phase I safety of retrovirally transduced human chondrocytes expressing transforming growth factor-beta-1 in degenerative arthritis patients.* Cytotherapy 14, 247–256 (2012).

Halai M, Ker A, Meek RD, Nadeem D, Sjostrom T, Su B, McNamara LE, Dalby MJ, Young PS. *Scanning electron microscopical observation of an osteoblast/osteoclast co-culture on micropatterned orthopaedic ceramics.* J Tissue Eng. 5, 1–10 (2014).

Handorf AM & Li WJ. *Fibroblast growth factor-2 primes human mesenchymal stem cells for enhanced chondrogenesis.* PloS One. 6, e22887 (2011).

Harborth J, Elbashir SM, Bechert K, Tuschl T, Weber K. *Identification of essential genes in cultured mammalian cells using small interfering RNAs.* J Cell Sci. 114, 4557–4565 (2001).

Hayden RS, Quinn KP, Alonzo CA, Georgakoudi I, Kaplan DL. *Quantitative characterization of mineralized silk film remodeling during long-term osteoblast-osteoclast co-culture.* Biomaterials. 35, 3794–3802 (2014).

Heinemann C, Heinemann S, Worch H, Hanke T. *Development of an osteoblast/osteoclast co-culture derived by human bone marrow stromal cells and human monocytes for biomaterials testing.* Eur Cell Mater. 21, 80–93 (2011).

Heinemann S, Heinemann C, Wenisch S, Alt V, Worch H, Hanke T. *Calcium phosphate phases integrated in silica/collagen nanocomposite xerogels enhance the bioactivity and ultimately manipulate the osteoblast/osteoclast ratio in a human co-culture model.* Acta Biomater. 9, 4878–4888 (2013).

Hellingman CA, Davidson EN, Koevoet W, Vitters EL, van den Berg WB, van Osch GJ, van der Kraan PM. *Smad signaling determines chondrogenic differentiation of bone-marrow-derived mesenchymal stem cells: inhibition of Smad1/5/8P prevents terminal differentiation and calcification.* Tissue Eng Part A. 17, 1157–1167 (2011).

Hemavathy K, Guru SC, Harris J, Chen JD, Ip YT. *Human slug is a repressor that localizes to sites of active transcription.* Mol Cell Biol. 20, 5087–5095 (2000).

Hollander AP, Dickinson SC, Kafienah W. *Stem cells and cartilage development: complexities of a simple tissue.* Stem Cells. 28, 1992–1996 (2010).

Hong E & Reddi AH. *Dedifferentiation and redifferentiation of articular chondrocytes from surface and middle zones: changes in microRNAs-221/-222, -140, and -143/145 expression.* Tissue Eng Part A. 19, 1015–1022 (2013).

Hong E & Reddi AH. *MicroRNAs in chondrogenesis, articular cartilage, and osteoarthritis: implications for tissue engineering.* Tissue Eng Part B Rev. 18, 445–453 (2012).

Huang AH, Motlekar NA, Stein A, Diamond SL, Shore EM, Mauck RL. *High-throughput screening for modulators of mesenchymal stem cell chondrogenesis.* Ann Biomed Eng. 36, 1909–1921 (2008).

Huang YF, Chang CT, Muo CH, Tsai CH, Shen YF, Wu CZ. *Impact of bisphosphonate-related osteonecrosis of the jaw on osteoporotic patients after dental extraction: a population-based cohort study.* PLoS One. 10, e0120756 (2015).

Hunziker EB, Lippuner K, Keel MJ, Shintani N. *An educational review of cartilage repair: precepts & practice – myths & misconceptions – progress & prospects.* Osteoarthritis Cartilage. 23, 334–350 (2015).

Hutchison CJ. *B-type lamins in health and disease.* Semin Cell Dev Biol. 29, 158–163 (2014).

Im GI, Kim HJ, Lee JH. *Chondrogenesis of adipose stem cells in a porous PLGA scaffold impregnated with plasmid DNA containing SOX trio (SOX-5,-6 and -9) genes.* Biomaterials. 32, 4385–4392 (2011).

Jacome-Galarza C, Lee SK, Lorenzo JA, Aguila HL. *Identification, characterization, and isolation of a common progenitor for osteoclasts, macrophages, and dendritic cells from murine bone marrow and periphery.* J Bone Miner Res. 28, 1203–1213 (2013).

Jash A, Yun K, Sahoo A, So JS Im SH. *Looping mediated interaction between the promoter and 3' UTR regulates type II collagen expression in chondrocytes.* PLoS One. 7, e40828 (2012).

Jay GD, Britt DE, Cha CJ. *Lubricin is a product of megakaryocyte stimulating factor gene expression by human synovial fibroblasts.* J Rheumatol. 27, 594–600 (2000).

Johnstone B, Alini M, Cucchiarini M, Dodge GR, Eglin D, Guilak F, Madry H, Mata A, Mauck RL, Semino CE, Stoddart MJ. *Tissue engineering for articular cartilage repair--the state of the art.* Eur Cell Mater. 25, 248–267 (2013).

Johnstone B, Hering TM, Caplan AI, Goldberg VM, Yoo JU. *In vitro chondrogenesis of bone marrow-derived mesenchymal progenitor cells.* Exp Cell Res. 238, 265–272 (1998).

Jones GL, Motta A, Marshall MJ, El Haj AJ, Cartmell SH. *Osteoblast: osteoclast co-cultures on silk fibroin, chitosan and PLLA films.* Biomaterials. 30, 5376–5384 (2009).

Kaji H, Camci-Unal G, Langer R, Khademhosseini A. *Engineering systems for the generation of patterned co-cultures for controlling cell-cell interactions.* Biochim Biophys Acta. 1810, 239–250 (2011).

Karlsen TA, Shahdadfar A, Brinchmann JE. *Human primary articular chondrocytes, chondroblasts-like cells, and dedifferentiated chondrocytes: differences in gene, microRNA, and protein expression and phenotype.* Tissue Eng Part C Methods. 17, 219–227 (2011).

Kean TJ & Dennis JE. *Synoviocyte derived-extracellular matrix enhances human articular chondrocyte proliferation and maintains re-differentiation capacity at both low and atmospheric oxygen tensions.* PLoS One. 10, e0138409 (2015).

Kessler MW & Grande DA. *Tissue engineering and cartilage.* Organogenesis 4, 28–32 (2008).

Khan IM, Evans SL, Young RD, Blain EJ, Quantock AJ, Avery N, Archer CW. *Fibroblast growth factor 2 and transforming growth factor β1 induce precocious maturation of articular cartilage.* Arthritis Rheum. 63, 3417–3427 (2011).

Kim D, Song J, Jin EJ. *MicroRNA-221 regulates chondrogenic differentiation through promoting proteosomal degradation of slug by targeting Mdm2.* J Biol Chem. 285, 26900–26907 (2010).

Kim HJ, Kim YH, Lee DS, Chung JK, Kim S. *In vivo imaging of functional targeting of miR-221 in papillary thyroid carcinoma.* J Nucl Med. 49, 1686–1693 (2008).

Kim S, Hwang do W, Lee DS. *A study of microRNAs in silico and in vivo: bioimaging of microRNA biogenesis and regulation.* FEBS J. 276, 2165–2174 (2009).

Knight E & Przyborski S. *Advances in 3D cell culture technologies enabling tissue-like structures to be created in vitro*. J Anat. 227, 746–756 (2015).

Knutsen G, Drogset JO, Engebretsen L, Grøntvedt T, Isaksen V, Ludvigsen TC, Roberts S, Solheim E, Strand T, Johansen O. *A randomized trial comparing autologous chondrocyte implantation with microfracture. Findings at five years.* J Bone Joint Surg Am. 89, 2105–2112 (2007).

Kotagama K, Babb CS, Wolter JM, Murphy RP, Mangone M. *A human 3'UTR clone collection to study post-transcriptional gene regulation.* BMC Genomics. 16, 1036 (2015).

Kozhemyakina E, Lassar AB, Zelzer E. *A pathway to bone: signaling molecules and transcription factors involved in chondrocyte development and maturation.* Development. 142, 817–831 (2015).

Kuttenberger J, Polska E, Schaefer BM. *A novel three-dimensional bone chip organ culture.* Clin Oral Investig. 17, 1547–1555 (2013).

Lam JK, Chow MY, Zhang Y, Leung SW. *siRNA Versus miRNA as Therapeutics for Gene Silencing.* Mol Ther Nucleic Acids. 4, e252 (2015).

Lambertini E, Lisignoli G, Torreggiani E, Manferdini C, Gabusi E, Franceschetti T, Penolazzi L, Gambari R, Facchini A, Piva R. *Slug gene expression supports human osteoblast maturation.* Cell Mol Life Sci. 66, 3641–3653 (2009).

Lambertini E, Lolli A, Vezzali F, Penolazzi L, Gambari R, Piva R. *Correlation between Slug transcription factor and miR-221 in MDA-MB-231 breast cancer cells.* BMC Cancer. 12, 445 (2012).

Le LT, Swingler TE, Clark IM. *The role of microRNAs in osteoarthritis and chondrogenesis.* Arthritis Rheum. 65, 1963–1974 (2013).

Lee HH, Chang CC, Shieh MJ, Wang JP, Chen YT, Young TH, Hung SC. *Hypoxia enhances chondrogenesis and prevents terminal differentiation through PI3K/Akt/FoxO dependent anti-apoptotic effect.* Sci Rep. 3, 2683 (2013).

Lee JM & Im GI. *SOX trio-co-transduced adipose stem cells in fibrin gel to enhance cartilage repair and delay the progression of osteoarthritis in the rat.* Biomaterials. 33, 2016–2024 (2012).

Lefebvre V & Smits P. *Transcriptional control of chondrocyte fate and differentiation.* Birth Defects Res C Embryo Today. 75, 200–212 (2005).

Li G, Wu P, Xu Y, Yu Y, Sun L, Zhu L, Ye D. *The effect of Lipoxin A4 on the interaction between macrophage and osteoblast: possible role in the treatment of aseptic loosening.* BMC Musculoskelet Disord. 10, 57–68 (2009).

Li Y, Wei X, Zhou J, Wei L. *The age-related changes in cartilage and osteoarthritis.* Biomed Res Int. 916530 (2013).

Li Z & Rana TM. *Therapeutic targeting of microRNAs: current status and future challenges.* Nat Rev Drug Discov. 13, 622–638 (2014).

Liao J, Shi K, Ding Q, Qu Y, Luo F, Qian Z. *Recent developments in scaffold-guided cartilage tissue regeneration.* J Biomed Nanotechnol. 10, 3085–3104 (2014).

Lin EA, Kong L, Bai XH, Luan Y, Liu CJ. *miR-199a*, a bone morphogenic protein 2-responsive microRNA, regulates chondrogenesis via direct targeting to Smad1.* J Biol Chem. 284, 11326–11335 (2009).

Lin JH, Chen IW, deLuna FA. *On the absorption of alendronate in rats*. J Pharm Sci. 83, 1741–1746 (1994).

Lin JH. *Bisphosphonates: a review of their pharmacokinetic properties.* Bone. 18, 75–85 (1996).

Lisignoli G, Cristino S, Piacentini A, Toneguzzi S, Grassi F, Cavallo C, Zini N, Solimando L, Mario Maraldi N, Facchini A. *Cellular and molecular events during chondrogenesis of human mesenchymal stromal cells grown in a three-dimensional hyaluronan based scaffold.* Biomaterials. 26, 5677–5686 (2005).

Lisignoli G, Manferdini C, Lambertini E, Zini N, Angelozzi M, Gabusi E, Gambari L, Penolazzi L, Lolli A, Facchini A, Piva R. *Chondrogenic potential of Slug-depleted hMSCs.* Tissue Eng Part A. 20, 2795–2805 (2014).

Lisignoli G, Toneguzzi S, Grassi F, Piacentini A, Tschon M, Cristino S, Gualtieri G, Facchini A. *Different chemokines are expressed in human arthritic bone biopsies: IFN-gamma and IL-6 differently modulate IL-8, MCP-1 and rantes production by arthritic osteoblasts.* Cytokine. 20, 231–238 (2002).

Loeser RF, Goldring SR, Scanzello CR, Goldring MB. *Osteoarthritis: a disease of the joint as an organ.* Arthritis Rheum. 64, 1697–1707 (2012).

Lolli A, Lambertini E, Penolazzi L, Angelozzi M, Morganti C, Franceschetti T, Pelucchi S, Gambari R, Piva R. *Pro-chondrogenic effect of miR-221 and slug depletion in human MSCs.* Stem Cell Rev. 10, 841–855 (2014).

Mackay AM, Beck SC, Murphy JM, Barry FP, Chichester CO, Pittenger MF. *Chondrogenic differentiation of cultured human mesenchymal stem cells from marrow.* Tissue Eng. 4, 415–428 (1998).

Madeira C, Santhagunam A, Salgueiro JB, Cabral JM. *Advanced cell therapies for articular cartilage regeneration.* Trends Biotechnol. 33, 35–42 (2015).

Madry H & Cucchiarini M. *Clinical potential and challenges of using genetically modified cells for articular cartilage repair.* Croat Med J. 52, 245–261 (2011).

Madry H & Cucchiarini M. *Tissue-engineering strategies to repair joint tissue in osteoarthritis: nonviral gene-transfer approaches.* Curr Rheumatol Rep. 16, 450 (2014).

Madry H, Kaul G, Cucchiarini M, Stein U, Zurakowski D, Remberger K, Menger MD, Kohn D, Trippel SB. *Enhanced repair of articular cartilage defects "in vivo" by transplanted chondrocytes overexpressing insulin-like growth factor I (IGF-I).* Gene Ther. 12, 1171–1179 (2005).

Madry H, Kaul G, Zurakowski D, Vunjak-Novakovic G, Cucchiarini M. *Cartilage constructs engineered from chondrocytes overexpressing IGF-I improve the repair of osteochondral defects in a rabbit model.* Eur Cell Mater. 25, 229–247 (2013).

Mahmoudifar N & Doran PM. *Chondrogenesis and cartilage tissue engineering: the longer road to technology development.* Trends Biotechnol. 30, 166–176 (2012).

Malik TH, Shoichet SA, Latham P, Kroll TG, Peters LL, Shivdasani RA. *Transcriptional repression and developmental functions of the atypical vertebrate GATA protein TRPS1*. EMBO J. 20, 1715–1725 (2001).

Manning K, Rachakonda PS, Rai MF, Schmidt MF. *Co-expression of insulin-like growth factor-1 and interleukin-4 in an in vitro inflammatory model.* Cytokine. 50, 297–305 (2010).

Marcacci M, Zaffagnini S, Iacono F, Vascellari A, Loreti I, Kon E, Presti ML. *Intra- and extra-articular anterior cruciate ligament reconstruction utilizing autogeneous semitendinosus and gracilis tendons: 5-year clinical results.* Knee Surg Sports Traumatol Arthrosc. 11, 2–8 (2002).

Mardones R, Jofré CM, Minguell JJ. *Cell therapy and tissue engineering approaches for cartilage repair and/or regeneration.* Int J Stem Cells. 8, 48–53 (2015).

Mariani E, Pulsatelli L, Facchini A. *Signaling pathways in cartilage repair.* Int J Mol Sci. 15, 8667–8698 (2014).

Martin JA & Buckwalter JA. *Roles of articular cartilage aging and chondrocyte senescence in the pathogenesis of osteoarthritis.* Iowa Orthop J. 21, 1–7 (2001).

Martinez-Sanchez A, Dudek KA, Murphy CL. *Regulation of human chondrocyte function through direct inhibition of cartilage master regulator SOX9 by microRNA-145 (miRNA-145).* J Biol Chem. 287, 916–924 (2012).

Mateos J, De la Fuente A, Lesende-Rodriguez I, Fernández-Pernas P, Arufe MC, Blanco FJ. *Lamin A deregulation in human mesenchymal stem cells promotes an impairment in their chondrogenic potential and imbalance in their response to oxidative stress.* Stem Cell Res. 11, 1137–1148 (2013).

Mazor M, Lespessailles E, Coursier R, Daniellou R, Best TM, Toumi H. *Mesenchymal stem-cell potential in cartilage repair: an update.* J Cell Mol Med. 18, 2340–2350 (2014).

McCormick F, Cole BJ, Nwachukwu BU, Harris JD, Adkisson HD, Farr J. *Treatment of focal cartilage defects with a juvenile allogeneic 3-dimensional articular cartilage graft.* Oper Tech Sports Med. 21, 95–99 (2013).

Medici D, Hay ED, Olsen BR. *Snail and Slug promote epithelial-mesenchymal transition through beta-catenin-T-cell factor-4-dependent expression of transforming growth factor-beta3*. Mol Biol Cell. 19, 4875–4887 (2008).

Mendelson A, Frank E, Allred C, Jones E, Chen M, Zhao W, Mao JJ. *Chondrogenesis by chemotactic homing of synovium, bone marrow, and adipose stem cells in vitro.* FASEB J. 25, 3496–3504 (2011).

Mesallati T, Buckley CT, Kelly DJ. *Engineering articular cartilage-like grafts by self-assembly of infrapatellar fat pad-derived stem cells.* Biotechnol Bioeng. 111, 1686–1698 (2014).

Mirzamohammadi F, Papaioannou G, Kobayashi T. *microRNAs in cartilage development, homeostasis, and disease.* Curr Osteoporos Rep. 12, 410–419 (2014).

Mobasheri A, Kalamegam G, Musumeci G, Batt ME. *Chondrocyte and mesenchymal stem cell-based therapies for cartilage repair in osteoarthritis and related orthopaedic conditions.* Maturitas. 78, 188–198 (2014).

Moseley JB, O'Malley K, Petersen NJ, Menke TJ, Brody BA, Kuykendall DH, Hollingsworth JC, Ashton CM, Wray NP. *A controlled trial of arthroscopic surgery for osteoarthritis of the knee.* N Engl J Med. 347, 81–88 (2002).

Murphy L & Helmick CG. *The Impact of Osteoarthritis in the United States: a population-health perspective.* Orthop Nurs. 31, 85–91 (2012).

Musumeci G, Aiello FC, Szychlinska MA, Di Rosa M, Castrogiovanni P, Mobasheri A. *Osteoarthritis in the XXIst century: risk factors and behaviours that influence disease onset and progression.* Int J Mol Sci. 16, 6093–6112 (2015).

Napierala D, Sam K, Morello R, Zheng Q, Munivez E, Shivdasani RA, Lee B. *Uncoupling of chondrocyte differentiation and perichondrial mineralization underlies the skeletal dysplasia in tricho-rhino-phalangeal syndrome.* Hum Mol Genet. 17, 2244–2254 (2008).

Narcisi R, Cleary MA, Brama PA, Hoogduijn MJ, Tüysüz N, ten Berge D, van Osch GJ. *Long-term expansion, enhanced chondrogenic potential, and suppression of endochondral ossification of adult human MSCs via WNT signaling modulation.* Stem Cell Reports. 4, 459–472 (2015).

Narcisi R, Quarto R, Ulivi V, Muraglia A, Molfetta L, Giannoni P. *TGF β-1 administration during ex vivo expansion of human articular chondrocytes in a serum-free medium redirects the cell phenotype toward hypertrophy.* J Cell Physiol. 227, 3282–3290 (2012). (a)

Narcisi R, Signorile L, Verhaar JA, Giannoni P, van Osch GJ. *TGFβ inhibition during expansion phase increases the chondrogenic re-differentiation capacity of human articular chondrocytes.* Osteoarthritis Cartilage. 20, 1152–1160 (2012). (b)

Nishi M, Matsumoto R, Dong J, Uemura T. *Regeneration of bone tissue in a controlled in vitro environment with a Rotating Wall Vessel Bioreactor.* Nano Biomedicine. 3, 267–274 (2011).

Nooeaid P, Salih V, Beier JP, Boccaccini AR. *Osteochondral tissue engineering: scaffolds, stem cells and applications.* J Cell Mol Med. 16, 2247–2270 (2012).

Noren Hooten N, Abdelmohsen K, Gorospe M, Ejiogu N, Zonderman AB, Evans MK. *microRNA expression patterns reveal differential expression of target genes with age.* PLoS One. 5, e10724 (2010).

Oldershaw RA. *Cell sources for the regeneration of articular cartilage: the past, the horizon and the future.* Int J Exp Pathol. 93, 389–400 (2012).

Ono Y, Sakai T, Hiraiwa H, Hamada T, Omachi T, Nakashima M, Ishizuka S, Matsukawa T, Knudson W, Knudson CB, Ishiguro N. *Chondrogenic capacity and alterations in hyaluronan synthesis of cultured human osteoarthritic chondrocytes.* Biochem Biophys Res Commun. 435, 733–739 (2013).

Otto S, Schreyer C, Hafner S, Mast G, Ehrenfeld M, Stürzenbaum S, Pautke C. *Bisphosphonate-related osteonecrosis of the jaws – characteristics, risk factors, clinical features, localization and impact on oncological treatment.* J Craniomaxillofac Surg. 40, 303–309 (2012).

Palmer GD, Steinert A, Pascher A, Gouze E, Gouze JN, Betz O, Johnstone B, Evans CH, Ghivizzani SC. *Gene-induced chondrogenesis of primary mesenchymal stem cells in vitro.* Mol Ther. 12, 219–228 (2005).

Palomares KT, Gleason RE, Mason ZD, Cullinane DM, Einhorn TA, Gerstenfeld LC, Morgan EF. *Mechanical stimulation alters tissue differentiation and molecular expression during bone healing.* J Orthop Res. 27, 1123–1132 (2009).

Papadimitropoulos A, Scherberich A, Güven S, Theilgaard N, Crooijmans HJ, Santini F. *A 3D in vitro bone organ model using human progenitor cells*. Eur Cell Mater. 21, 445–458 (2011).

Pasquinelli G, Orrico C, Foroni L, Bonafè F, Carboni M, Guarnieri C, Raimondo S, Penna C, Geuna S, Pagliaro P, Freyrie A, Stella A, Caldarera CM, Muscari C. *Mesenchymal stem cell interaction with a non-woven hyaluronan-based scaffold suitable for tissue repair.* J Anat. 213, 520–530 (2008).

Pavesio A, Abatangelo G, Borrione A, Brocchetta D, Hollander AP, Kon E, Torasso F, Zanasi S, Marcacci M. *Hyaluronan-based scaffolds (Hyalograft C) in the treatment of knee cartilage defects: preliminary clinical findings.* Novartis Found Symp. 249, 203–217 (2003).

Pei M, He F, Wei L. *Three-dimensional cell expansion substrate for cartilage tissue engineering and regeneration: a comparison in decellularized matrix deposited by synovium-derived stem cells and chondrocytes.* J Tissue Sci Eng. 2, 104 (2011).

Pelttari K, Winter A, Steck E, Goetzke K, Hennig T, Ochs BG, Aigner T, Richter W. *Premature induction of hypertrophy during in vitro chondrogenesis of human mesenchymal stem cells correlates with calcification and vascular invasion after ectopic transplantation in SCID mice.* Arthritis Rheum. 54, 3254–3266 (2006).

Penick KJ, Solchaga LA, Welter JF. *High-throughput aggregate culture system to assess the chondrogenic potential of mesenchymal stem cells.* Biotechniques. 39, 687–691 (2005).

Penolazzi L, Mazzitelli S, Vecchiatini R, Torreggiani E, Lambertini E, Johnson S, Badylak SF, Piva R, Nastruzzi C. *Human mesenchymal stem cells seeded on extracellular matrix-scaffold: viability and osteogenic potential.* J Cell Physiol. 227, 857–866 (2012).

Penolazzi L, Tavanti E, Vecchiatini R, Lambertini E, Vesce F, Gambari R, Mazzitelli S, Mancuso F, Luca G, Nastruzzi C, Piva R. *Encapsulation of mesenchymal stem cells from Wharton's jelly in alginate microbeads.* Tissue Eng Part C Methods. 16, 141–155 (2010).

Pi Y, Zhang X, Shao Z, Zhao F, Hu X, Ao Y. *Intra-articular delivery of anti-Hif-2α siRNA by chondrocyte-homing nanoparticles to prevent cartilage degeneration in arthritic mice.* Gene Ther. 22, 439–448 (2015).

Piersanti S, Remoli C, Saggio I, Funari A, Michienzi S, Sacchetti B, Robey PG, Riminucci M, Bianco P. *Transfer, analysis, and reversion of the fibrous dysplasia cellular phenotype in human skeletal progenitors.* J Bone Miner Res. 25, 1103–1116 (2010).

Piva R, Penolazzi L, Lambertini E, Giordano S, Gambari R. *Induction of apoptosis of human primary osteoclasts treated with a transcription factor decoy mimicking a promoter region of estrogen receptor alpha.* Apoptosis. 10, 1079–1094 (2005).

Pleumeekers MM, Nimeskern L, Koevoet WL, Kops N, Poublon RM, Stok KS, van Osch GJ. *The in vitro and in vivo capacity of culture-expanded human cells from several sources encapsulated in alginate to form cartilage.* Eur Cell Mater. 27, 264–280 (2014).

Reszka AA & Rodan GA. *Bisphosphonate mechanism of action*. Curr Rheumatol Rep. 5, 65–74 (2003).

Richardson SM, Kalamegam G, Pushparaj PN, Matta C, Memic A, Khademhosseini A, Mobasheri R, Poletti FL, Hoyland JA, Mobasheri A. *Mesenchymal stem cells in regenerative medicine: Focus on articular cartilage and intervertebral disc regeneration.* Methods. S1046-2023(15)30091-8 (2015).

Ríos CN, Skoracki RJ, Mathur AB. *GNAS1 and PHD2 short-interfering RNA support bone regeneration in vitro and in an in vivo sheep model.* Clin Orthop Relat Res. 470, 2541–2553 (2012).

Roelofs AJ, Rocke JP, De Bari C. *Cell-based approaches to joint surface repair: a research perspective.* Osteoarthritis Cartilage. 21, 892–900 (2013).

Roobrouck VD, Vanuytsel K, Verfaillie CM. *Concise review: culture mediated changes in fate and/or potency of stem cells.* Stem Cells, 29, 583–589 (2011).

Roscigno G, Quintavalle C, Donnarumma E, Puoti I, Diaz-Lagares A, Iaboni M, Fiore D, Russo V, Todaro M, Romano G, Thomas R, Cortino G, Gaggianesi M, Esteller M, Croce CM, Condorelli G. *MiR-221 promotes stemness of breast cancer cells by targeting DNMT3b.* Oncotarget. 7, 580–592 (2015).

Rosini S, Rosini S, Bertoldi I, Frediani B. *Understanding bisphosphonates and osteonecrosis of the jaw: uses and risks.* Eur Rev Med Pharmacol Sci. 19, 3309–3317 (2015).

Ruggiero SL, Dodson TB, Fantasia J, Goodday R, Aghaloo T, Mehrotra B, O'Ryan F; American Association of Oral and Maxillofacial Surgeons. *American Association of Oral and Maxillofacial Surgeons position paper on medication-related osteonecrosis of the jaw--2014 update.* J Oral Maxillofac Surg. 72, 1938–1956 (2014).

Satija NK, Gurudutta GU, Sharma S, Afrin F, Gupta P, Verma YK, Singh VK, Tripathi RP. *Mesenchymal stem cells: molecular targets for tissue engineering.* Stem Cells Dev. 16, 7–23 (2007).

Sato M, Yamato M, Hamahashi K, Okano T, Mochida J. *Articular cartilage regeneration using cell sheet technology.* Anat Rec (Hoboken). 297, 36–43 (2014).

Scharstuhl A, Glansbeek HL, van Beuningen HM, Vitters EL, van der Kraan PM, van den Berg WB. *Inhibition of endogenous TGF-beta during experimental osteoarthritis prevents osteophyte formation and impairs cartilage repair.* J Immunol. 169, 507–514 (2002).

Schnabel M, Marlovits S, Eckhoff G, Fichtel I, Gotzen L, Vécsei V, Schlegel J. *Dedifferentiation-associated changes in morphology and gene expression in primary human articular chondrocytes in cell culture.* Osteoarthritis Cartilage. 10, 62–70 (2002).

Scotti C, Piccinini E, Takizawa H, Todorov A, Bourgine P, Papadimitropoulos A, Barbero A, Manz MG, Martin I. *Engineering of a functional bone organ through endochondral ossification.* Proc Natl Acad Sci U S A. 110, 3997–4002 (2013).

Scotti C, Tonnarelli B, Papadimitropoulos A, Scherberich A, Schaeren S, Schauerte A, Lopez-Rios J, Zeller R, Barbero A, Martin I. *Recapitulation of endochondral bone formation using human adult mesenchymal stem cells as a paradigm for developmental engineering.* Proc Natl Acad Sci U S A. 107, 7251–7256 (2010).

Seidl CI, Martinez-Sanchez A, Murphy CL. *Derepression of miRNA-138 contributes to loss of the human articular chondrocyte phenotype.* Arthritis Rheumatol. 68, 398–409 (2016).

Seki K, Fujimori T, Savagner P, Hata A, Aikawa T, Ogata N, Nabeshima Y, Kaechoong L. *Mouse Snail family transcription repressors regulate chondrocyte, extracellular matrix, type II collagen, and aggrecan.* J Biol Chem. 278, 41862–41870 (2003).

Sekine H, Shimizu T, Sakaguchi K, Dobashi I, Wada M, Yamato M. *In vitro fabrication of functional three-dimensional tissues with perfusable blood vessels.* Nat Commun. 4, 1399 (2013).

Seo S & Na K. *Mesenchymal stem cell-based tissue engineering for chondrogenesis.* J Biomed Biotechnol. 806891 (2011).

Seyedin SM, Thompson AY, Bentz H, Rosen DM, McPherson JM, Conti A, Siegel NR, Galluppi GR, Piez KA. *Cartilage-inducing factor-A. Apparent identity to transforming growth factor-beta.* J Biol Chem. 261, 5693–5695 (1986).

Shen J, Li S, Chen D. *TGF-β signaling and the development of osteoarthritis.* Bone Res. 2, 14002 (2014).

Sims NA & Martin TJ. *Coupling the activities of bone formation and resorption: a multitude of signals within the basic multicellular unit.* Bonekey Rep. 3, 481 (2014).

Steinert AF, Ghivizzani SC, Rethwilm A, Tuan RS, Evans CH, Nöth U. *Major biological obstacles for persistent cell-based regeneration of articular cartilage.* Arthritis Res Ther. 9, 213 (2007).

Steinert AF, Nöth U, Tuan RS. *Concepts in gene therapy for cartilage repair.* Injury. Suppl 1:S97–113 (2008).

Studer D, Millan C, Öztürk E, Maniura-Weber K, Zenobi-Wong M. *Molecular and biophysical mechanisms regulating hypertrophic differentiation in chondrocytes and mesenchymal stem cells.* Eur Cell Mater. 24, 118–135 (2012).

Sun W, Julie Li YS, Huang HD, Shyy JY, Chien S. *microRNA: a master regulator of cellular processes for bioengineering systems*. Annu Rev Biomed Eng. 12, 1–27 (2010).

Swift J, Ivanovska IL, Buxboim A, Harada T, Dingal PC, Pinter J, Pajerowski JD, Spinler KR, Shin JW, Tewari M, Rehfeldt F, Speicher DW, Discher DE. *Nuclear lamin-A scales with tissue stiffness and enhances matrix-directed differentiation.* Science. 341, 1240104 (2013).

Tang QO, Carasco CF, Gamie Z, Korres N, Mantalaris A, Tsiridis E. *Preclinical and clinical data for the use of mesenchymal stem cells in articular cartilage tissue engineering.* Expert Opin Biol Ther. 12, 1361–1382 (2012).

Temenoff JS & Mikos AG. *Review: tissue engineering for regeneration of articular cartilage. Biomaterials.* 21, 431–440 (2000).

Thomson DW, Bracken CP, Goodall GJ. *Experimental strategies for microRNA target identification.* Nucleic Acids Res. 39, 6845–6853 (2011).

Tiku ML & Sabaawy HE. *Cartilage regeneration for treatment of osteoarthritis: a paradigm for nonsurgical intervention.* Ther Adv Musculoskelet Dis. 7, 76–87 (2015).

Tonnarelli B, Centola M, Barbero A, Zeller R, Martin I. *Re-engineering development to instruct tissue regeneration.* Curr Top Dev Biol. 108, 319–338 (2014).

Torreggiani E, Bianchini C, Penolazzi L, Lambertini E, Vecchiatini R, Canella A, Gambari R, Magri E, Pelucchi S, Pastore A, Piva R. *Osteogenic potential of cells derived from nasal septum*. Rhinology. 49, 148–154 (2011).

Torreggiani E, Lisignoli G, Manferdini C, Lambertini E, Penolazzi L, Vecchiatini R, Gabusi E, Chieco P, Facchini A, Gambari R, Piva R. *Role of Slug transcription factor in human mesenchymal stem cells.* J Cell Mol Med. 16, 740–751 (2012).

Tortelli F & Cancedda R. *Three-dimensional cultures of osteogenic and chondrogenic cells: a tissue engineering approach to mimic bone and cartilage in vitro.* Eur Cell Mater. 17, 1–14 (2009).

Tortelli F, Pujic N, Liu Y, Laroche N, Vico L, Cancedda R. *Osteoblast and osteoclast differentiation in an in vitro three-dimensional model of bone*. Tissue Eng Part A. 15, 2373–2383 (2009).

Tsuchiya H, Kitoh H, Sugiura F, Ishiguro N. *Chondrogenesis enhanced by overexpression of sox9 gene in mouse bone marrow-derived mesenchymal stem cells.* Biochem Biophys Res Commun. 301, 338–343 (2003).

Umlauf D, Frank S, Pap T, Bertrand J. *Cartilage biology, pathology, and repair.* Cell Mol Life Sci. 67, 4197–4211 (2010).

van Beuningen HM, Glansbeek HL, van der Kraan PM, van den Berg WB. *Osteoarthritis-like changes in the murine knee joint resulting from intra-articular transforming growth factor-beta injections.* Osteoarthritis Cartilage. 8, 25–33 (2000).

van Osch GJ, Brittberg M, Dennis JE, Bastiaansen-Jenniskens YM, Erben RG, Konttinen YT, Luyten FP. *Cartilage repair: past and future--lessons for regenerative medicine.* J Cell Mol Med. 13, 792–810 (2009).

Vecchiatini R, Penolazzi L, Lambertini E, Angelozzi M, Morganti C, Mazzitelli S, Trombelli L, Nastruzzi C, Piva R. *Effect of dynamic three-dimensional culture on osteogenic potential of human periodontal ligament-derived mesenchymal stem cells entrapped in alginate microbeads*. J Periodontal Res. 50, 544–553 (2015).

Vinatier C, Bouffi C, Merceron C, Gordeladze J, Brondello JM, Jorgensen C, Weiss P, Guicheux J, Noël D. *Cartilage tissue engineering: towards a biomaterial-assisted mesenchymal stem cell therapy.* Curr Stem Cell Res Ther. 4, 318–329 (2009). (a)

Vinatier C, Mrugala D, Jorgensen C, Guicheux J, Noël D. *Cartilage engineering: a crucial combination of cells, biomaterials and biofactors.* Trends Biotechnol. 27, 307–314 (2009). (b)

Vindigni V, Cortivo R, Iacobellis L, Abatangelo G, Zavan B. *Hyaluronan benzyl ester as a scaffold for tissue engineering.* Int J Mol Sci. 10, 2972–2985 (2009).

Wachsmuth L, Soder S, Fan Z, Finger F, Aigner T. *Immunolocalization of matrix proteins in different human cartilage subtypes.* Histol Histopathol. 21, 477–485 (2006).

Wang ZH, Li XL, He XJ, Wu BJ, Xu M, Chang HM, Zhang XH, Xing Z, Jing XH, Kong DM, Kou XH, Yang YY. *Delivery of the Sox9 gene promotes chondrogenic differentiation of human umbilical cord blood-derived mesenchymal stem cells in an in vitro model.* Braz J Med Biol Res. 47, 279–86 (2014).

Wang ZH, Yang ZQ, He XJ, Kamal BE, Xing Z. *Lentivirus-mediated knockdown of aggrecanase-1 and -2 promotes chondrocyte-engineered cartilage formation in vitro.* Biotechnol Bioeng. 107, 730–736 (2010).

Widbiller M, Lindner SR, Buchalla W, Eidt A, Hiller KA, Schmalz G, Galler KM. *Three-dimensional culture of dental pulp stem cells in direct contact to tricalcium silicate cements*. Clin Oral Invest. doi: 10.1007/s00784-015-1515-3 (2015).

Wu C, Tian B, Qu X, Liu F, Tang T, Qin A, Zhu Z, Dai K. *MicroRNAs play a role in chondrogenesis and osteoarthritis (review).* Int J Mol Med. 34, 13–23 (2014).

Wuelling M, Kaiser FJ, Buelens LA, Braunholz D, Shivdasani RA, Depping R, Vortkamp A. *Trps1, a regulator of chondrocyte proliferation and differentiation, interacts with the activator form of Gli3.* Dev Biol. 328, 40–53 (2009).

Xian CJ & Foster BK. *Repair of injured articular and growth plate cartilage using mesenchymal stem cells and chondrogenic gene therapy.* Curr Stem Cell Res Ther. 1, 213–229 (2006).

Xu Y, Malladi P, Chiou M, Bekerman E, Giaccia AJ, Longaker MT. *In vitro expansion of adipose-derived adult stromal cells in hypoxia enhances early chondrogenesis.* Tissue Eng. 13, 2981–2993 (2007).

Yang B, Guo H, Zhang Y, Chen L, Ying D, Dong S. *MicroRNA-145 regulates chondrogenic differentiation of mesenchymal stem cells by targeting Sox9.* PloS One. 6, e21679 (2011).

Yang J & Weinberg RA. *Epithelial-mesenchymal transition: at the crossroads of development and tumor metastasis.* Dev Cell. 14, 818–829 (2008).

Yang M, Zhang L, Gibson GJ. *Chondrocyte miRNAs 221 and 483-5p respond to loss of matrix interaction by modulating proliferation and matrix synthesis.* Connect Tissue Res. 56, 236–243 (2015).

Ye K, Di Bella C, Myers DE, Choong PF. *The osteochondral dilemma: review of current management and future trends.* ANZ J Surg. 84, 211–217 (2014).

Zhang F, Yao Y, Hao J, Zhou R, Liu C, Gong Y, Wang DA. *A dual-functioning adenoviral vector encoding both transforming growth factor-beta3 and shRNA silencing type I collagen: construction and controlled release for chondrogenesis.* J Control Release. 142, 70–77 (2010).

Zhang L, Hu J, Athanasiou KA. *The role of tissue engineering in articular cartilage repair and regeneration.* Crit Rev Biomed Eng. 37, 1–57 (2009).

Zhang M & Huang B. *The multi-differentiation potential of peripheral blood mononuclear cells.* Stem Cell Res Ther. 3, 48–58 (2012).

Zhen G, Wen C, Jia X, Li Y, Crane JL, Mears SC, Askin FB, Frassica FJ, Chang W, Yao J, Carrino JA, Cosgarea A, Artemov D, Chen Q, Zhao Z, Zhou X, Riley L, Sponseller P, Wan M, Lu WW, Cao X. *Inhibition of TGF-β signaling in mesenchymal stem cells of subchondral bone attenuates osteoarthritis.* Nat Med. 19, 704–712 (2013).

Book chapters

Gordeladze JO, Reseland JE, Karlsen TA, Jakobsen RB, Engebretsen L, Lyngstadaas SP, Duroux-Richard I, Jorgensen C, Brinchmann JE. *Bone and cartilage from stem cells: growth optimalization and stabilization of cell phenotypes.* Regenerative medicine and tissue engineering - cells and biomaterials. Ch. 2, 23–56 (2011). Prof. Daniel Eberli (Ed.), ISBN: 978-953-307-663-8, InTech.

Miranda-Duarte A. *Epigenetic Mechanisms in Osteoarthritis*. Osteoarthritis - Progress in Basic Research and Treatment. Ch. 2, 15–39 (2015). Prof. Qian Chen (Ed.), ISBN: 978-953-51-2136-7, InTech.

Oseni AO, Crowley C, Boland MZ, Butler PE, Seifalian AM. *Cartilage tissue engineering: the application of nanomaterials and stem cell technology.* Tissue engineering for tissue and organ regeneration. Ch. 12, 233–266 (2011). Prof. Daniel Eberli (Ed.), ISBN: 978-953-307-688-1, InTech.

Websites

http://www.unfpa.org/ageing

Appendix: list of publications

Peer-reviewed journal articles

Lolli A, Lambertini E, Penolazzi L, Angelozzi M, Morganti C, Pelucchi S, Gambari R, Piva R. *Pro-chondrogenic effect of miR-221 and Slug depletion in human MSCs.* Stem Cell Rev. 10, 841–855 (2014). **Chapter 2.**

Piva R, Lambertini L, Manferdini C, Capanni C, Penolazzi L, Gabusi E, Paolella F, Angelozzi M, Lolli A, Lattanzi G, Lisignoli G. *Slug transcription factor and nuclear Lamin B1 are upregulated in osteoarthritic chondrocytes.* Osteoarthritis Cartilage. 23, 1226–1230 (2015). **Chapter 3.**

Lisignoli G, Manferdini C, Lambertini E, Zini N, Torreggiani E, Gabusi E, Gambari L, Penolazzi L, Lolli A, Facchini A, Piva R. *Chondrogenic potential of Slug-depleted hMSCs.* Tissue Eng Part A. 20, 2795–2805 (2014). **Chapter 4.**

Penolazzi L, Lolli A, Sardelli L, Angelozzi M, Lambertini E, Trombelli L, Ciarpella F, Vecchiatini R, Piva R. *Establishment of a 3D-dynamic osteoblasts-osteoclasts co-culture model to simulate the jawbone microenvironment in vitro.* Life Sciences. In press (2016). **Chapter 5.**

Lolli A, Narcisi R, Lambertini E, Penolazzi L, Angelozzi M, Kops N, Gasparini S, van Osch GJVM, Piva R. *Silencing of anti-chondrogenic microRNA-221 in human mesenchymal stem cells promotes cartilage repair in vivo.* Stem Cells. In press (2016). **Chapter 6.**

Communications for scientific meetings

European Chapter Meeting of the Tissue Engineering and Regenerative Medicine International Society (TERMIS-EU 2013). 2013, Istanbul, Turkey. Angelozzi M, Penolazzi L, Miotto M, Morganti C, Lolli A, Lambertini E, Mazzitelli S, Piva R, Nastruzzi C. *Encapsulation of Osteochondroprogenitors in Hydrogel Composite Microfibers: implications for bone tissue engineering.* **Poster communication.**

4th Meeting Stem Cell Research Italy Society. 2013, Brescia, Italy. Angelozzi M, Penolazzi L, Lolli A, Lambertini E, Morganti C, Di Ciano M, Pedriali N, Mazzitelli S, Nastruzzi C, Piva R. *Optimization of hMSCs culture conditions in biocomposite scaffolds for bone and cartilage tissue engineering.* **Poster communication.**

MicroRNA: from basic research to therapeutic applications. 2013, Ferrara, Italy. Lolli A, Lambertini E, Angelozzi M, Morganti C, Di Ciano M, Pedriali N, Penolazzi L, Piva R. *Silencing of mir-221 in human MSCs: effect on chondrogenesis.* **Oral communication.** Oral presentation award.

57th National Meeting of the Italian Society of Biochemistry and Molecular Biology. 2013, Ferrara, Italy. Lolli A, Lambertini E, Angelozzi M, Morganti C, Di Ciano M, Pedriali N, Penolazzi L, Piva R. *Silencing of mir-221 in human MSCs: effect on chondrogenesis.* **Poster communication.**

57th National Meeting of the Italian Society of Biochemistry and Molecular Biology. 2013, Ferrara, Italy. Angelozzi M, Penolazzi L, Lolli A, Lambertini E, Morganti C, Di Ciano M, Pedriali N, Mazzitelli S, Nastruzzi C, Piva R. *Optimization of hMSCs culture conditions in biocomposite scaffolds for bone and cartilage tissue engineering.* **Poster communication.**

World Conference on Regenerative Medicine. 2013, Leipzig, Germany. Lolli A, Lambertini E, Penolazzi L, Angelozzi M, Morganti C, Di Ciano M, Pedriali N, Piva R. *Enhanced chondrogenic potential of Slug and miR-221 silenced human MSCs.* **Poster communication.**

World Conference on Regenerative Medicine. 2013, Leipzig, Germany. Angelozzi M, Penolazzi L, Lolli A, Lambertini E, Morganti C, Di Ciano M, Pedriali N, Mazzitelli S, Piva R, Nastruzzi C. *Development of composite microfibrous scaffolds for the incapsulation of osteochondroprogenitors: a promising approach for bone and cartilage tissue engineering.* **Poster communication.**

5th Meeting Stem Cell Research Italy Society. 2014, Salerno, Italy. Lambertini E, Manferdini C, Capanni C, Penolazzi L, Lolli A, Di Ciano M, Lattanzi G, Lisignoli G, Piva R. *Lamin B participates in cartilage senescence and degeneration.* **Poster communication.**

5th Meeting Stem Cell Research Italy Society. 2014, Salerno, Italy. Angelozzi M, Penolazzi L, Lambertini E, Lolli A, Miotto M, Vezzali F, Mazzitelli S, Pelucchi S, Pastore A, Nastruzzi C, Piva R. *Encapsulation of dedifferentiated nasal septal chondrocytes in alginate based scaffolds for cartilage tissue engineering.* **Poster communication.**

56th Annual Meeting of the Italian Cancer Society (SIC): "Dangerous Liaisons: translating cancer biology into better patients management". 2014, Ferrara, Italy. Angelozzi M, Lolli A, Lambertini E, Vezzali F, Di Ciano M, Penolazzi L, Piva R. *miR-221 and SLUG interplay in human mesenchymal stem cells and breast cancer cells.* **Poster communication.**

Netherlands Institute of Regenerative Medicine (NIRM) – Consortium Meeting. 2014, Rotterdam, The Netherlands. Lolli A, Lambertini E, Penolazzi L, Narcisi R, Angelozzi M, Vezzali F, Miotto M, van Osch GJVM, Piva R. *Enhanced chondrogenic potential of Slug and miR-221 depleted human MSCs.* **Poster communication.**

Netherlands Institute of Regenerative Medicine (NIRM) – Consortium Meeting. 2014, Rotterdam, The Netherlands. Han Arikan O, Narcisi R, Lolli A, ten Berge D, van Osch GJVM. *Investigating the role of canonical Wnt signalling in maintaining the multilineage differentiation capacity of human mesenchymal stem cells.* **Poster communication.**

23rd Annual Meeting of the Netherlands Society for Biomaterials and Tissue Engineering (NBTE). 2014, Lunteren, The Netherlands. Lolli A, Lambertini E, Penolazzi L, Narcisi R, Angelozzi M, Vezzali F, Miotto M, van Osch GJVM, Piva R. *Enhanced chondrogenic potential of Slug and miR-221 depleted human MSCs.* **Oral communication.**

4th Joint Meeting of the European Calcified Tissue Society (ECTS) and the International Bone and Mineral Society (IBMS). 2015, Rotterdam, The Netherlands. Lolli A, Lambertini E, Penolazzi L, Narcisi R, Angelozzi M, van Osch GJVM, Piva R. *Enhanced chondrogenic potential of miR-221 and Slug depleted human MSCs.* **Poster communication.**

4th Joint Meeting of the European Calcified Tissue Society (ECTS) and the International Bone and Mineral Society (IBMS). 2015, Rotterdam, The Netherlands. Angelozzi M, Miotto M, Penolazzi L, Lolli A, Mazzitelli S, Badylak SF, Piva R, Nastruzzi C. *Composite ECM-alginate microfibers produced by microfludics as scaffolds with biomineralisation potential.* **Poster communication.**

6th Meeting Stem Cell Research Italy Society. 2015, Bari, Italy. Lolli A, Lambertini E, Penolazzi L, Angelozzi M, Narcisi R, van Osch GJVM, Piva R. *Enhanced chondrogenic potential of miR-221 and Slug depleted human MSCs.* **Oral communication.**

6th Meeting Stem Cell Research Italy Society. 2015, Bari, Italy. Penolazzi L, Lolli A, Sardelli L, Angelozzi M, Ciarpella F, Vecchiatini R, Lambertini E, Piva R. *Establishment of a 3D-dynamic osteoblasts-osteoclasts co-culture model to simulate the jawbone microenvironment in vitro.* **Poster communication.**

6th Meeting Stem Cell Research Italy Society. 2015, Bari, Italy. Angelozzi M, Ciarpella F, Penolazzi L, Lambertini E, Lolli A, Lisignoli G, Pinton P, Piva R. *Osteogenic differentiation of human MSCs: specific occupancy of the mitochondrial DNA by NFATc1 transcription factor.* **Poster communication.**